ZooKeys 707: 1–46 (2017)
doi: 10.3897/zookeys.707.13042
http://zookeys.pensoft.net

RESEARCH ARTICLE

A peer-reviewed open-access journal
ZooKeys
Launched to accelerate biodiversity research

Abyssal fauna of the UK-1 polymetallic nodule exploration area, Clarion-Clipperton Zone, central Pacific Ocean: Mollusca

Helena Wiklund[1], John D. Taylor[1], Thomas G. Dahlgren[2,3], Christiane Todt[4,5], Chiho Ikebe[1], Muriel Rabone[1], Adrian G. Glover[1]

1 *Life Sciences Department, Natural History Museum, London SW7 5BD, UK* **2** *Uni Research, Bergen, Norway* **3** *Department of Marine Sciences, University of Gothenburg, Box 463, 40530 Gothenburg, Sweden* **4** *University Museum of Bergen, University of Bergen, Allégt. 41, 5007 Bergen, Norway* **5** *Rådgivande Biologer AS, Bredsgården, Bryggen 5003 Bergen, Norway*

Corresponding author: *Adrian G. Glover* (a.glover@nhm.ac.uk)

Academic editor: *E. Neubert* | Received 3 April 2017 | Accepted 8 June 2017 | Published 10 October 2017

http://zoobank.org/6A0BCD99-2749-450C-874B-440D0C0A232C

Citation: Wiklund H, Taylor JD, Dahlgren TG, Todt C, Ikebe C, Rabone M, Glover AG (2017) Abyssal fauna of the UK-1 polymetallic nodule exploration area, Clarion-Clipperton Zone, central Pacific Ocean: Mollusca. ZooKeys 707: 1–46. https://doi.org/10.3897/zookeys.707.13042

Abstract

We present the first DNA taxonomy publication on abyssal Mollusca from the Clarion-Clipperton Zone (CCZ), central Pacific ocean, using material collected as part of the Abyssal Baseline (ABYSSLINE) environmental survey cruise 'AB01' to the UK Seabed Resources Ltd (UKSRL) polymetallic-nodule exploration area 'UK-1' in the eastern CCZ. This is the third paper in a series to provide regional taxonomic data for a region that is undergoing intense deep-sea mineral exploration for high-grade polymetallic nodules.

Taxonomic data are presented for 21 species from 42 records identified by a combination of morphological and genetic data, including molecular phylogenetic analyses. These included 3 heterodont bivalves, 5 protobranch bivalves, 4 pteriomorph bivalves, 1 caudofoveate, 1 monoplacophoran, 1 polyplacophoran, 4 scaphopods and 2 solenogastres. Gastropoda were recovered but will be the subject of a future study. Seven taxa matched published morphological descriptions for species with deep Pacific type localities, and our sequences provide the first genetic data for these taxa. One taxon morphologically matched a known cosmopolitan species but with a type locality in a different ocean basin and was assigned the open nomenclature '*cf*' as a precautionary approach in taxon assignments to avoid over-estimating species ranges. One taxon is here described as a new species, *Ledella knudseni* sp. n. For the remaining 12 taxa, we have

determined them to be potentially new species, for which we make the raw data, imagery and vouchers available for future taxonomic study. The Clarion-Clipperton Zone is a region undergoing intense exploration for potential deep-sea mineral extraction. We present these data to facilitate future taxonomic and environmental impact study by making both data and voucher materials available through curated and accessible biological collections.

Keywords
New species, Bivalvia, Caudofoveata, Monoplacophora, Polyplacophora, Scaphopoda, Solenogastres, Aplacophora

Introduction

The abyssal zone of the world's oceans has been defined as that between 3000 m and 6000 m depth, a bathymetric zone that encompasses 54% of the geographic surface of the planet (Smith et al. 2008). Molluscs form a characteristic and abundant group in this region, and many of them, most prominently among the bivalves, are deposit feeders that can sustain themselves on the steady rain of organic matter from surface regions. Current online databases list 1204 mollusc species recorded at abyssal depths from between 3000 m and 6000 m (OBIS 2017) out of a total of 3229 accepted 'deep-sea' mollusc species recorded from depths greater than 500 m (Glover et al. 2017).

The Clarion-Clipperton Zone (hereafter, CCZ) is so called as it lies between the Clarion and Clipperton Fracture Zones, topographical highs that extend longitudinally across almost the entire Pacific Ocean. There is no strict definition of the region, but it has come to be regarded as the area between these fracture zones that lies within international waters and encompasses the main areas of commercial interest for polymetallic nodule mining. Exploration licenses issued by the International Seabed Authority (ISA 2017) extend from 115°W (the easternmost extent of the UK-1 exploration area) to approximately 158°W (the westernmost extent of the COMRA exploration area), as such we use from hereafter a working definition of the CCZ as the box: 13°N158°W; 18°N118°W; 10°N112°W; 2°N155°W. This is an area of almost exactly 5 million sq km, approximately 1.4% of the ocean's surface.

The Challenger expedition between 1872 and 1876 is said to be the start of modern oceanography, and in total about 4700 new species were described from it. However, in the Pacific Ocean they went from Japan to the Hawaiian Islands and after that fairly straight south down to about 40°S where they turned towards Valparaiso in Chile, and thus they did only touch the western-most part of the CCZ (Tizard et al. 1885). From 1891 to 1905 Agassiz did three expeditions onboard Albatross, after which Dall described 218 new species of molluscs and brachiopods from off the coast of Central and South America (Dall 1908). The Danish Galathea II deep-sea expedition went around the world in 1950-1952, but in the Pacific they went from New Zealand to Hawaii and then up north towards San Fransisco (Bruun et al. 1956), and did not collect anything in the actual CCZ.

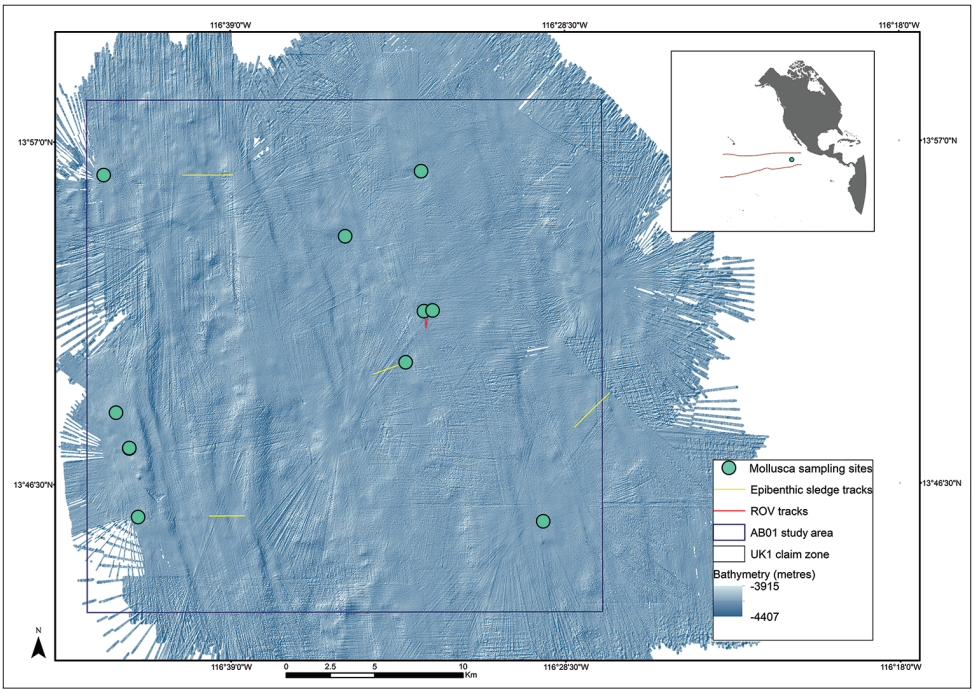

Figure 1. The UK Seabed Resources Ltd 'UK-1' polymetallic nodule exploration contract area ABYSSLINE (AB01) Stratum A, a 30 × 30 km survey box in the northern sector of the 58,000 km^2 exploration area. Bathymetric survey and sample localities from the AB01 RV *Melville* survey cruise, October 2013, data courtesy Craig R. Smith (University of Hawaii), UK Seabed Resources Ltd and Seafloor Investigations, LLC.

Within the entire 5 million sq km CCZ, as defined above, online databased sources prior to this publication list only one benthic mollusc record when specifying depth between 3000-6000 m, and a further four records just south of CCZ (OBIS 2017). This result is due to lack of sampling and/or taxonomic knowledge given that an abundant and diverse mollusc fauna is suspected in the region based on anecdotal reports from past environmental surveys (e.g. ISA 1999; Ebbe et al. 2010). The goal of the DNA taxonomy part of the Abyssal Baseline (ABYSSLINE) program is to start to rectify these gaps in our knowledge and make data publically available that will eventually allow for a complete taxonomic synthesis of the CCZ supported by openly-available molecular and morphological data. We present results from a DNA taxonomy survey of abyssal benthic Mollusca collected as part of the first ABYSSLINE environmental survey cruise 'AB01' to the UK Seabed Resources Ltd (UKSRL) polymetallic nodule exploration contract area 'UK-1' (Fig. 1) in the eastern Clarion-Clipperton Zone (CCZ), central Pacific Ocean (Smith et al. 2013). Here we provide the first version of the Mollusca taxonomic synthesis, consisting of taxon records, images, genetic data and short descriptions from the first research cruise (AB01) aboard the RV *Melville* in October 2013. Gastropoda

is not included in this version (subject to a future study), and we report on Bivalvia, Caudofoveata, Monoplacophora, Polyplacophora, Scaphopoda and Solenogastres.

This paper aims to provide regional taxonomic information for an area that is undergoing intense deep-sea mineral exploration for high-grade polymetallic nodules regulated by Sponsoring States (here the United Kingdom Government) and the International Seabed Authority (ISA 2017). The study is not a comprehensive faunal guide to the region, but a taxonomic data paper that will be updated with new additions following future collections and analyses. This publication is supported by similar data publications on other taxa from the CCZ. Two have been published (Echinodermata, Glover et al. 2016b and Cnidaria, Dahlgren et al. 2016), while other taxa are in preparation, forming a suite of taxonomic syntheses of biodiversity in the region, supported by a contract between the company UK Seabed Resources Ltd and the Natural History Museum, London and Uni Research, Bergen.

Materials and methods

Knowledge of baseline biodiversity and biogeography in the CCZ is severely hampered by a lack of modern DNA-supported taxonomic studies (Glover et al. 2016a). With this in mind, three fundamental principles underpin our methodological pipeline: (1) the careful sorting and collection of live samples at sea using a 'cold-chain' pipeline by trained taxonomists, (2) the use of combined multiple-marker DNA sequences and morphological data in phylogenetics-based species descriptions or re-descriptions/records and (3) integrated data and sample management to push openly-available taxonomic data through online repositories linked to curated molecular and morphological collections in national museums.

Fieldwork

The ABYSSLINE environmental baseline survey consists of a series of 30 × 30 km survey boxes (strata), three within the UK-1 exploration area, and an additional reference site outside the exploration area (Smith et al. 2013). Within each survey box, sample sites for a variety of benthic sampling gears are selected randomly – a randomized, stratified sampling design that assumes no *a priori* knowledge of the benthic environment. The UK-1 strata are being sampled in a series of oceanographic cruises during the course of the project, which commenced in July 2013, with the first cruise (AB01) taking place in October 2013 aboard the RV *Melville* (hereafter, cruise 'AB01'). During this cruise, the first stratum was comprehensively mapped and sampled for a range of environmental and geophysical parameters (Fig. 1, Smith et al. 2013).

A comprehensive description of our DNA taxonomy pipeline is provided in Glover et al. (2016a). In summary, deep-sea benthic specimens from the AB01 strata were

collected using a range of oceanographic sampling gears including box core (BC), epibenthic sledge (EBS), remotely operated vehicle (ROV) and multiple core (MC). Geographic data from sampling activities was recorded on a central GIS database (Fig. 1). Live-sorting of specimen samples was carried out aboard the RV *Melville* in a 'cold-chain' pipeline, in which material was immediately transferred and maintained in chilled, filtered seawater held at 2-4°C. Specimens were preliminary identified at sea and imaged live using stereomicroscopes with attached digital cameras. The specimens were then transferred to individual microtube vials containing an aqueous solution of 80% non-denatured ethanol, numbered and barcoded into a database and kept chilled until return to the Natural History Museum, London.

Laboratory work

In the laboratory, specimens were re-examined using stereo and compound microscopes, identified and described to best possible taxonomic level with key morphological features photographed with digital cameras and a small tissue-sample taken for DNA extraction.

Extraction of DNA was done with DNeasy Blood and Tissue Kit (Qiagen) using a Hamilton Microlab STAR Robotic Workstation. About 1800 bp of 18S, 450 bp of 16S, and 650 bp of cytochrome c oxidase subunit I (COI) were amplified using primers listed in Table 1. PCR mixtures contained 1 µl of each primer (10 µM), 2 µl template DNA and 21 µl of Red Taq DNA Polymerase 1.1X MasterMix (VWR) in a mixture of total 25 µl. The PCR amplification profile consisted of initial denaturation at 95°C for 5 min, 35 cycles of denaturation at 94°C for 45 s, annealing at 55°C for 45 s, extension at 72°C for 2 min, and a final extension at 72°C for 10 min. PCR prod-

Table 1. Primers used for PCR and sequencing of 18S, COI and 16S.

Primer	Sequence 5'-3'	Reference
18S		
18SA	AYCTGGTTGATCCTGCCAGT	Medlin et al. 1988
18SB	ACCTTGTTACGACTTTTACTTCCTC	Nygren and Sundberg 2003
620F	TAAAGYTGYTGCAGTTAAA	Nygren and Sundberg 2003
1324R	CGGCCATGCACCACC	Cohen et al. 1998
COI		
LCO1490	GGTCAACAAATCATAAAGATATTGG	Folmer et al. 1994
HCO2198	TAAACTTCAGGGTGACCAAAAAATCA	Folmer et al. 1994
16S		
ann16SF	GCGGTATCCTGACCGTRCWAAGGTA	Sjölin et al. 2005
16SbrH	CCGGTCTGAACTCAGATCACGT	Palumbi et al. 1996

ucts were purified using Millipore Multiscreen 96-well PCR Purification System, and sequencing was performed on an ABI 3730XL DNA Analyser (Applied Biosystems) at The Natural History Museum Sequencing Facility, using the same primers as in the PCR reactions plus two internal primers for 18S (Table 1). Overlapping sequence fragments were merged into consensus sequences using Geneious (Kearse et al. 2012) and aligned using MAFFT (Katoh et al. 2002) for 18S and 16S, and MUSCLE (Edgar 2004) for COI, both programs used as plugins in Geneious, with default settings. Bayesian phylogenetic analyses (BA) were conducted with MrBayes 3.2 (Ronquist et al. 2012). Analyses were run for 10-30 million generations, of which the first 25% generations were discarded as burn-in.

Data handling

The field and laboratory work created a series of databases and sample sets that are integrated into a data-management pipeline. This includes the transfer and management of data and samples between a central collections database, a molecular collections database and external repositories (GenBank, WoRMS, OBIS, GBIF, ZooBank) through DarwinCore archive. This provides a robust data framework to support DNA taxonomy, in which openly-available data and voucher material is key to quality data standards. A further elaboration of the data pipeline is published in Glover et al. (2016a).

Taxonomic assignments

All future studies of biogeographic and bathymetric ranges, gene-flow, extinction risks, natural history, reproductive ecology, functional ecology and geochemical interactions of CCZ species are dependent on accurate identifications faciliated by taxonomy. This taxonomy is dependent on a sound theoretical underpinning – a species concept - coupled with the availability of both raw data and voucher samples. Here we use a phylogenetic species concept *sensu* Donoghue (1985) with species determined by DNA-based phylogenetic analysis and the recognition of distinct monophyletic groups as species. For those taxa where the typical morphological data that allows determination of species are missing, we provide the lowest-level taxonomic name possible, but include determination with genetic data. All materials (vouchers including archived frozen tissue) and genetic data are accessible together with the morphological data presented in this paper. A full list of all taxa including Natural History Museum Accession Numbers, NHM Molecular Collection Facility (NHM-MCF) FreezerPro numbers and NCBI GenBank Accession numbers is provided in Table 2.

Table 2. Taxon treatments presented in this paper. Includes Class, DNA Taxonomy ID (a species-level identification based on combined DNA and morphological evidence), GUID (Global Unique Identifier link to data record on http://data.nhm.ac.uk), ABYSSLINE Record number, NHM Accession number, NHM Molecular Collection Facility (MCF) sample ID number (NHMUK_MCF#) and NCBI GenBank accession number (Genbank#) for successfully sequenced genetic markers.

Class, sub-class	DNA Taxonomy ID	GUID#	ABYSS LINE record#	NHMUK Acc#	NHMUK MCF#	Gen Bank#
Bivalvia, Heterodonta	*Myonera* sp. (NHM_186)	45033e06-fb54-49d5-b632-767e63c1cfd3	NHM_186	20170037	175138970	MF157481 MF157508
Bivalvia, Heterodonta	*Thyasira* sp. (NHM_180)	49b2f599-bda4-4177-932f-59effe8a3320	NHM_051	20170038	175139015	MF157468 MF157501
Bivalvia, Heterodonta	*Thyasira* sp. (NHM_180)	b84e470d-73bc-413b-88f9-3d702509a37a	NHM_180	20170039	175139013	MF157478
Bivalvia, Heterodonta	*Vesicomya galatheae*	c609ed0c-f881-44c9-a6a0-3e36f0934997	NHM_143	20170040	175139017	MF157474
Bivalvia, Heterodonta	*Vesicomya galatheae*	314ef160-7cfa-4705-b091-640c3e69ad1a	NHM_255	20170041	175138995	MF157460 MF157487 MF157509
Bivalvia, Heterodonta	*Vesicomya galatheae*	3add2560-71c1-4879-afb8-0a5ed1449c89	NHM_260	20170042	175138988	MF157488 MF157510
Bivalvia, Protobranchia	*Bathyspinula calcar*	3ab74908-1a5d-465f-890c-49373a44906c	NHM_181	20170043	175138994	MF157479 MF157507
Bivalvia, Protobranchia	*Bathyspinula calcar*	61f15e3c-f070-48a1-b484-780b37f7feb6	NHM_146	20170044	175138993	MF157475 MF157505
Bivalvia, Protobranchia	*Bathyspinula calcar*	c44da298-9b61-4d6d-a1cd-2d6c3bd70859	NHM_149A	20170045	175138969	MF157506
Bivalvia, Protobranchia	*Bathyspinula calcar*	ad2cb87b-1fce-415d-ab45-1619bbc4352b	NHM_284	20170046	175139011	MF157514
Bivalvia, Protobranchia	*Ledella knudseni* sp. n.	8aec47f4-dcec-4668-8398-9e4b0c28ecb8	NHM_288A	20170047	175138963	MF157515
Bivalvia, Protobranchia	*Ledella knudseni* sp. n.	f1886d78-22bf-403e-bdb2-784b91c0eb12	NHM_288C	20170048	175139136	MF157491 MF157516
Bivalvia, Protobranchia	*Ledella* sp. (NHM_381)	8f077dac-baac-4fef-b6a1-7fd02d5f0070	NHM_381	20170049	175139009	MF157494 MF157521
Bivalvia, Protobranchia	*Ledella* sp. (NHM_381)	08d5c39f-b1e4-43d7-a8ea-2fe9abc05752	NHM_144	20170050	175139014	MF157458 MF157504

Class, sub-class	DNA Taxonomy ID	GUID#	ABYSS LINE record#	NHMUK Acc#	NHMUK MCF#	Gen Bank#
Bivalvia, Protobranchia	*Nucula profundorum*	f2133256-1cad-4255-a5cb-bd5331417127	NHM_141	20170051	175139038	MF157457 MF157473 MF157503
Bivalvia, Protobranchia	*Nucula profundorum*	f96a470e-237e-46b4-ba85-4c6196106071	NHM_274A	20170052	175138964	MF157512
Bivalvia, Protobranchia	*Nucula profundorum*	65f8d1ed-dd6a-4265-90d2-daf07491cd76	NHM_378	20170053	175138949	MF157464 MF157520
Bivalvia, Protobranchia	*Yoldiella* sp. (NHM_190)	621deeed-8f8a-4d2e-9136-4e30794fc68e	NHM_042	20170054	175139016	MF157467
Bivalvia, Protobranchia	*Yoldiella* sp. (NHM_190)	6dfa8946-aa7a-448d-9f4f-703a3b2a10d9	NHM_185	20170055	175138989	MF157480
Bivalvia, Protobranchia	*Yoldiella* sp. (NHM_190)	b6e48ff4-2e02-42dc-b9ed-286d297d1459	NHM_190	20170056	175138965	MF157482
Bivalvia, Protobranchia	*Yoldiella* sp. (NHM_190)	7a6c76df-989b-4fcd-9e9c-a442d0a02443	NHM_194	20170057	175139019	MF157485
Bivalvia, Protobranchia	*Yoldiella* sp. (NHM_190)	37b2493a-a725-4ec4-a720-cc9dd12fb49d	NHM_246	20170058	175139012	MF157486
Bivalvia, Protobranchia	*Yoldiella* sp. (NHM_190)	17d54bb4-9f38-4073-9bb6-17637773b058	NHM_289	20170059	175139034	MF157492 MF157517
Bivalvia, Protobranchia	*Yoldiella* sp. (NHM_190)	8923576e-4542-4fc7-9a89-016e8fb564cb	NHM_193	20170060	175139036	MF157484
Bivalvia, Pteriomorpha	*Bentharca* cf. *asperula*	9d29d7ec-55cd-4b41-929a-2379be221263	NHM_108	20170061	175138968	MF157470 MF157502
Bivalvia, Pteriomorpha	*Bentharca* cf. *asperula*	96bfe548-f511-49c4-b2a3-0a9a45f9154b	NHM_150	20170062	175138966	MF157476
Bivalvia, Pteriomorpha	*Bentharca* cf. *asperula*	8d9beefd-2fbc-4204-9bf8-90551419ac1c	NHM_170	20170063	175139018	MF157477
Bivalvia, Pteriomorpha	*Bentharca* cf. *asperula*	ccdd114d-c8a8-47da-ba84-8b8ca5125a6a	NHM_282	20170064	175139035	MF157490 MF157513
Bivalvia, Pteriomorpha	*Bentharca* cf. *asperula*	1d462c2a-bb98-4369-afc3-63a7c33a4bdd	NHM_427	20170065	175139023	MF157496
Bivalvia, Pteriomorpha	*Bentharca* cf. *asperula*	a30eab51-5f52-4fec-89d7-d47152895c92	NHM_454	20170066	175138984	MF157499
Bivalvia, Pteriomorpha	*Dacrydium panamensis*	180e485f-f1c2-41e1-b858-f02ba537804b	NHM_117	20170067	175138967	MF157471
Bivalvia, Pteriomorpha	*Limopsis* sp. (NHM_453)	ce9cbed0-82cc-420d-baad-fdfff7cc0986	NHM_453	20170069	175138999	MF157498 MF157524
Bivalvia, Pteriomorpha	*Catillopecten* sp. (NHM_105)	24f5c5bb-e419-48ef-baaa-4a6493f691d9	NHM_105	20170070	175138991	MF157469
Caudofoveata	Prochaetodermatidae sp. (NHM_344)	e68608f9-4b83-4eb9-89f2-0de4f89c21b0	NHM_344	20170071	175138997	MF157462

Class, sub-class	DNA Taxonomy ID	GUID#	ABYSS LINE record#	NHMUK Acc#	NHMUK MCF#	Gen Bank#
Monoplaco-phora	*Veleropilina oligotropha*	bf968b01-1991-43b7-87e4-25da4d5a9dc5	NHM_405	20170072	175138950	MF157465 MF157495 MF157522
Polyplaco-phora	*Leptochiton macleani*	d69b581d-8a79-4c4d-8f70-88b2ec07d86e	NHM_446	20170073	175139008	MF157466 MF157497 MF157523
Scaphopoda	*Fissidentalium* sp. (NHM_261)	679fa0ca-d647-446d-87c5-e8d33949efe2	NHM_261	20170074	175138971	MF157461 MF157489 MF157511
Scaphopoda	Gadilida sp. (NHM_192)	fc0e3ae8-9cce-46a0-bb8b-fafe0e2cb46b	NHM_192	20170075	175138946	MF157459 MF157483
Scaphopoda	*Gadila* sp. (NHM_345)	c301a72f-54cb-435e-8aae-17cf4d37675f	NHM_345	20170076	175138986	MF157463 MF157493 MF157518
Scaphopoda	Gadilida sp. (NHM_132)	6a1906d9-9ed1-4f6e-a0cf-2d53e2289a01	NHM_132	20170077	175138944	MF157456 MF157472
Solenogastres	Acanthomeniidae sp. (NHM_367)	c0577fc9-7302-4fec-bc8c-87a17a38bc91	NHM_367	20170078	175138973	MF157519
Solenogastres	Lophomeniinae sp. (NHM_027)	319fd186-b07f-4be7-986c-b96c20f63723	NHM_027	20170079	175139039	MF157500

Systematics

Bivalvia
Heterodonta
Anomalodesmata
Cuspidariidae Dall, 1886
***Myonera* Dall & E.A Smith, 1886**

***Myonera* sp. (NHM_186)**

Materials examined. NHM_186 NHMUK 20170037, collected 2013-10-13, 13.93482 -116.55018, 4082 m. http://data.nhm.ac.uk/object/45033e06-fb54-49d5-b632-767e63c1cfd3

Description. Shell thin, translucent, sub-ovate tapering posteriorly. Postero-dorsal margin straight. Rostrum short, demarcated by single, carinate radial rib. Sculpture of a few strong, widely spaced, commarginal lamellae, reduced on rostrum. Shell surface minutely pustulose (Fig. 2). Maximum length 1.5 mm, maximum height 1 mm.

Genetic data. GenBank NHM_186 18S-MF157481, COI-MF157508.

Remarks. The species resembles the supposedly cosmopolitan form *Myonera alleni* Poutiers & Bernard, 1995, previously as *Myonera atlantica* (Allen & Morgan, 1981). However, the type locality for this species is from the deep north Atlantic and no genetic data are available for comparison. No similar species is recorded from deep water of the eastern Pacific. Forms a unique monophyletic clade with two other cuspidariid species distinct from all other AB01 specimens (Fig. 5). No genetic matches on GenBank.

Ecology. Found in polymetallic nodule province.

Lucinida
Thyasiridae Dall, 1900
Thyasira Lamarck, 1818

***Thyasira* sp. (NHM_180)**

Material examined. NHM_051 NHMUK 20170038, collected 2013-10-09, 13.8372 -116.55843, 4336 m. http://data.nhm.ac.uk/object/49b2f599-bda4-4177-932f-59ef-fe8a3320

NHM_180 NHMUK 20170039, collected 2013-10-13, 13.93482 -116.55018, 4082 m. http://data.nhm.ac.uk/object/b84e470d-73bc-413b-88f9-3d702509a37a

Description. Minute, thin-shelled, translucent, anteriorly extended, longer than high, umbones posterior of mid-line, posteriorly angulate, antero-dorsal margin long, evenly curved, shell surface smooth. Gill with single demibranch of about 10 widely spaced filaments, ventral edge of the gill does not cover the body pouches. Foot relatively large with distal bulb (Fig. 3). NHM_180 length 1.1 mm.

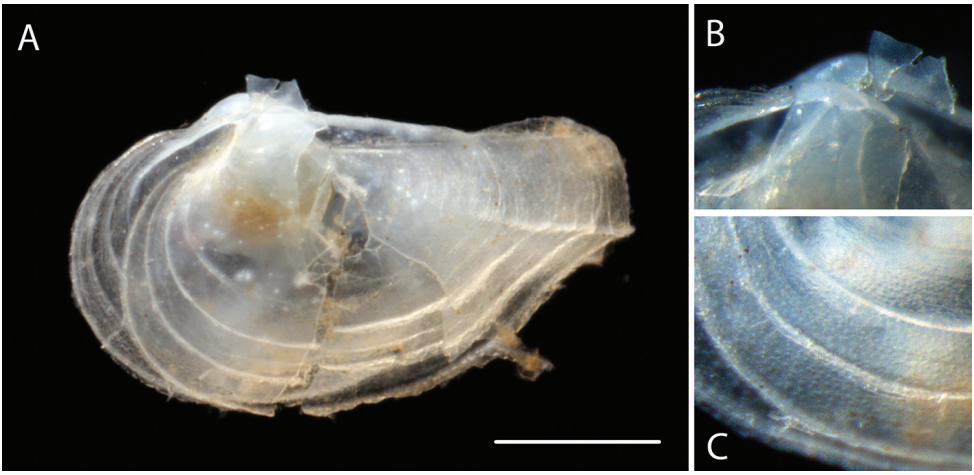

Figure 2. *Myonera* sp. (NHM_186) **A** Live specimen imaged at sea, slightly broken shell with live animal **B** Detail of hinge **C** Detail of shell ornamentation. Scale bar: 0.5 mm (**A**). Image attribution Glover, Dahlgren and Wiklund, 2017.

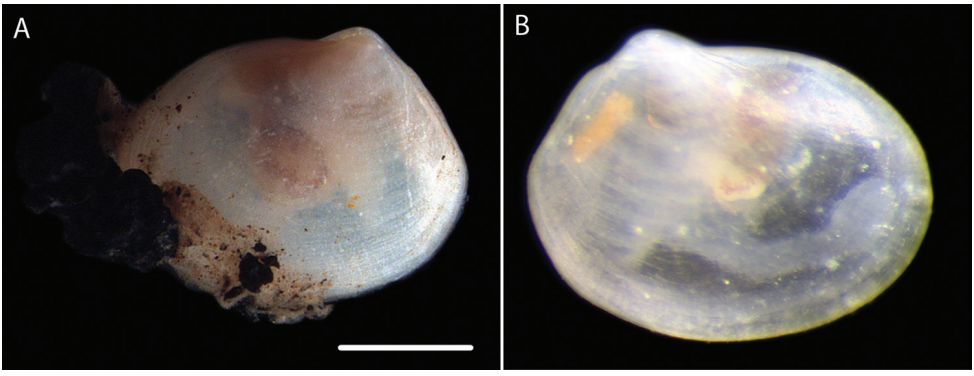

Figure 3. *Thyasira* sp. (NHM_180) **A** Preserved specimen (NHM_180) with pieces of polymetallic nodule adhered to shell margin **B** Additional small specimen (live imaged at sea) NHM_051. Scale bar: 0.5 mm (**A**). Image attribution Glover, Dahlgren and Wiklund, 2017.

Genetic data. GenBank NHM_051 18S-MF157468, COI-MF157501; NHM_180 18S-MF157478.

Remarks. Forms a monophyletic clade with four other thyasirid species (Fig. 5) and distinct from all other AB01 specimens. No genetic matches on GenBank. Morphologically the species is similar in shape to abyssal thyasirid species (*Thyasira inflata*, *T. transversa)* from the south Atlantic described and placed in *Thyasira* (*Mendicula*) by Payne & Allen (1991) but not similar to the type species of *Mendicula* (*Lucina*) *induta* Hedley, 1907 = *M. memorata* Iredale, 1924) or the widespread *Mendicula ferruginosa* (Forbes, 1844). No similarly shaped species has been recorded from the abyssal eastern Pacific.

Ecology. Found in polymetallic nodule province.

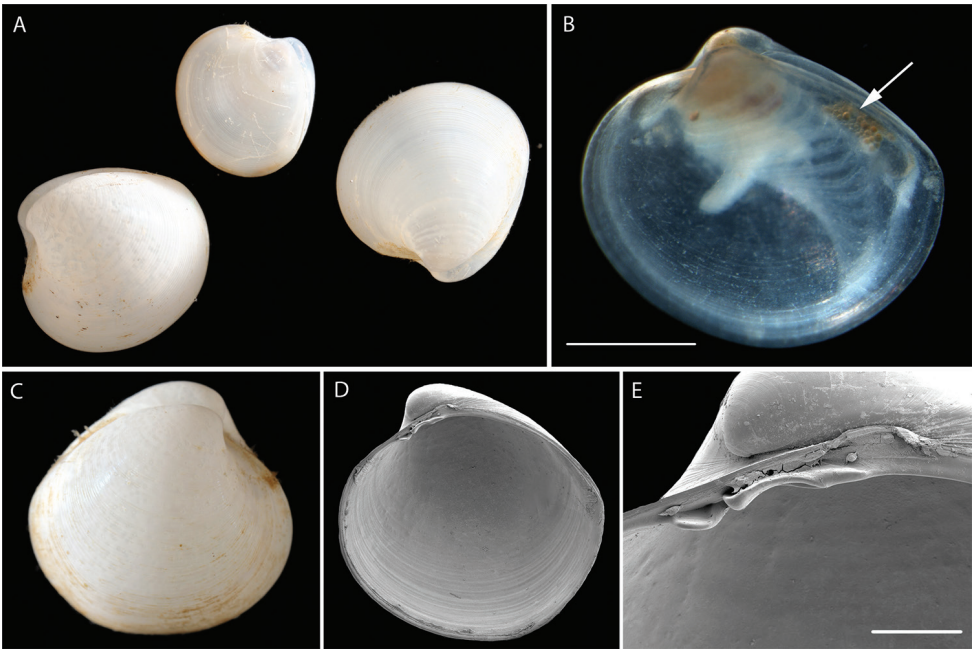

Figure 4. *Vesicomya galatheae* (Knudsen, 1970) **A** Live imaged specimens of NHM_260a,b,c habitus **B** Detail of NHM_143, probable juvenile, oil droplets arrowed **C** NHM_255 live imaged specimen **D–E** SEM detail of shell interior and hinge teeth of NHM_260a (right valve). Scale bars: 0.5 mm (**B, E**). Image attribution Glover, Taylor, Dahlgren & Wiklund, 2017.

Veneroida
Vesicomyidae Dall & Simpson, 1901
***Vesicomya* Dall, 1886**

***Vesicomya galatheae* (Knudsen, 1970)**

Material examined. NHM_143 NHMUK 20170040, collected 2013-10-11, 13.75833 -116.69852, 4080 m. http://data.nhm.ac.uk/object/c609ed0c-f881-44c9-a6a0-3e36f0934997

NHM_255 NHMUK 20170041, collected 2013-10-17, 13.75583 -116.48667, 4076 m. http://data.nhm.ac.uk/object/314ef160-7cfa-4705-b091-640c3e69ad1a

NHM_260 NHMUK 20170042.1-2, collected 2013-10-17, 13.75583 -116.48667, 4076 m. http://data.nhm.ac.uk/object/3add2560-71c1-4879-afb8-0a5ed1449c89

Description. Small, inflated sub-spherical. Sculpture of fine closely spaced low commarginal lamellae. Right valve with two cardinal teeth, posterior long, thin, anterior tooth small and short (Fig. 4). Specimen NHM_143 length 1.4 mm, height 1.2 mm.

Genetic data. GenBank NHM_143 18S-MF157474; NHM_255 16S-MF157460, 18S-MF157487, COI-MF157509; NHM_260 18S-MF157488, COI-MF157510.

Figure 5. Phylogenetic analysis of Bivalvia: Heterodonta. 50% majority rule consensus tree from the Bayesian analyses using 18S and COI. Asterisks denotes support values of 95 or above.

Remarks. *Vesicomya galatheae* was described from off Costa Rica and Panama at 2950- 3570 m. Morphologically similar to *Vesicomya pacifica* (Smith, 1885) holotype NHMUK 1887.2.9.2710-11 but Krylova et al. (2015) regard this as a northern Pacific species distinguished from *V. galatheae* by the shape, hinge teeth and number of siphonal tentacles. When comparing sequences from our CCZ specimens with the *Vesicomya pacifica* from Krylova et al. (2015), the K2P difference is 0.11. In the molecular tree (Fig. 5) it groups with a *Kelliella* species from the northwestern Atlantic and these two species form a sister clade to *Calyptogena* species. *Kelliella* species are very similar to *Vesicomya* and the relationships of species assigned to the two genera need clarification. Forms a unique monophyletic clade distinct from all other AB01 specimens. No genetic matches on GenBank.

Ecology. Found in polymetallic nodule province.

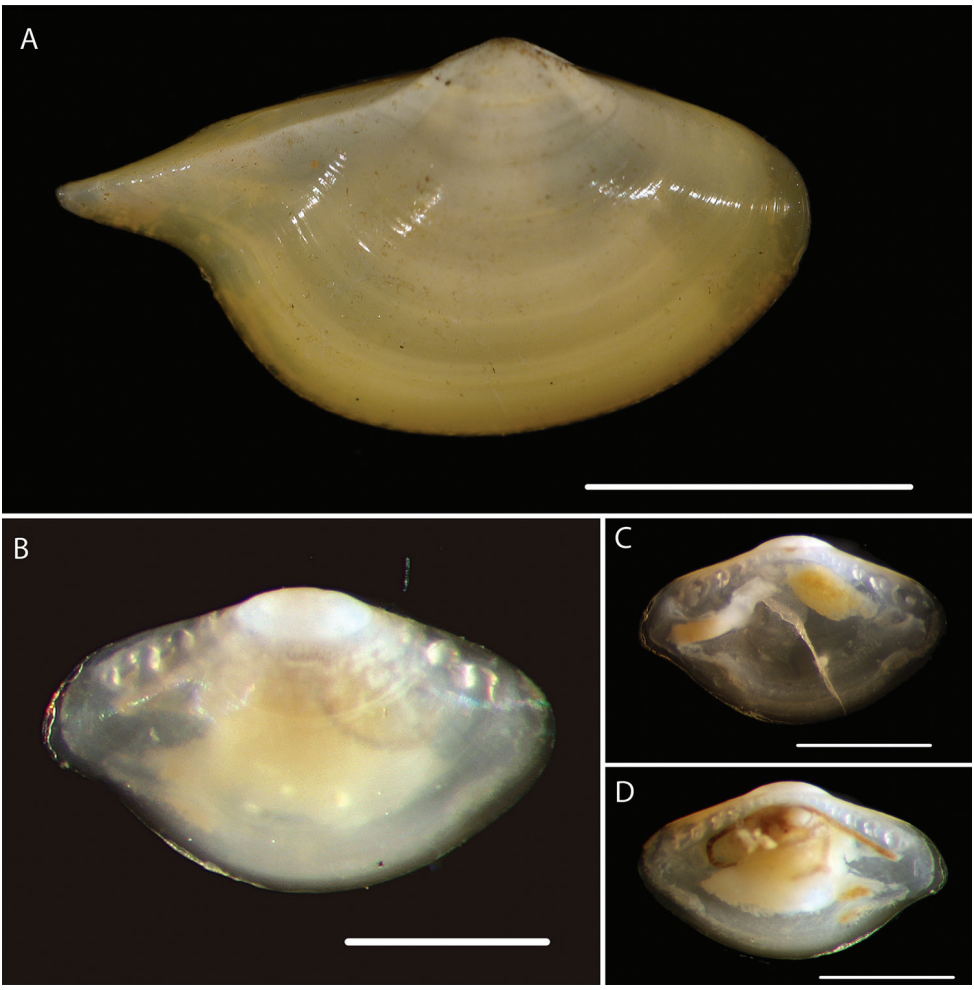

Figure 6. *Bathyspinula calcar* (Dall, 1908) **A** Specimen NHM_181, Image of live specimen after recovery, length 13.5 mm **B–D** Specimen NHM_149A confirmed juvenile *B. calcar* using DNA evidence, total length of animal ~2mm. Scale bars: 5 mm (**A**); 1 mm (**B–D**). Image attribution Glover, Taylor, Dahlgren & Wiklund, 2017.

Protobranchia
Nuculanoida
Bathyspinulidae Coan & Scott, 1997
***Bathyspinula* Allen & Sanders, 1982**

***Bathyspinula calcar* (Dall, 1908)**

Material examined. NHM_146 NHMUK 20170044, collected 2013-10-11, 13.75833 -116.69852, 4080 m. http://data.nhm.ac.uk/object/61f15e3c-f070-48a1-b484-780b37f7feb6

NHM_149A NHMUK 20170045, collected 2013-10-11, 13.75833 -116.69852, 4080 m. http://data.nhm.ac.uk/object/c44da298-9b61-4d6d-a1cd-2d6c3bd70859

NHM_181 NHMUK 20170043, collected 2013-10-13, 13.93482 -116.55018, 4082 m. http://data.nhm.ac.uk/object/3ab74908-1a5d-465f-890c-49373a44906c

NHM_284 NHMUK 20170046, collected 2013-10-17, 13.75583 -116.48667, 4076 m. http://data.nhm.ac.uk/object/ad2cb87b-1fce-415d-ab45-1619bbc4352b

Description. Shell sub-ovate, laterally compressed, with long, sharply pointed posterior rostrum. Periostracum shiny, medium brown. Posterior rostrum shorter, less defined in juveniles. Voucher specimen NHM_181 shell length 13.5 mm, width 7.6 mm (Fig. 6A).

Genetic data. GenBank NHM_146 18S-157475, COI-MF157505; NHM_149A COI-MF157506; NHM_181 18S-MF157479, COI-MF157507; NHM_284 COI-MF157514.

Remarks. Widely distributed in the eastern Pacific at depths of 400-5000 m (see Coan and Valentich-Scott 2012). The holotype (USNM 110573) was collected 725 km west of Trujillo, Peru at 2370 fathoms (4334 m). Forms a unique monophyletic clade distinct from all other AB01 specimens. Genetic match in 18S to *Bathyspinula calcar* (GenBank KC993875) from the north eastern Pacific (Sharma et al. 2013), but as the GenBank 18S sequence from *B. calcar* was only 289 bp long and as that specimen lacked COI, it was not included in the analyses. Some very small juvenile specimens (Fig. 6B–D) were recovered that superficially resemble *Ledella knudseni* sp. n. (Fig. 7) and may be easily confused. Genetic data confirmed these to be *Bathyspinula calcar* (Fig. 12). These may be distinguised from *Ledella* by the shiny and iridescent nature of the shell surface of *B. calcar*, which is preserved in the juveniles.

Ecology. Relatively large bivalve recovered from epibenthic sledge tow in polymetallic nodule province.

Nuculanidae H. Adams & A. Adams, 1858
***Ledella* Verrill & Bush, 1897**

***Ledella knudseni* Taylor & Wiklund, sp. n.**
http://zoobank.org/66E692B5-7C61-4ADC-9539-EFC085424147

Material examined. Paratype NHM_288A NHMUK 20170047.1-2, collected 2013-10-17, 13.75583 -116.48667, 4076 m. http://data.nhm.ac.uk/object/8aec47f4-dcec-4668-8398-9e4b0c28ecb8

Holotype NHM_288C NHMUK 20170048, collected 2013-10-17, 13.75583 -116.48667, 4076 m. http://data.nhm.ac.uk/object/f1886d78-22bf-403e-bdb2-784b91c0eb12

Description. Shell relatively thick, robust. Ovoid with short rostrum, umbones broad, prominent; postero ventral margin sinuous; broad, shallow sulcus extending from umbones to posteroventral margin. Sculpture of low, relatively broad, closely

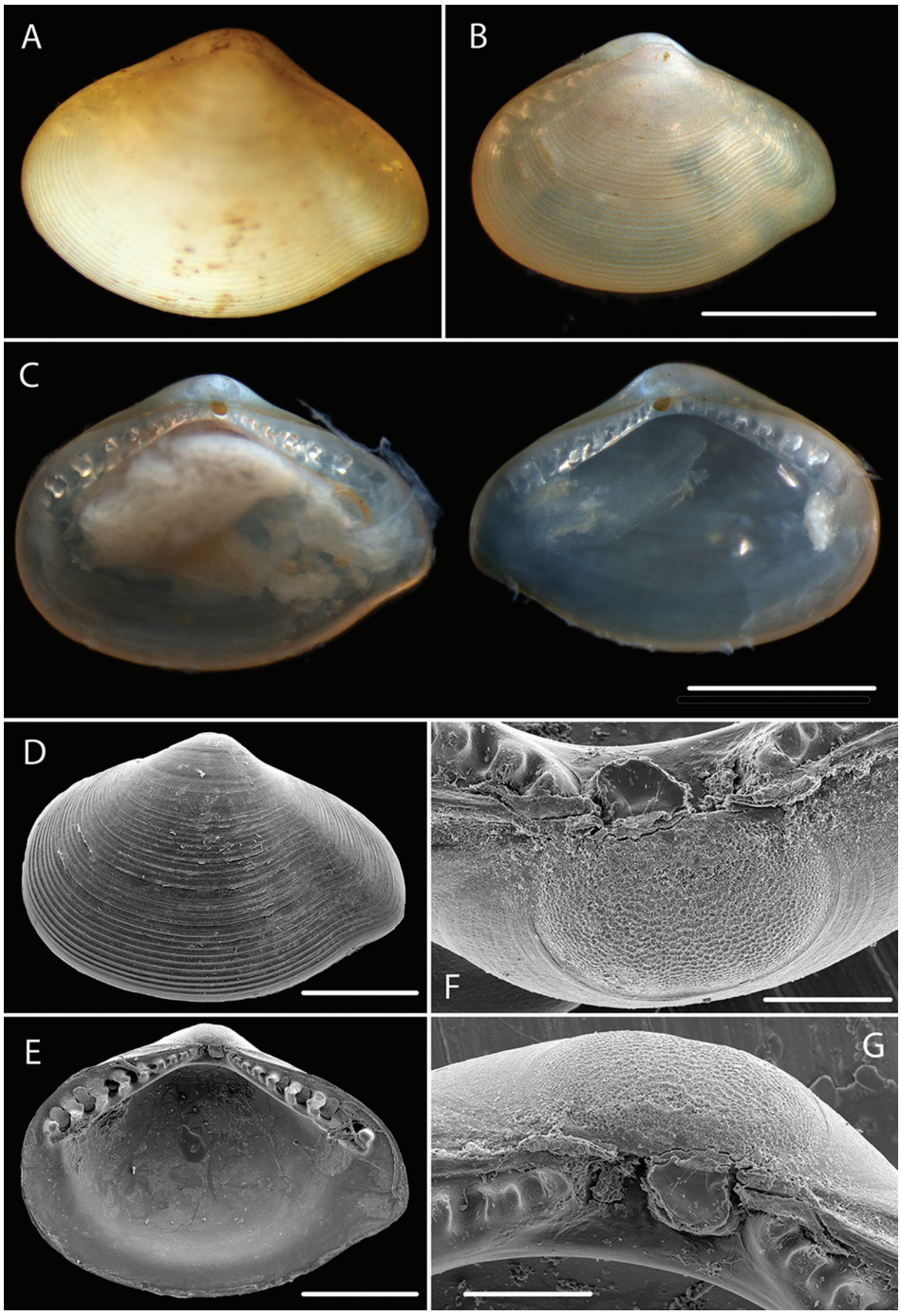

Figure 7. *Ledella knudseni* sp. n. **A** Holotype, specimen NHM_288c **B** Paratype, specimen NHM_288a **C** Specimen NHM 288a dissected prior to DNA sequencing and SEM **D–G** SEM of valve, hinge teeth and protoconch. Scale bars: 1 mm (**B–C**); 0.5 mm (**D–E**); 0.1 mm (**F–G**). Image attribution Glover, Taylor, Dahlgren & Wiklund, 2017.

spaced, commarginal lamellae; fine radial striations on rostrum and juvenile shell. Ligament internal, situated on broad resilium beneath umbones. Hinge robust, with 8-9 chevron shaped, blunt teeth to either side of ligament. Inner shell margin smooth. Prodissoconch large, ellipsoidal 0.3 mm long, with sharp rim, surface irregularly pitted. Holotype NHM_288C shell length 2.2 mm, width 1.5 mm; paratype NHM_288A shell length 2.1 mm, height 1.5 mm. (Figure 7).

Genetic data. GenBank NHM_288A COI-MF157515; NHM_288C 18S-MF157491, COI-MF157516.

Remarks. Similar in form to *Ledella ultima* (Smith, 1885) widespread in the abyssal Atlantic (Allen 2008), but has a less massive hinge with more teeth, 8-9 compared with 6-8 in *L. ultima*. Also similar is the species identified by Knudsen (1970) as *L. ultima* from the Sunda Trench in Indian Ocean at 3810 m. The only species recorded from the deep eastern Pacific is *Ledella dicella* (Dall, 1908) from 734-1200 m off Ecuador but this lacks the short rostrum and has 12-13 hinge teeth on each side of the ligament (Coan and Valentich-Scott 2012 pl. 26). No genetic matches on GenBank. *Ledella knudseni* groups in a small subclade with but is distinct from the Atlantic species *L. ultima* and *Ledella jamesi* Allen & Hannah, 1989, as well as another *Ledella* species from this study in the Pacific, *Ledella* sp. (NHM_381) (Figure 12). The new species can be confused with juveniles of *B. calcar* (see above), but shell is less shiny and iridescent, and ribs are more pronounced. DNA may be required to confirm identification.

Etymology. Named for Jørgen Knudsen (1918-2009), deep-sea bivalve systematist and author of the Galathea Report on abyssal and hadal Bivalvia.

Ecology. Found in polymetallic nodule province.

Ledella sp. (NHM_381)

Material examined. NHM_144 NHMUK 20170050, collected 2013-10-11, 13.75833 -116.69852, 4080 m. http://data.nhm.ac.uk/object/08d5c39f-b1e4-43d7-a8ea-2fe9abc05752

NHM_381 NHMUK 20170049, collected 2013-10-19, 13.93307 -116.71628, 4182 m. http://data.nhm.ac.uk/object/8f077dac-baac-4fef-b6a1-7fd02d5f0070

Description. Ovoid with short rostrum, shell shiny sub-translucent. Sculpture of fine closely spaced commarginal lamellae. Specimen NHM_381 length 2 mm (Fig. 8).

Genetic data. GenBank NHM_144 16S-MF157458, COI-MF157504; NHM_381 18S-MF157494, COI-MF157521.

Remarks. This species is morphologically very similar to the new *Ledella knudseni*, its sister taxon in the molecular phylogenetic analyses (Fig. 12), and DNA might be required to properly identify the species. No genetic matches on GenBank.

Ecology. Found in polymetallic nodule province.

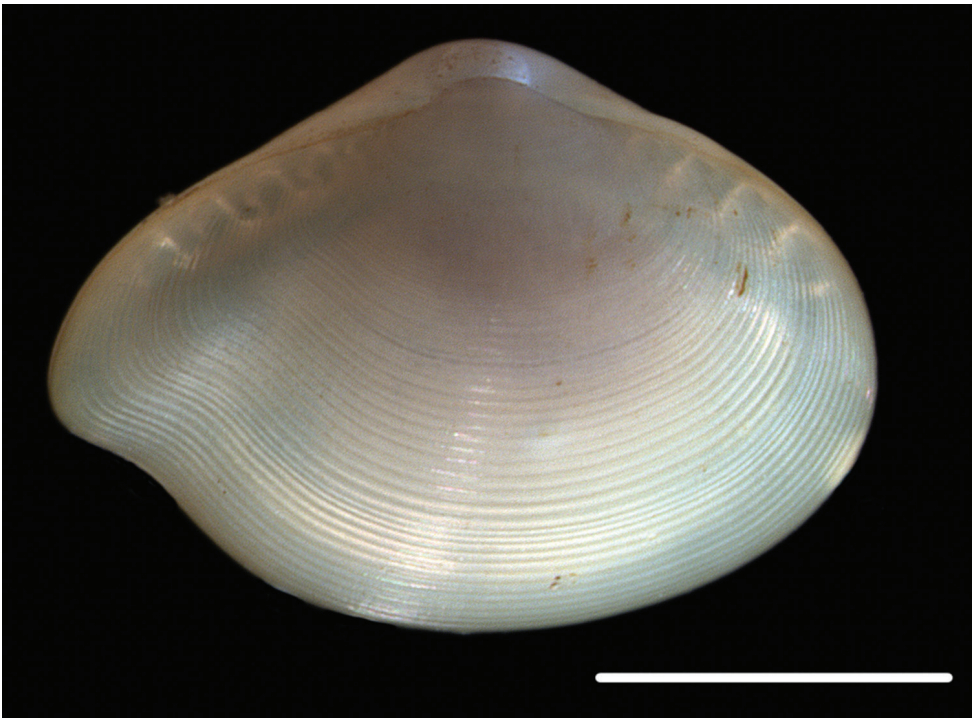

Figure 8. *Ledella* sp. (NHM_381). Scale bar: 1 mm. Image attribution Glover, Dahlgren & Wiklund, 2017.

Nuculida
Nuculidae Gray, 1824
***Nucula* Lamarck, 1799**

***Nucula profundorum* Smith, 1885**

Material examined. NHM_141 NHMUK 20170051, collected 2013-10-11, 13.75833 -116.69852, 4080 m. http://data.nhm.ac.uk/object/f2133256-1cad-4255-a5cb-bd5331417127

NHM_274A NHMUK 20170052, collected 2013-10-17, 13.75583 -116.48667, 4076 m. http://data.nhm.ac.uk/object/f96a470e-237e-46b4-ba85-4c6196106071

NHM_378 NHMUK 20170053.1-2, collected 2013-10-19, 13.93307 -116.71628, 4182 m. http://data.nhm.ac.uk/object/65f8d1ed-dd6a-4265-90d2-daf-07491cd76

Description. Small, trigonal- subovate. Periostracum light brown, shiny. Sculpture of fine radial lirae. Resilifer small. Hinge teeth: 5 anterior, 4 posterior. Inner shell margin finely denticulate. Voucher NHM_274A width 2 mm, height 1.8 mm (Fig. 9).

Genetic data. GenBank NHM_141 16S-MF157457, 18S-MF157473, COI-MF157503; NHM_274A COI-MF157512; NHM_378 16S-MF157464, COI-MF157520.

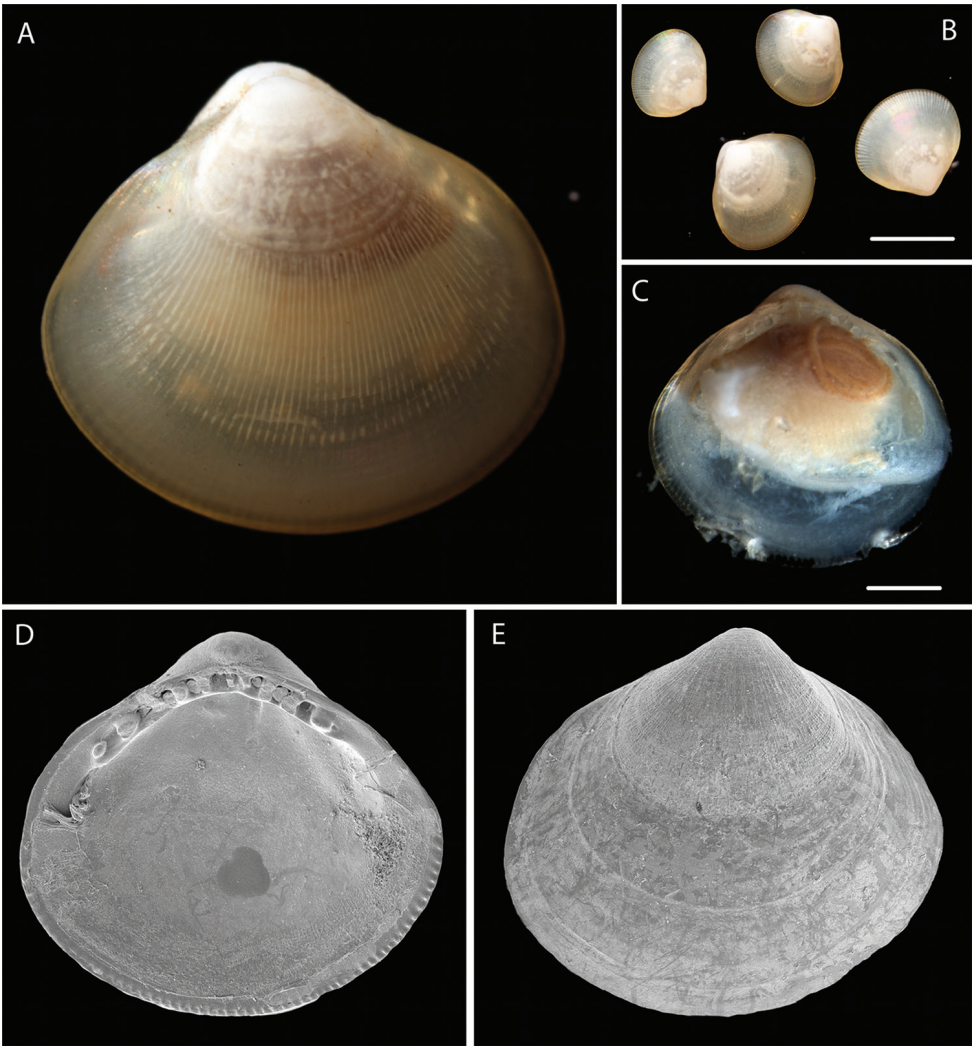

Figure 9. *Nucula profundorum* Smith, 1885 **A** Live specimen NHM_141 (for which 18S, CO1 and 16S sequences were obtained) **B** Live specimens NHM_274 (4 specimens from same sample) **C** Open shell from single individual NHM_274A with tissue sample taken for DNA sequencing **D–E** SEM of NHM_378 valve showing hinge teeth. Scale bars: 1.5 mm (**B**); 0.5 mm (**C**). Image attribution Glover, Taylor, Dahlgren & Wiklund, 2017.

Remarks. Morphologically matches *Nucula profundorum* Smith, 1885 based on examination of the syntype specimens [NHMUK 1887.2.9.2919]. In the molecular analysis of nuculoid protobranchs (Fig. 12) *Nucula profundorum* and the Atlantic *Nucula atacellana* Schenck, 1939 are well supported sister species. However the *N. profundorum* identified from the present samples differs genetically from the *N. profundorum* record in GenBank (accession nr KJ950274; Jennings and Etter 2014) which we believe may be misassigned. That sample came from 1045 m in the north eastern

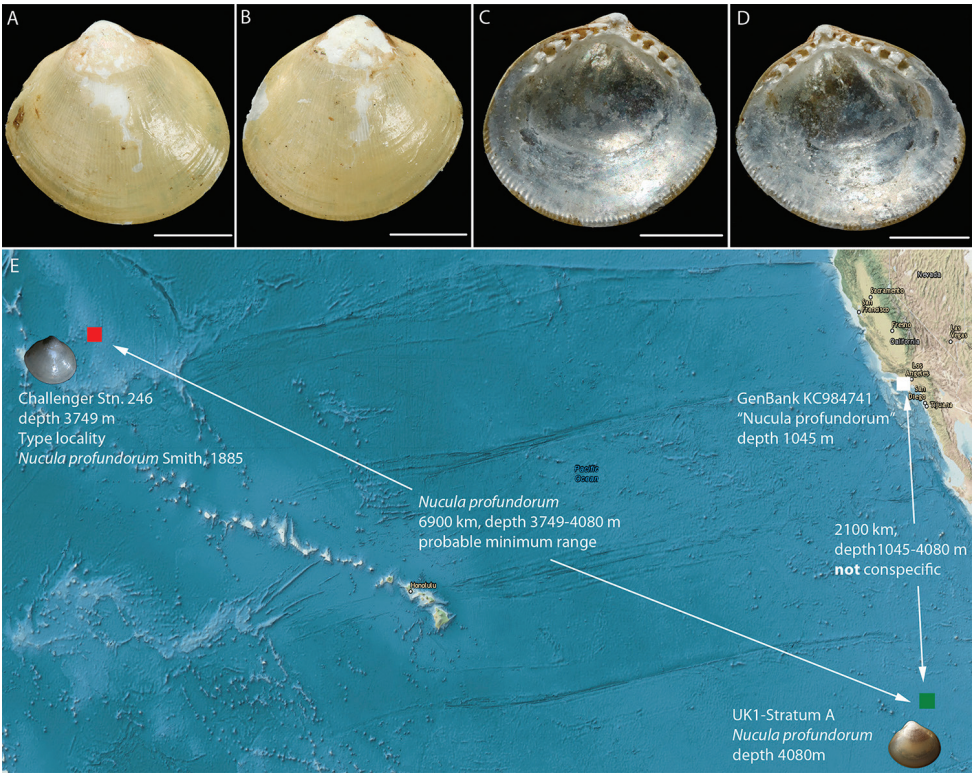

Figure 10. *Nucula profundorum* Smith, 1885. **A–D** Syntype BMNH 1887.2.9.2919, scalebars 1mm **E** Type locality (red) of *N. profundorum* from Challenger Expedition in relation to ABYSSLINE sampling location (green) and GenBank voucher specimen sampling location (white). Bathymetric data (**D**) from NOAA.

Pacific off San Diego (Figure 10). The shell illustrated by Coan and Valentich-Scott (2012 pl 12) as *N. profundorum* has more hinge teeth. There may be a complex of morphologically similar species in the eastern Pacific. No genetic matches on GenBank.

Ecology. The most abundant bivalve mollusc recorded in the ABYSSLINE sampling programme, frequently found in epibenthic sledge and box core samples from region of sediment and polymetallic nodules.

Yoldiidae
Yoldiella A.E Verrill & Bush, 1897

Yoldiella sp. (NHM_190)

Material examined. NHM_042 NHMUK 20170054, collected 2013-10-09, 13.8372 -116.55843, 4336 m. http://data.nhm.ac.uk/object/621deeed-8f8a-4d2e-9136-4e30794fc68e

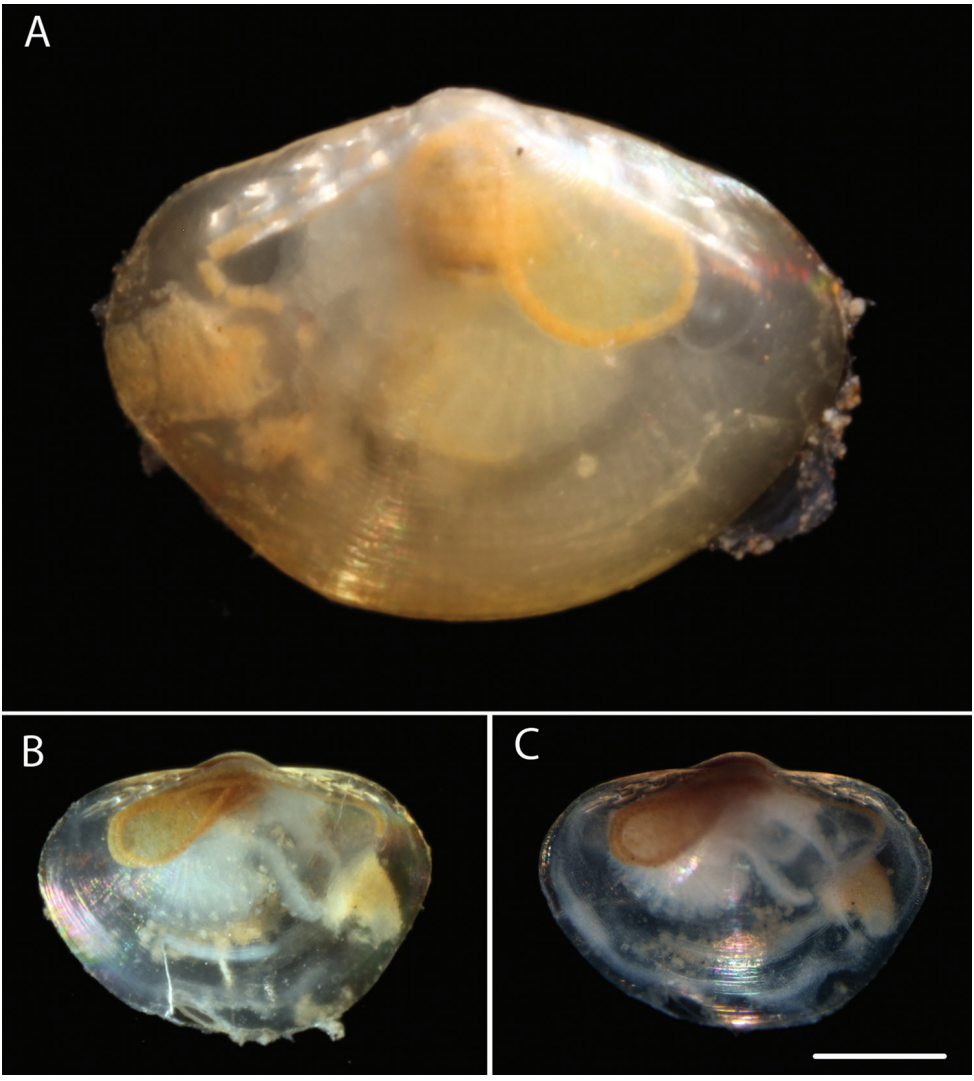

Figure 11. *Yoldiella* sp. (NHM_190) **A** Voucher specimen NHM_190 **B** Live specimens NHM_185 **C** NHM_185 after preservation in ethanol for 3 months prior to DNA sequencing. Scale bar: 0.5 mm (**C**). Image attribution Glover, Dahlgren & Wiklund, 2017.

NHM_185 NHMUK 20170055, collected 2013-10-13, 13.93482 -116.55018, 4082 m. http://data.nhm.ac.uk/object/6dfa8946-aa7a-448d-9f4f-703a3b2a10d9

NHM_190 NHMUK 20170056, collected 2013-10-13, 13.93482 -116.55018, 4082 m. http://data.nhm.ac.uk/object/b6e48ff4-2e02-42dc-b9ed-286d297d1459

NHM_193 NHMUK 20170060, collected 2013-10-13, 13.93482 -116.55018, 4082 m. http://data.nhm.ac.uk/object/8923576e-4542-4fc7-9a89-016e8fb564cb

NHM_194 NHMUK 20170057, collected 2013-10-13, 13.93482 -116.55018, 4082 m. http://data.nhm.ac.uk/object/7a6c76df-989b-4fcd-9e9c-a442d0a02443

NHM_246 NHMUK 20170058, collected 2013-10-16, 13.81166 -116.71, 4076 m. http://data.nhm.ac.uk/object/37b2493a-a725-4ec4-a720-cc9dd12fb49d

NHM_289 NHMUK 20170059, collected 2013-10-17, 13.75583 -116.48667, 4076 m. http://data.nhm.ac.uk/object/17d54bb4-9f38-4073-9bb6-17637773b058

Description. Small, sub-ovate, longer than high, umbone at mid-line, dorsal margin horizontal to slightly curved, ventral margin deeply rounded, thin-shelled, shiny, semi-transparent, smooth except for growth increments. Internal features not investigated but 4-5 anterior and posterior chevron teeth. Hindgut visible though the shell forms a simple rounded loop on right side of body. DNA voucher NHM_190 shell length 1.6 mm, height 1 mm. Voucher specimen NHM_185 shell length 1.5 mm, height 1 mm (Fig. 11).

Genetic data. GenBank NHM_042 18S-MF157467; NHM_185 18S-MF157480; NHM_190 18S-MF157482; NHM_193 18S-MF157484; NHM_194 18S-MF157485; NHM_246 18S-MF157486; NHM_289 18S-MF157492, COI-MF157517.

Remarks. Extremely small, semi-transparent bivalves typically about 1 mm in size. *Yoldiella* species are particularly difficult to identify (see Killeen and Turner 2009). Forms a unique monophyletic clade distinct from all other AB01 specimens. No genetic matches on GenBank. In the molecular tree (Fig. 12) the genus *Yoldiella* is not monophyletic, and the present species does not group with another Eastern Pacific bathyal species, *Yoldiella orcia* (Dall, 1916), which instead forms a well-supported subclade with two Atlantic species.

Ecology. Found in polymetallic nodule province.

Pteriomorphia
Arcoida
Arcidae Lamarck, 1809
***Bentharca* Verrill & Bush, 1898**

***Bentharca* cf. *asperula* (Dall, 1881)**

Material examined. NHM_108 NHMUK 20170061, collected 2013-10-11, 13.79335 -116.70308, 4081 m. http://data.nhm.ac.uk/object/9d29d7ec-55cd-4b41-929a-2379be221263

NHM_150 NHMUK 20170062.1-2, collected 2013-10-11, 13.75833 -116.69852, 4080 m. http://data.nhm.ac.uk/object/96bfe548-f511-49c4-b2a3-0a9a45f9154b

NHM_170 NHMUK 20170063, collected 2013-10-11, 13.7936 -116.70308, 4078 m. http://data.nhm.ac.uk/object/8d9beefd-2fbc-4204-9bf8-90551419ac1c

NHM_282 NHMUK 20170064, collected 2013-10-17, 13.75583 -116.48667, 4076 m. http://data.nhm.ac.uk/object/ccdd114d-c8a8-47da-ba84-8b8ca5125a6a

NHM_427 NHMUK 20170065, collected 2013-10-20, 13.86367 -116.54432, 4050 m. http://data.nhm.ac.uk/object/1d462c2a-bb98-4369-afc3-63a7c33a4bdd

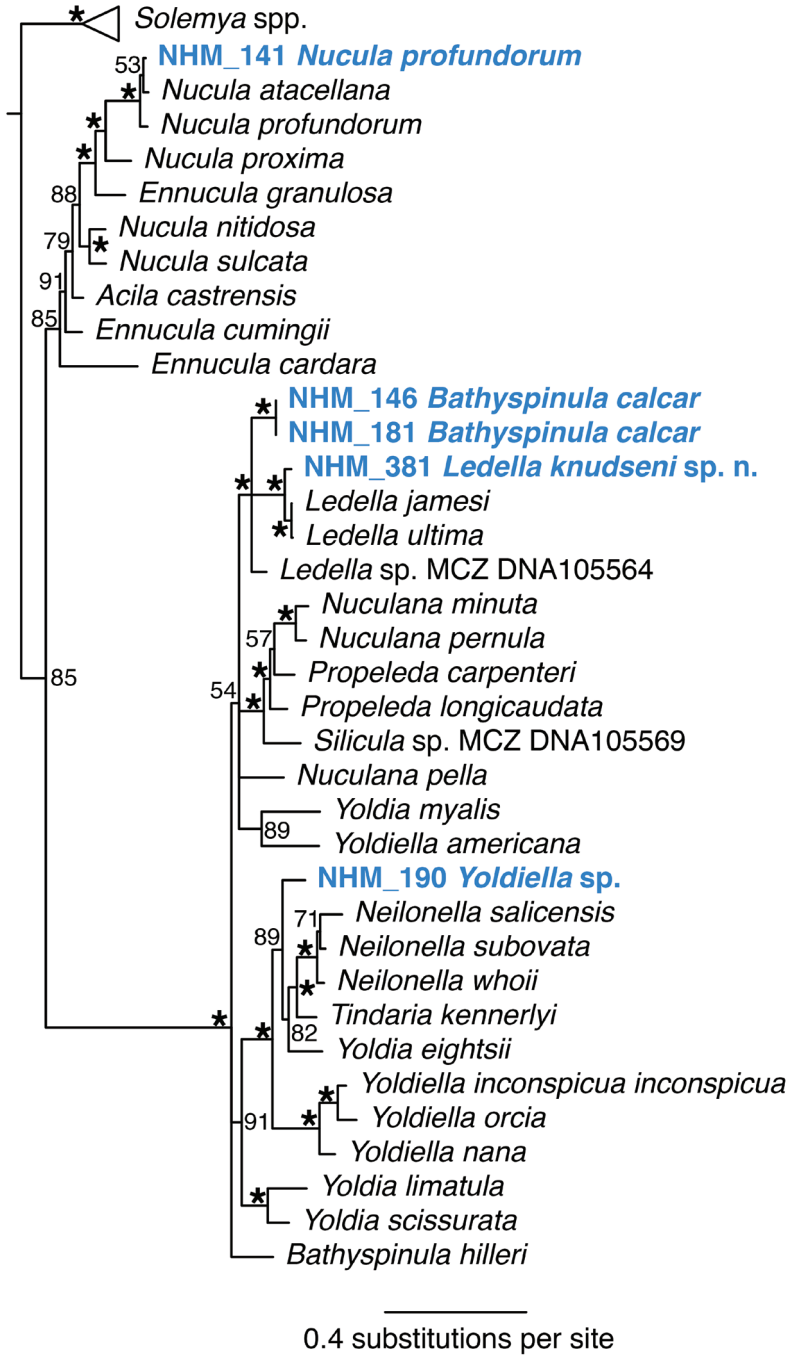

Figure 12. Phylogenetic analysis of Bivalvia: Protobranchia. 50% majority rule consensus tree from the Bayesian analyses using 18S and COI. Asterisks denotes support values of 95 or above.

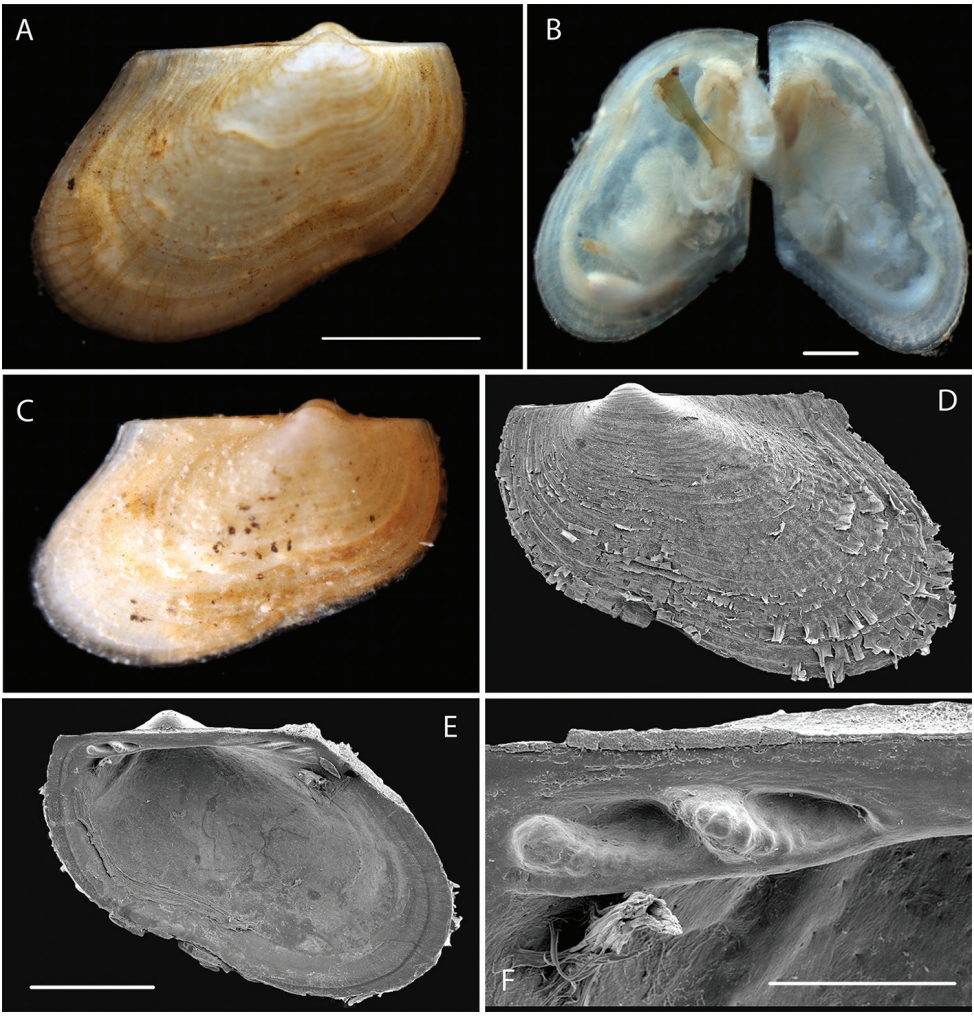

Figure 13. *Bentharca* cf. *asperula* (Dall, 1881) **A** Voucher specimen NHM_150 live after recovery **B** Specimen NHM_150 after preservation and dissection for DNA sample showing valves **C** Specimen NHM_108 Live **D–F** Specimen NHM_150 SEM showing shell ornamentation and hinge teeth. Scale bars: 1 mm (**A, E**); 0.5 mm (**B**); 0.2 mm (**F**). Image attribution Glover, Taylor, Dahlgren & Wiklund, 2017.

NHM_454 NHMUK 20170066, collected 2013-10-21, 13.90165 -116.59, 4163 m. http://data.nhm.ac.uk/object/a30eab51-5f52-4fec-89d7-d47152895c92

Description. Shell elongate, trapezoidal, strongly inequilateral, anteriorly attentuated and posteriorly expanded, umbones small, low, dorsal edge straight. Byssal sinus in ventral margin. Sculpture of irregular commarginal lamellae and low radial ribs but covered by a thick, shaggy, brown periostracum with projecting scales. Two pre- and post- umbonal hinge teeth with each tooth crossed by transverse grooves giving a lobate appearance (Fig. 13E, F). Inner shell margin smooth. DNA voucher NHM_150 shell length 3.2 mm shell width 1.9 mm.

Genetic data. GenBank NHM_108 18S-MF157470, COI-MF157502; NHM_150 18S-MF157476; NHM_170 18S-MF157477; NHM_282 18S-MF157490, COI-MF157513; NHM_427 18S-MF157496; NHM_454 18S-MF157499.

Remarks. *Bentharca asperula* has been regarded as a cosmopolitan deep-water species with a considerable recorded depth range of 430–5005 m (Knudsen 1967, 1970, Coan and Valentich-Scott 2012) from Atlantic, Indian and Pacific Oceans. The lectotype and paralectotypes (USNM 63174, 887339, 94363) originated from the Gulf of Mexico, off Yucatan, 2868 m (Blake stn 33). Because of its epifaunal, byssate life habit *B. asperula* shows considerable shape variation and Knudsen (1967) synonymised several nominal species and described how the number of hinge teeth increases with shell size (age). Without supporting genetic evidence from samples from different oceans it is impossible to test whether the species is truly cosmopolitan. Perhaps significantly, no shell has been described with as few hinge teeth as the present sample and none with the transverse grooves (Fig. 13F). No genetic matches on GenBank.

Ecology. Quite abundant. Found in polymetallic nodule province.

Mytiloida
Mytilidae Rafinesque, 1815
***Dacrydium* Torell, 1859**

***Dacrydium panamensis* Knudsen, 1970**

Material examined. NHM_117 NHMUK 20170067, collected 2013-10-11, 13.79335 -116.70308, 4081 m. http://data.nhm.ac.uk/object/180e485f-f1c2-41e1-b858-f02ba537804b

Description. Shell small, subovate, translucent, anterior-ventral margin slightly produced, highest point near mid-line. Voucher NHM_117 Shell length 1.7 mm, shell height 2.5 mm (Fig. 14).

Genetic data. GenBank NHM_117 18S-MF157471.

Remarks. Identified from figures in Knudsen (1970) and Coan & Valentich-Scott (2012). The holotype of *D. panamensis* was collected on the Galathea expedition (stn 726) at 3670-3270 m depth in Gulf of Panama. In the molecular analysis (Fig. 17) it aligns as a sister species to many shallow water Mytilidae. No genetic matches on GenBank.

Ecology. Found in polymetallic nodule province.

Limopsidae Dall, 1895
***Limopsis* Sassi, 1827**

***Limopsis* sp. (NHM_453)**

Material examined. NHM_453 NHMUK 20170069.1-2, collected 2013-10-21, 13.90165 -116.59, 4163 m. http://data.nhm.ac.uk/object/ce9cbed0-82cc-420d-baad-fdfff7cc0986

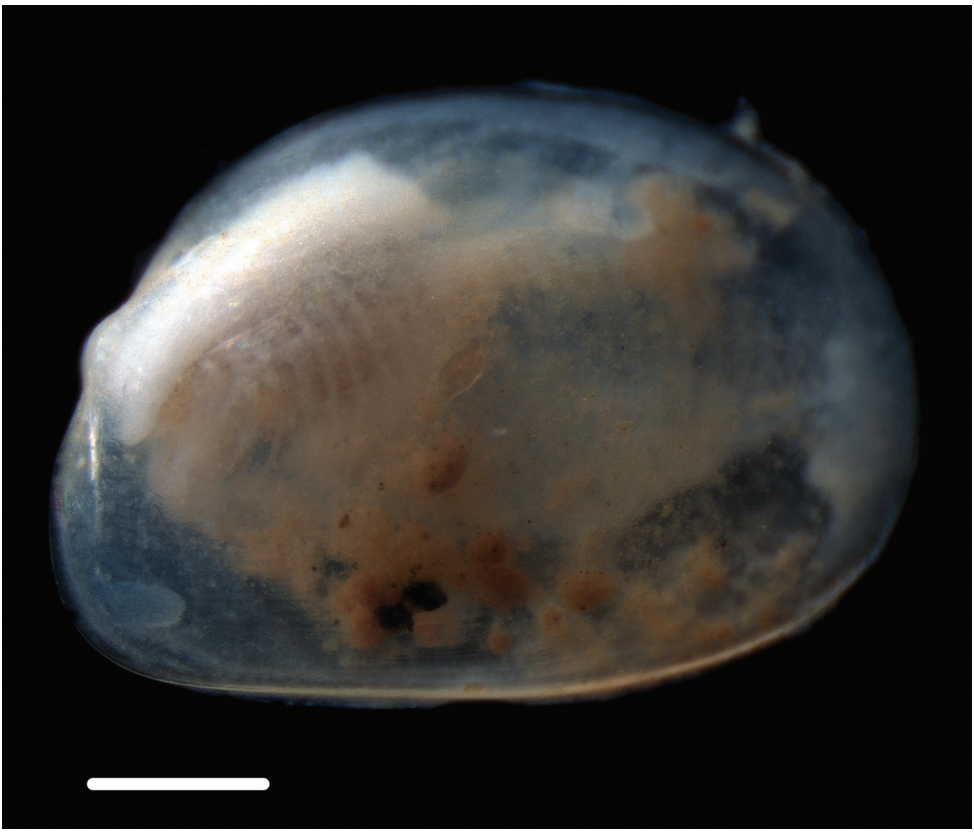

Figure 14. *Dacrydium panamensis* Knudsen, 1970 Specimen NHM_117. Scale bar: 0.5 mm. Image attribution Glover, Dahlgren & Wiklund, 2017.

Description. Subcircular to slightly oblique with slightly sinuous posterior margin. Periostracum with short, fine, bristles aligned in radial rows. Ligament small, triangular, set in shallow resilifer. Hinge teeth robust, 4 anterior and 5 posterior. Inner shell margin smooth. Voucher NHM_453 shell length 4.6 mm, height 4.3mm (Fig. 15).

Genetic data. GenBank NHM_453 18S-MF157498, COI-MF157524.

Remarks. Dissimilar in shape and periostracal bristle configuration to any recorded Eastern Pacific deep-water species (Coan & Valentich-Scott 2012). However, shape and number of hinge teeth are known to change with age/size in *Limopsis* species. In molecular analysis (Fig. 17) forms part of a well supported monophyletic clade with other *Limopsis* species and aligns closest to *Limopsis marionensis* Smith, 1885 from depths of 40–1000 m in the Southern Ocean. No genetic matches on GenBank.

Ecology. Found in polymetallic nodule province.

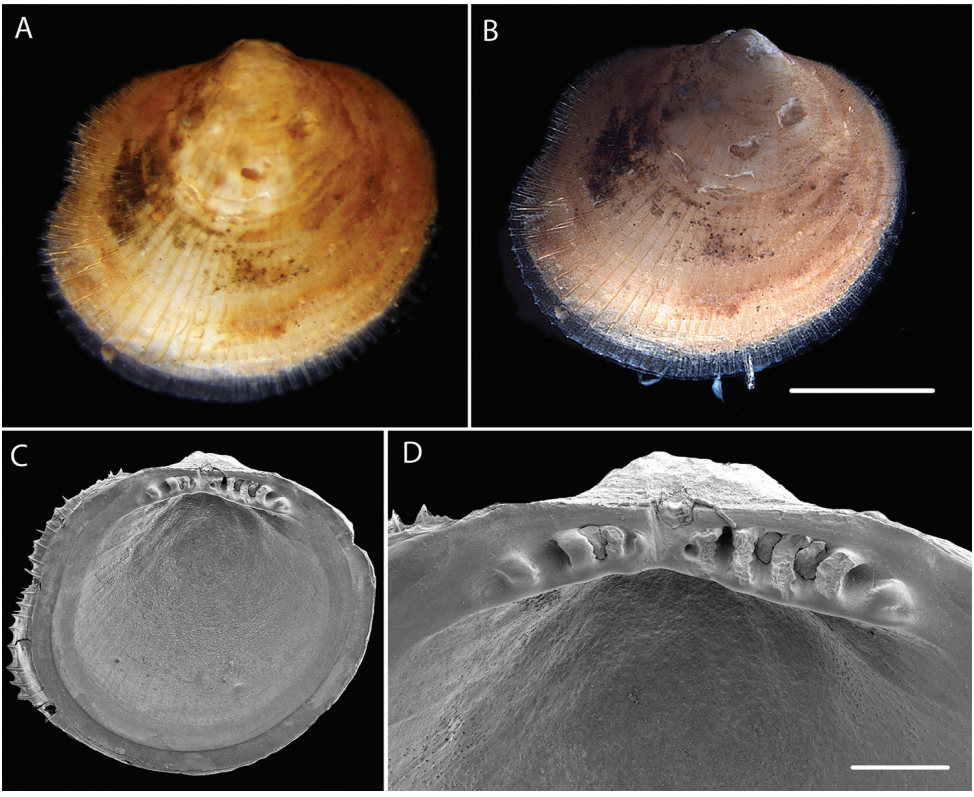

Figure 15. *Limopsis* sp. (NHM_453) **A** Specimen NHM_453 live after recovery **B** Specimen NHM_453 after preservation **C–D** SEM of interior of right valve showing hinge teeth. Scale bars: 2mm **B**, 0.5mm **D**. Image attribution Glover, Taylor, Dahlgren & Wiklund, 2017.

Pectinoida
Propeamussiidae Abbott, 1954
***Catillopecten* Iredale, 1939**

***Catillopecten* sp. (NHM_105)**

Material examined. NHM_105 NHMUK 20170070, collected 2013-10-11, 13.79335 -116.70308, 4081 m. http://data.nhm.ac.uk/object/24f5c5bb-e419-48ef-baaa-4a6493f691d9

Description. Small, thin-shelled, subcircular. Right valve flat, left valve slightly convex. Both valves with commarginal undulations that become stronger towards the margin, fine radial striations on both valves. Well defined anterior auricle and byssal notch. Voucher NHM_105 1.8 mm shell length, height 1.5 mm (Fig. 16).

Genetic data. GenBank NHM_105 18S-MF157469.

Remarks. Holotype (ZMUC) from Gulf of Panama, 3270–3670 m Galathea stn 726, figured by Coan and Valentich-Scott (2012 pl. 100). In the molecular tree it

Figure 16. *Catillopecten* sp. (NHM_105) live after recovery. Scale bar: 1 mm. Image attribution Glover, Dahlgren & Wiklund, 2017.

groups with two other species of Propeamussidae on a long branch and distinct from other Pectinoida, but a GenBank species (VLG_2013) identified as *Propeamussium* sp. is distinct from these (Fig. 17). Henk H. Dijkstra (Naturalis Biodiversity Center in Leiden, Netherlands) advised on identification of this species. Forms a unique monophyletic clade distinct from all other AB01 specimens. No genetic matches on GenBank.

Ecology. Found in polymetallic nodule province.

Caudofoveata
Prochaetodermatidae Salvini-Plawen, 1975

Prochaetodermatidae sp. (NHM_344)

Material examined. NHM_344 NHMUK 20170071.1-2, collected 2013-10-17, 13.75583 -116.48667, 4076 m. http://data.nhm.ac.uk/object/e68608f9-4b83-4eb9-89f2-0de4f89c21b0

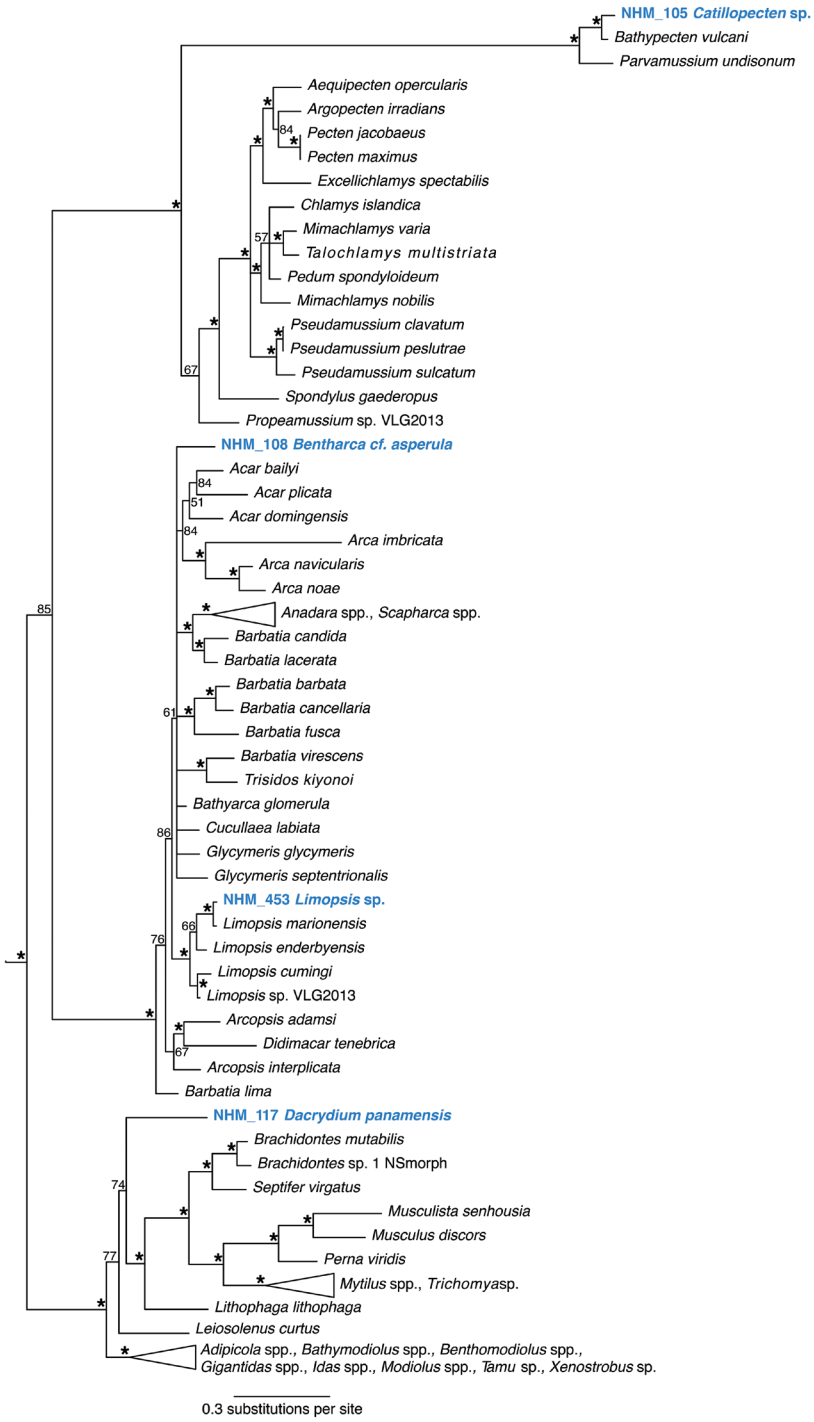

Figure 17. Phylogenetic analysis of Bivalvia: Pteriomorpha. 50% majority rule consensus tree from the Bayesian analyses using 18S and COI. Asterisks denotes support values of 95 or above.

Figure 18. Prochaetodermatidae sp. (NHM_344), abyssal aplacophoran mollusc, imaged after preservation. Scale bar: 0.5 mm. Image attribution Glover, Dahlgren & Wiklund, 2017.

Description. Voucher NHM_344 (Fig. 18) partially broken aplacophoran mollusc, maximum width 0.8 mm, length of fragment ~2.5 mm. Posterior body end lacking. Anterior body intact, with indistinct neck region. Trunk partly damaged. Trunk sclerites are scales with a slender tip confluent with the broad blade without a distinct shoulder region. Tip with keel, triangular in cross section. Blade without sculpture. Data and material, including a permanent preparation of sclerites (1 slide), made available for future study.

Genetic data. GenBank NHM_344 16S-MF157462.

Remarks. The specimen has the typical body shape and sclerite type of Prochaetodermatidae.

Ecology. Found in polymetallic nodule province. Burrows in soft sediment.

Monoplacophora
Neopilinidae Knight & Yochelson, 1958
***Veleropilina* Starobogatov & Moskalev, 1987**

***Veleropilina oligotropha* (Rokop, 1972)**

Material examined. NHM_405 NHMUK 20170072, collected 2013-10-20, 13.86328 -116.54885, 4050 m. http://data.nhm.ac.uk/object/bf968b01-1991-43b7-87e4-25da4d5a9dc5

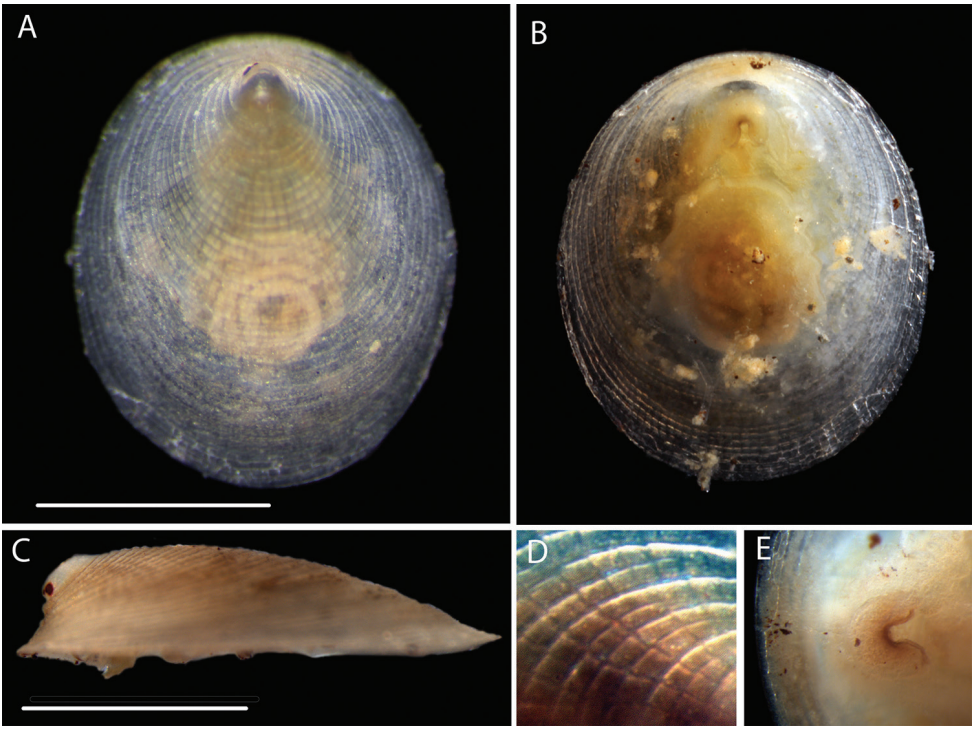

Figure 19. *Veleropilina oligotropha* (Rokop, 1972) Specimen NHM_405. **A** Dorsal view of living specimen **B** Ventral view of living specimen. **C** Lateral view of ethanol-preserved specimen **D** Dorsal shell sculpture detail, just below apex **E** Ventral view of mouth and shell margin. Scale bars: 1mm. Image attribution Glover, Dahlgren & Wiklund, 2017.

Description. Shell transparent, sculpture is reticulate, reticulation not covering the smooth apical area. Voucher specimen NHM_405, specimen length 2.2 mm, specimen width 1 mm (Fig. 19).

Genetic data. GenBank NHM_405 16S-MF157465, 18S-MF157495, COI-MF157522.

Remarks. Morphologically agrees with description of *Veleropilina oligotropha* (Rokop, 1972) described from ~6000 m water depth in the central North Pacific.

Forms a unique monophyletic clade distinct from all other AB01 specimens. No genetic matches on GenBank. In the molecular analyses based on the 16S gene, the Monoplacophora clade is strongly supported, but internal branches are unresolved or, when clades are present, they have low support (Fig. 20).

Ecology. Specimen collected from an epibenthic sledge tow across region of sediment and polymetallic nodules. Rokop (1972) did not observe the species directly on nodules, they were just recovered from the epibenthic sledge sample, as was the case in this study. The importance of the nodules as a habitat for the species remains uncertain until they are directly observed live on the seafloor.

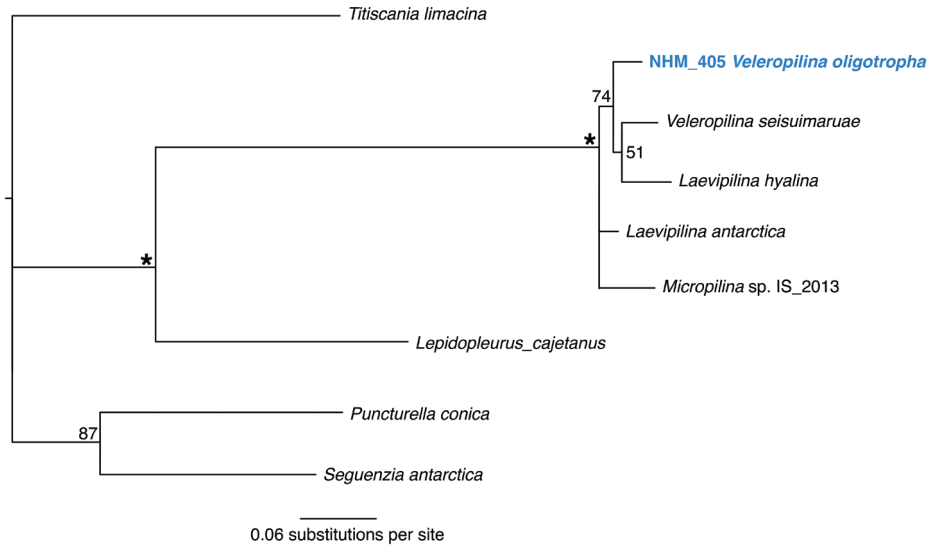

Figure 20. Phylogenetic analysis of Monoplacophora. 50% majority rule consensus tree from the Bayesian analyses using 16S. Asterisks denotes support values of 95 or above.

Polyplacophora
Leptochitonidae Dall, 1899
Leptochiton Gray, 1847

Leptochiton macleani Sirenko, 2015

Material examined. NHM_446 NHMUK 20170073.1-2, collected 2013-10-20, 13.86367 -116.54432, 4050 m. http://data.nhm.ac.uk/object/d69b581d-8a79-4c4d-8f70-88b2ec07d86e

Description. The form and pattern of tegmental granules together with the three aesthete pores are most similar to the images of *Leptochiton macleani* (Sirenko, 2015: figs 34–36). Voucher NHM_446 length approx 10 mm, width 3.2 mm (Fig. 21).

Genetic data. GenBank NHM_446 16S-MF157466, 18S-MF157497, COI-MF157523.

Remarks. Sirenko (2015) has recently reviewed *Leptochiton* of the southeastern Pacific Ocean and described several new species that had been previously confounded with *Leptochiton belknapi* Dall, 1878. The specimen morphologically matches *Leptochiton macleani,* type locality Peru-Chile Trench, East Pacific, 4600 m depth. Forms a unique monophyletic clade distinct from other AB01 specimens. No genetic matches on GenBank. In the molecular analyses based on the 18S and COI genes, it falls with strong support as sister taxon to two other *Leptochiton* species, but in the phylogenetic tree the genus *Leptochiton* is not monophyletic (Fig. 22).

Ecology. Specimen collected from an ROV scoop in region of sediment and polymetallic nodules, presumed living associated or on the nodule surface, but not directly observed doing so.

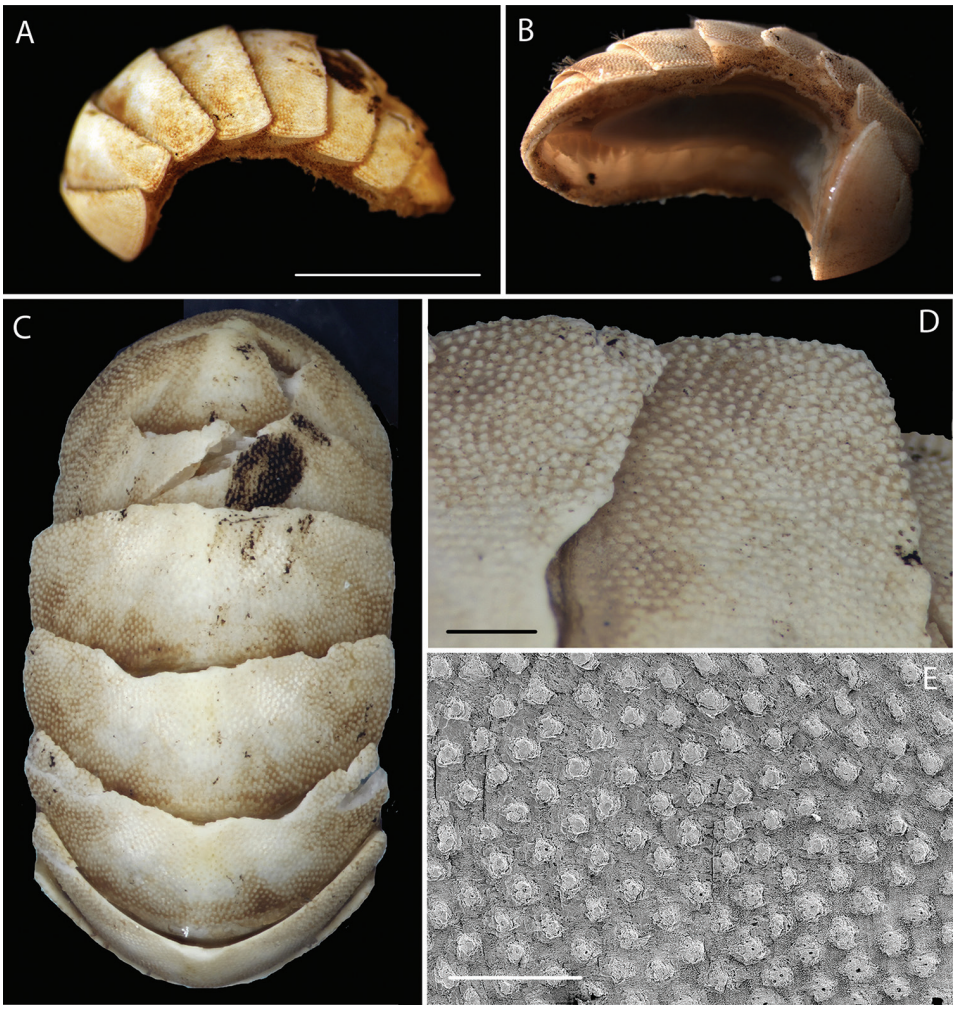

Figure 21. *Leptochiton macleani* Sirenko, 2015. NHM_446 voucher specimen. **A** Live specimen (lateral view) after recovery from the ROV scoop sample **B** Preserved specimen (ventro-lateral view) following DNA extraction **C** Dorsal view **D** surface detail **E** SEM of tegmentum surface and pores. Scale bars: 4 mm (**A**); 0.5 mm (**D**); 0.3 mm (**E**). Image attribution Glover, Taylor, Ikebe, Dahlgren & Wiklund, 2017.

Scaphopoda
Dentaliida Starobogatov, 1974
Dentaliidae Children, 1834
***Fissidentalium* Fischer, 1885**

***Fissidentalium* sp. (NHM_261)**

Material examined. NHM_261 NHMUK 20170074, collected 2013-10-17, 13.75583 -116.48667, 4076 m. http://data.nhm.ac.uk/object/679fa0ca-d647-446d-87c5-e8d33949efe2

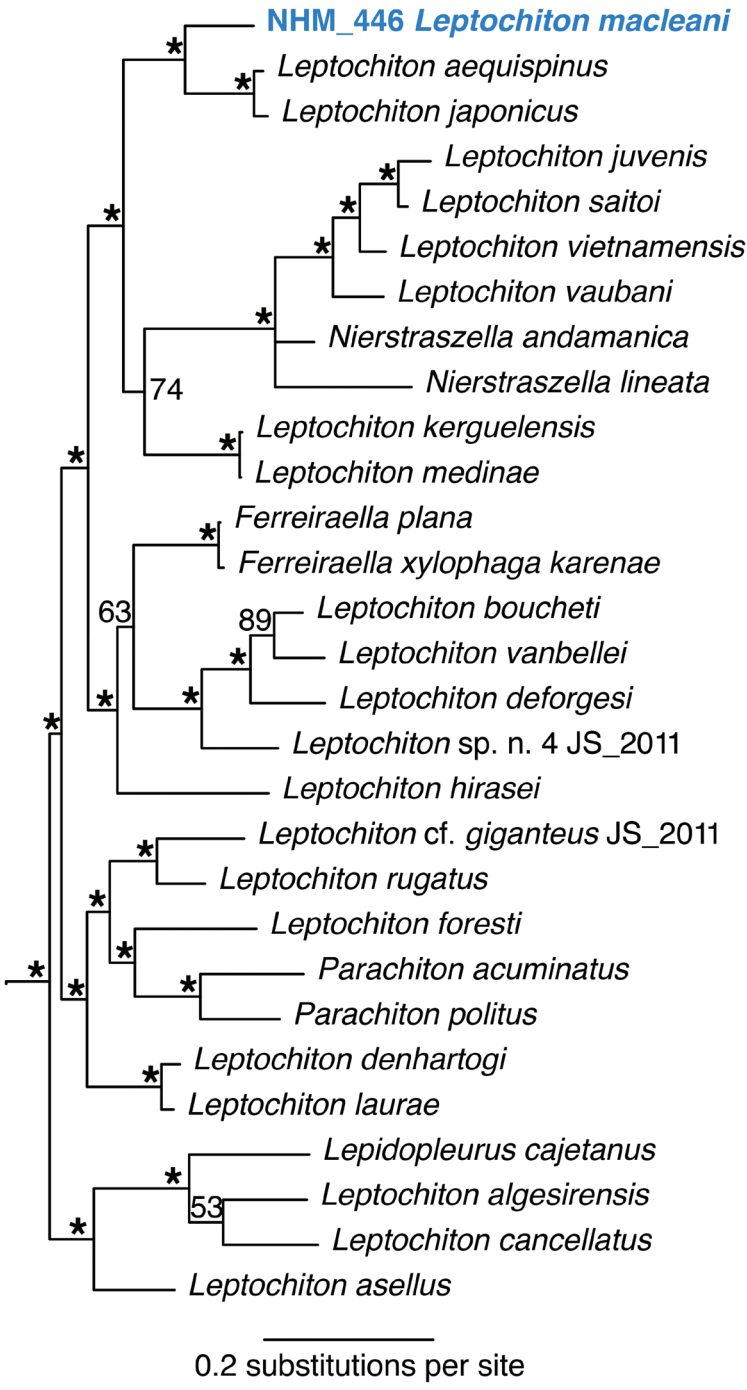

Figure 22. Phylogenetic analysis of Leptochitonidae, Polyplacophora. 50% majority rule consensus tree from the Bayesian analyses, combining 18S and COI. Asterisks denotes posterior probability values of 95 or above.

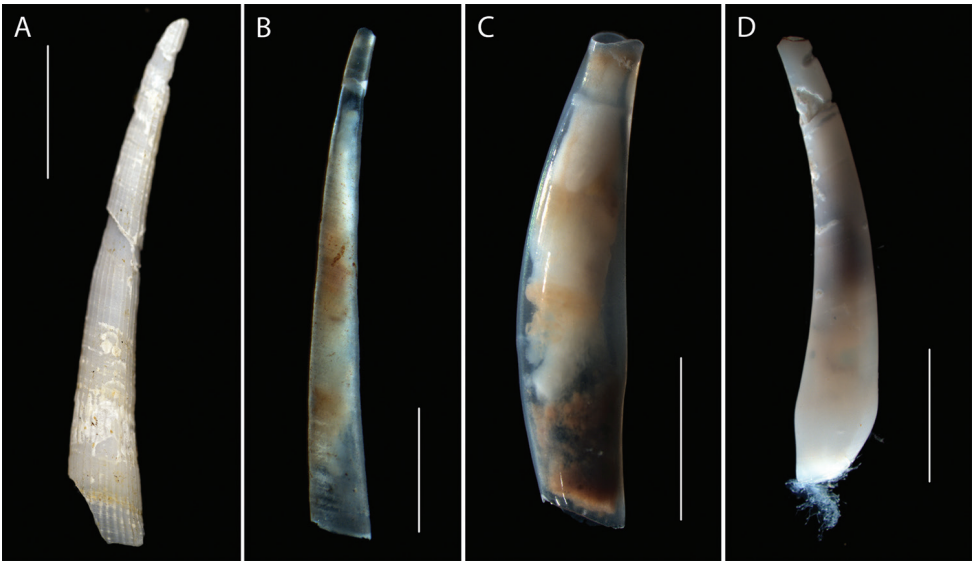

Figure 23. Scaphopoda spp. **A** *Fissidentalium* sp. (NHM_261) live specimen. **B** Gadilida sp. (NHM_192) live specimen **C** *Gadila* sp. (NHM_345) live specimen **D** Gadilida sp. (NHM_132) live specimen. Scale bars: 5 mm (**A, D**); 1 mm (**B**); 2 mm (**C**). Image attribution Glover, Dahlgren & Wiklund, 2017.

Description. A damaged shell with rib features and curvature similar to *Fissidentalium* species (see Scarabino, 1995). Voucher NHM_261, poor preservation, length 21 mm, maximum width 3.1 mm (Fig. 23A).

Genetic data. GenBank NHM_261 16S-MF157461, 18S-MF157489, COI-MF157511.

Remarks. Forms a unique monophyletic clade distinct from other AB01 specimens. In the molecular analysis it groups with other *Fissidentalium* species, but with very low support. No genetic matches on GenBank. Phylogenetic tree supports placement in order Dentaliida, family Dentaliidae (Fig. 24). Genetic data and imagery provided to facilitate future study.

Ecology. Specimen collected from an epibenthic sledge tow across region of sediment and polymetallic nodules.

Gadilida Starobogatov, 1974

Gadilida sp. (NHM_192)

Material examined. NHM_192 NHMUK 20170075, collected 2013-10-13, 13.93482 -116.55018, 4082 m. http://data.nhm.ac.uk/object/fc0e3ae8-9cce-46a0-bb8b-fafe0e2cb46b

Description. Slender, smooth, transparent, annular growth increments, maximum diameter at mouth. Voucher NHM_192, length 4 mm, maximum width 0.5 mm (Fig. 23B).

Genetic data. GenBank NHM_192 16S-MF157459, 18S-MF157483.

Remarks. Forms a unique monophyletic clade distinct from other AB01 specimens. No genetic matches on GenBank. Phylogenetic tree (Fig. 24) supports placement in order Gadilida with NHM_345. Genetic and image data made available for future study when better specimens available.

Ecology. Specimen collected from an epibenthic sledge tow across region of sediment and polymetallic nodules.

Gadilidae Stoliczka, 1868
***Gadila* Gray, 1847**

***Gadila* sp. (NHM_345)**

Material examined. NHM_345 NHMUK 20170076, collected 2013-10-17, 13.75583 -116.48667, 4076 m. http://data.nhm.ac.uk/object/c301a72f-54cb-435e-8aae-17cf4d37675f

Description. Short, glossy, transparent, maximum diameter near centre, ventral side curved, dorsal side near straight. Mouth simple, oblique. NHM_345 voucher specimen length 6 mm, width 1.4 mm (Fig. 23C).

Genetic data. GenBank NHM_345 16S-MF157463, 18S-MF157493, COI-MF157518.

Remarks. Forms a unique monophyletic clade distinct from other AB01 specimens. No genetic matches on GenBank. Phylogenetic tree supports placement in order Gadilida (Figure 24). Genetic and image data made available for future study when better specimens available.

Ecology. Specimen collected from an epibenthic sledge tow across region of sediment and polymetallic nodules.

Gadilida sp. (NHM_132)

Material examined. NHM_132 NHMUK 20170077, collected 2013-10-11, 13.75833 -116.69852, 4080 m. http://data.nhm.ac.uk/object/6a1906d9-9ed1-4f6e-a0cf-2d53e2289a01

Description. Shell slender, smooth, fairly transparent, increasing in diameter to a maximum about 2.5 mm from the anterior aperture, then decreasing towards the mouth. NHM_132 voucher specimen length 16.6 mm, max width 3 mm (Fig. 23D).

Genetic data. GenBank NHM_132 16S-MF157456, 18S-MF157472.

Remarks. Forms a unique monophyletic clade distinct from other AB01 specimens. No genetic matches on GenBank. Phylogenetic tree (Fig. 24) supports place-

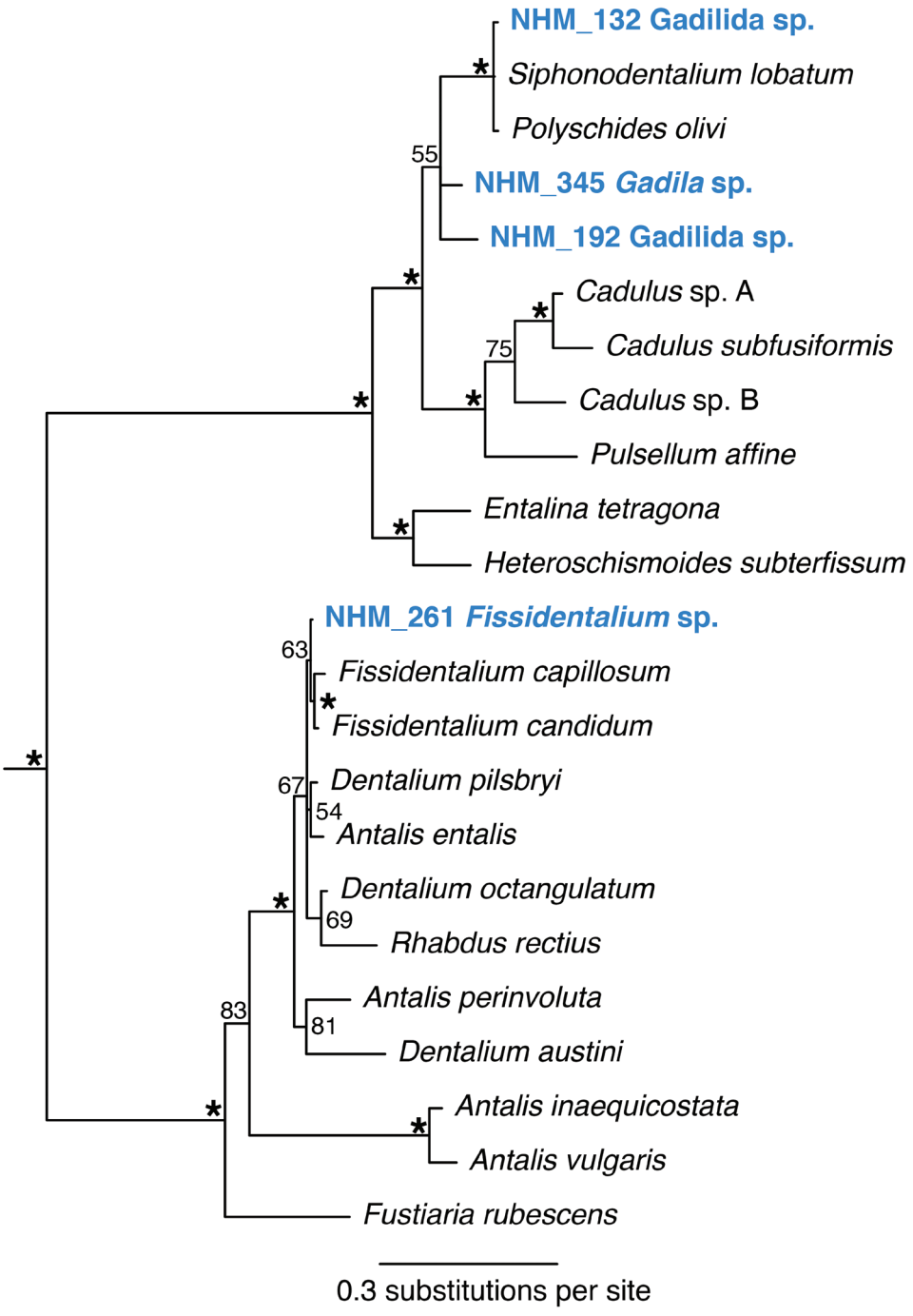

Figure 24. Phylogenetic analysis of Scaphopoda. 50% majority rule consensus tree from the Bayesian analyses using 18S. Asterisks denotes support values of 95 or above.

ment in order Gadilida. Genetic and image data made available for future study when better specimens available.

Ecology. Specimen collected from an epibenthic sledge tow across region of sediment and polymetallic nodules.

Solenogastres
Acanthomeniidae Salvini-Plawen, 1978

Acanthomeniidae sp. (NHM_367)

Material examined. NHM_367 NHMUK 20170078.1-2, collected 2013-10-19, 13.93307 -116.71628, 4182 m. http://data.nhm.ac.uk/object/c0577fc9-7302-4fec-bc8c-87a17a38bc91

Description. Voucher specimen NHM_367, small solenogaster specimen, anterior end lacking; fragment ca. 2.5 mm long and 0.5 mm in maximum diameter (Fig. 25). Main epidermal sclerites are slender, elongate and pointed scales with a thin, symmetrical rim, and hollow acicular spicules with voluminous cavities, thin walls, and short, pointed tips. Data and material, including a permanent preparation of sclerites (1 slide), made available for future study.

Genetic data. GenBank NHM_367 COI-MF157519.

Figure 25. Acanthomeniidae sp. (NHM_367). Living aplacophoran-like mollusc specimen recovered from sledge sample. Scale bar: 0.5 mm. Image attribution Glover, Dahlgren & Wiklund, 2017.

Remarks. The combination of scales and hollow spicules as main epidermal sclerites is diagnostic for the family Acanthomeniidae. Forms a unique monophyletic clade distinct from other AB01 specimens (Fig. 27). No genetic matches on GenBank.

Ecology. Specimen collected from an epibenthic sledge tow across region of sediment and polymetallic nodules.

Pruvotinidae Heath, 1911
Lophomeniinae Salvini-Plawen, 1978

Lophomeniinae sp. (NHM_027)

Material examined. NHM_027 NHMUK 20170079.1-2, collected 2013-10-09, 13.8372 -116.55843, 4336 m. http://data.nhm.ac.uk/object/319fd186-b07f-4be7-986c-b96c20f63723

Description. Voucher specimen NHM_027, small, probably juvenile, solenogaster specimen (Fig. 26). Main epidermal sclerites are very long hollow acicular spicules with simple pointed tips. Spicules slender, s-shaped and thin-walled; tips long and thin. Leaf-shaped pedal scales present. Data and material, including a permanent preparation of sclerites (1 slide), made available for future study.

Genetic data. GenBank NHM_027 COI-MF157500.

Remarks. Forms a unique monophyletic clade distinct from other AB01 specimens (Fig. 27). No genetic matches on GenBank. Body shape and sclerites are characteristic for the family Pruvotinidae and indicative of the subfamily Lophomeniinae. Placement as sister to *Hypomenia*, another pruvotinid species, in the phylogenetic analysis (Fig. 27) confirms the family-level affiliation.

Ecology. Specimen collected from an epibenthic sledge tow across region of sediment and polymetallic nodules.

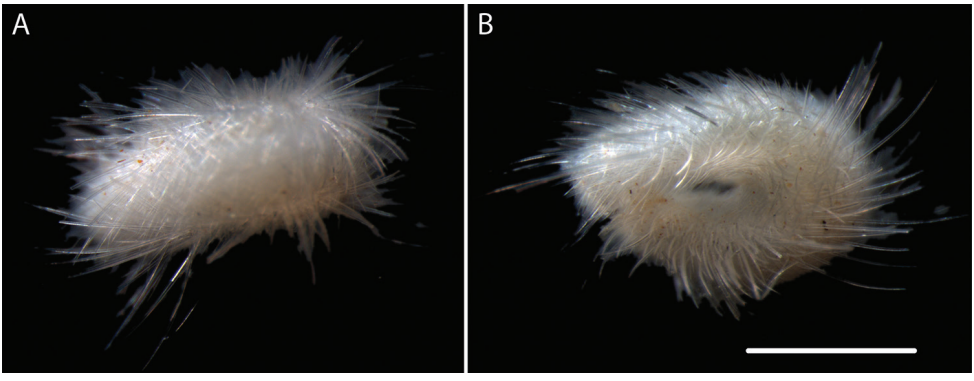

Figure 26. Lophomeniinae sp. (NHM_027) **A** Dorsal view of preserved specimen **B** Preserved specimen (ventro-lateral view) following DNA extraction. Scale bar: 0.5 mm. Image attribution Glover, Dahlgren & Wiklund, 2017.

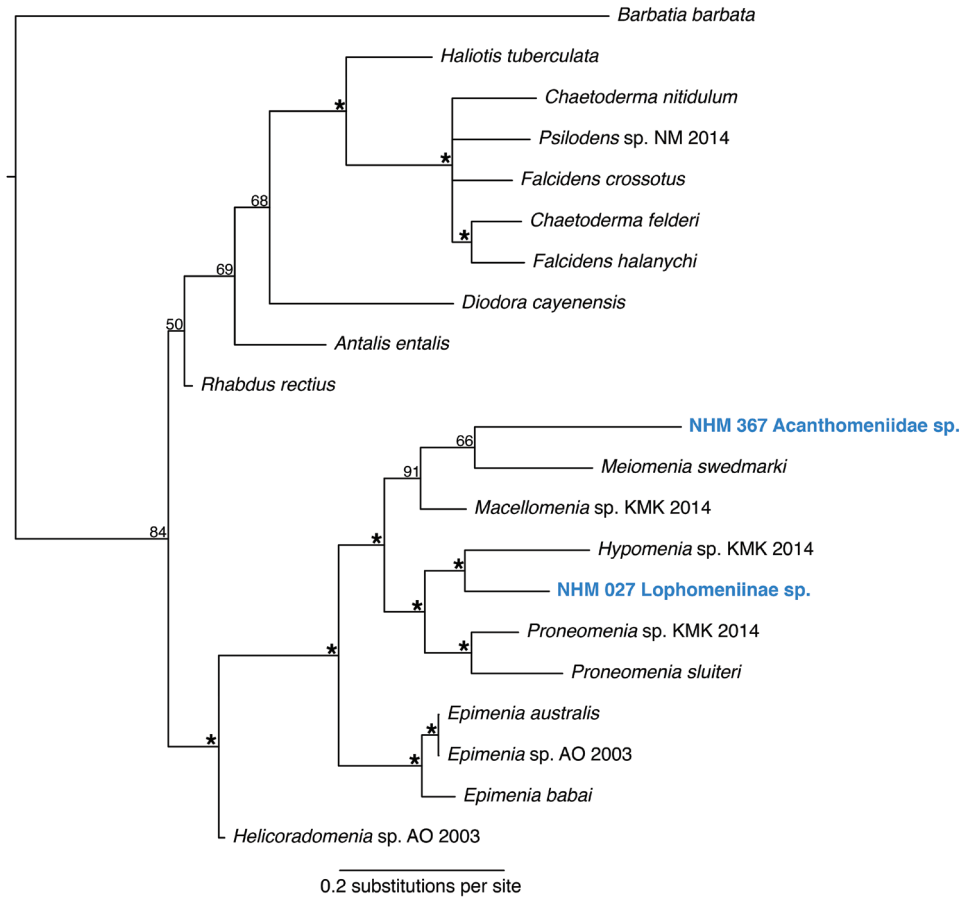

Figure 27. Phylogenetic analysis of Solenogastres, 50% majority rule consensus tree from the Bayesian analyses using COI. Asterisks denotes support values of 95 or above.

Discussion

Only one record of benthic mollusc taxa in the CCZ is hitherto reported on OBIS (OBIS 1017; iobis.org), with a further four just south of CCZ. In this study we report 42 records for 21 taxa, of which one is described as a new species. All our data and material from this study are made publicly available through this publication, and through depositing DNA extractions and tissue for further molecular analyses in the Molecular Collections Facility as well as morphological vouchers at the Natural History Museum in London, UK.

Mollusca is a diverse group with its members having very differing life histories, and in this study there are representatives of both sediment-dwelling species and nodule fauna. Not much is known about the mollusc species distribution and connectivity within the CCZ, an information deficit that makes it impossible to assess

impact from anthropogenic activities. Genetic data is crucial for distribution analyses as some taxa look very similar and can be difficult to separate to species level based on morphology only, e.g. the new species *Ledella knudseni* and its sister taxon *Ledella* sp. (NHM_381). In our study we have used a precautionary approach when reporting taxa that are preliminary identified as described species with type locality far from CCZ, e.g. our *Bentharca* cf. *asperula* which is very similar to *Bentharca asperula* with type locality in Gulf of Mexico. Without genetic information from specimens collected at the type locality, we can not rule out that ours is a different species despite the similarity in morphology.

The protobranch bivalve *Nucula profundorum* is the most abundant bivalve mollusc in our samples, and population connectivity analyses are underway (Dahlgren et al. in prep). Morphologically it is identical to type material of the original *Nucula profundorum*, which was described from collections of HMS Challenger in the mid-North Pacific (36°N, 178°E) at about 3750 m depth (Fig. 10), and although our specimens were collected further south and east, the depth is almost the same. However, as we compare our sequences with published *N. profundorum* sequences on GenBank it is obvious that those two are different species. The sequences already published on GenBank come from specimens collected at about 1000 m depth off San Diego. Based on morphological similarity only, and the general observation that depth is a stronger barrier to dispersal than geographic distance (e.g Etter & Rex, 1990), our hypothesis is that our specimens are likely to correspond to *N. profundorum* and that the sequences attributed to *N. profundorum* on GenBank are erroneously identified.

There are very few DNA sequences from a few faunal groups from the CCZ available on GenBank, e.g. echinoderms (Glover et al. 2016b), cnidarians (Dahlgren et al. 2016) and polychaetes and crustaceans (Janssen et al. 2015). With our study including both morphological and molecular data we add greatly to our knowledge of genetic information in the CCZ and aim to improve the taxonomic understanding of benthic fauna in the CCZ to get a better picture of the distribution of taxa. These are essential data for the establishment of conservation strategies in the light of future mineral extraction.

Acknowledgements

The ABYSSLINE (ABYSSal baseLINE) environmental survey of the UK-1 exploration area was supported by a collaborative partnership between six non-profit global academic research institutes (University of Hawaii (UH) at Manoa, Natural History Museum (NHM), Uni Research, National Oceanography Centre, Senckenberg Institute, IRIS Norway) and through an arrangement with UK Seabed Resources Ltd. We gratefully acknowledge the leadership of Prof Craig R Smith (UH) on this project and during the research cruises. Additional support for the project was provided by the Swedish research council FORMAS (TGD). We would like to acknowledge the support of Maggie Georgieva (NHM) and Iris Altamira (UH) in sorting on board ship, and Henk H. Dijkstra from Naturalis Biodiversity Center in Leiden, Netherlands for taxonomic

advice on *Catillopecten*. We would also like to acknowledge the expert support from the Senckenberg Institute team in the deployment and recovery of successful Brenke Epibenthic Sledge samples on the first ABYSSLINE cruise (Nils Brenke, Pedro Martinez Arbizu and Inga Mohrbeck). This study was made possible only by the dedicated help from the entire scientific party and the Masters and Crew of the Research Vessel Melville during the first cruise of the ABYSSLINE project in October 2013. Thanks also to Jackie Mackenzie-Dodds at the NHM Molecular Collection Facility, and Ben Scott of the NHM Diversity and Informatics group for work on the NHM Data Portal.

References

Abbott RT (1954) American seashells. Van Nostrand Company, New York, 541 pp.

Adams H, Adams A (1858) The genera of recent Mollusca arranged according to their organisation. J. van Voorst, London.

Allen JA (2008) Bivalvia of the deep Atlantic. Malacologia 50: 57–103. https://doi.org/10.4002/0076-2997-50.1.57

Allen JA, Hannah FJ (1989) Studies on the deep sea Protobranchia: the subfamily Ledellinae (Nuculanidae). The Natural History Museum (London), Bulletin (Zoology) 55: 123–171.

Allen JA, Morgan RE (1981) The functional morphology of Atlantic deep water species of the families Cuspidariidae and Poromyidae (Bivalvia): an analysis of the evolution of the septibranch condition. Philosophical Transactions of the Royal Society of London 294: 413–546. https://doi.org/10.1098/rstb.1981.0117

Allen JA, Sanders HL (1982) Studies on the deep sea Protobranchia: the subfamily Spinulinae (family Nuculanidae). Bulletin of the Museum of Comparative Zoology 150: 1–30.

Bruun AF, Greve S, Mielche H, Spärck R (Eds) (1956) The Galathea deep sea expedition 1950–1952. Described by members of the expedition. George Allen and Unwin Ltd, London, 296 pp.

Children JG (1834) Synopsis of the contents of the British Museum (28th edition). British Museum, London, 240 pp.

Coan EV, Scott PH (1997) Checklist of marine bivalves of the northeastern Pacific Ocean. Santa Barbara Museum of Natural History, Contributions in Science 1: 1–28.

Coan EV, Valentich-Scott PH (2012) Bivalve seashells of tropical west America: Marine bivalves from Baja California to northern Peru. Santa Barbara Museum of Natural History Monographs 6: 1–1258.

Cohen BL, Gawthrop A, Cavalier-Smith T (1998) Molecular phylogeny of brachiopods and phoronids based on nuclear-encoded small subunit ribosomal RNA gene sequences. Philosophical Transactions of the Royal Society B Biological Sciences 353: 2039–2061. https://doi.org/10.1098/rstb.1998.0351

Dahlgren TG, Wiklund H, Rabone M, Amon DJ, Ikebe C, Watling L, Smith CR, Glover AG (2016) Abyssal fauna of the UK-1 polymetallic nodule exploration area, Clarion-Clipperton Zone, central Pacific Ocean: Cnidaria. Biodiversity Data Journal 4: e9277. https://doi.org/10.3897/BDJ.4.e9277

Dall WH (1908) The Mollusca and the Brachiopoda. Reports on the dredging operations off the west coast of Central America to the Galapagos, to the west coast of Mexico, and in the Gulf of California, in charge of Alexander Agassiz. Bulletin of the Museum of Comparative Zoology 43: 203–487.

Dall WH (1881) Reports on the results of dredging, under the supervision of Alexander Agassiz, in the Gulf of Mexico and in the Caribbean Sea (1877-78), by the United States Coast Survey Steamer "Blake", Lieutenant-Commander C.D. Sigsbee, U.S.N., and Commander J.R. Bart. Bulletin of the Museum of Comparative Zoology at Harvard College 9: 33–144.

Dall WH (1900) Contributions to the Tertiary fauna of Florida, with especial reference to the Miocene silex-beds of Tampa and the Pliocene beds of the Calooshatchie River. Transactions of the Wagner Free Institute of Science of Philadelphia 3: 949–1189.

Dall WH (1878) Descriptions of new forms of mollusks from Alaska contained in the collection of the National Museum. Proceedings of the United States National Museum 1: 1–3. https://doi.org/10.5479/si.00963801.1

Dall WH (1895) Science results of explorations by the US Fish Commission Steamer Albatross. No. 34. Report on Mollusca and Brachiopoda dredged in deep water, chiefly near the Hawaiian Islands, with illustrations of the hitherto unfigured species from northwest America. In: US Nat. Mus., Proc., 675–733.

Dall WH (1886) Reports on the results of dredging, under the supervision of Alexander Agassiz, in the Gulf of Mexico (1877–78) and in the Carribean Sea (1879–80), by the U.S. Coast Survey steamer "Blake", Lieut.-Commander C.D. Sigsbee, U.S.N. and Commander J.R. Bartlett. Bulletin of the Museum of Comparative Zoology at Harvard College 12: 171–318.

Dall WH (1916) Diagnoses of new species of marine bivalve mollusks from the northwest coast of America in the collection of the United States National Museum. Proceedings of the United States National Museum 52: 393–417. https://doi.org/10.5479/si.00963801.52-2183.393

Dall WH, Simpson CT (1901) The Mollusca of Puerto Rico. Bulletin of the US Fish Commission 20: 351–524.

Donoghue MJ (1985) A Critique of the Biological Species Concept and Recommendations for a Phylogenetic. The Bryologist 88: 172–181. https://doi.org/10.2307/3243026

Ebbe B, Billett DSM, Brandt A, Ellingsen K, Glover A, Keller S, Malyutina M, Martínez Arbizu P, Molodtsova T, Rex M, Smith C, Tselepides A (2010) Diversity of Abyssal Marine Life. In: Life in the World's Oceans. Wiley-Blackwell, 139–160. https://doi.org/10.1002/9781444325508.ch8

Edgar RC (2004) MUSCLE: multiple sequence alignment with high accuracy and high throughput. Nucleic Acids Research 32: 1792–1797. https://doi.org/10.1093/nar/gkh340

Etter RJ, Rex MA (1990) Population differentiation decreases with depth in deep-sea gastropods. Deep Sea Research Part A, Oceanographic Research Papers 37: 1251–1261. https://doi.org/10.1016/0198-0149(90)90041-S

Fischer P (1885) 1880-1887. Manuel de conchyliologie et de paleontologie conchyliologique ou histoire naturelle des mollusques vivants et fossiles. Libraire F. Savy, Paris, 1369 pp.

Folmer O, Black M, Hoeh W, Lutz R, Vrijenhoek R (1994) DNA primers for amplification of mitochondrial cytochrome c oxidase subunit I from diverse metazoan invertebrates. Mo-

lecular Marine Biology and Biotechnology 3: 294–299. https://doi.org/10.1371/journal.pone.0013102

Forbes E (1844) On the Mollusca and Radiata of the Aegean Sea and on their distribution, considered as bearing on geology. Report of the British Association for the Advancement of Science 1843: 130–193.

Glover AG, Dahlgren TG, Wiklund H, Mohrbeck I, Smith CR (2016a) An End-to-End DNA Taxonomy Methodology for Benthic Biodiversity Survey in the Clarion-Clipperton Zone, Central Pacific Abyss. Journal of Marine Science and Engineering 4: 2. https://doi.org/10.3390/jmse4010002

Glover AG, Wiklund H, Rabone M, Amon DJ, Smith CR, O'Hara T, Mah CL, Dahlgren TG (2016b) Abyssal fauna of the UK-1 polymetallic nodule exploration area, Clarion-Clipperton Zone, central Pacific Ocean: Echinodermata. Biodiversity Data Journal 4: e7251. https://doi.org/10.3897/BDJ.4.e7251

Gray JE (1824) Shells. In: Parry WE (Ed.) Supplement to Appendix, Parry's Voyage for the Discovery of a north-west passage in the years 1819-1820, containing an account of the subjects of Natural History London, John Murray. Appendix 10, Zool: 240–246.

Gray JE (1847) A list of the genera of recent Mollusca, their synonymy and types. Proceedings of the Zoological Society London 15: 129–206.

Heath H (1911) Reports on the scientific results of the expedition to the Tropical Pacific, in charge of Alexander Agassiz, by the U. S. Fish Commission Steamer Albatross, from August 1899 to June 1900, Commander Jefferson F. Moser. XVI. The Solenogastres. Memoirs of the Museum of Comparative Zoology at Harvard College 45: 1–182.

Hedley C (1907) The results of deep-sea investigation in the Tasman Sea. II. The expedition of the 'Woy Woy.' Records of the Australian Museum 6: 356–364. https://doi.org/10.3853/j.0067-1975.6.1907.1020

Hendrickx M, Valentich-Scott P, Suárez-Mozo N (2016) Deep-water bivalve mollusks collected during the TALUD XV cruise off the west coast of the southern Baja California Peninsula, Mexico. Biodiversity Data Journal 4: e8661. https://doi.org/10.3897/BDJ.4.e8661

International Seabed Authority (1999) Deep-Seabed Polymetallic Nodule Exploration: Development of Environmental Guidelines. Kingston, Jamaica

Iredale T (1924) Results from Roy Bell's molluscan collections. Proceedings of the Linnean Society of New South Wales 49: 179–278.

Janssen A, Kaiser S, Meißner K, Brenke N, Menot L, Arbizu PM (2015) A reverse taxonomic approach to assess macrofaunal distribution patterns in abyssal pacific polymetallic nodule fields. PLoS ONE. https://doi.org/10.1371/journal.pone.0117790

Jennings RM, Etter RJ (2014) Phylogeographic estimates of colonization of the deep Atlantic by the protobranch bivalve Nucula atacellana. Polish Polar Research 35: 261–278. https://doi.org/10.2478/popore-2014-0017

Katoh K, Misawa K, Kuma K, Miyata T (2002) MAFFT: a novel method for rapid multiple sequence alignment based on fast Fourier transform. Nucleic acids research 30: 3059–3066. https://doi.org/10.1093/nar/gkf436

Kearse M, Moir R, Wilson A, Stones-Havas S, Cheung M, Sturrock S, Buxton S, Cooper A, Markowitz S, Duran C, Thierer T, Ashton B, Meintjes P, Drummond A (2012) Geneious

Basic: An integrated and extendable desktop software platform for the organization and analysis of sequence data. Bioinformatics 28: 1647–1649. https://doi.org/10.1093/bioinformatics/bts199

Killeen IJ, Turner JA (2009) Yoldiella and Portlandia (Bivalvia) from the Faroe-Shetland Channel and Rockall Trough, Northeast Atlantic. Journal of Conchology 39: 733–778.

Knight JB, Yochelson EL (1958) A reconsideration of the Monoplacophora and the primitive Gastropoda. Proceedings of the Malacological Society of London 33: 37–48.

Knudsen J (1967) The deep-sea Bivalvia. John Murray Expedition Scientific Reports 11: 237–343.

Knudsen J (1970) The systematics and biology of abyssal and hadal Bivalvia. Galathea Reports 11: 1–241.

Krylova EM, Kamenev GM, Vladychenskaya IP, Petrov NB (2015) Vesicomyinae (Bivalvia: Vesicomyidae) of the Kuril-Kamchatka Trench and adjacent abyssal regions. Deep-Sea Research Part II: Topical Studies in Oceanography 111: 198–209. https://doi.org/10.1016/j.dsr2.2014.10.004

Lamarck J-B (1818) Histoire naturelle des animaux sans vertèbres ... précédée d'une introduction offrant la détermination des caractères essentiels de l'animal, sa distinction du végétal et des autres corps naturels, enfin, l'exposition des principes fondamentaux de la zool. Verdière, Paris, 1–636. http://www.biodiversitylibrary.org/item/46337 [March 15, 2017]

Lamarck J-B (1799) Prodrome d'une nouvelle classification des coquilles, comprenant une rédaction appropriée des caractères génériques, et l'établissement d'un grand nombre de genres nouveaux. Mémoires de la Société d'Histoire Naturelle de Paris: 63–91.

Medlin L, Elwood HJ, Stickel S, Sogin ML (1988) The characterization of enzymatically amplified eukaryotic 16S-like rRNA-coding regions. Gene 71: 491–499. https://doi.org/10.1016/0378-1119(88)90066-2

Nygren A, Sundberg P (2003) Phylogeny and evolution of reproductive modes in Autolytinae (Syllidae, Annelida). Molecular Phylogenetics and Evolution 29: 235–249. https://doi.org/10.1016/S1055-7903(03)00095-2

Payne CM, Allen JA (1991) The Morphology of Deep-Sea Thyasiridae (Mollusca: Bivalvia) from the Atlantic Ocean. Philosophical Transactions of the Royal Society B: Biological Sciences 334: 481–562. https://doi.org/10.1098/rstb.1991.0128

Poutiers J, Bernard F (1995) Carnivorous bivalve molluscs (Anomalodesmata) from the tropical western Pacific Ocean, with a proposed classification and a catalogue of Recent species. Mémoires du Muséum National d'Histoire Naturelle 167: 107–187.

Rafinesque CS (1815) Analyse de la nature ou tableau de l'univers et des corps organisés. Published by the author, Palerme, 214 pp. https://doi.org/10.5962/bhl.title.106607

Rokop FJ (1972) A new species of monoplacophoran from the abyssal north Pacific. Veliger 15: 91–95.

Ronquist F, Teslenko M, Van Der Mark P, Ayres DL, Darling A, Höhna S, Larget B, Liu L, Suchard MA, Huelsenbeck JP (2012) Mrbayes 3.2: Efficient bayesian phylogenetic inference and model choice across a large model space. Systematic Biology 61: 539–542. https://doi.org/10.1093/sysbio/sys029

Salvini-Plawen L (1978) Antarktische und subantarktische Solenogastres (eine Monographie: 1898-1974). Zoologica 128: 1–305.

Salvini-Plawen L (1975) Mollusca Caudofoveata. Marine invertebrates of Scandinavia, 4. Universitetsforlaget, Oslo, 54 pp.

Sassi A (1827) Saggio geologico sopra il Bacino terziario di Albenga. Giornale ligustico di scienze: 467–484.

Scarabino V (1995) Scaphopoda of the tropical Pacific and Indian Oceans, with description of 3 new genera and 42 new species. Mémoires du Muséum National d'Histoire Naturelle 167: 189–379.

Schenck G (1939) Revised nomenclature for some nuculid pelecypods. Journal of Paleontology 13: 21–41.

Sharma PP, Zardus JD, Boyle EE, González VL, Jennings RM, McIntyre E, Wheeler WC, Etter RJ, Giribet G (2013) Into the deep: A phylogenetic approach to the bivalve subclass Protobranchia. Molecular Phylogenetics and Evolution 69: 188–204. https://doi.org/10.1016/j.ympev.2013.05.018

Sirenko B (2015) Shallow and deep-sea chitons of the genus Leptochiton Gray, 1847 (Mollusca: Polyplacophora: Lepidopleurida) from Peruvian and Chilean waters. Zootaxa 4033: 151–202. https://doi.org/10.11646/zootaxa.4033.2.1

Sjölin E, Erséus C, Källersjö M (2005) Phylogeny of Tubificidae (Annelida, Clitellata) based on mitochondrial and nuclear sequence data. Molecular Phylogenetics and Evolution 35: 431–441. https://doi.org/10.1016/j.ympev.2004.12.018

Smith CR, Dahlgren TG, Drazen J, Gooday A, Glover AG, Kurras G, Martinez-Arbizu P, Shulse C, Spickermann R, Sweetman AK, Vetter E (2013) Abyssal Baseline Study (ABYSSLINE) Cruise Report. Seafloor Investigations Report 2013-1304-051J-SRDL-AB01.

Smith CR, De Leo FC, Bernardino AF, Sweetman AK, Arbizu PM (2008) Abyssal food limitation, ecosystem structure and climate change. Trends in Ecology and Evolution 23: 518–528. https://doi.org/10.1016/j.tree.2008.05.002

Smith EA (1885) Report on the Lamellibranchiata collected by HMS Challenger during the years 1873-1876. Reports of the scientific results of the voyage of H.M.S. "Challenger", Zoology 13: 1–341.

Starobogatov YI (1974) Xenoconchias and their bearing on the phylogeny and systematics of some molluscan classes. Paleontologicheskii Zhurnal 1: 3–18.

Starobogatov YI, Moskalev LI (1987) Systematics of the Monoplacophora. In: Starobogatov YI, Golikov AN, Likarev IM (Eds) Molluscs, results and perspectives of investigation. USSR Academy of Sciences, Zoological Institute, Leningrad.

Tizard TH, Moseley HN, Buchanan JY, Murray J (1885) Narrative of the cruise of HMS Challenger with a general account of the scientific results of the expedition. HMSO, London.

Torell O (1859) Bidrag till Spitsbergens Mollusk-fauna. Föreningens Boktryckeri, Stockholm, 154 pp.

Verrill AE, Bush KJ (1897) Revision of the genera of Ledidae and Nuculidae of the Atlantic coast of the United States. American Journal of Science 3: 51–63. https://doi.org/10.2475/ajs.s4-3.13.51

ZooKeys 707: 47–61 (2017)
doi: 10.3897/zookeys.707.13493
http://zookeys.pensoft.net

RESEARCH ARTICLE

A peer-reviewed open-access journal
ZooKeys
Launched to accelerate biodiversity research

A new species of the water mite genus *Sperchon* Kramer, 1877 from China, with identifying *Sperchon rostratus* Lundblad, 1969 through DNA barcoding (Acari, Hydrachnidia, Sperchontidae)

Jian-Hua Ding[1], Jing-Lan Sun[1], Xu Zhang[1]

1 *School of Life Sciences, Huaibei Normal University; Huaibei 235000, China*

Corresponding author: *Xu Zhang* (xuzhang03@hotmail.com)

Academic editor: *V. Pesic* | Received 1 May 2017 | Accepted 7 September 2017 | Published 10 October 2017

http://zoobank.org/8AFD7FB5-EC4C-44A8-A739-C87B60D98AB3

Citation: Ding J-H, Sun J-L, Zhang X (2017) A new species of the water mite genus *Sperchon* Kramer, 1877 from China, with identifying *Sperchon rostratus* Lundblad, 1969 through DNA barcoding (Acari, Hydrachnidia, Sperchontidae). ZooKeys 707: 47–61. https://doi.org/10.3897/zookeys.707.13493

Abstract

A new species of the water mite genus *Sperchon* Kramer, 1877 from China, *Sperchon fuxiensis* Zhang, **sp. n.**, is described and illustrated in this article. DNA barcoding for the new species is documented for future use. Descriptions of both male and female of *Sperchon rostratus* Lundblad, 1969 are given in the present study, and DNA barcoding for identifying *S. rostratus* is also discussed.

Keywords

China, DNA Barcoding, Hydrachnidia, new species, *Sperchon*

Introduction

Sperchon Kramer, 1877 is the most species-rich genus in the family Sperchontidae Thor, 1900. It is widely distributed in the Holarctic, Oriental, and Ethiopian regions (Cook 1974, Di Sabatino et al. 2008). At present, 22 species of the genus have been recorded from China: *Sperchon beijingensis* Zhang & Jin, 2010; *S. brevipalpis* Jin, 1997; *S. curvipalpis* Zhang & Jin, 2010; *S. fluviatilis* Uchida, 1934; *S. garhwalensis* Kumar, Kumar & Pesic, 2007; *S. gracilipalpis* Lundblad, 1941; *S. heteropoda* Zhang & Jin,

2010; *S. huangshanenses* Zhang & Jin, 2010; *S. lanigerus* Guo & Jin, 2011; *S. mirabilis* (Lundblad, 1941); *S. nikkoensis* Imamura, 1976; *S. oligospinis* Jin, 1997; *S. orbipatella* Zhang & Jin, 2011; *S. perspicuus* Zhang & Jin, 2011; *S. placodermus* (Lundblad, 1967); *S. plumifer* Thor, 1902; *S. rostratus* Lundblad, 1969; *S. sounkyo* Imamura, 1954; *S. synsetus* Zhang & Jin, 2012; *S. turfanensis* Zhang & Jin, 2010; *S. urumqiensis* Zhang & Jin, 2011; and *S. xiaoqikongensis* Zhang & Jin, 2012 (Jin 1997, Zhang et al. 2007, Jin et al. 2010, Zhang & Jin 2010, Zhang et al. 2010, Zhang & Jin 2011, Zhang et al. 2011, Zhang et al. 2012).

Species identification based on the 658bp sequence of mitochondrial cytochrome oxidase I gene (COI) is known as "DNA barcoding". This technique has been widely applied in many invertebrates, but rarely in Hydrachnidia (Hebert et al. 2004, Feng et al. 2011, Zhang and Zhang 2014). The study of DNA barcoding for *Sperchon* has not been reported yet.

During checking of a recent collection of water mites, three species (*S. plumifer*, *S. rostratus,* and *Sperchonopsis echphyma* Prasad & Cook, 1972) and a new species (*S. fuxiensis* sp. n.) were found. The descriptions and illustrations of *S. fuxiensis* sp. n. are given herein. DNA barcoding for these four species is also provided. DNA barcoding for indentifying *S. rostratus* is discussed in the present study.

Materials and methods

Water mites were collected by hand netting and preserved in absolute ethanol in 1.5ml centrifuge tubes. The centrifuge tubes were transported to the laboratory and stored at -20°C°C. The information of the samples used in this study is given in Table 1.

Molecular analysis

For molecular examination, each mite was transferred in individual 1.5ml tubes, and washed several times with sterile deionized water. Non-destructive DNA extraction was done on the whole mite. The genomic DNA was extracted by using the DNeasy Blood & Tissue kit (Qiagen, Hilden, Germany), following the manufacturer's instructions. Then, the mites were fixed in absolute ethanol and stored at -20°C for morphological analysis.

The standard COI barcoding fragments (658bp) were amplified with the universal primers LCO 1490 (5'-GGTCAACAAATCATAAAGATATTGG-3') and HCO 2198 (5'-TAAACTTCAGGGTGACCAAAAAATCA-3') (Folmer et al. 1994). Primers were synthesized by Shanghai Sangon Biotechnology (Shanghai, China). All amplification reactions were done in a total volume of 25μl, containing 1–5μl DNA; 12.5μl 2×Taq PCR MasterMix (Tiangen, Beijing, China) and deionized water. The PCR amplification was performed with the following profile: 5 min at 94°C;35 cycles of 30 sec at

Table 1. Samples examined in this study.

Species	Sex	BOLD process ID	GenBank accession numbers
Sperchon rostratus	Male	SPER001-17	MF124260
Sperchon rostratus	Male	SPER002-17	MF124259
Sperchon rostratus	Female	SPER003-17	MF124258
Sperchon rostratus	Female	SPER004-17	MF124257
Sperchon plumifer	Female	SPER005-17	MF124256
Sperchon plumifer	Male	SPER006-17	MF124255
Sperchon plumifer	Male	SPER007-17	MF124254
Sperchon plumifer	Male	SPER008-17	MF124253
Sperchonopsis echphyma	Male	SPER009-17	MF124252
Sperchon fuxiensis sp. n.	Female	SPER010-17	MF124251

94°C, 30 sec at 51°C, 45 sec at 72°C; final extension 10 min at 72°C. PCR products were purified by using QIAquick Gel Extraction kit (Qiagen, Hilden, Germany). The pure segments were ligated into the pGEM-Teasy vector (Promega, Madison, WI, USA) and introduced into *Escherichia coli* DH5a cells. Bacteria were cultured in LB medium after blue/white selection, and then inserts were sequenced with M13 primers. Each insert was sequenced twice with ABI 3730 automated DNA sequencer by Shanghai Sangon. All sequences were submitted to BOLD and GenBank. The BOLD process ID and the GenBank accession numbers are provided in Table 1.

All the sequence data were analysed by using MEGA (ver. 6; Tamura et al. 2013), and were aligned by ClustalW. Genetic distances within and between species were calculated with a K2P model. Phylogenetic trees were constructed with neighbur-joining (NJ) and maximum-likelihood (ML) using K2P model. The sequence of *Sperchonopsis echphyma* was used as the outgroup. Bootstrap values were obtained from 1000 replicates.

Morphometric analysis

For morphological examination, the mite was dissected as described elsewhere (e.g. Cook 1974). Terms follow Jin (1997). The following abbreviations are used:

A1, A2 = antennal glandularia 1 and 2; ACG = anterior coxal group (CxI + CxII); CxI–CxIV = coxae I–IV; D1–D4 = dorsoglandularia 1–4; E1–E4 = epimeroglandularia 1–4; L1–L4 = lateroglandularia l–4; O1, O2 = ocularia l and 2; PCG = posterior coxal group (CxIII + CxIV); P-I–P-V = palpal segments 1–5; V1–V4 = venteroglandularia 1–4; I-L-1–I-L-6 = the first leg segments 1–6; II-L-1–II-L-6 = the second leg segments 1–6; III-L-1–III-L-6 = the third leg segments 1–6; IV-L-1–IV-L-6 = the fourth leg segments 1–6.

The type specimens are deposited in School of Life Sciences, Huaibei Normal University, China. All measurements are given in μm.

Systematics

Family Sperchontidae Thor, 1900
Genus *Sperchon* Kramer, 1877

***Sperchon fuxiensis* Zhang, sp. n.**
http://zoobank.org/0B23E95E-F928-4734-AC9C-C0FF6E99F006
Figures 1–9

Type series. Holotype: Female, Anhui Province, Fuxi village, Monkey Valley scenic area, an unnamed stream (30°04'16"N; 118°09'26"E), 8 September 2016, coll. Xu Zhang. Paratypes: 1 female, the same data as the holotype.

Diagnosis. Integument fine spinules arranged in hexagonal pattern; A1 smooth; excretory pore surrounded by a sclerotized ring; P-II with a long ventro-distal projection and one thick seta; third to fifth segments of leg I-IV with short plumose setae.

Description. Female (n = 2): *Body* oval in shape, 948 (965) in length, 837 (842) in width. Integument yellow in colour, covered with very fine spinules arranged in hexagonal pattern (Fig. 3). A1 short, smooth and thick, other dorsal setae long and thin. Chitinous plates and glandular plates on both dorsum and venter well developed as illustrated in Fig. 1 and Fig. 2. The heart-shaped platelet between D2 somewhat bluish. Coxae in four groups, surface of coxae reticulated. ACG 92 (98) in length, apodeme well developed. E2 laterally between ACG and PCG. PCG 220 (231) in length. E4 absent from CxIII. Distance between anterior end of ACG and posterior end of PCG 373 (380). Genital field 205 (207) in length, 171 (175) in width. Pre- and postgenital sclerites developed. Three pairs of genital acetabula, the first pair of genital acetabula elliptical, the second pair somewhat triangular, and the third pair rounded and larger than the anterior two pairs. V1 on small sclerites and without accompanying glandularia. Excretory pore between V2, and with a sclerotized ring.

Capitulum with a long rostrum, length 213 (219). Chelicera total length 219 (226), basal segment length 158 (164), claw length 61 (62), ratio of basal segment / claw length 2.6. Dorsal lengths of the palpal segments: P-I, 22 (23); P- II, 123 (127); P-III, 172 (178); P-IV, 178 (183); P-V, 36 (37). P-I short and without seta. P-II with a long ventro-distal projection bearing one long setae. Approximately ten setae on the lateral and dorsal side of P-II and none of them plumose. The ventral side of P-III nearly straight and without seta, four short smooth setae on the lateral and dorsal side. P-IV with two small peg-like ventral setae, one larger almost in the middle, another one near the ventral distal end.

Legs. Dorsal lengths of leg I: I-L-1, 53 (55); I-L-2, 76 (80); I-L-3, 78 (81); I-L-4, 132 (139); I-L-5, 138 (142); I-L-6, 130 (137). Dorsal lengths of leg IV: IV-L-1, 92 (99); IV-L-2, 126 (135); IV-L-3, 129 (137); IV-L-4, 231 (243); IV-L-5, 225 (231); IV-L-6, 193 (198). Third to fifth segments of leg I-IV with rather short plumose setae

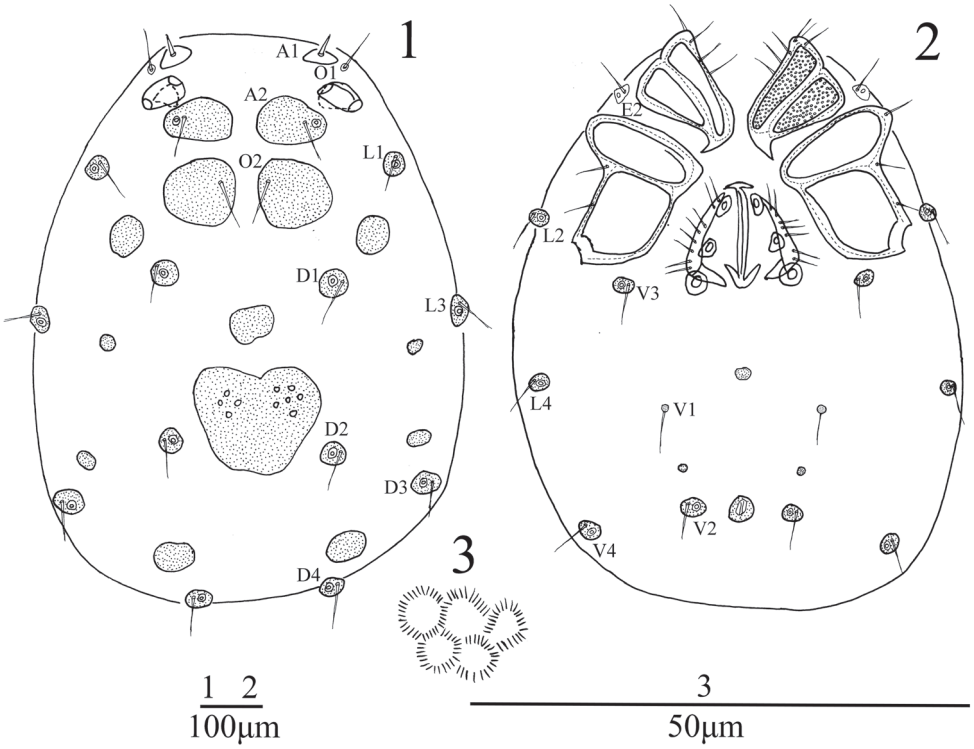

Figures 1–3. *Sperchon fuxiensis* sp. n., Female **1** idiosoma, dorsal view **2** idiosoma, ventral view **3** structure of integument.

in longitudinal rows (Fig. 9). Ambulacrum with two claws. Claws with well protruded claw-blade and two small claws, a long dorsal and a shorter ventral one (Fig. 8).

Etymology. The species is named after the village where it was collected.

Remarks. Due to the shape of the integument, P- II with a very long ventrodistal projection, excretory pore surrounded by sclerotized ring, and third to fifth segments of leg I-IV with plumose setae, the new species is similar to *S. hispidus* Koenike, 1895 and *Sperchon indicus* Kumar, Kumar & Pesic, 2007 (Kumar et al. 2007, Tuzovskij 2010). However, the new species differs from the two species in the shape of the acetabula. In *S. hispidus* and *S. indicus*, three pairs of acetabula are large and arranged densely, whereas in the new species, the three pairs of acetabula are relatively small and arranged loosely with large gaps. The new species also differs from *S. hispidus* and *S. indicus* in the shape of apodemes of anterior coxae, which are indistinct in *S. hispidus* and *S. indicus*, but well developed in the new species. Besides, E4 is situated on CxIII in *S. hispidus* and *S. indicus*, but absent from CxIII in the new species.

Distribution. China (Anhui Province).

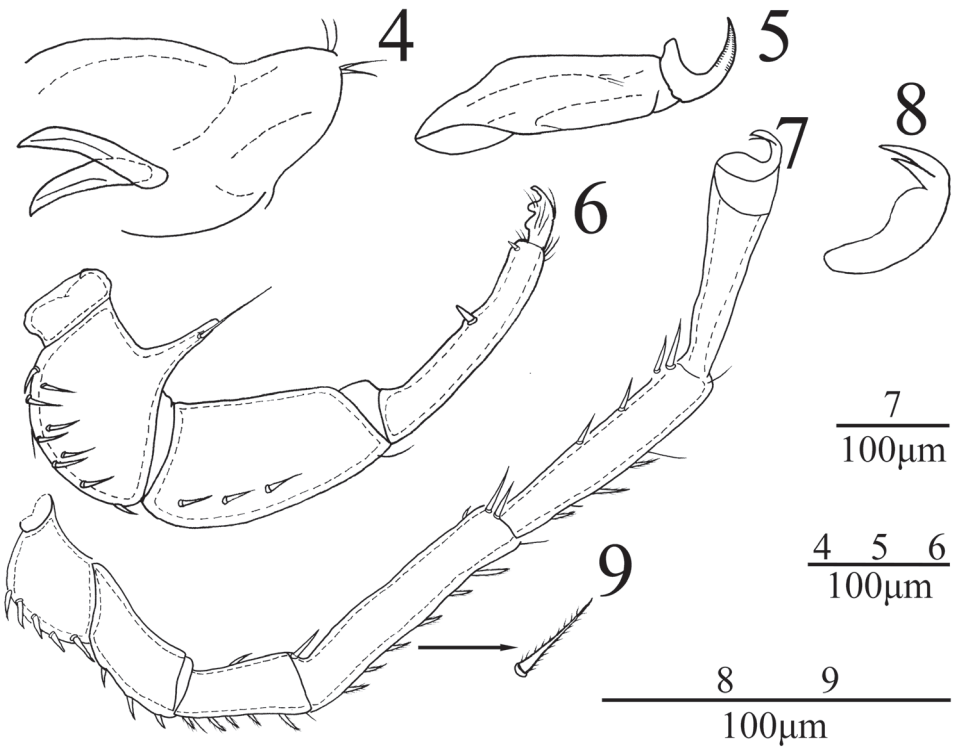

Figures 4–9. *Sperchon fuxiensis* sp. n., Female **4** infracapitulum **5** chelicera **6** palp **7** IV-L-1–IV-L-6 **8** claw **9** dorsal seta of IV-L-5.

Sperchon rostratus Lundblad, 1969

Figures 10–19

Material examined. 2 females, Guizhou Province, Fanjingshan National Nature Reserve, an unnamed stream (27°54'06"N; 108°36'44"E), 29 July 2001, coll. Jian-Jun Guo; 1 male and 1 female, Guizhou Province, Leigongshan National Nature Reserve, an unnamed stream (26°21'06"N; 108°12'39"E), 3 October 2005, coll. Xu Zhang; 2 male and 5 females, Anhui Province, Fuxi village, an unnamed stream (30°04'16"N; 118°09'26"E), 8 September 2016, coll. Xu Zhang.

Description. Male (n = 3): *Body* oval in shape, 533 (545-576) in length, 432 (441-476) in width, color yellow-brown. Integument with very fine spinules arranged in hexagonal pattern (Fig. 12). Chitinous plates in dorsum and venter well developed as illustrated in Fig. 10 and Fig. 11. All glandularia and O2 surrounded by a platelet. A1 short and smooth, other dorsal setae thin and long. Coxae in four groups, surface of coxae reticulated. ACG 136 (138-152) in length, posterior apodeme indistinct. E2 laterally between ACG and PCG. PCG 194 (204-216) in length, widely separated. E4 absent from CxIII. Distance between anterior end of ACG and posterior end of PCG 329 (347-361). Genital field 135 (142-156) in length, 121 (128-137) in width,

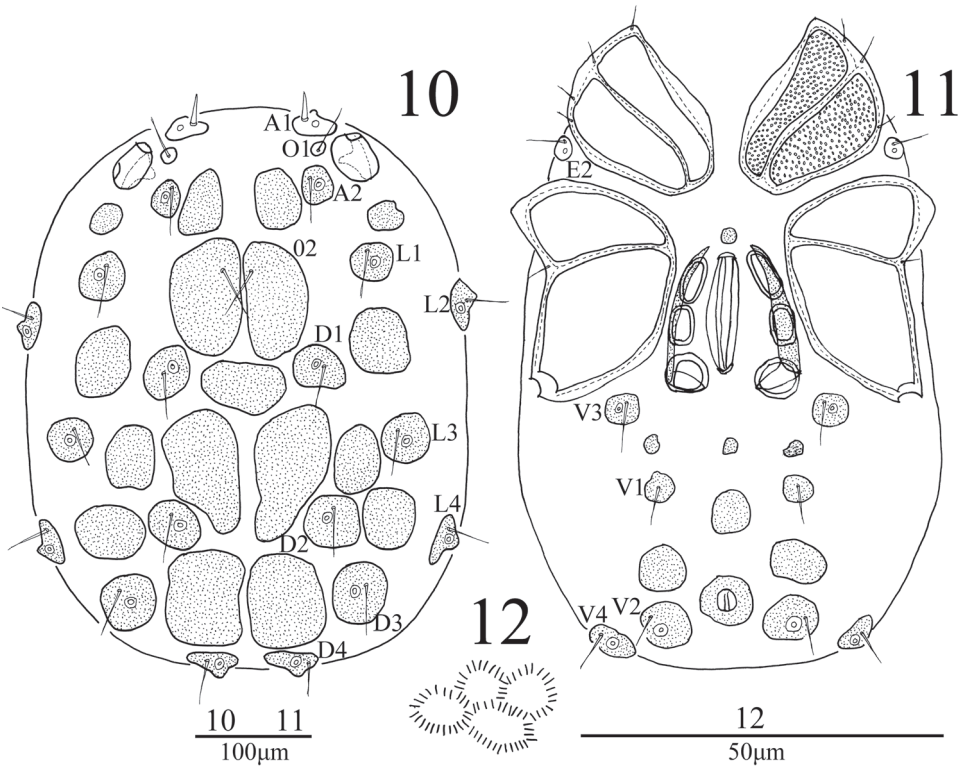

Figures 10–12. *Sperchon rostratus* Lundblad, 1969, Male **10** idiosoma, dorsal view **11** idiosoma, ventral view **12** structure of integument.

with a small and rounded platelet in front. Three pairs of genital acetabula, first and second pairs of acetabula elongate and oval, third pair more or less rounded. Pre- and postgenital sclerite not developed. V1 without accompanying glandularia but on sclerites of medium size. Excretory pore slightly anterior to V2, and surrounded by a well-developed sclerotized ring.

Capitulum with a long rostrum, length 219 (228-236). Chelicera total length 205 (220-227), basal segment length 166 (179-185), claw length 39 (41-42), ratio of basal segment /claw length (4.3-4.4). Dorsal lengths of the palpal segments: P-I, 26 (27-28); P-II, 103 (107-116); P-III, 147 (156-166); P-IV, 152 (161-170); P-V, 36 (39-43). P-I short and without seta. P-II with one thin seta instead of ventro-distal projection. Eight seta on the dorsal and lateral side of the P-II, none of them plumose. The venter margin of P-III without setae, five smooth setae on the lateral and dorsal side. P-IV with two small peg-like setae, one almost in the middle of the segment and with two small setae, another one near the distal end of the segment.

Legs. Dorsal lengths of leg I: I-L-1, 41 (44-52); I-L-2, 62 (69-78); I-L-3, 78 (82-94); I-L-4, 86 (89-97); I-L-5, 100 (110-126); I-L-6, 97 (103-117). Dorsal lengths of leg IV: IV-L-1, 76 (82-90); IV-L-2, 83 (92-104); IV-L-3, 107 (113-126); IV-L-4, 113

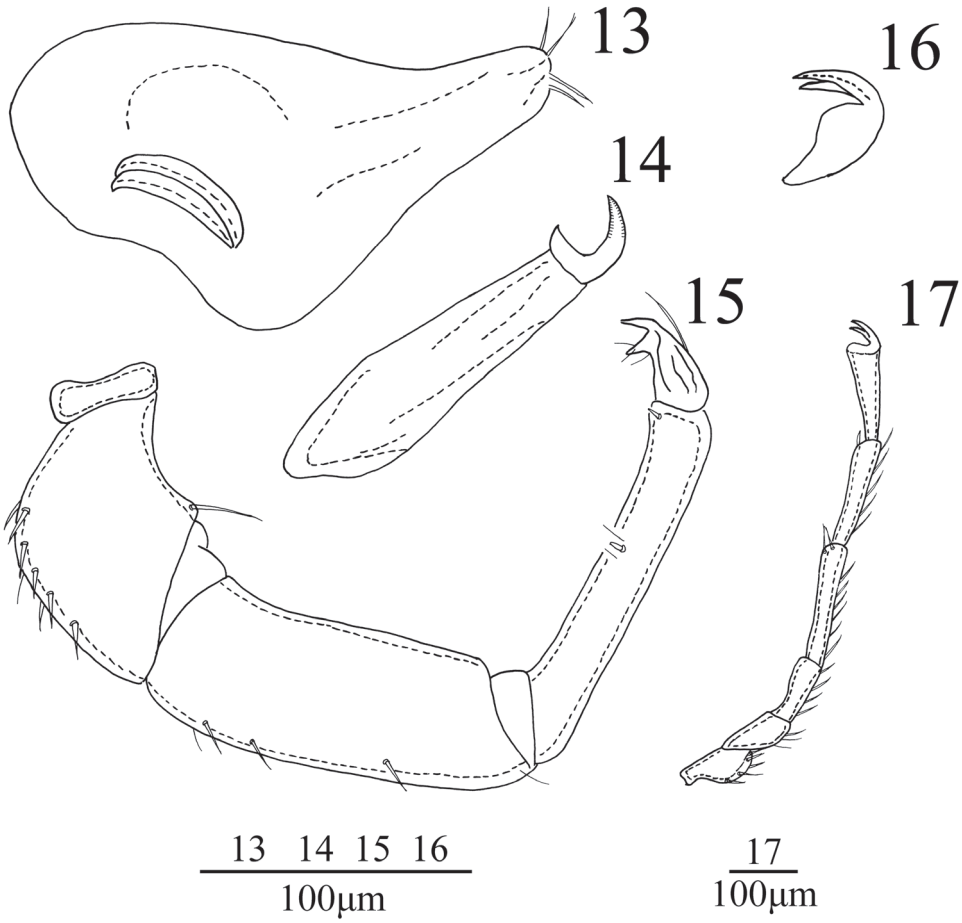

Figures 13–17. *Sperchon rostratus* Lundblad, 1969, Male **13** infracapitulum **14** chelicera **15** palp **16** claw **17** IV-L-1–IV-L-6.

(124-138); IV-L-5, 175 (192-201); IV-L-6, 152 (165-178). Ambulacrum with two claws. Claws with protruding claw blade and two small claws, a long dorsal claw and a shorter ventral one (Fig. 16).

Female (n = 8): Similar to male except for the morphology of genital field and the size of idiosoma. Idiosoma 847 (810-905) in length, 583 (536-618) in width. ACG 173 (154-195) in length, PCG 230 (207-264) in length. Distance between anterior end of ACG and posterior end of PCG 410 (388-435). Genital field 168 (139-192) in length, 152 (138-173) in width. Pregenital sclerite crescent-shaped, and more developed than the postgenital sclerite. Infracapitulum length 288 (264-317). Chelicera total length 286 (278-305), basal segment length 231 (221-248), claw length 55 (57-61), basal segment/claw length ratio 4.2 (4.1-4.4). Dorsal lengths of the palpal segments: P-I, 36 (34-45); P-II, 144 (128-166); P-III, 204 (194-225); P-IV, 212 (200-259); P-V, 57

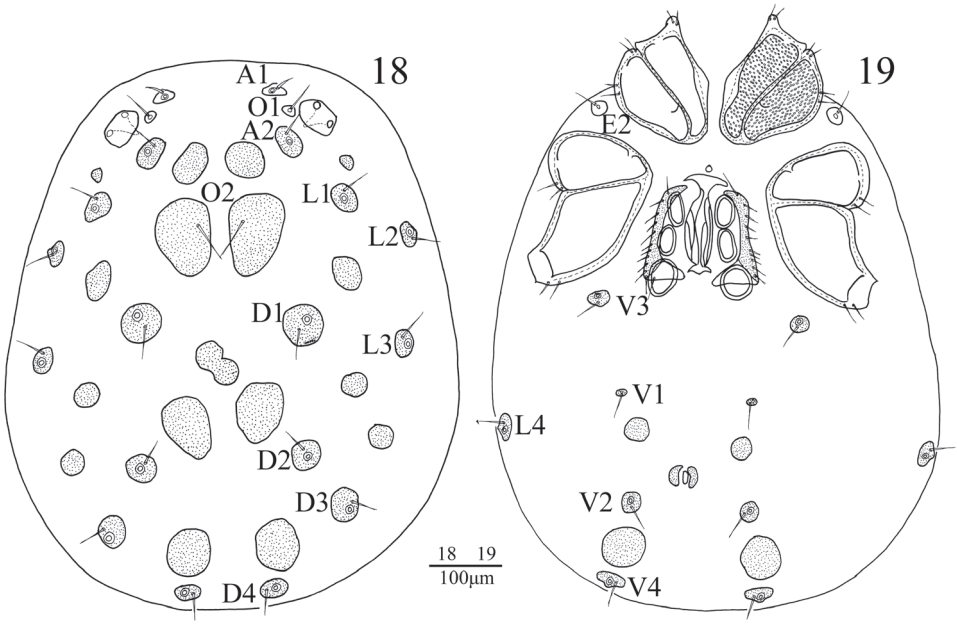

Figures 18–19. *Sperchon rostratus* Lundblad, 1969, Female **18** idiosoma, dorsal view **19** idiosoma, ventral view.

(50-64). Dorsal lengths of the first leg: I-L-1, 57 (48-66); I-L-2, 86 (71-98); I-L-3, 109 (92-127); I-L-4, 120 (107-146); I-L-5, 142 (130-170); I-L-6, 135 (116-154). Dorsal lengths of the fourth leg: IV-L-1, 93 (80-104); IV-L-2, 112 (107-134); IV-L-3, 173 (157-204); IV-L-4, 296 (272-324); IV-L-5, 267 (257-295); IV-L-6, 234 (227-264).

Remarks. *Sperchon rostratus* was first described from Burma by Lundblad (1969). However, the description and illustration given in the literature are short and insufficient. The species was subsequently recorded from China (Guizhou Province, Taiwan), Iran, and Turkey (Smit 1995, Boyaci 2007, Pešić and Vafaei 2009, Pešić et al. 2012, Pešić et al. 2014). Although the species has been reported many times, an illustration of the idiosoma for the male was given only once (from Turkey) (Boyaci 2007).

Due to the shape of integument, E4 absent from CxIII, P-II with one thin seta, and P-IV with two small peg-like setae, the female from China shows a general conformity with *S. rostratus*, a species previously reported from China, however, the morphological characters of the male show obvious differences between the specimens in our study and the Turkish specimens. It is obvious that the platelets of the dorsum and venter of *S. rostratus* are large and close together (Fig 10–11), but small and arranged loosely in the Turkish specimens (see details of *S. rostratus* in Boyaci 2007). In addition, the pre- and postgenital sclerites are small in our specimens but relatively large in Turkish specimens, and the pregenital sclerite is somewhat crescent-shaped in Turkish specimens. Additionally, our specimens possess a rounded platelet in front of the genital field, which is absent in the Turkish specimens.

Although there are many differences between the male of *S. rostratus* in our study and the Turkish specimens, considering most characters of our specimens (eg., the shape of integument, E4 absent from CxIII, P-II with one thin seta, P-IV with two small peg-like setae and same habitat of the female), we attribute the male specimens to *S. rostratus*. In order to test whether the male and the female are conspecific, we used DNA barcoding technology for *S. rostratus*. The results are given below (see Results of molecular analysis).

Distribution. Burma, China (Anhui, Guizhou, Taiwan), Turkey, Iran.

Results of molecular analysis

The ten nucleotide sequences of 658 bp obtained belong to four species (*S. fuxiensis*, *S. plumifer*, *S. rostratus,* and *Sperchonopsis echphyma*) and two genera (*Sperchon* and *Sperchonopsis*). Sequence of *S. fuxiensis* is documented as DNA barcoding for future use, the others were constructed for a phylogenetic tree and analysed for genetic distances. Phylogenetic tree based on neighbour-joining (NJ) and maximum-likelihood (ML) gave the same result, with minor difference in bootstrap support values only (Figure 20). The male and female of *S. rostratus* were clustered in a clade together with *S. plumifer*.

Genetic distances (K2P) for barcode region of CO I between the species analysed in this study were shown in Table 2. The sequence divergence between the both sexes was 0.6%–1.1% in *S. rostratus*, and 0.9–1.2% in *S. plumifer*, respectively. The intraspecific sequence divergence was 0–1.2% (average is 0.62%) in *S. plumifer*, and 0.2–1.1% (average is 0.73%) in *S. rostratus*, respectively (Table 2). Interspecific divergence between *S. plumifer* and *S. rostratus* was 15.7%–17.1% (average is 16.53%). Intergeneric divergence between *Sperchon* and *Sperchonopsis* was 32.0%–36.6%.

Table 2. Genetic distances (K2P) for barcode region of CO I among the *Sperchon* species analysed in this study. ('F' indicates female and 'M' indicates male).

	1	2	3	4	5	6	7	8
1 *S. plumifer* F								
2 *S. plumifer* M	0.012							
3 *S. plumifer* M	0.009	0.003						
4 *S. plumifer* M	0.009	0.003	0.000					
5 *S. rostratus* M	0.168	0.171	0.167	0.167				
6 *S. rostratus* M	0.170	0.169	0.169	0.169	0.002			
7 *S. rostratus* F	0.166	0.168	0.164	0.164	0.006	0.008		
8 *S. rostratus* F	0.158	0.161	0.157	0.157	0.009	0.011	0.009	
9 *S. echphyma* M	0.364	0.366	0.366	0.366	0.324	0.322	0.322	0.322

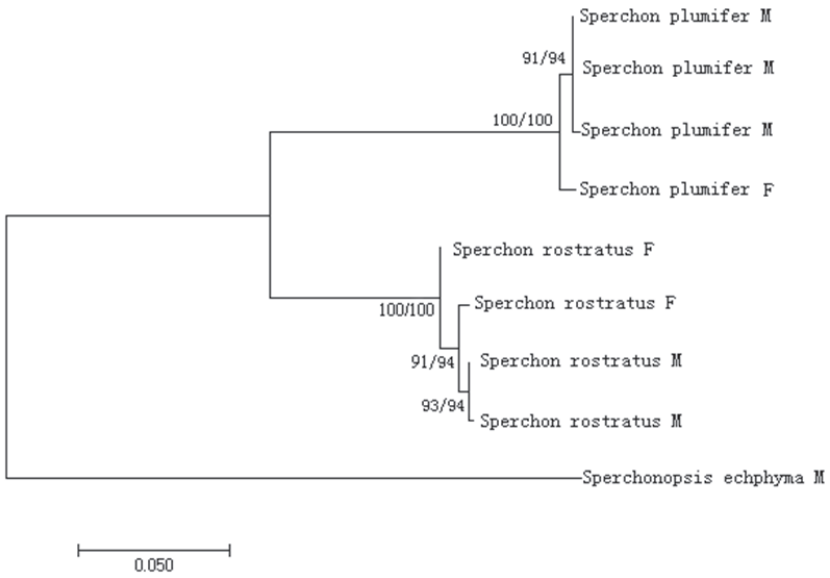

Figure 20. Phylogenetic tree based on barcode region of COI of *Sperchon plumifer*, *Sperchon rostratus,* and *Sperchonopsis echphyma*. The bootstrap proportions of neighbour-joining and maximum-likelihood are indicated above each branch in the format of NJ/ML. *Sperchonopsis echphyma* was used as the outgroup.

Discussion

In this study, the female of *S. rostratus* coincided with the species as previously reported, but the male specimens showed differences in the size of chitinous plates and genital field. In order to verify whether the male specimens belong to *S. rostratus*, we attempted to use the molecular identification known as "DNA barcoding" to construct a polygenetic tree and analyse genetic distance. Our attribution of the male specimens to *S. rostratus* was supported by molecular data. Phylogenetic tree showed that the male and the female of *S. rostratus* in our study could cluster in the same clade. In addition, the divergence between the male and the female was 0.6%-1.1%, which approximately agrees with the divergence of both sexes of *S. plumifer* (0.9-1.2%).

The morphological characters of the male *S. rostratus* showed obviously differences between China and Turkey. Many characters of the Chinese male specimens in our study, such as with extended and fused chitinous plates in dorsum and venter, pre- and postgenital sclerite weakly developed, and with a rounded platelet in front of the genital field (Figures 10-11), are typical characters of the male sex. On the contrary, most characters of the Turkish male specimens, e.g., with smaller and unfused chitinous plates, the pregenital sclerite is crescent-shaped and without a rounded platelet in front of the genital field, are the typical characters of the female sex (Di Sabatino et al. 2010). In our study, the Chinese male specimens also match the female of *S. rostratus* with the support of molecular data. Therefore, the male specimens of *S. rostratus* re-

ported from Turkey are female and not male. Although *S. rostratus* has been reported many times, the description and illustration are still incomplete. Our study represents the first description and illustration of both sexes.

In recent years, the research of molecular identification and phylogeny have been reported in many genera of water mites, such as *Brachypodopsis*, *Hygrobates*, *Monatractides*, *Neumania*, *Torrenticola*, and *Unionicola* (Ernsting et al. 2010, Pešić et al. 2012, Pešić and Smit 2014, 2016, 2017, Pešić et al. 2017). However, previous research rarely involved molecular analysis of both sexes. Pešić et al. (2012) reported that divergence value between the female and male of *Torrenticola lundbladi* is 0.15% (different in one nucleotide), which is much lower than the divergences in our study (0.6%–1.1% in *S. rostratus* and 0.9–1.2% in *S. plumifer*). However, only one female and one male of *T. lundbladi* were compared in the their study, so that the molecular data is hardly representative.

Hebert et al. (2004) reported that an appropriate threshold for DNA barcoding sequence should certainly be high enough to separate only specimens that very likely belong to different species. Their research also suggested the 10× rule threshold value method, in which interspecific divergences should be nearly ten times higher than intraspecific divergences (Hebert et al. 2004). In our study, the ratio of interspecific divergences to intraspecific divergences in the genus *Sperchon* is 22.64-26.66, which indicates that the DNA barcoding of COI gene may be a useful tool for identifying the *Sperchon* species.

According to the previous research and our study, the intra- and interspecific divergences of water mites were variable among different groups. For example, the intraspecific divergence value was 0.2% in *Torrenticola sabahensis* (Pešić and Smit 2014) and *Brachypodopsis truncata* (Pešić and Smit 2016), 0.3% in *Torrenticola lukai* (Pešić 2012) and *Brachypodopsis crockerensis* (Pešić and Smit 2016), 0.62% in *S. rostratus* (the present study), 1.8% in *Torrenticola kinabaluensis* (Pešić and Smit 2014), and 5.1% in *Torrenticola neoindica* (Pešić and Smit 2014). The interspecific divergence value was 11.6-11.8% in *Torrenticola* (Pešić et al. 2012), 10.7-23.5% in *Brachypodopsis* (Pešić and Smit 2016), 15.7%-17.1% in *Sperchon* (the present study), and 21.8% in *Monatractides* (Pešić and Smit 2014).

The instable divergences among the different species of water mites may be ascribed to limited data and researches on DNA barcoding for water mites. More molecular researches on water mites are required to solve this problem.

Acknowledgements

We are very grateful to Dr. Jian-Jun Guo (Guizhou University, China) for the specimen collection and Dr. Dao-Chao Jin (Guizhou University, China) for his help in many ways. Furthermore, we are grateful to Dr. Ling-Ying Shuai (Huaibei Normary University, China) for providing helpful comments and suggestions on this manuscript. This study was supported by The National Science Foundation of China (No. 31301895).

References

Boyaci YO (2007) *Limnolegeria longiseta* Motas, 1928 and *Sperchon rostratus* Lundblad, 1969: Two Water Mite Species (Acari: Hydrachnidia) from Turkey. Turkish Journal of Zoology 31: 281–286.

Cook DR (1974) Water mite genera and subgenera. Memoirs of the American Entomological Institute 21: 1-860.

Di Sabatino A, Gerecke R, Gledhill T, Smit H (2010) Chelicerata: Acari II. In: Gerecke R (Ed.) 2006. Chelicerata: Araraneae, Acari I. Süßwasserfauna von Mitteleuropa, Vol. 7, 2–2, Elsevier Spektrum Akademischer Verlag, München, 234 pp.

Di Sabatino A, Smit H, Gerecke R, Goldschmidt T, Matsumoto N, Cicolani B (2008) Global diversity of water mites (Acari, Hydrachnidia; Arachnida) in freshwater. Hydrobiologia 595: 303–315. https://doi.org/10.1007/s10750-007-9025-1

Ernsting BR, Edwards DD, Vidrine MF, Myers KS, Harmon CM (2006) Phylogenetic relationships among species of the subgenus *Parasitatax* (Acari: Unionicolidae: *Unionicola*) based on DNA sequence of the mitochondrial cytochrome oxidase I gene. International Journal of Acarology 32(2): 195–202. https://doi.org/10.1080/01647950608684461

Feng YW, Li Q, Kong LF, Zheng XD (2011) DNA barcoding and phylogenetic analysis of Pectinidae (Mollusca: Bivalvia) based on mitochondrial COI and 16S rRNA genes. Molecular Biology Reports 38(1): 291–299. https://doi.org/10.1007/s11033-010-0107-1

Folmer O, Black M, Hoeh W, Lutz R, Vrijenhoek R (1994) DNA primers for amplification of mitochondrial cytochrome oxidase subunit I from diverse metazoan invertebrates. Molecular Marine Biology Biotechnology 3: 294–299.

Hebert PDN, Penton EH, Burns JM, Janzen DH, Hallwachs W (2004) Ten species in one: DNA barcoding reveals cryptic species in the neotropical skipper butterfly *Astraptes fulgerator*. Proceedings of the National Academy of Sciences of the United States of America 101(41): 14812–14817.

Hebert PDN, Stoeckle MY, Zemlak TS, Francis CM (2004) Identification of birds through DNA barcodes. PLoS Biology 2(10): 1657–1663. https://doi.org/10.1371/journal.pbio.0020312

Hebert PDN, Cywinska A, Ball SL, deWaard JR (2003) Biological identifications through DNA barcodes. Proceedings of the Royal Society of London, Series B: Biological Sciences 270: 313–321. https://doi.org/10.1098/rspb.2002.2218

Jin DC (1997) Hydrachnellae: morphology, systematics; a primary study of Chinese fauna. Guizhou science and technology publishing house, Guiyang, 356 pp. [In Chinese]

Jin DC, Yi TC, Guo JJ (2010) A review of progress in taxonomy of water mites from China (Acari: Hydrachnidia). Zoosymposia 4: 106–119.

Kumar N, Kumar K, Pešić V (2007) Two new species of Sperchon Kramer (Acari: Hydrachnidia: Sperchontidae) from the Garhwal Himalayas (India). Systematic & Applied Acarology 12: 31–36. https://doi.org/10.11158/saa.12.1.5

Lundblad O (1969) Indische Wassermilben, hauptsächlich von Hinterindien. Arkiv för Zoologi 22: 1–126.

Pešić V, Asadi M, Cimpean M, Dabert M, Esen Y, Gerecke R, Martin P, Savic A, Smit H, Stur E (2017) Six species in one: evidence of cryptic speciation in the *Hygrobates fluviatilis* com-

plex (Acariformes, Hydrachnidia, Hygrobatidae). Systematic and Applied Acarology 22(9): 1327–1377. https://doi.org/10.11158/saa.22.9.4

Pešić V, Smit H (2014) Torrenticolid water mites (Acari: Hydrachnidia: Torrenticolidae) from Malaysian Borneo. Zootaxa 3840(1): 1–72. https://doi.org/10.11646/zootaxa.3840.1.1

Pešić V, Smit H (2016) Evidence of cryptic and pseudocryptic speciation in *Brachypodopsis baumi* species complex (Acari, Hydrachnidia, Aturidae) from Borneo, with description of three new species. Systematic and Applied Acarology 21(8): 1092–1106. https://doi.org/10.11158/saa.21.8.10

Pešić V, Smit H (2017) *Neumania kyrgyzica* sp. nov. a new water mite from Kyrgyzstan based on morphological and molecular data (Acari, Hydrachnidia: Unionicolidae). Systematic and Applied Acarology 22(6): 885–894. https://doi.org/10.11158/saa.22.6.12

Pešić V, Smit H, Saboori A (2014) Checklist of the water mites (Acari, Hydrachnidia) of Iran: Second supplement and description of one new species. Ecologica Montenegrina 1(1): 30–48.

Pešić V, Vafaei R (2009) New records of water mites (Acari: Hydrachnidia) from Iran, with the first descriptions of the male of *Nilotonia persica* Pesic & Saboori, 2006 and *Atractides mirkopesici* Pesic, 2004. Systematic & Applied Acarology 14: 153–160. https://doi.org/10.11158/saa.14.2.7

Pešić V, Valdecasas AG, García-Jimenez R (2012) Simultaneous evidence for a new species of *Torrenticola* Piersig, 1896 (Acari, Hydrachnidia) from Montenegro. Zootaxa 3515: 38–50.

Pešić V, Yam RSW, Chan BKK, Chatterjee T (2012) Water mites (Acari, Hydrachnidia) from Baishih River drainage in Northern Taiwan, with description of two new species. ZooKeys 203: 65–83. https://doi.org/10.3897/zookeys.203.3356

Smit H (1995) New records of water mites from Turkey, with 11 species new for the Turkish fauna (Acari, Hydrachnellae) Storkia 4: 10–15.

Stålstedt J, Bergsten J, Ronquist F (2013) "Forms" of water mites (Acari: Hydrachnidia): intraspecific variation or valid species?. Ecology and Evolution 3(10): 3415–3435. https://doi.org/10.1002/ece3.704

Tamura K, Stecher G, Peterson D, Filipski A, Kumar S (2013) MEGA6: molecular evolutionary genetics analysis version 6.0. Molecular Biology Evolution 30: 2725–2729. https://doi.org/10.1093/molbev/mst197

Tuzovskij PV (2010) On Diagnostics of the Water Mite *Sperchon hispidus* (Acariformes, Sperchontidae). Entomological Review 90(4): 473–480. https://doi.org/10.1134/S0013873810040081

Zhang RL, Zhang B (2014) Prospects of using DNA barcoding for species identification and evaluation of the accuracy of sequence databases for ticks (Acari: Ixodida). Ticks and Tick-Borne Diseases 5(3): 352–358. https://doi.org/10.1016/j.ttbdis.2014.01.001

Zhang X, Jin DC (2010) Three new species and one new record of the subgenus *Hispidosperchon* Thor, 1901 within the genus *Sperchon* Kramer, 1877 from China. Zootaxa 2684: 14–24.

Zhang X, Jin DC (2011) New records of water mites of the family Sperchontidae Thor, 1900 from China (Acari, Hydrachnidia), with descriptions of two new species. ZooKeys 158: 89–109. https://doi.org/10.3897/zookeys.158.1970

Zhang X, Jin DC, Guo JJ (2011) Two new water mites species of the genus *Sperchon* Kramer, 1877 (Acari, Hydrachnidia, Sperchontidae). Acta Zootaxonomica Sinica 36(2):221–226.

Zhang X, Jin DC, Guo JJ (2012) Descriptions of two new species of the genus *Sperchon* Kramer, 1877 (Acari: Hydrachnidia, Sperchontidae) from China. International Journal of Acarology 38(1): 23–29. https://doi.org/10.1080/01647954.2011.577452

Zhang X, Jin DC, Guo JJ, Yi TC (2010) Descriptions of two new species of *Mixosperchon* Viets, a newly recorded subgenus of water mites, from China (Acari, Hydrachnellae, Sperchontidae). Acta Zootaxonomica Sinica 35(3): 435–439.

Zhang X, Jin DC, Guo JJ, Zhu Q (2007) Three species of the Family Sperchontidae (Acari, Hydrachnellae, Sperchontidae) as new records from China. Science paper Online. (2007-12-28): 1–5. http://www.paper.edu.cn/index.php/ default/releasepaper/downPaper/200712-845/2 [In Chinese]

ZooKeys 707: 63–72 (2017)
doi: 10.3897/zookeys.707.20759
http://zookeys.pensoft.net

RESEARCH ARTICLE

A peer-reviewed open-access journal
ZooKeys
Launched to accelerate biodiversity research

Two new species of the rare Neotropical caddisfly genus *Amphoropsyche* Holzenthal (Trichoptera, Leptoceridae)

Ernesto Rázuri-Gonzales[1], Ralph W. Holzenthal[1], Blanca Ríos-Touma[2]

1 *University of Minnesota, Department of Entomology, 1980 Folwell Ave., 219 Hodson Hall, St. Paul, Minnesota 55108 U.S.A.* **2** *Universidad de Las Américas, Facultad de Ingenierías y Ciencias Agropecuarias, Ingeniería Ambiental, Campus Queri, Calle José Queri, Edificio #8, PB, Quito, Ecuador*

Corresponding author: *Ralph W. Holzenthal* (holze001@umn.edu)

Academic editor: *A. Previšić* | Received 1 September 2017 | Accepted 25 September 2017 | Published 10 October 2017

http://zoobank.org/3B332B5B-DDEC-4EED-B798-0295DA8A4032

Citation: Rázuri-Gonzales E, Holzenthal RW, Ríos-Touma B (2017) Two new species of the rare Neotropical caddisfly genus *Amphoropsyche* Holzenthal (Trichoptera: Leptoceridae). ZooKeys 707: 63–72. https://doi.org/10.3897/zookeys.707.20759

Abstract

Two new species in the rare, endemic Neotropical caddisfly genus *Amphoropsyche* Holzenthal, 1985 are described from Ecuador (*A. carchi* **sp. n.**) and Peru (*A. matsigenka* **sp. n.**) bringing to 17 the number of species known in the genus. Almost all species are known from only a few individuals and from even fewer localities. The new species belong to a group of 10 other species that have tergum X in the male genitalia divided into a mesal process and a pair of lateral processes. *Amphoropsyche carchi* can be separated from those species by the rounded mesal concavity, the short mesobasal lobe, and the short 2nd article of the inferior appendage, while *A. matsigenka* can be diagnosed by the very slender and straight inferior appendage, which bears a pair of spine-like mesoventral projections. We also present a new record for *Amphoropsyche tandayapa* Holzenthal & Rázuri-Gonzales, 2011, from Ecuador, previously known only from the male holotype.

Keywords

Endemic, new species, taxonomy, Ecuador, Peru, Neotropics, male genitalia, Andes, South America

Introduction

The recently published *Catalog of the Neotropical Trichoptera* lists more than 3,200 species occurring in the region of Mexico, the Caribbean, and Central and South America (Holzenthal and Calor 2017). This figure represents an increase in more than 1,000 new species described since the last catalog of the fauna was published, about 20 years ago (Flint et al. 1999). New species continue to be described, especially from unexplored areas (e.g., Quinteiro and Holzenthal 2017; Souza and Santos 2017) indicating that the caddisfly fauna of the Neotropics holds many more species.

In this paper, we add two new species in the genus *Amphoropsyche* Holzenthal, 1985, a member of the long-horned caddisfly family Leptoceridae, to the Neotropical fauna. The family contains more than 221 species in the Neotropics. Eight of the 16 genera occurring in the region are endemic (Holzenthal and Calor 2017). The endemic genus *Amphoropsyche* currently includes 15 species (one further divided into two subspecies), 13 from South America, and the remaining from the Lesser Antilles (Holzenthal and Calor 2017). All these species are very rare; individuals are only very infrequently attracted to UV lights or caught in Malaise traps, standard methods for collecting adult caddisflies, and most of the described species are known from only one or two specimens (Holzenthal and Rázuri-Gonzales 2011, Holzenthal and Ríos-Touma 2016). On the other hand, Flint and Holzenthal observed a large swarm of individuals of *Amphoropsyche woodruffi* Flint & Sykora, 1993 flying during the day above a small shallow stream in Venezuela, indicating that the species in the genus may be day active and not as rare as suggested from light trap collections alone. The larva of only one species is known (Holzenthal 1986) and its life history is unknown. Knowledge of adult behavior is non-existent, except for the swarming behavior observed for *A. woodruffi*. The two new species described in this paper from Ecuador and Peru are known from only 3 individuals, and no biological information was observed.

Material and methods

The Ecuadorian specimen was collected during an ongoing project by the authors and their colleagues to document the Trichoptera fauna of the country while the Peruvian specimens were collected during an inventory carried out prior to the exploitation of the Camisea natural gas reserve in southeastern Peru. Specimens were either collected using UV lights (Ecuadorian specimen) or a Malaise trap (Peruvian). Techniques and procedures used in the preparation and examination of the specimens were outlined by Blahnik and Holzenthal (2004) and Blahnik et al. (2007). The illustrations of the genitalia were prepared from pencil sketches made with the aid of a drawing tube mounted on an Olympus BX41 compound microscope. The pencil sketches were then scanned and placed into an Adobe Illustrator (version CC, Adobe Systems, Inc.) document, to serve as a template, and then digitally drawn to create a vector graphic illustration. A graphic tablet and pen (Intuous TM, Wacom Technology Co.) facilitated careful drawing of the original image.

Terminology used in describing male and female genitalia follows that of Holzenthal and Ríos-Touma (2016). The types will be deposited in the Museo Ecuatoriano de Ciencias Naturales, Quito, Ecuador (MECN) and the Museo de Historia Natural, Universidad Nacional Mayor de San Marcos, Lima, Peru (MUSM), as specified below. Each specimen bears an accession number from the University of Minnesota Insect Collection and the specimen and collection data are stored in the collection's database.

Systematics

***Amphoropsyche carchi* Rázuri-Gonzales, Holzenthal & Ríos-Touma, sp. n.**
http://zoobank.org/B82E8DB8-2F36-4F10-9898-74BED8262B35
Fig. 1

Diagnosis. This species is diagnosed by the structure of the inferior appendage and the phallic apparatus, especially the rounded mesal concavity, the short mesobasal lobe and the short 2nd article of the inferior appendage, and the phallobase with paired apicolateral projections each bearing a short, apical spine-like seta. This new species belongs to a group of 10 species whose males have segment X divided into a mesal process and a pair of lateral processes (*A. ayura* Holzenthal, 1985, *A. cauca* Holzenthal, 1985, *A. choco* Holzenthal, 1985, *A. flinti* Holzenthal, 1985, *A. napo* Holzenthal, 1985, *A. quebrada* Holzenthal, 1985, *A. real* Holzenthal & Ríos-Touma, 2016, *A. spinifera* Holzenthal, 1986, *A. stellata* Holzenthal, 1985, and *A. tandayapa* Holzenthal & Rázuri-Gonzales, 2011). Among these, *A. carchi* sp. n., is most similar to *A. quebrada* based on the structure of the inferior appendage (short 2nd segment, deep mesal concavity in ventral view), but the mesal notch on the preanal appendage of the new species is not as deep as in *A. quebrada.* Additionally, *A. carchi* lacks parameres in the phallic apparatus, but has a pair of apicolateral projections each with an apical spine-like seta, and the lateral process of tergum X in the new species lacks any spine-like setae apically. In the key to males of the genus provided by Holzenthal and Ríos-Touma (2016), the new species will lead to *A. spinifera*, but the paired apicolateral processes of the phallobase are not bifid as they are in *A. spinifera*.

Description. Male. Forewing length 5.5 mm (n=1). Body and legs brown, no discernable color pattern, antennae cream colored (specimen pinned, base of wings slightly denuded). Genitalia as in Fig. 1A–D. Segment IX annular, sternum with anterior margin straight not extended anteriorly (Fig. 1A). Segment X composed of single mesal process and pair of lateral processes (Fig. 1A–B); mesal process very lightly sclerotized, slightly longer than preanal appendages, triangular, apex acute (Fig. 1B); lateral process broadly crescent-shaped, without any spine-like setae; apically, lateral process with about 5-6 small setae (Fig. 1A). Preanal appendages large, oval, fused basally but divided apically to 1/3 their lengths (apical emargination broad); with large reticulate internal gland and small subapicoventral pore (Fig. 1A–B); apically with pair of short, digitate, membranous dorsomesal processes (Fig. 1B). Inferior appendage narrow, elongate, bent

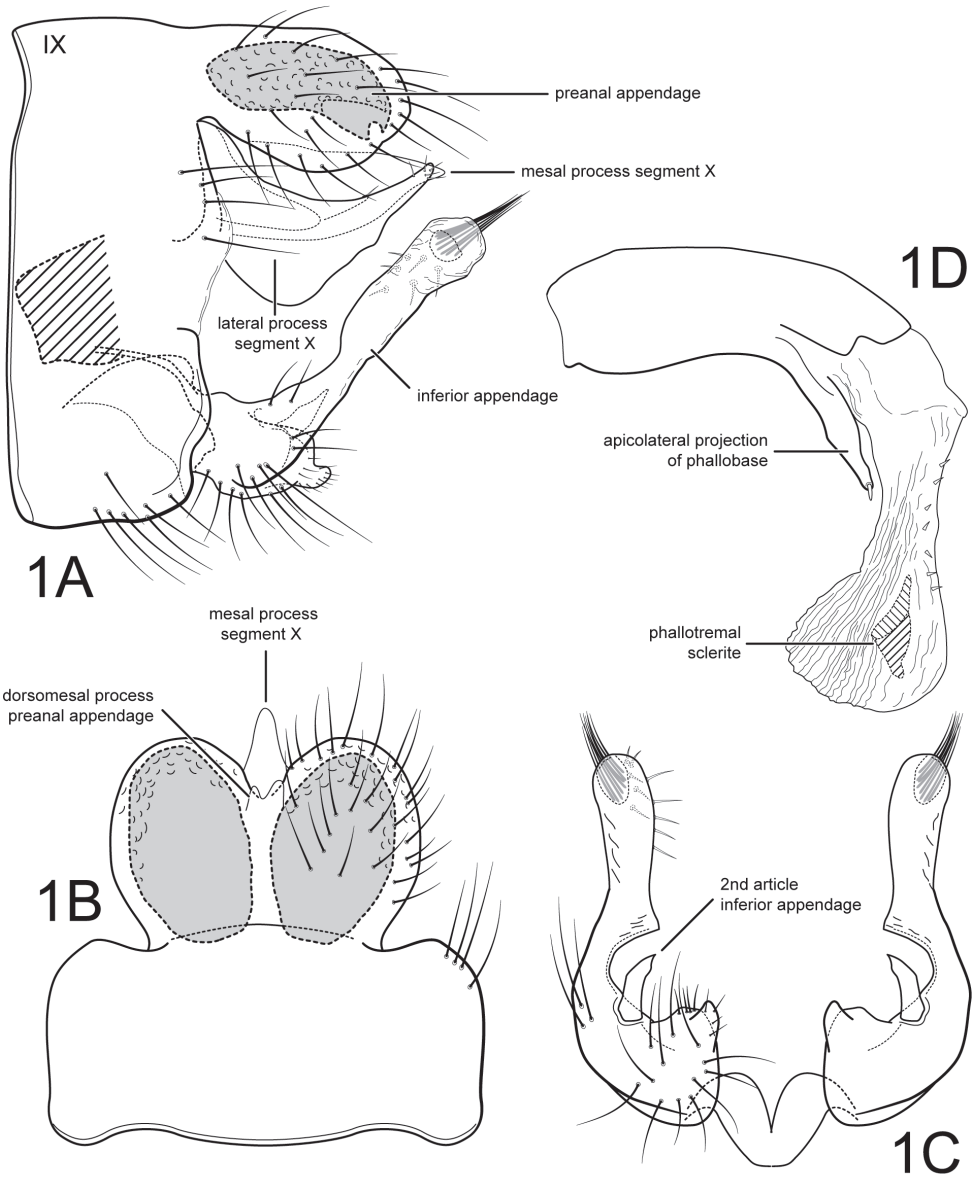

Figure 1. *Amphoropsyche carchi*, new species. Male genitalia **A** segments IX-X, lateral **B** segments IX-X, dorsal **C** inferior appendages, ventral **D** phallus, lateral. IX=abdominal segment IX.

dorsad from base, with short basoventral projection bearing short setae (Fig. 1A, C); in ventral view, with deep, rounded mesal concavity with sharp posterior angle; ending in bulbous, semi-membranous apex, bearing subterminal tuft of closely appressed setae emerging from membranous pocket and with prominent setae on mesal face; 2nd article of inferior appendage short, thin, slightly curved inwards in ventral view, apex

acute; 2nd article sitting on ridge at base of mesal concavity (Fig. 1C). Phallic apparatus (Fig. 1D) with phallobase well-developed, with sclerotized apicolateral projection on each side, bearing stout apical spine-like seta; parameres absent; endothecal membranes well-developed, everted on specimen, with row of small spicules anterodorsally; phallotremal sclerite U-shaped, well-developed, triangular in lateral view.

Holotype. Male. ECUADOR: Carchi: Quebrada San Francisco (Hacienda San Francisco), ca. 1.8 km W Las Juntas, 00.80330°N, 78.17081°W, el. 1241 m, 15.ii.2017, Ríos-Touma & Amigo (UMSP000114269) (MECN).

Etymology. This species is named after the Province of Carchi, where the type was collected.

***Amphoropsyche matsigenka* Rázuri-Gonzales, Holzenthal & Ríos-Touma, sp. n.**
http://zoobank.org/6444085A-E7FC-455D-A4B5-FC42254375B5
Figs 2, 3

Diagnosis. This species is mainly diagnosed by the structure of the inferior appendage, the phallic apparatus, and the mesal process of tergum X. The inferior appendage is very slender and straight and bears a pair of spine-like mesoventral projections. One or both of these spine-like mesoventral projections could represent the 2nd article that has become fused to the body (1st article) of the inferior appendage; however, while these are positioned where the 2nd article occurs in those species that possess one, no indication of articulation or fusion is apparent). The phallic apparatus has a strongly sclerotized apicolateral projection of the phallobase and the endothecal membranes have a pair of lightly sclerotized spine-like projections dorsally. Finally, the mesal process of segment X is elongate, talon-like, curved ventrad apically, and much longer than the preanal appendages. As with *A. carchi* species, this new species is related to the group of species with divided tergum X. It resembles *A. spinifera*, due to the very slender and almost straight inferior appendage, but differs in the spine-like mesoventral projections (if these are interpreted to be the 2nd article, their structure is different). The lateral processes of tergum X are also similar between the 2 species, but the mesal processes are quite different; in *A. spinifera* the process is only slightly shorter than the preanal appendages and the apex is rounded, but in *A. matsigenka* it is much longer than the preanal appendages and the apex is sharply pointed. In the key to males of the genus provided by Holzenthal and Ríos-Touma (2016), *A. matsigenka* will lead to couplet 14 containing *A. cauca* and *A. ayura* if the 2nd article of the inferior appendage is assumed absent, but the new species lacks the phallic parameres found in those species.

Description. Male. Forewing length 5.5 mm (n=1). Body and appendages brown (specimen preserved in 80% ethyl alcohol, wings denuded). Genitalia as in Fig. 2A–D. Segment IX annular, sternum with anterior margin slightly extended anteriorly (Fig. 2A). Segment X composed of single mesal process and pair of lateral processes (Fig. 2A–B); mesal process elongate, talon-like, curved ventrad apically, and much longer than preanal appendage; lateral process broadly crescent-shaped, with spine-like seta subapically on

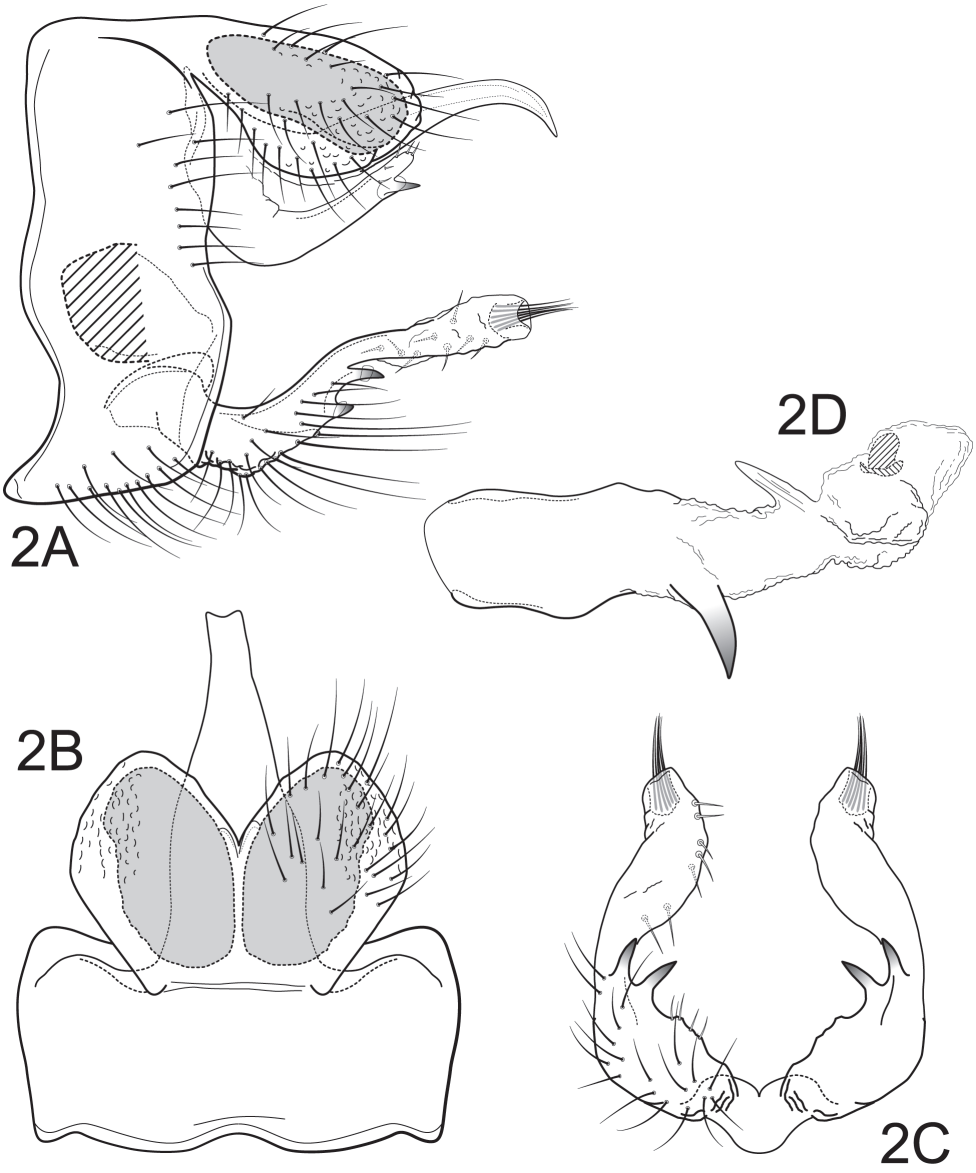

Figure 2. *Amphoropsyche matsigenka*, new species. Male genitalia **A** segments IX-X, lateral **B** segments IX-X, dorsal **C** inferior appendages, ventral **D** phallus, lateral.

ventral margin; apically lateral process with ca. 5 small setae (Fig. 2A). Preanal appendages large, oval, fused basally but divided apically to 1/2 their lengths (apical emargination acute); with large reticulate internal gland and small subapicoventral pore (Fig. 2A–B); apically with pair of very reduced, digitate, membranous dorsomesal processes (Fig. 2B). Inferior appendage narrow, elongate, almost straight, with pair of spine-like mesoventral

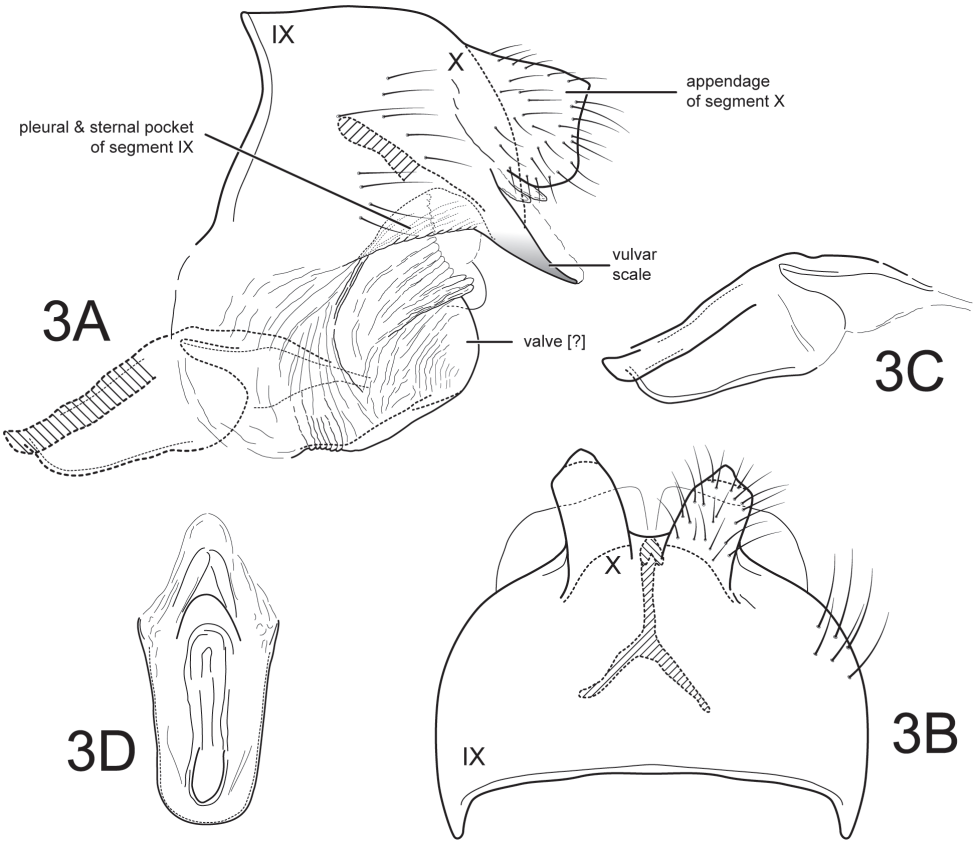

Figure 3. *Amphoropsyche matsigenka*, new species. Female genitalia **A** segments IX-X, lateral **B** segments IX-X, dorsal **C** vaginal apparatus, lateral **D** vaginal apparatus, ventral. IX=abdominal segment IX, X=abdominal segment X.

projections (Fig. 2A, C); in ventral view, concave mesally; ending in bulbous, semimembranous apex, bearing subterminal tuft of closely appressed setae emerging from membranous pocket and with prominent setae on mesal face; 2nd article of inferior appendage absent [or one or both of the spine-like mesoventral projections could represent the 2nd article that has become fused to the first article] (Fig. 2C). Phallic apparatus (Fig. 2D) with phallobase well-developed, with sclerotized apicolateral projection on each side, without apical spine-like seta; parameres absent; endothecal membranes well-developed, everted on specimen, with pair of lightly sclerotized spine-like projections dorsally; phallotremal sclerite U-shaped, well-developed, oval in lateral view.

Female. Forewing length 5.5 mm (n=1). Color and structure similar to male's (specimen preserved in 80% ethyl alcohol, wings denuded). Genitalia as in Fig. 3A–D. Abdominal tergum IX + X complete; dorsomesal margin entire; distinctive Y-shaped sclerite internally. Appendages of segment X quadrate, longer than wider, setose, directed laterad. Valves posterolateral, rounded, wider than longer, bare, but with highly folded membranous surface and prominemt dorsal ridge of folded membrane [these

structures are less evident than the valves in other species so their homology as valves is uncertain]. Vulvar scale thin, more sclerotized than surrounding tissues, narrow in lateral view, round in dorsal view with slight mesal excavation. Pleuron region and sternum IX laterally forming large, prominent pocket-like structure. Vaginal apparatus (spermathecal sclerite complex) (see Fig. 3C, D) with broad, oval, posterior base bearing central "keyhole-shaped" structure; middle region to apex with narrow lightly sclerotized plates and membrane.

Holotype. Male. PERU: Cusco: La Convención, Echarate, Cashiriari-3 [Shell prospecting and development project], 11.86667°S, 72.65°W, el. 690 m, xi-xii.1997, S. Córdoba, (UMSP000114270) (MUSM). **Paratypes:** Same data as holotype, 1 female (UMSP000114271) (MUSM).

Etymology. This species is named after the Matsigenka ethnic group, whose communities are spread throughout the departments of Cusco and Madre de Dios in southeastern Peru, more specifically, the Cashiriari community that inhabits the area where the holotype was collected.

***Amphoropsyche tandayapa* Holzenthal & Rázuri-Gonzales, 2011**
urn:lsid:zoobank.org:act:405CE4BA-B14D-4CEB-827E-BFE295FD12F0

New record. ECUADOR: Pichincha: Bellavista Cloud Forest Reserve and Lodge, small stream, pan trap, 0.01212°S, 78.68958°W, 13–14.vii.2017, el. 2614 m, col. Andrea Tapia, 2 males (MECN).

Discussion

Amphoropsyche matsigenka was collected in the Urubamba River basin, which eventually drains into the Amazon River in northeastern Peru. This new species was collected some 170 km northwest of the only other species known from the country (*A. spinifera*; Flint 1996), which appears to be restricted to the Beni River basin, which also flows into the Amazon in northern Brazil. Conversely, *A. carchi* is only the 2nd species of *Amphoropsyche* known from the western slope of the Andes (*A. tandayapa* is the other), and these 2 species are separated from each other by roughly 100 km. However, the rivers on the Pacific side of the Andes are shorter and do not form extensive watersheds like those on the Amazon slopes, but they can be much more complex. These smaller western watersheds are isolated from one another by the topographical complexity of the Andes and this could have acted as barriers that allowed these 2 species to diverge. On the other hand, the record of *A. spinifera* from the Amazonian slope of Bolivia (Holzenthal 1986) is roughly 956 km SE of the record of the same species from Manu, Peru, indicating that the Amazonian species in the genus are not as isolated and may be more widespread, but probably still restricted to particular basins.

The rarity of the members of this genus limits the study of their diversity, habitat preferences, and life history features, and to date, all additional individuals collected in the northern Andes, on either slope, since Holzenthal's (1985) revision have been new species. *Amphoropsyche matsigenka* is only the 2nd species collected from the large country of Peru since Flint's (1996) record of *A. spinifera*. Similarly, *A. carchi* is the 4th species recorded or described from Ecuador. Even with our recent concentrated efforts to expand the knowledge of Ecuadorian Trichoptera (Ríos-Touma et al. 2017) and our studies in Peru, the localities and the number of individuals known for *Amphoropsyche* are very limited. Given the apparent localized distribution of the species in this genus, it is highly probable that any specimens of this genus discovered in the future will be new to science, especially with increased sampling effort and the exploration of new regions in the other northern and central Andean countries (Bolivia, Colombia, and Venezuela).

Acknowledgements

The authors wish to thank Santiago Villamarín and Christian Villamarín for their hospitality and support during our field studies in Carchi, Ecuador during February of 2017. Xavier Amigo, *Nature Experience*, and Jolanda Huisman also provided very generous support in the field. This study was supported by Universidad de Las Americas project AMB.BRT.17.005 "Diversidad y Distribucion de Trichoptera de Ecuador," Minnesota Agricultural Experiment Station projects MIN-17-017 and 17-029, and USDA National Institute of Food and Agriculture project 1013092. ERG was funded through a doctoral fellowship from Cienciactiva, Consejo Nacional de Ciencia, Tecnologia, e Innovacion Tecnologica Peru (contract 277-2015- FONCECYT). The Ministerio del Ambiente, Ecuador, granted the study permit (MAE-DNB-CM-2016-0045). This support is gratefully acknowledged. We thank Dr Brian Armitage, Dr Tatiana Arefina-Armitage, Dr Ana Previsic, and an anonymous reviewer for providing very useful suggestions to improve the manuscript.

References

Blahnik RJ, Holzenthal RW (2004) Collection and curation of Trichoptera, with an emphasis on pinned material. *Nectopsyche*, Neotropical Trichoptera Newsletter 1: 8–20.

Blahnik RJ, Holzenthal RW, Prather AL (2007) The lactic acid method for clearing Trichoptera genitalia. In: Bueno-Soria J, Barba-Álvarez R, Armitage BJ (Eds) Proceedings of the 12th International Symposium on Trichoptera. The Caddis Press, Columbus, Ohio, 9–14.

Flint OS Jr. (1996) The Trichoptera collected on the expeditions to Parque Manu, Madre de Dios, Peru. In: Wilson DE, Sandoval A (Eds) Manu, the biodiversity of southeastern Peru. Smithsonian Institution, Washington, D.C., 369–430.

Flint OS Jr., Holzenthal RW, Harris SC (1999) Catalog of the Neotropical Caddisflies (Trichoptera). Special Publication, Ohio Biological Survey, Columbus, Ohio, 1–239.

Flint OS Jr., Sykora J (1993) New species and records of caddisflies (Insecta: Trichoptera) from the Lesser Antilles, with special reference to Grenada. Annals of Carnegie Museum 62: 47–62.

Holzenthal RW (1985) Studies in Neotropical Leptoceridae (Trichoptera) II: *Amphoropsyche*, a new genus and species of Leptocerinae from northern South America. International Journal of Entomology 27: 255–269.

Holzenthal RW (1986) Studies in Neotropical Leptoceridae (Trichoptera), a new species of *Amphoropsyche*, with a redescription of the immature stages of *A. insularis* (Flint). Annals of the Entomological Society of America 79: 251–255. https://doi.org/10.1093/aesa/79.1.251

Holzenthal RW, Calor AR (2017) Catalog of the Neotropical Trichoptera (Caddisflies). ZooKeys 654: 1–566. https://doi.org/10.3897/zookeys.654.9516

Holzenthal RW, Rázuri-Gonzales LE (2011) A new species of *Amphoropsyche* (Trichoptera, Leptoceridae) from Ecuador, with a key to the species in the genus. ZooKeys 211: 59–65. https://doi.org/10.3897/zookeys.111.813

Holzenthal RW, Ríos-Touma B (2016) A new Ecuadorian species of the rare Neotropical caddisfly genus *Amphoropsyche* Holzenthal (Trichoptera, Leptoceridae). ZooKeys 640: 59–67. https://doi.org/10.3897/zookeys.640.10344

Quinteiro FB, Holzenthal RW (2017) Fourteen new species of *Oecetis* McLachlan, 1877 (Trichoptera: Leptoceridae) from the Neotropical region. PeerJ 5: e3753. https://doi.org/10.7717/peerj.3753

Ríos-Touma B, Holzenthal RW, Huisman J, Thomson R, Rázuri-Gonzales E (2017) Diversity and distribution of the Caddisflies (Insecta: Trichoptera) of Ecuador. PeerJ 5: e2851. https://doi.org/10.7717/peerj.2851

Souza WRM de, Santos APM (2017) Taxonomic study of the genus *Oxyethira* Eaton 1873 (Trichoptera: Hydroptilidae) from Northeast Brazil: Eleven new species and distributional records. Zootaxa 4236: 484–506. https://doi.org/10.11646/zootaxa.4236.3.4

ZooKeys 707: 73–130 (2017)
doi: 10.3897/zookeys.707.12649
http://zookeys.pensoft.net

MONOGRAPH

A peer-reviewed open-access journal
ZooKeys
Launched to accelerate biodiversity research

Austromonticola, a new genus of broad-nosed weevil (Coleoptera, Curculionidae, Entiminae) from montane areas of New Zealand

Samuel D. J. Brown[1,2]

1 *Bio-Protection Research Centre, PO Box 85084, Lincoln University 7647, Canterbury, New Zealand*
2 *AgResearch, Gerald St, Lincoln, Canterbury, New Zealand*

Corresponding author: *Samuel D. J. Brown* (sam.brown@lincoln.ac.nz)

Academic editor: *M. Alonso-Zarazaga* | Received 17 March 2017 | Accepted 20 August 2017 | Published 10 October 2017

http://zoobank.org/0DF0C91D-3B1D-450D-80F3-F32F8EE7801D

Citation: Brown SDJ (2017) *Austromonticola*, a new genus of broad-nosed weevil (Coleoptera, Curculionidae, Entiminae) from montane areas of New Zealand. ZooKeys 707: 73–130. https://doi.org/10.3897/zookeys.707.12649

Abstract

Austromonticola **gen. n.** is proposed for a group of eight New Zealand alpine broad-nosed weevil species, all of which are here described: *A. atriarius* **sp. n.** (type locality: Umbrella Mountains, Central Otago), *A. caelibatus* **sp. n.** (type locality: Ohau Range, Mackenzie), *A. furcatus* **sp. n.** (type locality: Old Man Range, Central Otago), *A. inflatus* **sp. n.** (type locality: Hawkdun Range, Central Otago), *A. planulatus* **sp. n.** (type locality: St Marys Range, Central Otago), *A. postinventus* **sp. n.** (type locality: Kirkliston Range, South Canterbury), *A. mataura* **sp. n.** (type locality: Mt Dick, Otago Lakes) and *A. rotundus* **sp. n.** (type locality: Old Man Range, Central Otago). All species occur exclusively above 1000 m elevation in the mountains of Central Otago and South Canterbury in the South Island. A phylogeny of the genus, including six outgroups, was inferred from 33 morphological characters. It resolved the genus as monophyletic, and revealed two strongly supported clades within *Austromonticola*. DNA sequences of four gene regions were obtained from five species. Of these, the 3' end of COI proved to be the most suitable for the identification of specimens. Females of all species have diagnostic secondary sexual structures on the elytra and ventrites. These structures are hypothesised to have evolved to assist with oviposition in and beside cushion plants or by selection for structures to mitigate the costs to females of prolonged mating.

Keywords

Biodiversity, taxonomy, alpine, speciation, functional morphology

Introduction

The indigenous entimine weevil fauna of New Zealand currently consists of 28 described genera, containing 247 species. Taxonomic research on these weevils, especially at the genus level, has been dominated by the works of Francis Polkinghorne Pascoe (1875, 1877, 1876a, 1876b), Thomas Broun (1880, 1881, 1886, 1903, 1909a, 1909b, 1911, 1913, 1915, 1921) and David Sharp (1886) in the late 19th and early 20th centuries. Since then, few additional species have been described (Marshall 1926, 1931, 1937; Barratt and Kuschel 1996), and—with the exception of several generic synonyms proposed by Kuschel (1964, 1969, 1972, 1982)—the composition of most New Zealand entimine weevil genera has remained largely unmodified since Broun's (1921) last work on the group. Recent research, however, indicates that understanding of the genus diversity of broad-nosed weevils in New Zealand has been obscured by imprecise and polyphyletic generic concepts (Brown 2017), and many species and genera remain undescribed. This paper describes a new genus of entimine weevils that is restricted to high-alpine vegetation types and whose females exhibit exaggerated ornamentation on the abdominal ventrites.

The mountains of New Zealand are some of the most dramatic and recognisable landscapes of the country. Areas above 1000 m in elevation form a significant proportion of the available land area in the South Island. Geological evidence reveals that these landscapes have been formed relatively recently, with most ranges only appearing in the past five million years (Youngson et al. 1998; Craw et al. 2012). Despite this youth, these alpine regions harbour a rich flora and fauna, which are both endemic to New Zealand and restricted to alpine areas (Mark 2012). The alpine endemic biota include plants (McGlone et al. 2001), birds (Michelsen-Heath and Gaze 2007), lizards (Whitaker 1984; Bell and Patterson 2008), beetles (Leschen and Buckley 2015; Seago et al. 2015), moths (Gaskin 1975; Hoare 2012), cicadas (Buckley and Simon 2007; Dugdale and Fleming 1978), cockroaches (Chinn and Gemmell 2004) and Orthoptera (Trewick et al. 2000; Trewick 2008). Resolving this paradox of distinctive and highly endemic biota in a recent landscape has been a research priority in recent decades (Heenan and McGlone 2013; Buckley and Simon 2007; Winkworth et al. 2005).

Materials and methods

Field collected specimens were killed in 100% ethanol or placed directly into a freezer at -20°C. Ethanol-preserved specimens were used preferentially for DNA extraction and sequencing.

Genitalia were examined by softening specimens for a short time in warm water, before removing the abdomen by inserting fine forceps between the metaventrite and ventrite 1. The abdomen was digested in porcine pancreatin enzyme solution for c. 36 h (Álvarez Padilla and Hormiga 2008), the lysate of which was subsequently used

for DNA extraction. If specimens had not cleared satisfactorily at the end of this time, or were unsuitable for DNA extraction, abdomens were digested in room-temperature 10g/l KOH for up to two hours.

After clearing, the abdomen was flayed by cutting down the right side of the abdomen with spring scissors. Male genitalia were removed by severing the strong ligaments connecting sternite 8 to tergite 8, then cutting through the pretegminal membrane between the phallobase and the anus. Female genitalia were stained briefly by immersion in a 1g/l solution of Chlorazol Black in 70% ethanol, then removed by cutting through the membranes connecting tergites 7 and 8. Sternite 8 and tergite 8 were separated from the gonocoxites by cutting through their connecting membranes. Genitalia were photographed, then mounted on a card using dimethyl hydantoin formaldehyde (DMHF) (Liberti 2005), which was then pinned below the specimen.

Genitalia illustrations were prepared from photographs, using the program Inkscape (v. 0.91, Inkscape Team 2004-2017). Other line drawings were made with a Zeiss Stemi SV6 stereo microscope fitted with a camera lucida. These drawings were scanned and inked digitally in Inkscape. Habitus photographs were taken using a Nikon DS-Ri1 microscope fitted with a digital camera and a mechanical z-stepper. The program Nikon NIS Elements v. 4.10 was used to prepare the image stack and to produce the final montaged image.

Terminology follows Oberprieler et al. (2014), Lawrence et al. (2010) and Wanat (2007). Body length was measured in lateral view, from the anterior margin of the eyes to the apex of the elytra. Rostrum width was measured across the antennal insertions in dorsal view. Legs are described in their idealised laterally extended position, thereby having dorsal, ventral, anterior and posterior surfaces. Everted ovipositors were measured from the centre of the ovipositor level with the apices of sternite 8 and tergite 8, to the apex of the gonocoxites. Pappolepidia (Brown 2017) are multiply finely divided scales (Fig. 114, "multifid hairs" of Kuschel 1969), found in abundance on the abdominal and thoracic ventrites of some species. The term 'dolabriform' is used to describe relatively short, broad scales that have a similar shape to an adze blade (Torre-Bueno 1979).

Descriptions of colour follow the terminology provided by the National Bureau of Standards (Kelly and Judd 1976). The NBS centroid colours are a comprehensive dictionary of colours, with natural-language descriptions. Digital representations of these colours have been provided by Jaffer (2011). The difference in colour contrast between elongate setiform scales ('setae') and their surrounding appressed scales is given using the rough descriptors `pale', `concolorous' and `dark'.

Specimens were prepared for scanning electron microscopy (SEM) by separating the abdomen from the specimen, removing the tergites and genitalia and brushing down the sternites. Specimens were then air-dried before being mounted with double-sided carbon tape onto aluminium SEM stubs (11 mm high, 12 mm diameter). Specimens were coated with gold using a Emitech K975X sputter coater. Photographs were taken using a JEOL JSM-7000F field emission scanning electron microscope (JEOL, Tokyo, Japan), with an accelerating voltage of 3 kV.

Specimens were obtained and deposited in the following collections:

AMNZ	Auckland War Memorial Museum, Auckland, New Zealand
ANIC	Australian National Insect Collection, CSIRO, Canberra, Australia
CMNZ	Canterbury Museum, Christchurch, New Zealand
IACC	Invermay Agricultural Centre Collection, Mosgiel, New Zealand
LUNZ	Lincoln University Entomology Research Museum, Lincoln, Canterbury, New Zealand
MONZ	Te Papa Tongarewa, National Museum of New Zealand, Wellington, New Zealand
NHM	The Natural History Museum, London, United Kingdom
NZAC	New Zealand Arthropod Collection, Manaaki Whenua Landcare Research, Tamaki, Auckland, New Zealand
USNM	Smithsonian Institution National Museum of Natural History, Washington D.C., United States of America

Label data of holotypes are transcribed using the following conventions. Data of individual labels are enclosed using quotes ('…'), lines are indicated with a solidus (/) and metadata are given in square brackets ([…]).

Two-letter area codes follow the bioregionalisation system proposed by Crosby et al. (1998). The following codes are used in this paper; CO (Central Otago), MK (Mackenzie), OL (Otago Lakes), SC (South Canterbury). Coordinates given after the locality names are in the WGS84 datum. Coordinates tagged "R" (Recorded) were obtained from coordinates on the label when given or from consultation with the collector. Coordinates tagged "A" (Approximate) were determined by using available gazetteers, primarily the New Zealand Gazetteer of Place Names (Land Information New Zealand 2016). These georeferenced data were used to extract estimated elevations from 25 m resolution digital elevation models of New Zealand provided by Landcare Research (Landcare Research 2010a, 2010b).

A generative conception of species (Wilkins 2009) is followed, where morphological data are used as the primary criteria to justify inclusion within each species. Species are defined by character sets that allow differentiation between groups that form diagnosable entities. These taxa are recognised as phenomena that require explanation through further evolutionary and ecological study (Wilkins 2010).

Data resources

Occurrence data from the specimens examined in this paper are deposited at GBIF, the Global Biodiversity Information Facility, http://ipt.pensoft.net/resource.do?r=austromonticoladistribution. DNA alignments and analysis scripts are available from FigShare, http://dx.doi.org/10.6084/m9.figshare.5367457

Table 1. Markers and PCR primer combinations used in this research.

Marker	Primer name	Direction	Primer sequence	Reference
COI	C1-J-2183	Forward	5'-CAA CAT TTA TTT TGA TTT TTT GG-3'	Simon et al. 1994
	LCO1490-JJ	Forward	5'-CHA CWA AYC ATA AAG ATA TYG G-3'	Astrin and Stüben 2008
	HCO2198-JJ	Reverse	5'-AWA CTT CVG GRT GVC CAA ARA ATC A-3'	Astrin and Stüben 2008
	TL2-N-3014	Reverse	5'-TCC AAT GCA CTA ATC TGC CAT ATT A-3'	Simon et al. 1994
28S	S3660	Forward	5'-GAG AGT TMA ASA GTA CGT GAA AC-3'	Sequeira et al. 2000
	28S-Ff	Reverse	5'-TTA CAC ACT CCT TAG CGG AT-3'	Gómez-Zurita et al. 2005
ArgK	ArgKforB4	Forward	5'-GAY CCC ATC ATC GAR GAC TAC C-3'	McKenna et al. 2009
	ArgKrevB1	Reverse	5'-TCN GTR AGR CCC ATW CGT CTC-3'	McKenna et al. 2009
CAD	CADfor4	Forward	5'-TGG AAR GAR GTB GAR TAC GAR GTG GTY CG-3'	Jordal et al. 2011
	CADrev1mod	Reverse	5'-GCC ATY RCY TCB CCY ACR CTY TTC AT-3'	Jordal et al. 2011

DNA sequencing and analysis

Only freshly collected specimens were used for sequencing. Genomic DNA was extracted from the pancreatin lysate (see above) using the Zymo Quick g-DNA Miniprep Kit (Zymo Research Corporation, Irvine, CA, U. S. A.), following the manufacturer's instructions for a proteinase k extraction. Four gene regions were sequenced: the cytochrome *c* oxidase subunit I (COI) mitochondrial gene, the D2-D3 region of the 28S ribosomal RNA gene, the nuclear protein-coding gene arginine kinase (ArgK) and the nuclear protein-coding carbamoyl-phosphate synthetase 2-aspartate transcarbamylase-dihydroorotase (CAD) gene.

DNA was amplified using a 25 µl polymerase chain reaction (PCR) consisting of 1.25 U iStar Taq (iNtRON Biotechnology, Seongnam, South Korea), 0.4 mM dNTP, 1.5 mM $MgCl_2$ and 0.2 µM of forward and reverse primers (Table 1). The COI primer combination LCO1490-JJ/TL2-N-3014 was used preferentially in order to amplify the whole gene, which was then sequenced using all four primers. If amplification using this combination was unsuccessful, C1-J-2183/TL2-N-3014 was used. Reactions were run on a C1000 Touch thermal cycler (Bio-Rad Laboratories Inc., Hercules, CA, USA) or a MJ Mini thermal cycler (Bio-Rad Laboratories Inc.) with an initial denature at 94 °C for 2 min, followed by 40 cycles at 94 °C (20 s), variable annealing temperature (20 s) and 72 °C (60 s), and with a final extension at 72 °C for 5 min. Annealing temperatures were 45 °C for COI, and 52 °C for 28S reactions. ArgK and CAD reactions were amplified using a touchdown protocol, with annealing temperatures starting at 50 °C, decreasing by 1 °C per cycle for 5 cycles, followed by 35 cycles at 45 °C. Purified PCR products were sequenced by Macrogen (Seoul, Korea) using ABI BigDye 3.1 technology on an ABI3730XL platform (Applied Biosystems).

Sequences were aligned by eye in Seaview (version 4.5.4) (Guoy et al. 2010). Uncorrected genetic distances (*p*-distances) were calculated using Ape (version 3.5) (Paradis et al. 2004), which were then decomposed into interspecific and intraspecific components using Spider (version 1.4-2) (Brown et al. 2012). Diagnostic nucleotides (Sarkar et al. 2008) for each species were identified using Spider.

Table 2. Character matrix for cladistic analysis of relationships within *Austromonticola*.

Taxon	1	6	11	16	21	26	31
Austromonticola atriarius	02100	00100	11000	11011	10010	01101	11?
Austromonticola caelibatus	12101	00010	00001	1?21?	0????	???01	021
Austromonticola furcatus	02101	00100	11000	01011	10010	11101	111
Austromonticola inflatus	12101	00010	00001	01210	00110	11101	021
Austromonticola planulatus	12100	00000	00000	10211	01010	01111	011
Austromonticola postinventus	12101	00010	00001	01210	00110	01101	021
Austromonticola mataura	02101	00100	11000	11011	10010	11101	111
Austromonticola rotundus	02101	00100	00000	10011	00010	01111	01?
Irenimus parilis	00110	00001	00000	10000	01021	00020	000
Brachyolus punctatus	00010	01000	00000	00100	01000	00000	010
Inophloeus sulcifer	11001	01000	01110	00100	01011	00001	011
Zenagraphus metallescens	11000	11000	00110	00000	01011	02100	010
Inophloeus sternalis	10000	01001	00000	10100	00021	00001	021
Undescribed genus and species	11000	10000	1001?	00100	00010	00120	021

Morphological phylogenetic analysis

A total of 33 morphological characters were scored for 14 species (Table 2), including six outgroup taxa: *Irenimus parilis* Pascoe, 1876, *Brachyolus punctatus* White, 1846, *Inophloeus sulcifer* Broun, 1886, *Zenagraphus metallescens* Broun, 1915, "*Inophloeus*" *sternalis* Broun, 1904, and an undescribed genus and undescribed species represented by specimens collected from Chancellor Hut, Fox Glacier, Westland Te Poutini National Park. Specimens of this last taxon have been deposited in NZAC with specimen numbers IRE7143, IRE7144, IRE7145 and IRE7147.

The phylogenetic matrix was prepared using Mesquite (version 3.10) (Maddison and Maddison 2016). Parsimonious cladograms were inferred using the parsimony ratchet (Nixon 1999), as implemented in Phangorn (version 2.0.4) (Schliep 2011), using Fitch parsimony with a random starting tree and subtree pruning and regrafting (SPR) rearrangements. The ratchet was run 100 times to ensure thorough sampling of the treespace. Bootstrap and jackknife (delete-half method, Felsenstein 2004) support values were calculated using Phangorn with 100 replicates each. Due to *A. planulatus*, *A. caelibatus* and *A. postinventus* not having suitable specimens available for DNA sequencing, morphological and sequence data were not combined.

Taxonomic treatment

Austromonticola **Brown, gen. n.**
http://zoobank.org/51010275-E6EE-47B9-B84B-1D868054AD07

Type species. *Austromonticola mataura* new species, here designated. Gender: masculine.

Diagnosis. Integument densely covered with small, grey appressed scales, elongate setiform scales ('setae') conspicuous along elytral interstriae. Rostrum stout, in dorsal

view about 1.5 times longer than wide; subparallel proximally; scrobes lateral; ventral curvature with head capsule approximately 90°. Pronotum in dorsal view evenly convex. Elytra with small, shallow punctures, interstriae flat. Metanepisternal sutures complete. Metatibiae with apex simple. Penis tubular. Bursa copulatrix with a single sclerite.

Differential diagnosis. The combination of characters given above allows separation of *Austromonticola* from all other New Zealand weevils. The complete metanepisternal sutures distinguish them from *Chalepistes* Brown, 2017, in which the sutures are lacking. The abrupt 90° deflexion of the rostrum distinguish them from *Catoptes* Schönherr, 1842, which has a smoothly deflexed rostrum, angled about 120° with the ventral surface of the head capsule. The ridged appressed scales, conspicuous setae, evenly convex pronotum and small strial punctures separate *Austromonticola* from species of *Inophloeus* Pascoe, 1875 and *Zenagraphus* Broun, 1915, which have smooth appressed scales, inconspicuous setae, sculptured pronota and large, deep strial punctures. The subparallel rostrum and lateral scrobes, distinguish *Austromonticola* from *Nicaeana* Pascoe, 1877 and *Haplolobus* Broun, 1893, which have proximally widening rostra and dorsally situated scrobes.

Description. Body length ranging from 3.4 mm to 8.9 mm. Densely covered with appressed scales on all surfaces, interspersed with elongate setiform scales ('setae'); appressed scales on dorsum oval, 35–55 μm long, ridges visible at 30 × magnification, generally coloured bluish grey, brownish grey or blackish grey, easily abraded. **Rostrum**. Subparallel proximally in dorsal view, widened at antennal insertions. Epistome punctate, plurisetose, slightly raised above frons but separation indistinct. Epifrons with longitudinal median carina, lacking sulci; continuous with occiput, without distinct dorsal separation between head capsule and rostrum. **Antennae**. Sockets dorsolateral, situated in apical 1/3 of rostrum. Scapes clavate, reaching posterior margin of eye in repose. Funicular segments clavate, subspherical or oblately spheroid, moderately to loosely articulated, segments 7 almost as wide as club. Clubs two times longer than wide, tapering apicad. **Head capsule**. Interocular width in dorsal view greater than width of rostrum at base. Eyes large, lateral, flat, ovate to subcircular with long axis vertical, parallel with sagittal axis. Ventral curvature of head capsule and rostrum in lateral view angulate, approximately 90°. **Pronotum**. Disc in dorsal view smooth, evenly convex. Postocular lobes poorly to well developed; fringed with numerous short vibrissae attaining a maximum length of 1/3 times anterior-posterior length of eye. **Elytra**. In dorsal view approximately parallel-sided in anterior 2/3. Setae arising from interstriae. Elytral declivity in lateral view rounded in males, but sutural margin at top of declivity developed into tubercles in females of several species. Interstriae 3 above the declivity slightly swollen in both sexes of most species, interstriae 5 above the declivity rarely swollen. Ventral margin in lateral view sinuous, highest point near level of metacoxae. **Thorax**. Procoxae contiguous. Prosternum visible behind procoxae as a raised tubercle ("prosternellum"). Metaventrite with median suture visible only as a small, circular fovea posteriorly. Metanepisternal sutures complete. **Abdomen**. Ventrites 1 and 2 fused, subequal in length in middle; ventrites 3 and 4 subequal in length, approximately 0.5 times shorter than 1 or 2; ventrite 5 approximately equal in length to 1 or 2. Suture separating ventrites 1 and 2 curved anteriad in middle, other sutures straight. **Wings**. Absent. **Legs**. Uniformly and densely covered with appressed scales and setae, except for the posterior

surface of the metafemora. Femora unarmed, maximum girth at about distal quarter. Pro- and mesotibiae with indistinct denticles along ventral margin and mucrones at apex; protibiae wider in distal 1/3 than proximal 1/3, incurved at apex. Metatibiae with dorsal and ventral margins subparallel; apical setal comb arcuate, pale; mucrones small, inconspicuous; without corbel. Tarsi with long, coarse setae on dorsal surface, without appressed scales; underside of segments 1 to 3 with short, dense setae forming pads medially divided by an inconspicuous glabrous line. Claws simple, separate, diverging. **Male genitalia**. Hemisternites 8 fully separate, with a forked membranous sclerite on the anterior margin of the membrane connecting them ('spiculum relictum', Thompson 1992; Wanat 2007; Franz and Cardona-Duque 2013). Penis with pedon tubular, strongly curved, lateral lobes meeting or narrowly separated dorsally; temones shorter than pedon. Endophallus moderate in length, usually reaching anterior 1/3 of temones when in repose; armed with a variably-shaped sclerite surrounding the primary gonopore ('gonoporial sclerite'), other sclerites variably present. Tegmen with ring complete; parameroid lobes moderately developed, 0.35 times length of manubrium (Figs 85, 86); manubrium shorter than temones. **Female genitalia**. Sternite 8 with spiculum ventrale more than twice as long as blade. Gonocoxites divided into two parts; proximal part about 2.3 times longer than distal part, largely unsclerotised except for a strongly sclerotised rod; rods ventrally situated, broadening at proximal end; distal gonocoxite moderately sclerotised. Bursa copulatrix with a single sclerite.

Distribution. Restricted to alpine regions in Otago and South Canterbury, New Zealand.

Etymology. Derived from the Latin *australis*, meaning 'southern' and *monticola*, meaning 'mountain dweller', alluding to the habitat of the species of this genus, being confined to the mountains of the southern part of the South Island. Gender masculine.

Biology. Specimens of the genus have been collected in fellfield and cushionfield vegetation communities (Mark, 2012), commonly on top of, and close beside, cushion plants of the genera *Phyllachne* J. R. et G. Forst., 1776 (Stylidiaceae), *Scleranthus* L., 1753 (Caryophyllaceae), *Veronica* L., 1753 (Plantaginaceae), *Hectorella* Hook. f., 1864 (Montiaceae), *Dracophyllum* Labill., 1798 (Ericaceae) and *Raoulia* Hook. f., 1846 (Asteraceae), particularly when the plants have been in flower. Some species have also been found under specimens of *Celmisia* Cass., 1825 (Asteraceae) and *Geum* L., 1753 (Rosaceae). The larvae are as yet unknown.

Most specimens have been collected by hand collecting, though some have been captured in pitfall traps or by heat extraction from litter and turf samples.

Austromonticola atriarius Brown, sp. n.

http://zoobank.org/3E3220A4-9418-4B2E-A080-F7E48B50FBF2
Figs 1, 2, 17, 18, 39, 40, 41, 42, 43, 44, 45, 100, 101, 116

Diagnosis. Body size medium, 4 mm in length. Pronotum with median furrow. Elytral declivity in females with sutural tubercle; margin of ventrite 4 produced into a

lamina, with bifurcate median process (Fig. 100); margin of ventrite 5 with a slim horn on either side of genital opening (Fig. 100).

Description. Body length 3.60 mm to 4.55 mm ($\bar{X}$ = 4.19 mm, s = 0.36, n = 8). Integument black. Dorsum densely covered with moderate yellowish brown to greyish brown appressed scales, pale "V" on elytral declivity often present; pronotum same colour as elytra, with pale posterolateral maculae lining up with pale maculae on humeral angles of elytra, especially prominent in females. Femora and tibiae with dense appressed scales concolorous with elytral scales, usually with pale band in distal 1/4 of femora. Tarsi with integument deep orange. **Rostrum**. Length 0.72 mm to 0.96 mm ($\bar{X}$ = 0.85 mm, s = 0.09, n = 7), width 0.52 mm to 0.65 mm ($\bar{X}$ = 0.59 mm, s = 0.05, n = 7), length/width ratio 1.33 to 1.55 ($\bar{X}$ = 1.44, s = 0.07, n = 7). Epifrons with appressed scales imbricate; setae dolabriform, decumbent, dark; median and lateral carinae not evident. Dorsal carinae arched over antennal insertions. Lateral area ventral of antennal insertions with thick setae, without appressed scales. **Antennae**. Scapes in repose reaching hind margin of eye; covered with appressed scales and setae. Funicular segments moderately articulated; segments 1 clavate, subequal in length to 2; segments 2 clavate, about two times longer than 3; segments 3 to 4 clavate; segments 5 to 7 oblately spheroid. **Pronotum**. Length 1.07 mm to 1.29 mm ($\bar{X}$ = 1.16 mm, s = 0.09, n = 7), width 1.58 mm to 2.08 mm ($\bar{X}$ = 1.88 mm, s = 0.20, n = 7), length/width ratio 0.77 to 0.97 ($\bar{X}$ = 0.87, s = 0.07, n = 7); in dorsal view widest in anterior 1/4, lateral margins evenly curved. Anterior margin slightly emarginate medially, posterior margin straight. Disc in dorsal view evenly convex, with median furrow; appressed scales imbricate; setae dolabriform to claviform, decumbent, dark to concolorous. Postocular lobes moderately developed. **Elytra**. Length 2.40 mm to 3.09 mm ($\bar{X}$ = 2.78 mm, s = 0.26, n = 7), width 1.58 mm to 2.08 mm ($\bar{X}$ = 1.88 mm, s = 0.20, n = 7), length/width ratio 1.39 to 1.61 ($\bar{X}$ = 1.48, s = 0.08, n = 7). Anterior margin curved posteriad in middle, humeral angles rounded. Appressed scales imbricate. Setae claviform, decumbent, concolorous. Striae moderately impressed; interstriae slightly convex. Interstriae 1 at declivity flat in males, produced into a tubercle in females. Interstriae 3 and 5 at declivity swollen in both sexes. Apex in lateral view square in males; produced ventrad in females. **Thoracic ventrites**. Mesoventral process rounded. Mesanepisterna, mespimera, metanepisterna and metaventrite densely clothed with pappolepidia. **Abdomen**. Ventrites sparsely clothed, appressed scales most numerous medially, pappolepidia becoming dominant laterally. Apex rounded. Males with ventrite 1 strongly depressed medially; ventrite 5 flat. Females with ventrite 1 flat; ventrite 4 with posterior margin produced medially into a bifurcated lamina (Figs 100, 101); ventrite 5 with median furrow, posterior margin broadly emarginate with a strong horn on either side of emargination. **Male genitalia**. Figs 39, 40. Penis with apex acute, upturned; ostial region thickened, forming a crest. Endophallus with lightly sclerotised plate proximally from primary gonopore, gonoporial sclerite large, with distinct posterior lobes. Temones 0.72 times as long as pedon. **Female genitalia**. Figs 41–45. Distal gonocoxites slender, 2.7 times longer than high. Bursa copulatrix long; not constricted anteriorly of proximal gonocoxite; sclerite horseshoe-shaped,

squat. Sternite 8 narrowly rounded apically, membranous laterally. Everted ovipositor 3.44 mm in length, 0.75 times body length.

DNA sequences. COI. KX191432. **28S**. KX192009. **ArgK**. KX191719. **CAD**. KX191161.

Type material examined. Holotype. Female (NZAC). Specimen mounted on card teardrop; abdomen removed, dissected and mounted in DMHF on white card below specimen; otherwise entire; elytra parted at apex. Labelled 'NEW ZEALAND CO / Gem Lake / Umbrella Mountains / 10 Feb 2014 / SDJ Brown' [printed, cream card], 'On *Phyllachne* cushion / 1430 m / 45.5703°S, 169.1021°E [printed, cream card], '*Irenimus* taxonomy / and systematics / SDJ Brown / PhD Thesis 2012–2015 / IRE4875' [printed, cream card], 'HOLOTYPE / *Austromonticola* / *atriarius* / Brown 2017' [printed, red card]. Genomic DNA extract from enzyme digestion of abdomen: E300 (NZAC). CAD sequence KX191167; COI sequence KX191438; ArgK sequence KX191722; 28S sequence KX192015.

Paratypes. A total of 7 specimens (4 males, 3 females) designated as paratypes, bearing blue paratype label. Paratype specimens deposited in NHM, IACC, LUNZ, NZAC.

CO. Gem Lake [45°34.236'S, 169°6.384'E, A], 14–15 Dec 1985, Barratt BIP, 1300 m (NHM: 1); Gem Lake [45°34.236'S, 169°6.384'E, A], 14–15 Dec 1985, Barratt BIP, 1400 m (IACC: 1); Gem Lake [45°34.236'S, 169°6.384'E, A], 15 Dec–15 Jan 1986, Barratt BIP, 1430 m (NHM: 1, IACC: 1, LUNZ: 2, NZAC: 1).

Distribution. Fig. 116. South Island: **CO**: Umbrella Mountains.

Elevational range. Label data: 1300 m to 1430 m ($\bar{X}$ = 1410 m, s = 46, n = 8). Georeferenced data: 1297 m to 1423 m ($\bar{X}$ = 1313 m, s = 44, n = 8).

Etymology. From the Latin noun *atriarius*, 'porter, doorkeeper', in reference to the armature surrounding the female genital opening and alluding to a possible function of preventing unwanted mating attempts. The name is a noun in apposition.

Biology. Found in cushionfield, with a single specimen recorded in association with *Phyllachne*.

Austromonticola caelibatus Brown, sp. n.

http://zoobank.org/423B4D86-6AD7-4214-8A57-0B21CC7670B0
Figs 15, 16, 46, 47, 48, 49, 115

Diagnosis. Body size large, 8 mm in length. Epifrons flat, with semi-erect setae. Funicle segments 7 subconical. Pronotum evenly convex. Elytra with erect, piliform setae.

Description. Body length 7.83 mm to 8.91 mm ($\bar{X}$ = 8.28 mm, s = 0.41, n = 5). Integument black. Dorsum densely covered with fine blackish blue appressed scales without metallic reflections. Femora and tibiae with appressed scales, unicolorous, concolorous with elytral scales. Tarsi with integument blackish red. **Rostrum**. Length 1.60 mm to 1.72 mm ($\bar{X}$ = 1.65 mm, s = 0.05, n = 5), width 0.80 mm to 1.00 mm ($\bar{X}$ = 0.94 mm, s = 0.08, n = 5), length/width ratio 1.68 to 2.04 ($\bar{X}$ = 1.77, s = 0.15, n

= 5). Epifrons with appressed scales tessellate; setae piliform, semi-erect, concolorous; median and lateral carinae evident. Dorsal carinae arched over antennal insertions. Lateral area ventral of antennal insertions with fine setae and appressed scales. **Antennae**. Scapes in repose reaching beyond hind margin of eyes; covered with appressed scales and setae. Funicular segments loosely articulated; segments 1 clavate, roughly as long as 2; segments 2 clavate, about two times longer than 3; segments 3 to 6 clavate, getting progressively shorter; segments 7 subconical. **Pronotum**. Length 1.90 mm to 2.24 mm ($\bar{X}$ = 2.05 mm, s = 0.13, n = 5), width 3.08 mm to 3.25 mm ($\bar{X}$ = 3.16 mm, s = 0.07, n = 5), length/width ratio 0.88 to 1.02 ($\bar{X}$ = 0.94, s = 0.05, n = 5); in dorsal view widest in anterior 1/3, lateral margins evenly curved. Anterior margin entire, posterior margin straight. Disc in dorsal view evenly curved; appressed scales tessellate; setae piliform, semi-erect, concolorous. Postocular lobes moderately developed. **Elytra**. Length 5.15 mm to 5.61 mm ($\bar{X}$ = 5.36 mm, s = 0.23, n = 5), width 3.08 mm to 3.25 mm ($\bar{X}$ = 3.16 mm, s = 0.07, n = 5), length/width ratio 1.63 to 1.76 ($\bar{X}$ = 1.70, s = 0.05, n = 5). Anterior margin slightly curved posteriad in middle, humeral angles rounded. Appressed scales tessellate. Setae piliform, semi-erect to erect, concolorous on disc, pale laterally and posteriorly. Striae moderately impressed; interstriae flat. Interstriae 1 at declivity flat in males; females unknown. Apex in lateral view square in males; females unknown. **Thoracic ventrites**. Mesoventral process rounded. Sutures between mesepimera and metanepisterna raised into a carina. Metaventrite densely covered with appressed scales. **Abdomen**. Ventrites sparsely clothed with appressed scales. Apex rounded. Males with ventrite 1 depressed medially, ventrite 5 flat. Females unknown. **Male genitalia**. Figs 46–49. Hemisternites with spiculum relictum large, bulbous and strongly pigmented. Penis with apex acute, upturned; ostial region unmodified. Endophallus with small gonoporial sclerite with reduced posterior lobes. Temones 0.52 times as long as pedon. **Female genitalia**. Unknown.

DNA sequences. No DNA sequences obtained.

Type material examined. Holotype. Male (CMNZ). Specimen pinned through right elytron; entire. Labelled '3832 Lake Ohau Ski Field / 1600–1650 m Johns, PM; / Nicholls, D 15.i.04' [printed, cream card], '2007.215.2060' [printed, white card], '*Irenimus* taxonomy / and systematics / SDJ Brown / PhD Thesis 2012–2015 / IRE4031' [printed, cream card], 'HOLOTYPE / *Austromonticola* / *caelibatus* / Brown 2017' [printed, red card].

Paratypes. A total of 4 specimens (4 males) designated as paratypes, bearing blue paratype label. Paratype specimens deposited in CMNZ.

MK: Lake Ohau Ski Field [44°13.44'S, 169°46.59'E, A], 15 Jan 2004, Johns PM, Nicholls D, 1600-1650 m (CMNZ: 4).

Distribution. Fig. 115. South Island: **MK**: Lake Ohau Ski Field.

Elevational range. Label data: 1625 m (n = 5). Georeferenced data: 1574 m (n = 5).

Etymology. From the Latin noun *caelibatus*, 'celibacy', an allusion to the fact that the species is thus far known only from the male sex; the species name is a noun.

Biology. No plant associations recorded.

***Austromonticola furcatus* Brown, sp. n.**
http://zoobank.org/0B3B6FC4-0CC0-4F66-8D01-C54894022B56
Figs 5, 6, 21, 22, 37, 50, 51, 52, 53, 54, 55, 56, 57, 102, 103, 116

Diagnosis. Body size medium, 4 mm in length. Dense pappolepidia on venter. Elytral declivity in females with sutural tubercle; margin of ventrite 4 produced into a lamina, with deep median emargination (Fig. 102); margin of ventrite 5 with a broad horn on either side of the genital opening (Fig. 102).

Description. Body length 3.67 mm to 4.22 mm ($\bar{X}$ = 3.98 mm, s = 0.19, n = 8). Integument black. Dorsum densely covered with brownish black to dark greyish yellowish brown appressed scales; pale "V" on elytral declivity largely confined to summits of protuberances; other pale variegations usually present on elytra, not forming patterns. Scutellum densely covered with pale scales. Pronotum same colour as elytra; with striking, pale, posterolateral maculae corresponding to pale maculae on humeral angles, especially in females. Femora and tibiae with appressed scales dense, unicolorous, concolorous with elytral scales. Tarsi integument dark reddish orange to black. **Rostrum**. Length 0.77 mm to 1.04 mm ($\bar{X}$ = 0.90 mm, s = 0.09, n = 7), width 0.52 mm to 0.66 mm ($\bar{X}$ = 0.57 mm, s = 0.05, n = 7), length/width ratio 1.35 to 1.68 ($\bar{X}$ = 1.57, s = 0.11, n = 7). Epifrons with appressed scales imbricate; setae dolabriform, decumbent, concolorous; median and lateral carinae not evident. Dorsal carina arched over antennal insertions. Lateral area ventral of antennal insertions with fine setae, without appressed scales. **Antennae**. Scapes in repose reaching hind margin of eyes; covered with appressed scales and setae. Funicular segments moderately articulated; segments 1 clavate, about 1.25 times longer than 2; segments 2 clavate, about 1.4 times longer than 3; segments 3 to 4 subspherical; segments 5 to 7 oblately spheroid, subequal in length. **Pronotum**. Length 1.06 mm to 1.24 mm ($\bar{X}$ = 1.14 mm, s = 0.06, n = 7), width 1.61 mm to 2.16 mm ($\bar{X}$ = 1.88 mm, s = 0.18, n = 7), length/width ratio 0.80 to 0.92 ($\bar{X}$ = 0.86, s = 0.04, n = 7); in dorsal view widest in anterior 1/4, lateral margins strongly curved anteriorly, tapering posteriorly, more pronounced in females. Anterior margin slightly emarginate medially, posterior margin straight. Disc in dorsal view evenly curved; appressed scales imbricate; setae dolabriform, decumbent, dark to concolorous. Postocular lobes poorly developed. **Elytra**. Length 2.54 mm to 3.28 mm ($\bar{X}$ = 2.78 mm, s = 0.25, n = 7), width 1.61 mm to 2.16 mm ($\bar{X}$ = 1.88 mm, s = 0.18, n = 7), length/width ratio 1.39 to 1.58 ($\bar{X}$ = 1.48, s = 0.07, n = 7). Anterior margin nearly straight, humeral angles rounded. Appressed scales tessellate to narrowly imbricate. Setae claviform, decumbent, pale to concolorous. Striae moderately impressed; interstriae flat on disc, convex on elytral declivity. Interstriae 1 at declivity flat in males, produced into a strong tubercle in females. Interstriae 3 and 5 at declivity swollen in both sexes. Apex in lateral view square in males; produced ventrad in females. **Thoracic ventrites**. Mesoventral process rounded. Metaventrite densely covered with pappolepidia. **Abdomen**. Ventrites clothed almost exclusively with pappolepidia, ventrites 1 and 2 moderately densely clothed, ventrites 3 to 5 increasingly sparse. Apex rounded. Males with ventrite 1 strongly depressed medially; ventrite 5 flat. Females with ventrite 1 flat; ventrite 4 with posterior margin produced into a subtriangular lamina

with very deep apical emargination (Figs 102, 103); ventrite 5 disc with median furrow, posterior margin with narrow emargination with a horn either side of emargination. **Male genitalia**. Figs 50–53. Hemisternites with spiculum relictum slender. Penis with apex acute, ostial region thickened, forming a crest. Endophallus with gonoporial sclerite having pronounced anterior lobes, lacking posterior lobes. Temones 0.75 times as long as pedon. **Female genitalia**. Figs 54–57. Distal gonocoxites slender, 2.6 times longer than high. Bursa copulatrix long; not constricted anterior of proximal gonocoxite; sclerite horseshoe-shaped, long. Sternite 8 narrowly rounded at apex, membranous laterally. Everted ovipositor 2.14 mm in length, 0.57 times body length.

DNA sequences. COI. KX191344. **28S**. KX191914. **ArgK**. KX191626. **CAD**. KX191085.

Type material examined. Holotype. Female (NZAC). Specimen mounted on card teardrop; abdomen removed, dissected and mounted in DMHF on white card below specimen; otherwise entire; elytra parted at apex. Labelled 'NEW ZEALAND CO / Obelisk Range / Old Man Range / 14 Jan 2014/ SDJ Brown' [printed, cream card], 'On *Phyllachne* cushion / 1640 m / 45.3113°S 169.1956°E' [printed, cream card], '*Irenimus* taxonomy / and systematics / SDJ Brown / PhD Thesis 2012–2015 / IRE4771' [printed, cream card], 'HOLOTYPE / *Austromonticola* / *furcatus* / Brown 2017' [printed, red card]. Genomic DNA extract from enzyme digestion of abdomen: E196 (NZAC). CAD sequence KX191085; COI sequence KX191344; ArgK sequence KX191626; 28S sequence KX191914.

Paratypes. A total of 16 specimens (8 males, 8 females) designated as paratypes, bearing blue paratype label. Paratype specimens deposited in NHM, LUNZ, NZAC.

CO: Hyde Rock [45°23.358'S, 169°11.844'E, A], 15 Mar 1975, Watt JC, 1524 m, Litter (LUNZ: 1, NZAC: 1); Hyde Rock [45°23.358'S, 169°11.844'E, A], 22 Feb 1974, Dugdale JS, 1555-1616 m (NZAC: 1); Old Man Range [45°20.04'S, 169°12.534'E, A], 15 Mar 1975, May BM, 1524 m, Under *Celmisia* (NZAC: 1); Old Man Range [45°20.04'S, 169°12.534'E, A], 16 Jan 1965, Kuschel G, Townsend JI, 4500 feet, *Celmisia prorepens* (NHM: 1, NZAC: 4); Old Man Range [45°20.04'S, 169°12.534'E, A], 17 Jan 1965, Kuschel G, Townsend JI, 5000 feet (NHM: 1, NZAC: 1); Old Man Range [45°20.04'S, 169°12.534'E, A], 20 Feb 1974, Dugdale JS, 1615 m, Ex *Celmisia haastii* (NZAC: 1); Old Man Range [45°20.04'S, 169°12.534'E, A], 20 Feb 1974, Dugdale JS, 1615 m, ex *Celmisia sessiflora* (LUNZ: 1, NZAC: 1); The Herrons Station [45°24.739'S, 169°12.714'E, R], 17 Jan 2004, Emberson RM, Syrett P, 1590 m, Pitfall trap by tors in fell field (LUNZ: 1).

Distribution. Fig. 116. South Island: **CO**: Old Man Range.

Elevational range. Label data: 1372 m to 1640 m ($\bar{X}$ = 1509 m, s = 103, n = 16). Georeferenced data: 1583 m to 1665 m ($\bar{X}$ = 1641 m, s = 19, n = 17).

Etymology. From the Latin adjective *furcatus*, 'divided, forked', in reference to the form of the ventral lamina of the female; the name is an adjective.

Biology. Specimens have been collected in association with *Phyllachne* cushions and *Celmisia* daisies. In particular, the largest series was associated with *C. prorepens* Petrie, 1887, but specimens have also been found with *C. haastii* Hook.f., 1864, and *C. sessiliflora* Hook.f., 1864.

***Austromonticola inflatus* Brown, sp. n.**
http://zoobank.org/4389A53E-83C4-460C-90E4-30ACE7D1A523
Fig. 13, 14, 29, 30, 31, 35, 33, 58, 59, 60, 61, 62, 63, 64, 65, 66, 106, 107, 115

Diagnosis. Body size large, 8 mm in length. Rostrum with epifrons swollen (Fig. 33). Appressed scales on pronotum and elytra with metallic reflections. Females with ventrite 5 slightly emarginate and with median furrow (Fig. 106); elytra with sutural tubercle at top of elytral declivity.

Description. Body length 6.98 mm to 8.72 mm ($\bar{X}$ = 7.94 mm, s = 0.64, n = 8). Integument black. Dorsum densely covered with fine appressed scales coloured greyish blue to dark greyish blue, often with brassy or purplish metallic reflections. Femora and tibiae with appressed scales unicolorous, concolorous with elytral scales. Tarsi with integument blackish red to dark red. **Rostrum**. Length 1.29 mm to 1.72 mm ($\bar{X}$ = 1.60 mm, s = 0.15, n = 8), width 0.89 mm to 1.18 mm ($\bar{X}$ = 1.05 mm, s = 0.09, n = 8), length/width ratio 1.37 to 1.64 ($\bar{X}$ = 1.53, s = 0.09, n = 8). Epifrons swollen (Fig. 33); appressed scales imbricate; setae piliform, decumbent, concolorous; median and lateral carinae not evident. Dorsal carinae arched over antennal insertions. Lateral area ventral of antennal insertions with fine setae and appressed scales. **Antennae**. Fig. 35. Scapes in repose reaching beyond hind margin of eyes; covered with appressed scales and setae. Funicular segments loosely articulated; segments 1 clavate, 1.2 times longer than 2; segments 2 clavate, about 2 times longer than 3; segments 3 to 5 clavate, getting progressively shorter; segments 6 and 7 subspherical. **Pronotum**. Length 1.68 mm to 2.26 mm ($\bar{X}$ = 1.96 mm, s = 0.21, n = 7), width 2.63 mm to 3.62 mm ($\bar{X}$ = 3.17 mm, s = 0.34, n = 7), length/width ratio 0.84 to 0.94 ($\bar{X}$ = 0.89, s = 0.03, n = 7); in dorsal view widest in anterior 1/3, lateral margins evenly curved. Anterior margin entire, posterior margin straight. Disc in dorsal view with anterolateral and mediolateral impressions usually obscure, but occasionally pronounced; appressed scales imbricate; setae piliform, decumbent, concolorous. Postocular lobes moderately developed. **Elytra**. Length 4.60 mm to 6.19 mm ($\bar{X}$ = 5.41 mm, s = 0.54, n = 7), width 2.63 mm to 3.62 mm ($\bar{X}$ = 3.17 mm, s = 0.34, n = 7), length/width ratio 1.66 to 1.75 ($\bar{X}$ = 1.71, s = 0.04, n = 7). Anterior margin curved posteriad in middle, with humeral angles rounded. Appressed scales imbricate. Setae piliform, semi-erect to decumbent, pale. Elytral interstriae 1 flat in males; produced into elongate tubercle in females. Apex in lateral view square in males, produced ventrad in females. **Thoracic ventrites**. Mesoventral process truncate. Metaventrite sparsely covered with appressed scales. **Abdomen**. Ventrites sparsely clothed with appressed scales. Apex of abdomen broadly rounded. Males with ventrite 1 strongly depressed medially; ventrite 5 flat. Female with subtriangular prominence on disc of ventrite 1; ventrite 4 with posterior margin curved anteriad in middle and posterior face glabrous (Figs 106, 107); ventrite 5 with median furrow and apical notch. **Male genitalia**. Figs 58–61. Hemisternites with spiculum relictum slender. Penis with apex narrowly rounded; ostial region normally developed, not strongly thickened. Endophallus with gonoporial sclerite with broad posterior lobes. Temones 0.59 times as long as pedon. **Female genitalia**. Figs 62–66.

Distal gonocoxites stout, 1.3 times longer than high. Proximal gonocoxite with rods recurved distally. Bursa copulatrix stout; constricted anterior of proximal gonocoxite; sclerite large, pear-shaped. Sternite 8 broad, rounded at apex, membranous laterally.

DNA sequences. COI. KX191461, KX191462. **28S**. KX192043, KX192044, KX192045. **ArgK**. No sequences obtained. **CAD**. KX191187, KX191188.

Type material examined. Holotype. Female (NZAC). Specimen pinned through right elytron; abdomen removed and mounted in DMHF on white card pinned below specimen, genitalia dissected, ventrites coated in gold for SEM; left protarsus broken at base of segment 1, right mesotarsus lacking claw segment. Labelled 'NEW ZEALAND CO / 1680 m / Hawkdun Range / 10 Dec 2013/ SDJ Brown' [printed, cream card], 'On *Chionohebe* and under / stones close to / *Chionohebe* cushions / 44.788°S 169.994°E' [printed, cream card], '*Irenimus* taxonomy / and systematics / SDJ Brown / PhD Thesis 2012–2015 / IRE6389' [printed, cream card], 'HOLOTYPE / *Austromonticola* / *inflatus* / Brown 2017' [printed, red card]. Genomic DNA extract from enzyme digestion of abdomen: E336 (NZAC). CAD sequence KX191187; COI sequence KX191461; 28S sequence KX192043.

Paratypes. A total of 7 specimens (3 males, 4 females) designated as paratypes, bearing blue paratype label. Paratype specimens deposited in NHM, LUNZ, NZAC.

CO: Hawkdun Range [44°47.256'S, 169°59.694'E, R], 11 Dec 2013, Brown SDJ, 1730 m, On *Hectorella* cushion (NHM: 1); Hawkdun Range [44°47.28'S, 169°59.64'E, R], 10 Dec 2013, Brown SDJ, 1680 m, On *Chionohebe* and under stones close to *Chionohebe* cushions (NHM: 1, LUNZ: 2, NZAC: 1); Hawkdun Range [44°49.044'S, 169°59.922'E, R], 12 Dec 2013, Brown SDJ, 1720 m, On *Hectorella* cushion (LUNZ: 1, NZAC: 1).

Distribution. Fig. 115. South Island: **CO**: Hawkdun Range.

Elevational range. Label data: 1680 m to 1730 m ($\bar{X}$ = 1696 m, s = 23, n = 8). Georeferenced data: 1684 m to 1716 m ($\bar{X}$ = 1699 m, s = 11, n = 8).

Etymology. From the Latin participle *inflatus*, 'swollen, distended', in reference to the convex epifrons of this species; the species name is a participle.

Biology. Specimens have been collected on *Hectorella caespitosa* Hook.f., 1864 and on and beside cushions of the snow hebe group (formerly placed in *Chionohebe* B.G.Briggs & Ehrend., 1976) of *Veronica*.

Austromonticola planulatus Brown, sp. n.

http://zoobank.org/FDDF873C-1605-4D39-9631-AA0192D0675F

Figs 11, 12, 27, 28, 32, 67, 68, 69, 70, 71, 72, 73, 74, 75, 108, 109, 115

Diagnosis. Body size large, 8 mm in length. Protibia with large denticles on ventral margin (Fig. 32). Elytral disc somewhat flattened with interstriae 3 and 5 raised along length. Females with ventrite 4 with lateral laminae (Fig. 108), ventrite 5 slightly concave medially (Fig. 108); elytra interstriae 1 at top of elytral declivity flat.

Description. Body length 7.59 mm to 8.25 mm ($\bar{X}$ = 7.92 mm, s = 0.47, n = 2). Integument black. Dorsum covered with fine appressed scales, individual scales barely distinguishable, brownish black, with areas of brownish grey at sides of pronotum and base of rostrum. Femora and tibiae with appressed scales unicolorous, concolorous with elytral scales. Tarsi with integument black to strong red. **Rostrum**. Length 1.52 mm to 1.71 mm ($\bar{X}$ = 1.62 mm, s = 0.13, n = 2), width 0.96 mm to 0.99 mm ($\bar{X}$ = 0.98 mm, s = 0.02, n = 2), length/width ratio 1.58 to 1.73 ($\bar{X}$ = 1.66, s = 0.10, n = 2). Epifrons with appressed scales imbricate; setae claviform, decumbent, concolorous; median and lateral carinae distinct, lateral carinae especially so. Dorsal carinae arched over antennal insertions. Lateral area ventral of antennal insertions with fine setae and appressed scales. **Antennae**. Scapes in repose reaching beyond hind margin of eyes; covered with appressed scales and setae. Funicular segments loosely articulated; segments 1 and 2 clavate, subequal, about 2 times longer than 3; segments 3 to 6 clavate, getting progressively shorter; segment 7 subconical. **Pronotum**. Length 1.92 mm to 2.28 mm ($\bar{X}$ = 2.10 mm, s = 0.25, n = 2), width 3.22 mm to 3.47 mm ($\bar{X}$ = 3.35 mm, s = 0.18, n = 2), length/width ratio 0.89 to 0.93 ($\bar{X}$ = 0.91, s = 0.03, n = 2); in dorsal view widest in anterior 1/4, lateral margins evenly curved. Anterior margin sinuous, posterior margin straight. Disc in dorsal view evenly curved, except for median furrow extending from anterior 1/4 to posterior 1/8, deepest anteriorly; appressed scales imbricate; setae piliform to claviform, decumbent, dark. Postocular lobes strongly developed. **Elytra**. Length 5.21 mm to 5.39 mm ($\bar{X}$ = 5.30 mm, s = 0.13, n = 2), width 3.22 mm to 3.47 mm ($\bar{X}$ = 3.35 mm, s = 0.18, n = 2), length/width ratio 1.50 to 1.67 ($\bar{X}$ = 1.59, s = 0.12, n = 2). Anterior margin almost straight, humeral angles rounded. Disc subdepressed. Appressed scales imbricate. Setae piliform to claviform, decumbent to semi-erect, concolorous on disc, pale laterally and posteriorly. Striae strongly impressed; interstriae convex; interstriae 1 at top of elytral declivity flat in males, swollen in females; interstriae 3 and 5 raised throughout length in both sexes. Apex in lateral view square in males; slightly produced ventrad and with small subapical tubercles in females. **Thoracic ventrites**. Mesoventral process narrowly rounded. Metaventrite densely covered with appressed scales. **Abdomen**. Ventrites densely covered with appressed scales. Males with ventrite 1 flat; ventrite 5 flat. Females with ventrite 1 flat; ventrite 4 with posterior margin produced laterally into small subtriangular laminae (Figs 108, 109); ventrite 5 with median concavity. Apex rounded. **Legs**. Protibiae with conspicuous denticles on ventral margin. **Male genitalia**. Figs 67–70. Hemisternites with spiculum relictum inconspicuous, possibly absent. Penis with apex sagittate, broad; ostial region normally developed. Endophallus with papillae; gonoporial sclerite with long, thin posterior lobes. Temones 0.73 times as long as pedon. **Female genitalia**. Figs 71–75. Distal gonocoxites moderately stout, 1.9 times longer than high. Bursa copulatrix stout, not constricted anterior of proximal gonocoxite; sclerite horseshoe-shaped. Sternite 8 fully sclerotised, apex rounded.

DNA sequences. No DNA sequences obtained.

Type material examined. Holotype. Female (NZAC). Specimen pinned through right elytron; abdomen removed and mounted in DMHF on white card pinned below specimen, genitalia dissected, ventrites coated in gold for SEM; otherwise entire. Labelled ‘Mt Bitterness / St Mary Range CO:NZ / 1830–1900 m / P.M.Johns & /

M.H.Ingerfeld / 6–7.II.78' [printed, white card], 'stonefield with / occ. mat plants' [printed, white card], '*Irenimus* taxonomy / and systematics / SDJ Brown / PhD Thesis 2012–2015 / IRE7625' [printed, cream card], 'HOLOTYPE / *Austromonticola* / *planulatus* / Brown 2017' [printed, red card].

Paratypes. A total of 1 specimen (1 male) designated as paratype, bearing blue paratype label. Paratype specimen deposited in CMNZ.

CO: Mt Bitterness [44°45.24'S, 170°18.198'E, A], 6–7 Feb 1978, Johns PM, Ingerfeld MH, 1830-1900 m, Stonefield with occasional mat plants (CMNZ: 1).

Distribution. Fig. 115. South Island: **CO**: St Marys Range.

Elevational range. Label data: 1865 m (n = 2).Georeferenced data: 1905 m (n = 2).

Etymology. From the Latin adjective *planus*, 'flat, even', combined with the the diminutive *-ulus* and the possessive *-atus*, referring to the almost level dorsum of this species, as compared with others in the genus; the species name is an adjective.

Biology. Collected in fellfield. No plant associations recorded.

Austromonticola postinventus Brown, sp. n.

http://zoobank.org/0905AF10-6CBD-4E24-B7F2-24D099931F84
Figs 9, 10, 25, 26, 33, 36, 76, 77, 78, 79, 80, 81, 82, 83, 84, 110, 111, 115

Diagnosis. Body size large, 8 mm in length. Epifrons flat, with decumbent setae. Females with ventrite 5 emarginate and with median swelling (Fig. 110); elytra with interstriae 1 swollen at top of elytral declivity and the apex produced ventrad.

Description. Body length 7.26 mm to 8.42 mm ($\bar{X}$ = 7.84 mm, s = 0.82, n = 2). Integument black. Dorsum densely covered with fine brownish black appressed scales with purple and gold metallic reflectance, reflectance particularly pronounced laterally and posteriorly. Femora and tibiae with appressed scales dense, unicolorous, concolorous with elytral scales. Tarsi with integument strong red. **Rostrum**. Length 1.45 mm to 1.67 mm ($\bar{X}$ = 1.56 mm, s = 0.16, n = 2), width 0.90 mm to 1.02 mm ($\bar{X}$= 0.96 mm, s = 0.08, n = 2), length/width ratio 1.61 to 1.64 ($\bar{X}$ = 1.62, s = 0.02, n = 2). Epifrons with appressed scales tessellate; setae piliform, decumbent, pale; median and lateral carinae not evident. Dorsal carinae arched over antennal insertions. Lateral area ventral of antennal insertions with fine setae and appressed scales. **Antennae**. Fig. 36. Scapes in repose reaching hind margin of eyes; covered with appressed scales and setae. Funicular segments moderately articulated; segments 1 clavate, about 1.3 times longer than 2; segments 2 clavate, about 2 times longer than 3; segments 3 clavate, slightly longer than 4; segments 4 to 6 clavate, subequal; segments 7 subconical. **Pronotum**. Length 1.90 mm to 2.11 mm ($\bar{X}$ = 2.00 mm, s = 0.15, n = 2), width 2.85 mm to 3.53 mm ($\bar{X}$ = 3.19 mm, s = 0.48, n = 2), length/width ratio 0.85 to 0.90 ($\bar{X}$ = 0.88, s = 0.04, n = 2); in dorsal view widest in anterior 1/3, lateral margins evenly curved. Anterior margin entire, posterior margin straight. Disc in dorsal view evenly curved; appressed scales imbricate; setae piliform, decumbent, concolorous. Postocular lobes moderately developed. **Elytra**. Length 4.90 mm to 5.70 mm ($\bar{X}$ = 5.30 mm, s = 0.57, n = 2), width 2.85 mm to

3.53 mm ($\bar{X}$ = 3.19 mm, s = 0.48, n = 2), length/width ratio 1.61 to 1.72 ($\bar{X}$ = 1.67, s = 0.07, n = 2). Anterior margin almost straight, humeral angles rounded. Appressed scales imbricate. Setae piliform, erect, pale. Striae moderately impressed; interstriae flat; interstriae 1 at elytral declivity flat in males, with small tubercle in females. Apex in lateral view square in males, produced posteriad in females. **Thoracic ventrites**. Mesoventral process acutely rounded in males, broadly rounded in females. Metaventrite densely covered with appressed scales. **Abdomen**. Ventrites densely covered with appressed scales. Apex rounded. Males with ventrite 1 depressed medially; ventrite 5 flat. Females with ventrite 1 flat; ventrite 4 posterior margin curved anteriad in middle, with narrow laminae laterally (Figs 110, 111); ventrite 5 swollen medially, posterior margin broadly emarginate. **Male genitalia**. Figs 76–79. Hemisternites with spiculum relictum slender. Penis with apex narrowly rounded, upturned; ostial region normally developed. Endophallus with gonoporial sclerite small, posterior lobes reduced. Temones 0.63 times as long as pedon. **Female genitalia**. Figs 80–84. Distal gonocoxites stout, 1.4 times longer than high. Bursa copulatrix stout; constricted anterior of proximal gonocoxite; sclerite large, pear-shaped. Sternite 8 broad, rounded at apex, membranous laterally.

DNA sequences. No DNA sequences obtained.

Type material examined. Holotype. Female (NZAC). Specimen pinned through right elytron; abdomen removed and mounted in DMHF on white card pinned below specimen, genitalia dissected, ventrites coated in gold for SEM; right proleg missing, broken off from trochanter. Labelled 'Mt Kirkliston / 6000 / C.J.Burrows / 5.1.65 / understones' [first three lines printed, last two lines handwritten, off-white card], '*Irenimus* taxonomy / and systematics / SDJ Brown / PhD Thesis 2012–2015 / IRE1116' [printed, off-white card], 'HOLOTYPE / *Austromonticola* / *postinventus* / Brown 2017' [printed, red card].

Paratypes. A total of 1 specimen (1 male) designated as paratype, bearing blue paratype label. Paratype specimen deposited in NZAC.

SC: Kirkliston Range [44°32.124'S, 170°30.954'E, A], 8–9 Feb 1978, Johns PM, Ingerfeld MH, 1740-1770 m, Stonefield with occasional mat plants (NZAC: 1).

Distribution. Fig. 115. South Island: **SC**: Kirkliston Range.

Elevational range. Label data: 1755 m to 1829 m (n = 2). Georeferenced data: 1615 m to 1868 m (n = 2).

Etymology. From the Latin prefix *post*, 'after', and the participle *inventus*, 'discovered', referring to the recognition of this species after my PhD defence; the name is a participle.

Biology. Collected in fellfield. No plant associations recorded.

Austromonticola mataura Brown, sp. n.

http://zoobank.org/8F3D76BE-96EF-4C84-8833-54ED30B20938
Figs 3, 4, 19, 20, 85, 86, 87, 88, 89, 90, 91, 92, 104, 105, 116

Diagnosis. Body size medium, 4 mm in length. Venter with glossy appressed scales, pappolepidia sparse. Elytral declivity of females with sutural tubercle; margin of ven-

trite 3 with paired median processes; margin of ventrite 4 produced into a lamina, with deep median emargination; margin of ventrite 5 with a broad horn on either side of the genital opening.

Description. Body length 3.42 mm to 4.11 mm ($\bar{X}$ = 3.80 mm, s = 0.25, n = 13). Integument black. Dorsum densely covered with light bluish grey to dark greyish yellow appressed scales with metallic reflections; frequently with pale mottling sublaterally, and with scutellum, humeral area and hind pronotal angles bluish white; elytral declivity slightly paler than disc, especially in males. Pappolepidia of mesothoracic sternites light yellow. Femora appressed scales concolorous with elytral scales, often with obscure pale band in distal 1/4. Tarsi with integument deep orange to strong red. **Rostrum**. Length 0.72 mm to 0.88 mm ($\bar{X}$ = 0.84 mm, s = 0.06, n = 8), width 0.52 mm to 0.66 mm ($\bar{X}$ = 0.57 mm, s = 0.05, n = 7), length/width ratio 1.35 to 1.68 ($\bar{X}$ = 1.57, s = 0.11, n = 7). Epifrons with appressed scales imbricate; setae claviform, decumbent, concolorous; median carina weak; lateral carinae evident. Dorsal carinae arched over antennal insertions. Lateral area ventral of antennal insertions with fine setae, without appressed scales. **Antennae**. Scapes in repose reaching middle of eyes. Funicular segments moderately articulated; segments 1 and 2 clavate, subequal, about 2 times longer than 3; segments 3 and 4 clavate, subequal; segments 5 to 7 subspherical, subequal. **Pronotum**. Length 1.06 mm to 1.18 mm ($\bar{X}$ = 1.13 mm, s = 0.04, n = 8), width 1.61 mm to 2.16 mm ($\bar{X}$ = 1.88 mm, s = 0.18, n = 7), length/width ratio 0.80 to 0.92 ($\bar{X}$ = 0.86, s = 0.04, n = 7); in dorsal view widest in anterior 1/3, lateral margins strongly curved to widest point, gently curved behind. Anterior margin entire, posterior margin straight. Disc in dorsal view uneven, weak median furrow present, anterolateral depressions vague; appressed scales tessellate to imbricate; setae claviform, decumbent to semi-erect, concolorous. Postocular lobes poorly developed. **Elytra**. Length 2.30 mm to 3.04 mm ($\bar{X}$ = 2.79 mm, s = 0.23, n = 8), width 1.61 mm to 2.16 mm ($\bar{X}$ = 1.88 mm, s = 0.18, n = 7), length/width ratio 1.39 to 1.58 ($\bar{X}$ = 1.48, s = 0.07, n = 7). Anterior margin curved posteriad in middle, humeral angles rounded. Appressed scales tessellate to imbricate. Setae claviform, decumbent to semi-erect, concolorous. Interstriae 1 at elytral declivity flat in males, produced into tubercles in females. Interstriae 3 raised at base; swollen at elytral declivity in both sexes, though more pronounced in females. Interstriae 5 at elytral declivity swollen in both sexes. Humeral region strongly pronounced by deeply impressed striae 9. Apex in lateral view square in males, produced ventrad in females. **Thoracic ventrites**. Mesoventral process narrowly rounded. Mesanepisterna, mesepimera and metanepisterna covered with small pappolepidia, contrasting with metaventrite densely covered with appressed scales. **Abdomen**. Ventrites clothed almost exclusively with appressed scales; ventrites 1 and 2 densely clothed in females, scales dense laterally and sparser medially in males; ventrites 3 to 5 increasingly sparse. Males with ventrite 1 depressed medially; ventrite 5 flat. Females with ventrite 1 flat; ventrite 4 posterior margin produced into a lamina, usually with a deep median emargination (Fig. 104, 105) but variably shallower to entire; ventrite 5 disc with median furrow,

deeply emarginate with a broad horn on either side of emargination. Apex narrowly rounded. **Male genitalia**. Fig. 85–88. Hemisternites with spiculum relictum slender. Penis with apex acute, upturned; ostial region thickened, forming a crest. Endophallus with gonoporial sclerite small, anterior and posterior lobes reduced. Temones 0.71 times as long as pedon. **Female genitalia**. Fig. 89–92. Distal gonocoxites slender, 3.1 times longer than high. Proximal gonocoxite with rods recurved distally. Bursa copulatrix long; not constricted anterior of proximal gonocoxite; sclerite small, semicircular. Sternite 8 narrow, apex acute, membranous laterally.

DNA sequences. COI. KX191347, KX191348, KX191349. **28S**. KX191917, KX191918, KX191919. **ArgK**. KX191629, KX191630, KX191631. **CAD**. KX191088, KX191089, KX191090.

Type material examined. Holotype. Female (NZAC). Specimen mounted on card teardrop; abdomen removed, dissected and mounted in DMHF on white card below specimen; otherwise entire. Labelled 'NEW ZEALAND OL / Mt Dick / Kingston / 17 Jan 2014 / SDJ Brown' [printed, cream card], 'On *Phyllachne* cushion / 1690 m / 45.2652°S 168.6870°E' [printed, cream card], '*Irenimus* taxonomy / and systematics / SDJ Brown / PhD Thesis 2012–2015 / IRE4775' [printed, cream card], 'HOLOTYPE / *Austromonticola* / *mataura* / Brown 2017' [printed, red card]. Genomic DNA extract from enzyme digestion of abdomen: E200 (NZAC). CAD sequence KX191089; COI sequence KX191348; ArgK sequence KX191630; 28S sequence KX191918.

Paratypes. A total of 21 specimens (9 males, 12 females) designated as paratypes, bearing blue paratype label. Paratype specimens deposited in AMNZ, ANIC, NHM, CMNZ, IACC, LUNZ, MONZ, NZAC, USNM.

OL: Mt Dick [45°15.564'S, 168°40.926'E, R], 17 Jan 2014, Brown SDJ, 1600 m, On *Dracophyllum muscoides* cushion (AMNZ: 1, LUNZ: 2, MONZ: 2, NZAC: 1); Mt Dick [45°15.696'S, 168°41.016'E, R], 17 Jan 2014, Brown SDJ, 1680 m, On *Phyllachne* cushion (NHM: 1, USNM: 1); Mt Dick [45°15.81'S, 168°41.148'E, R], 17 Jan 2014, Brown SDJ, 1710 m, On *Raoulia haastii* (LUNZ: 1, USNM: 1); Mt Dick [45°17.112'S, 168°41.19'E, R], 16 Jan 2014, Brown SDJ, 1570 m, On *Phyllachne* cushion (ANIC: 1); Mt Dick [45°18.264'S, 168°41.496'E, R], 16 Jan 2014, Brown SDJ, 1510 m, On *Phyllachne* cushion (AMNZ: 1, ANIC: 1, NHM: 1, CMNZ: 1, LUNZ: 1, NZAC: 1); Symmetry Peaks [45°16.928'S, 168°34.56'E, A], 8 Jan 1987, Barratt BIP, 1750-1860 m (IACC: 1); Upper Mataura Valley [45°19.734'S, 168°26.07'E, A], 17 Jan 1971, 1524 m, Moss (NZAC: 3).

Distribution. Fig. 116. South Island: **OL**: Eyre Mountains; Mt Dick.

Elevational range. Label data: 1270 m to 1805 m ($\bar{X}$ = 1580 m, s = 107, n = 23). Georeferenced data: 878 m to 1682 m ($\bar{X}$ = 1479 m, s = 254, n = 23).

Etymology. This species is named after its distribution in the headwaters of the Mataura River; the name is a noun in apposition. The word mataura is Māori, of obscure meaning. Mataura was an ancestor of Ngatoro-i-rangi, the priest of the Arawa canoe. It may mean `glowing face', which is appropriate for its collection localities thus far have been on the eastern slopes of the Eyre Mountains.

Biology. Collected from *Raoulia hectorii* Hook.f., 1864, (recorded as *R. haastii* Hook.f., 1864, in error), moss, *Dracophyllum muscoides* Hook.f., 1864, and *Phyllachne* cushions. The majority of specimens were collected from *Phyllachne*.

***Austromonticola rotundus* Brown, sp. n.**
http://zoobank.org/3B99FAB1-E825-4593-8508-4411388A6D40
Figs 7, 8, 23, 24, 38, 93, 94, 95, 96, 97, 98, 99, 112, 113, 117

Diagnosis. Body size medium, 4.5 mm in length. Pronotum with subparallel lateral margins (Fig. 38), about as wide as base of elytra. Venter clothed with appressed scales, pappolepidia sparse. Females with elytral declivity distinctly rounded, without sutural tubercle; margin of ventrite 5 entire (Fig. 112).

Description. Body length 4.20 mm to 4.80 mm ($\bar{X}$ = 4.50 mm, s = 0.20, n = 11). Integument black. Dorsum densely covered with moderate olive to greyish brown appressed scales, some variegation usually present on elytra, but rarely forming distinct patterns; pronotum frequently with obscure lighter lines obliquely converging anteriorly. Femora and tibiae with dense appressed scales concolorous with elytral scales, usually with pale band in distal 1/4 of femur. Tarsi with integument deep orange. **Rostrum**. Length 0.89 mm to 0.99 mm ($\bar{X}$ = 0.94 mm, s = 0.04, n = 6), width 0.58 mm to 0.66 mm ($\bar{X}$ = 0.62 mm, s = 0.03, n = 6), length/width ratio 1.44 to 1.69 ($\bar{X}$ = 1.52, s = 0.09, n = 6). Epifrons with appressed scales imbricate; setae claviform, decumbent, concolorous; median and lateral carinae not evident. Dorsal carinae arched over antennal insertions. Lateral area ventral of antennal insertions with fine setae and with appressed scales. **Antennae**. Scapes in repose reaching hind margin of eyes; covered with appressed scales and setae. Funicular segments moderately articulated; segments 1 clavate, about 1.5 times longer than 2; segments 2 clavate, about 1.2 times longer than 3; segments 3 and 4 clavate; segments 5 to 7 subspherical, subequal in length. **Pronotum**. Length 1.26 mm to 1.39 mm ($\bar{X}$ = 1.32 mm, s = 0.05, n = 6), width 1.79 mm to 2.26 mm ($\bar{X}$ = 1.98 mm, s = 0.19, n = 6), length/width ratio 0.83 to 0.91 ($\bar{X}$ = 0.87, s = 0.03, n = 6); in dorsal view widest in anterior 1/3, lateral margins approximately subparallel (Fig. 38). Anterior margin entire, posterior margin curved. Disc in dorsal view evenly curved, but with obscure median depression in anterior 1/3; appressed scales imbricate; setae claviform, decumbent, concolorous. Postocular lobes poorly developed. **Elytra**. Length 2.79 mm to 3.52 mm ($\bar{X}$ = 3.02 mm, s = 0.26, n = 6), width 1.79 mm to 2.26 mm ($\bar{X}$ = 1.98 mm, s = 0.19, n = 6), length/width ratio 1.43 to 1.62 ($\bar{X}$ = 1.53, s = 0.07, n = 6). Anterior margin curved posteriad, humeral angles rounded. Appressed scales imbricate. Setae claviform, semi-erect, pale. Striae moderately impressed; interstriae slightly convex. Interstriae 1 at declivity flat in both sexes. Interstriae 3 at declivity flat in both sexes. Elytral declivity curved in females. Apex in lateral view square in males; produced ventrad in females. **Thoracic ventrites**. Mesoventral process rounded. Mesanepisterna, mesepimera, metanepisterna and metaventrite densely cov-

ered with appressed scales. **Abdomen**. Ventrites sparsely clothed with appressed scales. Apex broadly rounded. Males with ventrite 1 flat; ventrite 5 flat. Females with ventrite 1 flat; ventrite 4 with posterior margin produced into a broad lamina with a strong apical emargination (Figs 112, 113); ventrite 5 disc with shallowly concave, posterior margin entire. **Male genitalia**. Figs 93, 94. Penis with apex sagittate; ostial region receeding anteriorly, not thickened. Endophallus with gonoporial sclerite very small. Temones 0.78 times as long as pedon. **Female genitalia**. Figs 95–99. Distal gonocoxites slender, 3.0 times longer than high. Bursa copulatrix long; not constricted anterior of proximal gonocoxite; sclerite lanceolate. Sternite 8 apex rounded, fully sclerotised.

DNA sequences. COI. KX191445. **28S**. KX192022. **ArgK**. KX191729. **CAD**. KX191173.

Type material examined. Holotype. Female (NZAC). Specimen mounted on card teardrop; abdomen removed, dissected and mounted in DMHF on white card below specimen; otherwise entire. Labelled 'NEW ZEALAND CO / Obelisk Range / Old Man Range / 13 Jan 2014 / SDJ Brown' [printed, cream card], 'On *Dracophyllum* / *muscoides* cushion / 1590 m / 45.3126°S 169.2102°E' [printed, cream card], '*Irenimus* taxonomy / and systematics / SDJ Brown / PhD Thesis 2012–2015 / IRE4888' [printed, cream card], 'HOLOTYPE / *Austromonticola* / *atriarius* / Brown 2017' [printed, red card]. Genomic DNA extract from enzyme digestion of abdomen: E313 (NZAC). CAD sequence KX191173; COI sequence KX191445; ArgK sequence KX191729; 28S sequence KX192022.

Paratypes. A total of 17 specimens (6 males, 11 females) designated as paratypes, bearing blue paratype label. Paratype specimens deposited in NHM, IACC, LUNZ: 1, NZAC: 2.

CO: North Garvie Mountains, 9 Feb 1985, Barratt BIP, 1200 m, Ex *Geum parviflorum* (IACC: 1); Old Man Range [45°20.04'S, 169°12.534'E, A], 17 Jan 1965, Kuschel G, Townsend JI, 5000 feet (NZAC: 1); Old Woman Range [45°15.18'S, 169°3.54'E, A], 20 Nov 1974, Watt JC, 1389 m, Litter (LUNZ: 1, NZAC: 5); Rock Peak [44°59.442'S, 168°58.17'E, A], 27 Nov 1974, Dugdale JS, 1430-1460 m, Litter (NZAC: 1); Rock Peak [44°59.442'S, 168°58.17'E, A], 27 Nov 1974, Dugdale JS, 1430-1460 m, Mixed swards and litter (NHM: 2, LUNZ: 1, NZAC: 4); Rock Peak [44°59.442'S, 168°58.17'E, A], 27 Nov 1974, Dugdale JS, 1430-1460 m, Mixed swards litter (NZAC: 1).

Distribution. Fig. 117. South Island: **CO**: Garvie Mountains; Old Man Range; Old Woman Range; Crown Range.

Elevational range. Label data: 1200 m to 1590 m ($\bar{X}$ = 1428 m, s = 76, n = 18). Georeferenced data: 1329 m to 1717 m ($\bar{X}$ = 1477 m, s = 184, n = 17).

Etymology. From the Latin adjective *rotundus*, 'round, spherical' for the form of the female elytral declivity; the name is an adjective.

Biology. Specimens have been collected from *Geum parviflorum* Smith, 1805 and *Dracophyllum muscoides*. The majority of specimens, however, were collected from litter and turf (sward) samples.

Key to the species of *Austromonticola*

1 Larger species, greater than 7 mm in length **2**
– Smaller species, less than 5 mm in length..... **5**
2(1) Denticles on protibiae large, conspicuous (Fig. 32); lateral carinae of rostrum distinct; interstriae 3 and 5 raised along length ..... ***A. planulatus***
– Denticles on protibiae undeveloped (Fig. 31); lateral carinae of rostrum moderate or weak; interstriae 3 and 5 raised at base and/or on elytral declivity, not raised on disc **3**
3(2) Epifrons swollen, convex (Fig. 33). Funicle segments 7 subspherical (Fig. 35)..... ***A. inflatus***
– Epifrons flattened, level (Fig. 34). Funicle segments 7 subconical (Fig. 36)..... **4**
4(3) Epifrons with setae semi-erect. Setae along elytral interstriae 7 erect .... ***A. caelibatus***
– Epifrons with setae decumbent. Setae along elytral interstriae 7 decumbent.. ..... ***A. postinventus***
5(1) Pronotum hexagonal in outline, widest anteriorly, sides evenly converging toward base (Fig. 37). Females with elytral declivity roughly vertical, sutural tubercle present; ventrite 5 emarginate, possessing spines around the genital opening **6**
– Pronotum round in outline (Fig. 38). Female with elytral declivity rounded, without sutural tubercle; margin of ventrite 5 entire ..... ***A. rotundus***
6(5) Venter with dense pappolepidia, round appressed scales sparsely distributed **7**
– Venter with dense appressed scales, pappolepidia sparsely distributed .... ***A. mataura***
7(6) Pronotum with median furrow. Elongate elytral scales decumbent. Antennal funicle segments 3 longer than 4..... ***A. atriarius***
– Pronotum evenly curved. Elongate elytral scales semi-erect. Antennal funicle segments 3 of similar length as 4..... ***A. furcatus***

Molecular diagnostics

Specimens of five species of *Austromonticola* were available for DNA sequencing. No fresh specimens of *A. planulatus*, *A. caelibatus* and *A. postinventus* were collected. Multiple specimens were available only of *A. inflatus* and *A. mataura*, and only the latter yielded multiple sequences for all gene regions. Due to these low sample numbers, conclusions regarding intra-specific variability are necessarily limited.

The three protein-coding genes could all be unambiguously aligned, 28S being the only locus that required alignment gaps. The COI alignment was divided into two regions. The first represented the 5' region, corresponding to the region favoured for DNA barcoding (Hebert et al. 2003), and consisted of 669 bp, beginning at position

1239 of the *Tribolium castaneum* (Herbst, 1797) mitochondrial genome KM244661.1. This region was only sequenced for *A. mataura* and *A. rotundus* due to difficulties in amplifying it in other species. The second region, at the 3' end of the gene, consisted of 799 bp beginning at position 1909 of the same *T. castaneum* mitochondrial genome sequence. The 28S alignment was 756 bp long, beginning at position 1121 of the *Tenebrio* sp. reference sequence AY210843.1 (Gillespie et al. 2004). The ArgK alignment was 681 bp long, beginning at position 419 of the *T. castaneum* reference sequence XM_966707.4. The CAD alignment was 460 bp long, beginning at position 2082 of the *T. castaneum* reference sequence XM_967097.3.

Genetic variation existed in all gene regions, COI showing the greatest amount of variation, followed by CAD and ArgK, and 28S displaying the least (Figs 122–124). Of the genes sampled here, COI exhibited the greatest amount of genetic variation, as expected (Lin and Danforth 2004).

COI proved to be the most suitable gene for identifying specimens of *Austromonticola*. The 3' end of COI allowed unambiguous differentiation of all species with available data. This region has the greatest taxon coverage, though indications are that the 5' 'barcoding' end of the gene has higher levels of variation if amplification is successful (Fig. 122). ArgK is also a possible candidate for identification purposes, as all species displayed differences between them, however the level of variation was substantially lower than that of COI (Fig. 123). 28S and CAD are both unsuitable for specimen identification, due to there being some zero distances between species (Figs 124, 121).

The same pattern of variation in each gene region was observed when the number of diagnostic nucleotides was calculated (Figs 125–129). All species can be diagnosed using COI, with the number of nucleotides ranging between 7 and 20, and a median of 15. However, due to the lack of intra-specific sampling, these diagnostic sites should be used with caution.

Across all three protein-coding genes, *A. atriarius*, *A. furcatus* and *A. mataura* showed the smallest interspecific distances. In COI, *A. rotundus* was nearest to *A. inflatus* (Fig. 120), while in CAD and ArgK it was nearest to *A. atriarius* (Fig. 121, 123) and in 28S it was nearest to *A. mataura* (Fig. 124). There were no differences in the 28S sequences of *A. atriarius*, *A. furcatus* and *A. inflatus* (Fig. 124).

Phylogenetic analysis

Analysis of the character matrix (Table 2) resulted in a single most parsimonious cladogram (Fig. 118), with a length of 68 steps, a consistency index of 57 and a retention index of 70. Collapsing unsupported nodes (Fig. 119) increased the tree length to 78 steps.

In the discussion of characters below, the significance of synapomorphies is only discussed in relation to *Austromonticola*, due to limited representation of outgroup taxa.

1. Body length, as measured from the anterior margin of the eyes to the elytral declivity in lateral view: (0) less than 6 mm; (1) greater than 6 mm. As estimated by this phylogeny,

state 1 is the ancestral body size, while state 0 is homoplasious for the *A. rotundus–A. mataura* clade and *Irenimus parilis* + *Brachyolus punctatus* (ci = 0.5, ri = 0.8).

2. Body vestiture, form of appressed scales covering dorsum: (0) scales large, conspicuous, imbricate, coloured brown or bronze or pale yellow; (1) scales small, inconspicuous, tessellate, dome-shaped, black, ridges not visible at 50 × magnification; (2) scales small, tessellate, flat, coloured greys or browns, ridges visible at 30 × magnification. State 2 is a synapomorphy for *Austromonticola* (ci = 1, ri = 1).
3. Labium, form of base: (0) flat; (1) concave, with lateral areas raised relative to disc. State 1 is a synapomorphy for *Austromonticola* but convergently present in *Irenimus parilis* (ci = 0.5, ri = 0.75).
4. Labium, setation of disc: (0) bare; (1) with setae distally and laterally. The plesiomorphic state 0 is present in all species of *Austromonticola,* with state 1 being a synapomorphy for *Irenimus parilis* + *Brachyolus punctatus* (ci = 1, ri = 1).
5. Rostrum, ventral side, hypostomal-labial sutures: (0) strongly convergent to point distal of head capsule deflexion; (1) roughly parallel, converging to point proximal of head deflexion. State 1 is convergently present in *Inophloeus sulcifer* and *Austromonticola* excluding *A. planulatus*, though with a reversal in *A. atriarius* (ci = 0.33, ri = 0.67).
6. Frons, vestiture: (0) clothed with pale, thick, conspicuous setae; (1) clothed with inconspicuous setae. The plesiomorphic state 0 is present in all species of *Austromonticola*, with state 1 being a synapomorphy for *Zenagraphus metallescens* + the undescribed genus (ci = 1, ri = 1).
7. Pronotum, sculpture of disc: (0) evenly convex, without obvious sculpture; (1) with depressions or wrinkles laterally. State 0 is shared with the undescribed genus and *I. parilis* by all species of *Austromonticola* (ci = 0.33, ri = 0.33).
8. Pronotum, scale pattern: (0) without distinctive pattern; (1) with lateral vittae formed by pale scales, vittae extending onto humeral area. State 1 is a synapomorphy for the *A. rotundus–A. mataura* clade (ci = 1, ri = 1).
9. Protarsus, second segment: (0) transverse, or width subequal to length; (1) distinctly elongate, length greater than width. State 1 is a synapomorphy for the *A. caelibatus–A. inflatus* clade (ci = 1, ri = 1).
10. Metatibial apex: (0) simple, without corbel; (1) with bare corbel. The plesiomorphic state 0 is present in all species of *Austromonticola*. This phylogeny estimates that state 1 is convergently present in *Inophloeus sternalis* and *Irenimus parilis* (ci = 0.5, ri = 0).
11. Metanepisterna, vestiture: (0) consisting of round appressed scales; (1) consisting of pappolepidia. State 1 is a synapomorphy for the *A. atriarius–A. mataura* clade, but convergently present in the undescribed genus (ci = 0.5, ri = 0.67).
12. Metanepisterna, vestiture: (0) comprising two rows of scales; (1) comprising three or more rows of scales. State 1 is a synapomorphy for the *A. atriarius–A. mataura* clade but convergently present in *I. sulcifer* (ci = 0.5, ri = 0.67) (ci = 0.5, ri = 0.67).
13. Elytra, form of strial punctures: (0) shallow, circular, interstriae much wider than punctures; (1) deep, subquadrate, interstriae approximately equal in width as

punctures. The plesiomorphic state 0 is present in all species of *Austromonticola*. State 1 is convergently present in *Inophloeus sulcifer* and *Zenagraphus metallescens* (ci = 0.5, ri = 0).

14. Elytra, length and density of setae on disc: (0) long, conspicuous and evenly distributed; (1) short, sparse. The plesiomorphic state 0 is present in all species of *Austromonticola*. State 1 is a synapomorphy for the *Inophloeus sulcifer–Zenagraphus metallescens* clade (ci = 1, ri = 1).
15. Elytra, form of setae: (0) claviform; (1) piliform. State 1 is a synapomorphy for the *A. caelibatus–A. inflatus* clade (ci = 1, ri = 1).
16. Elytra, humeral region anteriorly of conjunction of striae 7 & 8: (0) evenly convex, not prominent in comparison with surroundings, stria 9 not deeply impressed at base; (1) strongly raised in comparison with surroundings, stria 9 deeply impressed at base. A complex character that does not show any clear relationships (ci = 0.25, ri = 0.5).
17. Elytra, form of sutural interval above elytral declivity in females: (0) flat; (1) developed into a prominent tubercle. State 1 is convergently present in the *A. caelibatus–A. inflatus* clade and the *A. atriarius–A. mataura* clades (ci = 0.5, ri = 0.75). The unknown female of *A. caelibatus* is predicted by this estimation to possess state 1.
18. Elytra, form of interstriae 3 above elytral declivity: (0) swollen, more so than on disc; (1) developed into prominent tubercles; (2) flat, no greater than on disc. State 2 is shared between *A. planulatus* and the *A. caelibatus–A. inflatus* clade. State 0 is a shared by all members of the *A. rotundus–A. mataura* clade but has also evolved elsewhere in the tree (ci = 0.5, ri = 0.67).
19. Elytra, form of interstriae near apex: (0) clearly impressed, confluence of interstriae 3 and 9 clearly raised above confluence of 2 and 10; (1) striae obsolete, confluence of interstriae 3 and 9 on same level as confluence of 2 and 10. State 1 is a synapomorphy for *Austromonticola* (ci = 1, ri = 1).
20. Ventrite 4 of females, form of posterior margin: (0) entire; (1) produced into a lamina. State 1 is a synapomorphy for *Austromonticola*, but a reversal to state 0 has occurred in *A. postinventus* and *A. inflatus* (ci = 0.5, ri = 0.75).
21. Ventrite 5 of females, form of apex: (0) entire or only slightly emarginate; (1) strongly emarginate, flanked by horns. State 1 is a synapomorphy for the *A. atriarius–A. mataura* clade (ci = 1, ri = 1).
22. Female genitalia, presence of rectal valve (Lyal and Favreau 2015): (0) absent; (1) present as a crimped ring. State 0 is inferred on this tree to be the derived state and shared by all members of the *A. caelibatus–A. mataura* clade. (ci = 0.33, ri = 0.5).
23. Female genitalia, length/height ratio of distal gonocoxite: (0) long and slender, ratio greater than 1.8; (1) stout, ratio less than 1.5. State 1 is a synapomorphy for the *A. caelibatus–A. inflatus* clade (ci = 1, ri = 1). The unknown female of *A. caelibatus* is predicted by this phylogeny to possess state 1.
24. Female genitalia, number of sclerites in the bursa copulatrix: (0) absent; (1) one present; (2) two present. This cladogram infers that a single bursal sclerite is the plesiomorphic state, which is shared by all species of *Austromonticola*. State 0 is

an apomorphy for *Brachyolus punctatus*, while state 2 is convergently present in *Inophloeus sternalis* and *Irenimus parilis* (ci = 1, ri = 1).

25. Female genitalia, form of vagina: (0) unsclerotised; (1) sclerotised. State 1 is a character uniting all species of *Austromonticola* but shared with *Brachyolus punctatus* and the undescribed genus (ci = 0.33, ri = 0.33).
26. Female genitalia, caudal shape of sclerotised rods on proximal gonocoxite: (0) straight in ventral view; (1) curved inwardly in ventral view. State 1 has arisen twice, in *A. furcatus–A. mataura* and apparently independently in *A. inflatus* (ci = 0.5, ri = 0.5).
27. Female genitalia, shape of sclerotised rods on proximal gonocoxite: (0) tapering proximally; (1) broadening proximally; (2) strongly broadening proximally, multiply divided. State 1 is a synapomorphy for *Austromonticola* (ci = 1, ri = 1).
28. Female genitalia, position of sclerotised rods on proximal gonocoxite in lateral view: (0) median; (1) ventral. State 1 unites all species of *Austromonticola*, but is shared with *Zenagraphus metallescens* and the undescribed genus (ci = 0.5, ri = 0.67).
29. Penis, apex in dorsal view: (0) acute; (1) sagittate; (2) truncate. State 0 is the usual form in *Austromonticola*, but state 1 has arisen twice, in *A. planulatus* and *A. rotundus* (ci = 0.5, ri = 0).
30. Penis, curvature in lateral view: (0) even from base to apex, maximum height near middle; (1) largely confined to base, maximum height near basal 1/3. The plesiomorphic state 1 is present in all species of *Austromonticola*. State 0 is a homoplasious synapomorphy for *Brachyolus punctatus* + *Irenimus parilis* and *Zenagraphus metallescens* + the undescribed genus (ci = 0.5, ri = 0.67).
31. Penis, form of ostial region: (0) tubular, unmodified; (1) thickened to form sclerotised crest (Fig. 40). State 1 is a synapomorphy for the *A. atriarius–A. mataura* clade (ci = 1, ri = 1).
32. Penis, length of temone in relation to length of pedon in lateral view: (0) longer than pedon; (1) shorter than pedon, but longer than 0.7 times length of pedon; (2) shorter than 0.7 times length of pedon. State 2 is a homoplasious character that unites the members of the *A. caelibatus–A. inflatus* clade but shared with the undescribed genus (ci = 0.5, ri = 0.5).
33. Male genitalia, shape of hemisternites 8: (0) roughly quadrate; (1) roughly triangular. The plesiomorphic state 1 is present in all species of *Austromonticola*. State 0 unites *Brachyolus punctatus* + *Irenimus parilis*, but is convergently present in *Zenagraphus metallescens* (ci = 0.5, ri = 0.5).

The species of *Austromonticola* are united by three unambiguous synapomorphies, scale structure (character 2), the obsolete striae at the elytral apex (character 19), and the proximally widening gonocoxal rods (character 27).

In *Austromonticola* there are two strongly supported clades, one consisting of the larger species *A. caelibatus*, *A. postinventus* and *A. inflatus* (the *A. inflatus* clade) and the other consisting of the smaller species possessing metanepisterna with three

rows of pappolepidia, a penis with an ostial crest and ventrite 5 with a strongly emarginate apex in the females, *A. atriarius*, *A. furcatus* and *A. mataura* (the *A. mataura* clade). Grouped with the latter clade is *A. rotundus*; however, the support for this relationship is weak, and the sagittate apex of the penis shared with *A. planulatus* hints at a possible relationship. Together, *A. planulatus* and *A. rotundus* provide a transitional series between the distinctly different *A. inflatus* clade and the *A. mataura* clade.

Discussion

Development of ventrites in females

The highly modified ventrites in many species of *Austromonticola* are a particularly fascinating feature of the genus. There is a range of developments of the posterior margin of ventrite 4 of the females. No laminae are found in *A. inflatus* and *A. postinventus*, rather the posterior margin of ventrite 4 is recurved anteriad. A short lamina with a wide emargination is present in *A. planulatus*. Long bifurcate laminae are found in *A. mataura* and *A. atriarius*, while *A. furcatus* has a broader lamina with a deep emargination. Finally, *A. rotundus* has a long, broad lamina with a shallow emargination. The unknown female of *A. caelibatus* is predicted in the phylogenetic tree inferred above to be lacking a lamina, but it is equally parsimonious to infer a lamina being present in *A. caelibatus*, given the basal position of the species in the clade. The form of the lamina in this species would be of interest. This range of development make *Austromonticola* a suitable system for investigating the function of these laminae. Two hypotheses are presented in detail here.

Preparation of oviposition sites

The first hypothesis is that these ventral structures assist in the preparation of oviposition sites in cushion plants. The cushion vegetational form is a distinctive feature of New Zealand alpine plants, such as *Raoulia* and *Phyllachne*. This growth habit presents densely packed foliage underlain by a peaty layer formed by decaying leaves still attached to the plant (Cockayne 1921). In this hypothesis, the long abdominal laminae and apical horns of *A. mataura* and related species are used to force aside the foliage of cushion plants to allow the ovipositor to extend into the underlying layer to deposit the eggs (Fig. 130). This model of function may explain the emargination present in the lamina, its correspondence with the horns around the genital orifice, the correlation of these structures with a long, flexible ovipositor that can be extended to 3/4 of the weevil's body length, and the damaged apex of the lamina in the specimen of *A. atriarius* (Fig. 100). Predictions made by this model are that oviposition occurs while

the female is sitting on top of the cushion plant, that females thus exposed will exhibit disruptive coloration and that eggs and early-instar larvae will be found in the centre of cushions, feeding on the peaty material beneath the foliage.

This hypothesis also provides an explanation for the recurved margin of ventrite 4 of *A. inflatus* and *A. postinventus*. In these species, it is hypothesised that the form of ventrite 4 allows maximum flexion of ventrite 5, which assists in ovipositing under the side of the cushion plants where the plant meets the surrounding substrate (Fig. 131). This model explains the much stouter ovipositor possessed by *A. inflatus* and *A. postinventus*. Predictions of this model include that eggs and early-instar larvae will be found towards the edges of the cushions, feeding on roots in the soil, that adult specimens will be more frequently found beside cushions rather than on top of them, and will be coloured like the surrounding substrate.

The rather different laminae of *A. planulatus* and *A. rotundus* suggest different oviposition behaviours or host plants from those of the two scenarios postulated above.

Mate hindrance

The second hypothesis is that these structures are mate hindrance devices. Mating pairs of entimine weevils are frequently encountered *in copula* in the field, and studies of their mating behaviour in captivity show that males will remain mounted on females for extended periods of time (D Watkin and SDJ Brown, unpub. data). The costs imposed by extended mounting include the energy expended in carrying males (Watson et al. 1998), potentially increased predation risk (Magnhagen 1991) and the losses involved in reduced foraging time (Stone 1995). Structures developed in *Austromonticola* females, such as elytral sutural tubercles, abdominal laminae and armature around the genital orifice, may enable prevention of unwanted mating attempts or assist in dislodging males if mounting becomes excessively prolonged. Evidence for this mechanism of sexual selection have been found in studies of water striders, which show similar exaggerated structures in females. Females of a number of species of *Gerris* Fabricius, 1794 (Heteroptera: Gerridae) possess elongate abdominal spines that decrease the duration of premating struggles, thereby decreasing energetic costs to the females (Arnqvist and Rowe 1995).

The two hypotheses presented above are not necessarily mutually exclusive. These two selection pressures may act synergistically, which may explain the rapid evolution of these structures. Further observations of oviposition and mating behaviour of *Austromonticola*, combined with experiments manipulating the form of the laminae, will be required to evaluate these hypotheses.

Other, alternate hypotheses for these ventral structures could include male stimulation during mating, pre-copulatory species recognition signals to prevent hybridisation, assisting the retraction of the ovipositor after oviposition has been completed and providing an area for sensory organs to determine optimum oviposition sites.

Modified ventrites in other weevils

Although unusual, the highly modified ventrites of *Austromonticola* females are not unique. In the New Zealand context, modified ventrites are also known in species of *Chalepistes* (e.g. *C. dugdalei* (Barratt & Kuschel, 1996), *C. curvus* (Barratt & Kuschel, 1996) and *C. patricki* (Barratt & Kuschel, 1996)) and *Nicaeana*, which have medial laminae on ventrite 4 or various swellings on ventrite 5 (Barratt and Kuschel 1996). Species of *Platyacus* Faust, 1897 (Celeuthetini) in the Solomon Islands have the posterior margin of ventrite 4 developed into a medial projection or a trifurcate lamina (Tanner 1969; Marshall 1956). Most species of the endemic Mauritian genus *Syzygops* Schönherr, 1826 (Ottistirini) have simple ventrites in both sexes (Williams 2000), but several have modifications that include a large, trifurcate lamina on ventrite 4 (*S. insignis* Williams, 2000), a thin median projection on ventrite 4 (*S. ornatus* Williams, 2000), and ventrite 4 being almost completely invaginated (*S. vinsoni* Hustache, 1939). Some populations of *Trichalophus caudiculatus* (Fairmaire, 1886) (Tropiphorini) found in the Chinese Himalayas possess a bifurcate lamina on ventrite 4 (Grebennikov 2015), which has a similar shape to that of *A. furcatus* (Fig. 102). Species of *Leptomias* Faust, 1886 (Tanymecini) from montane Kashmir possess variable numbers and shapes of abdominal laminae; whereas *L. costatus* (Faust, 1897) has a lamina on ventrite 4 only, *L. montanus* (Aslam, 1969), *L. fletcheri* (Aslam, 1969) and *L. rufus* (Aslam, 1969) have a lamina on ventrite 3 in addition to one on ventrite 4 (Aslam 1969). The species possessing these laminae were represented only by females, and there is no indication that Aslam (1969) recognised these structures as sexually dimorphic. Laminae are also known from some Himalayan species of *Leptomias* (Li Ren pers. comm.) and Central American *Sciomias* Sharp, 1911 (Sciaphilini) (R. Anderson pers. comm.), but no details have been published. Abdominal laminae are also known in the subfamily Cyclominae, with females of the *Nestrius bifurcus* Kuschel, 1964 group of species having laminae formed at the posterior margin of ventrite 3 (Kuschel 1964).

The cushion growth form is a feature of alpine vegetation worldwide, and is prevalent in the Himalayas (Chen et al. 2015, Dolezal et al. 2016), where several of the weevil species discussed above are found. Additionally, *Syzygops* is associated with ferns, which frequently present a dense rhizome mat. These observations lend support to the first hypothesis detailed above, which posits that abdominal laminae assist with preparation of oviposition sites in close-packed vegetational structures. Further investigation of the oviposition behaviour of these weevils will be necessary to accurately evaluate this hypothesis. It also predicts that weevils displaying abdominal laminae will be found in other regions where cushion vegetation is present, such as Tasmania (Gibson and Kirkpatrick 1985), the Andes (Molina-Montenegro et al. 2006) and Siberia (Volkov and Volkova 2015).

Relationships

The morphological phylogeny is largely consistent with the molecular data, in that both indicate a close relationship between *A. furcatus*, *A. atriarius* and *A. mataura*.

However, the position of *A. rotundus* in the morphology-based tree, placed as the sister taxon of the *A. mataura* clade, is not supported by the molecular data. The overall signal from the molecular data is that *A. rotundus* is the most distant of all the species for which DNA sequences were obtained, however no consensus was gained regarding its nearest relative. Results from COI and 28S are surprising. In the analysis of COI, *A. inflatus* was nearest to *A. rotundus*, whereas *A. inflatus* has the same 28S sequence as *A. atriarius* and *A. furcatus*. These results serve to bolster confidence that *A. inflatus*, *A. postinventus* and *A. caelibatus* are congeneric with the other members of the genus. Obtaining DNA sequences from the other species in the genus, especially the morphologically distinct *A. planulatus*, will be important for further insights into the relationships of species in the genus.

New Zealand alpine weevil fauna

Austromonticola is one of a number of weevils that inhabit the montane regions of New Zealand. Other weevil genera with representatives found above the treeline include *Baeosomus* Broun, 1904 (Brachycerinae), *Anagotus* Sharp, 1882, *Gromilus* Blanchard, 1853, *Liparogetus* Broun, 1915, *Lyperopais* Broun, 1893 (Cyclominae), *Lyperobius* Pascoe, 1876, "*Crisius*" Pascoe, 1876 (Molytinae), *Eugnomus* Schönherr, 1847, *Oreocalus* May 1993, *Pactolotypus* Broun, 1909, *Stephanorhynchus* White, 1846 (Curculioninae: Eugnomini), *Peristoreus* and *Simachus* (Curculioninae: Storeini). However, the Entiminae are best represented, with 13 genera (*Austromonticola*, *Sargon* Broun, 1903, *Inophloeus*, *Chalepistes*, *Catoptes*, *Nicaeana*, *Haplolobus*, *Zenagraphus*, *Neoevas* Broun, 1921, and four undescribed genera) having species found primarily or solely in montane environments over 1000 m in elevation.

This diverse community is at apparent odds with the young geological age of the environment. The Southern Alps began rising around 5 million years ago (Sutherland 1996). The Old Man Range is older, with uplift estimated to have begun in the middle Miocene (c. 15 mya) (Craw et al. 2012). The Hawkdun and Kirkliston Ranges are estimated to have begun rising in the late Miocene (Youngson et al. 1998; Forsyth 2001). Prior to this time, the landscape of the Central Otago region is inferred to have been a low-relief basin, dominated by the large, freshwater Lake Manuherikia (Mildenhall 1989).

A geobiological model of the origin of the New Zealand alpine flora posited by Heenan and McGlone (2013) infers that a sizable component of the modern flora is derived from the community of plants that inhabited infertile and boggy lowland environments. It is noteworthy that one of the plant genera mentioned explicitly by Heenan and McGlone (2013) as providing evidence for their model is *Phyllachne*, upon which several species of alpine Entiminae have been collected (SDJ Brown pers. obs.). This model predicts that closely related species or genera may be found in lowland bogs. Unfortunately, these habitats have been greatly diminished as a result of agricultural intensification. However, there remain relatively intact remnant wetland systems in Southland that have a similar vegetation community to alpine

bogs (McGlone 2009) and which may harbour sister taxa of alpine specialists. An example of this scenario is the crambid moth *Orocrambus thymiastes* Meyrick, 1901, which is found in alpine boggy regions, but has a population in the Awarua-Waituna Wetlands (Gaskin 1975).

An alternative possibility for the origin of the New Zealand alpine biota is dispersal from alpine regions in Australia, South America or the Northern Hemisphere. These areas have been the main sources for the majority of New Zealand alpine plant radiations (Winkworth et al. 2005). Dispersal from alpine areas elsewhere is an unlikely scenario for New Zealand's alpine weevils, as most of the genera are New Zealand endemics, with no close relatives elsewhere. However, little work has been done on the relationships of New Zealand weevils to other world faunas, and until these studies have been done, the dispersal hypothesis will remain untested.

Research into the mechanisms by which these weevil lineages have adapted to alpine environments, as has been investigated in other New Zealand alpine insects (Wharton 2011; Dunning et al. 2014), will be useful to inform further hypotheses of the origin of the New Zealand alpine weevil fauna.

Conservation significance

The localised distribution of most of the species of *Austromonticola* place them within the Naturally Uncommon (Range Restricted) threat classification category (Townsend et al. 2008). All species already have significant portions of their range administered by DOC as Stewardship Areas. The main threats to these species are likely to be predation by introduced mammals (O'Donnell et al. 2017) and encroachment of weeds. Non-target parasitism by adventive wasps is also a potential threat (Barlow et al. 2004; Barratt et al. 2007). All of these threats are expected to increase due to climate change (Halloy and Mark 2003). The much larger distribution of *A. rotundus* results in it being given the classification of Not Threatened.

Conclusion

Additional research into the biology, behaviour and physiology of the species of *Austromonticola* described here will offer insight into the function of the exaggerated abdominal structures of the females, and into processes by which sexual selection accelerates speciation. Further exploration and collecting, especially in areas such as the Mt Teviot/Manorburn region in Central Otago, the Pisa Range, Dunstan Mountains and Mt Aspiring National Park, will be vital for discovering additional species in the genus, which will provide further data for evaluating hypotheses of the role of historical contingency and environmental pressures on the evolution of alpine insects.

Plates

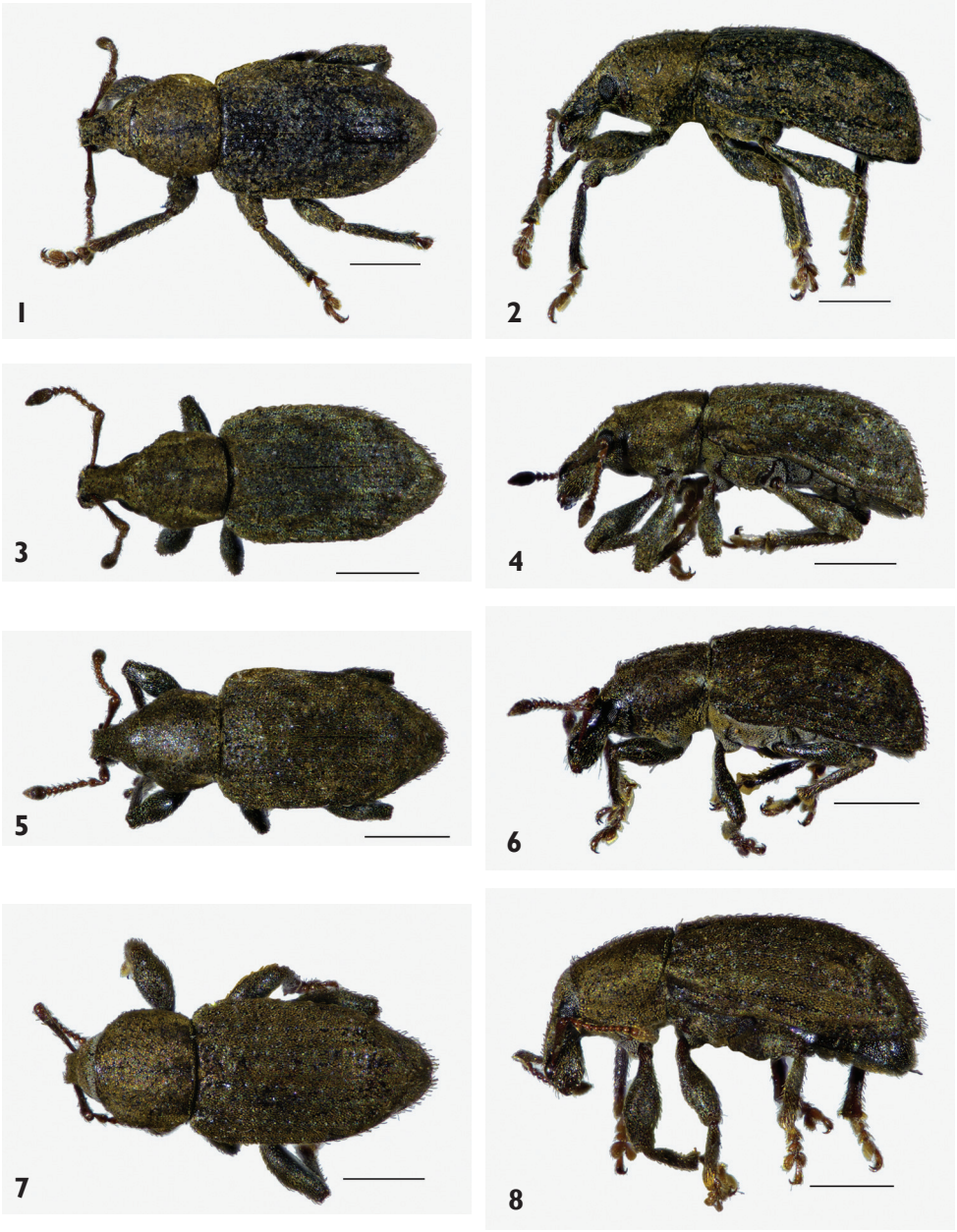

Figures 1–8. Habitus photographs of *Austromonticola* males. **1, 2** *A. atriarius* **3, 4** *A. mataura* **5, 6** *A. furcatus* **7, 8** *A. rotundus*. Scale bars = 1 mm.

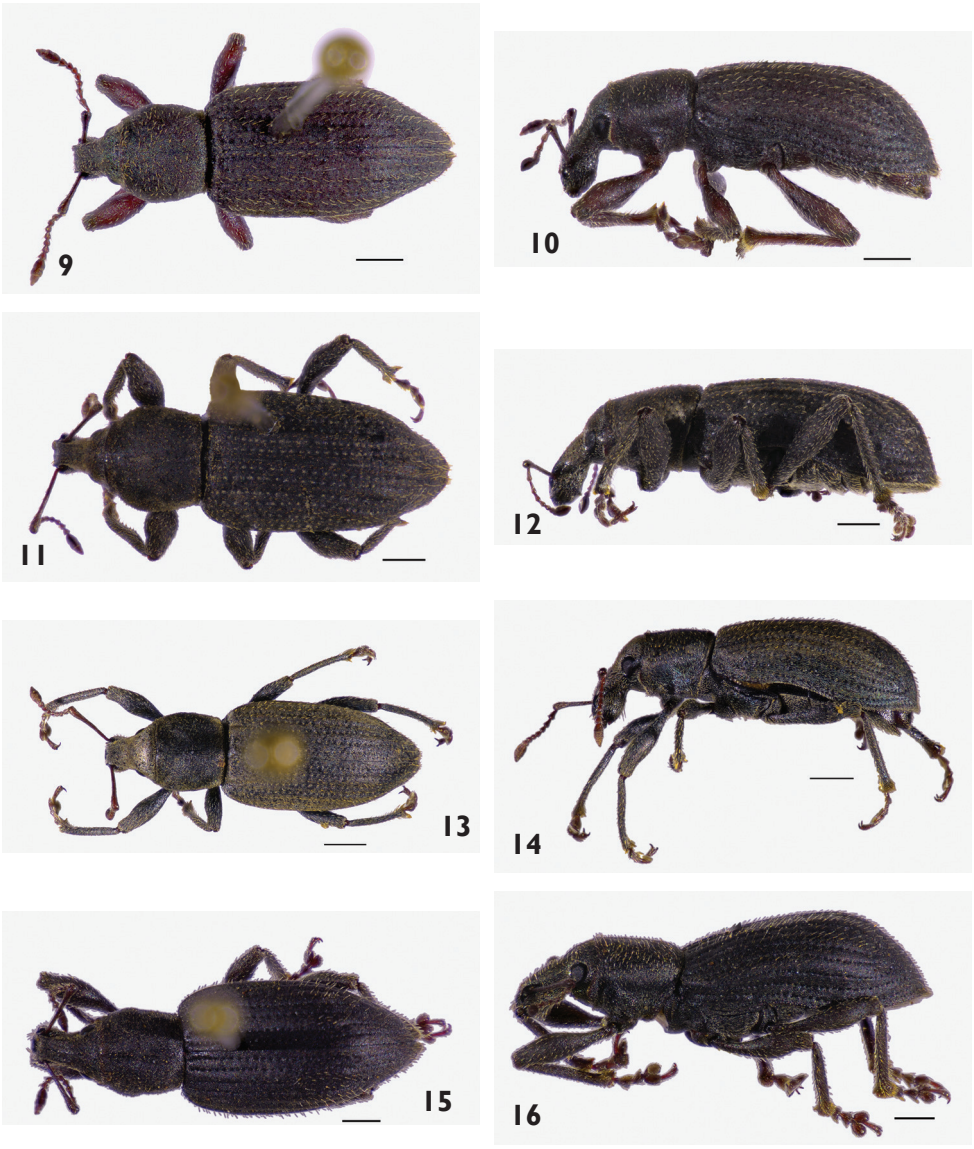

Figures 9–16. Habitus photographs of *Austromonticola* males. **9, 10** *A. postinventus* **11, 12** *A. planulatus* **13, 14** *A. inflatus* **15, 16** *A. caelibatus*, holotype. Scale bars = 1 mm.

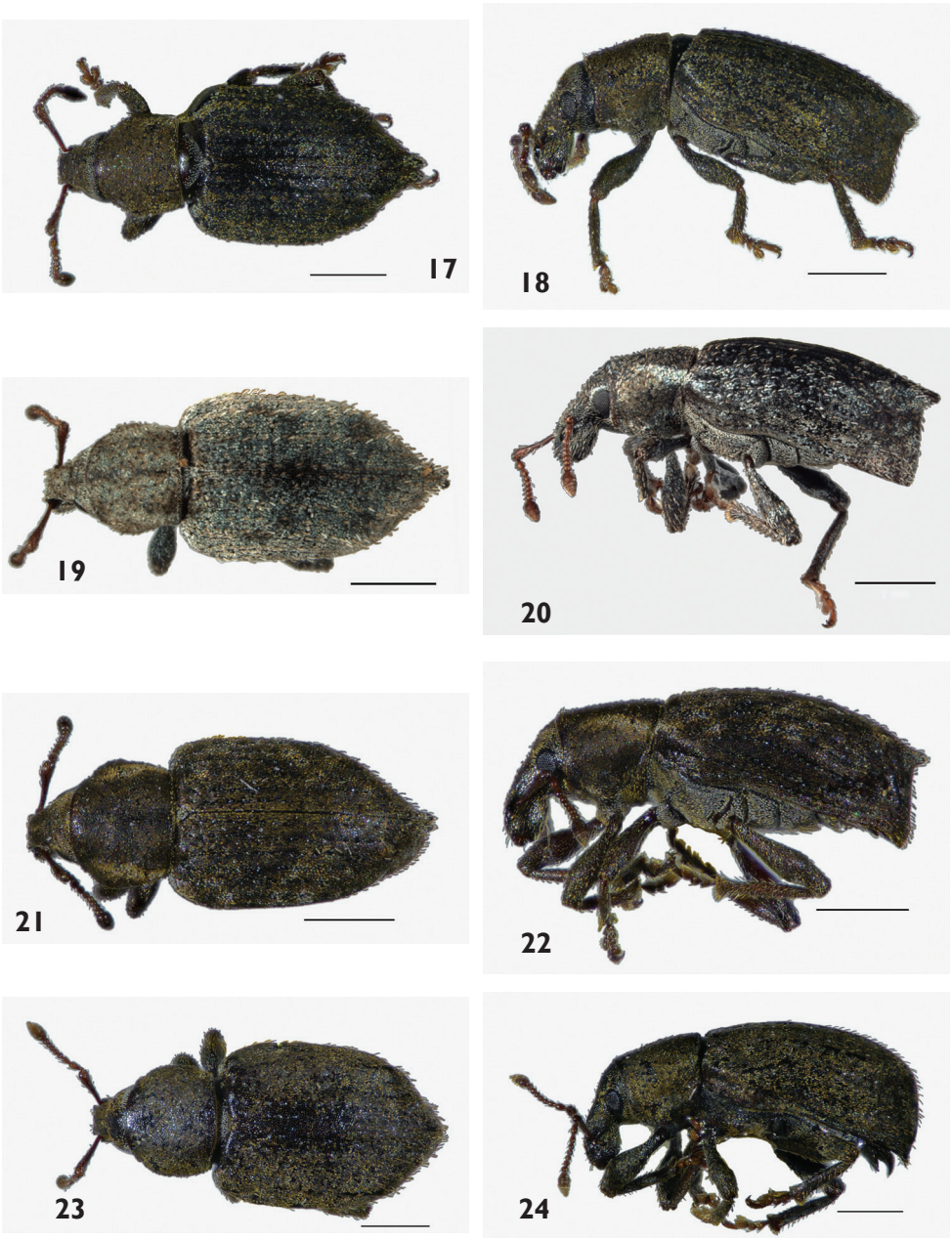

Figures 17–24. Habitus photographs of *Austromonticola* females. **17, 18** *A. atriarius* **19, 20** *A. mataura* **21, 22** *A. furcatus* **23, 24** *A. rotundus*. Scale bars = 1 mm.

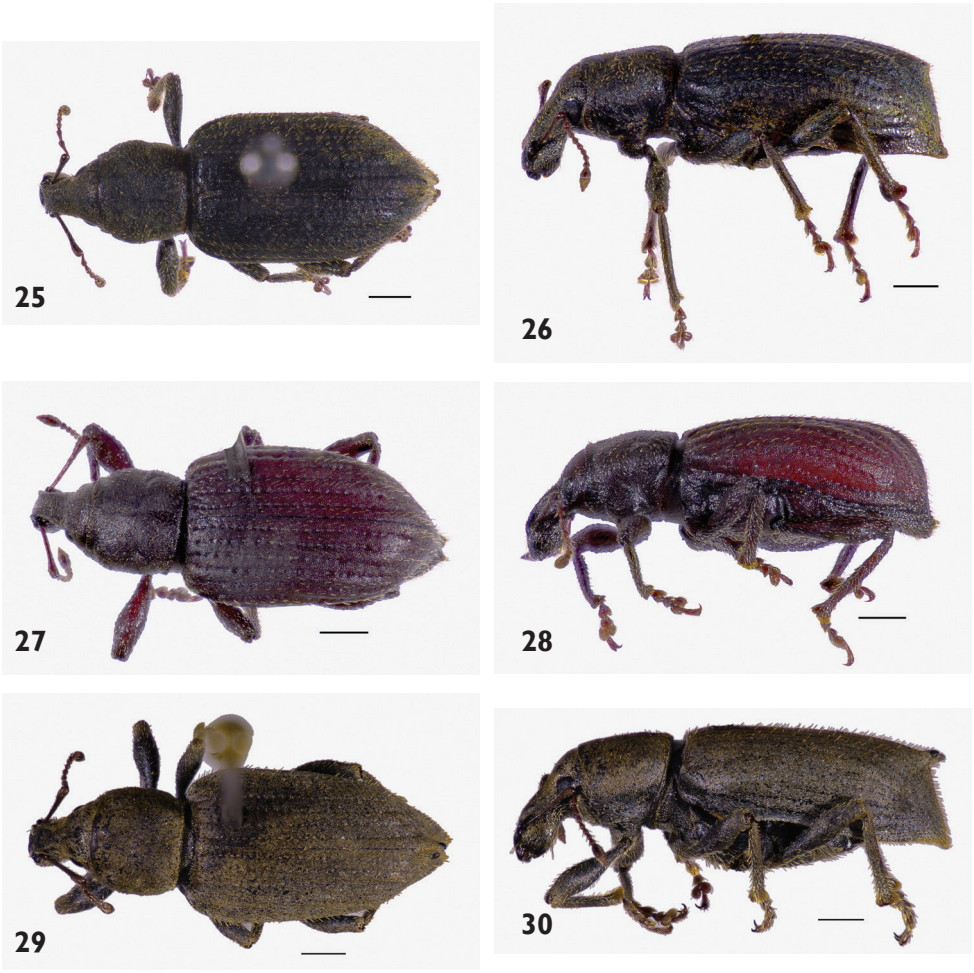

Figures 25–30. Habitus photographs of *Austromonticola* females. **25, 26** *A. postinventus*, holotype **27, 28** *A. planulatus*, holotype **29, 30** *A. inflatus*, holotype. Scale bars = 1 mm.

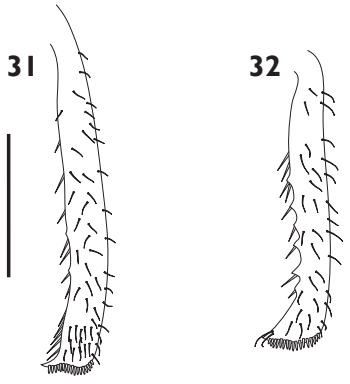

Figures 31–32. Left protibia, anterior view. **31** *Austromonticola inflatus*, holotype **32** *Austromonticola planulatus*, holotype. Scale bar = 1 mm.

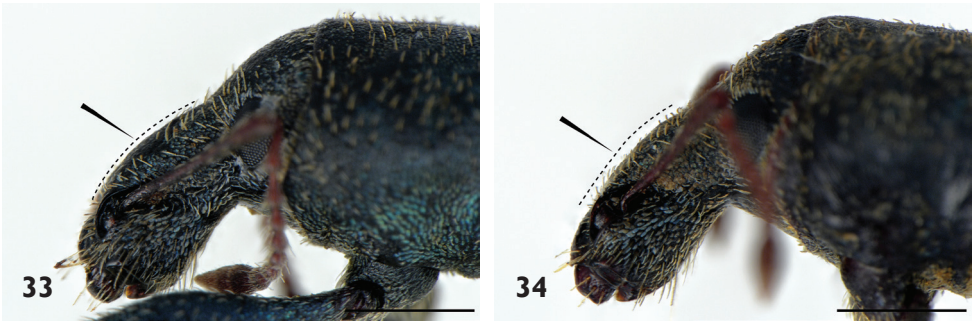

Figures 33–34. Rostrum, lateral view. **33** *Austromonticola inflatus*, arrow and dashed line indicates convex epifrons **34** *Austromonticola postinventus*, holotype, arrow and dashed line indicates flattened. Scale bars = 1 mm.

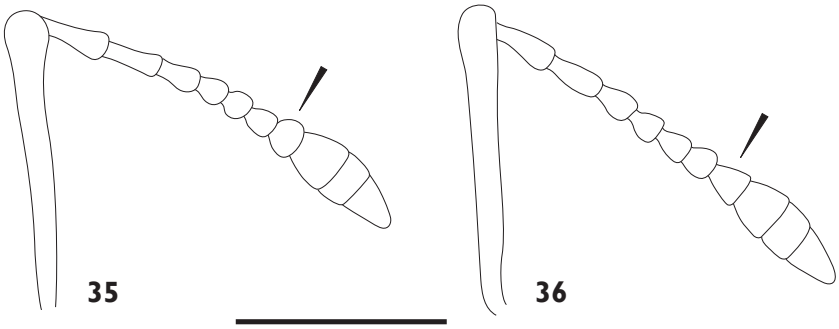

Figures 35–36. Left antenna, anterior view. **35** *Austromonticola inflatus*, holotype **36** *Austromonticola postinventus*, holotype. Arrows indicate funicle segment 7. Scale bar = 1 mm.

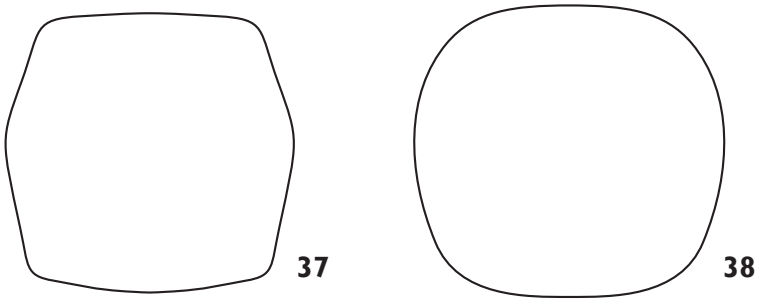

Figures 37–38. Pronotum, dorsal view. **37** *Austromonticola furcatus* **38** *Austromonticola rotundus*.

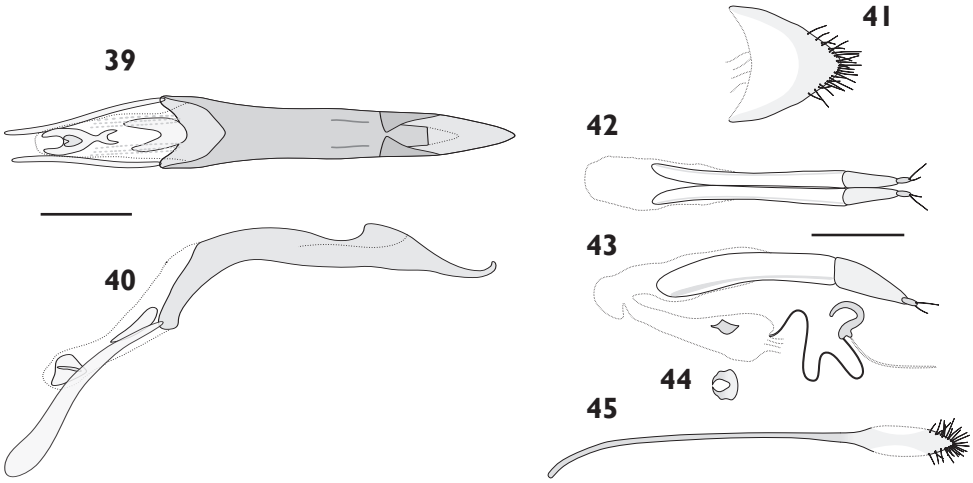

Figures 39–45. Genitalia of *Austromonticola atriarius*. **39** penis, dorsal view **40** aedeagus, lateral view **41** female tergite 8, dorsal view **42** ovipositor, dorsal view **43** ovipositor and spermatheca, lateral view **44** bursal sclerite, ventral view **45** female sternite 8, ventral view. Scale bars = 0.5 mm; **39–40** at same scale; **41–45** at same scale.

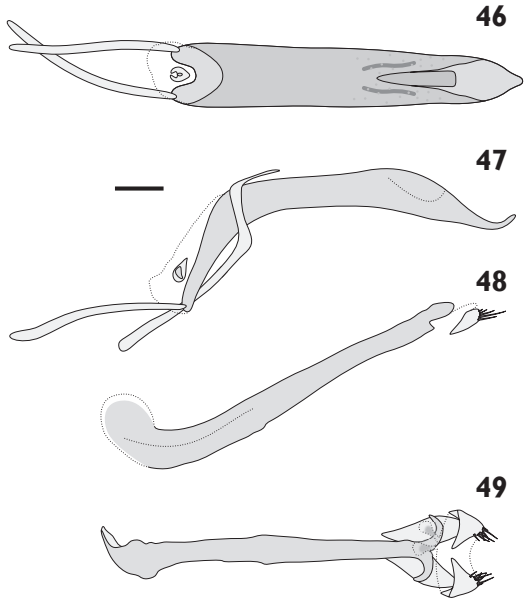

Figures 46–49. Genitalia of *Austromonticola caelibatus*. **46** penis, dorsal view **47** aedeagus, lateral view **48** male hemisternites 8 and spiculum gastrale, lateral view (membrane between hemisternites 8 and basal plate indicated) **49** male hemisternites 8 and spiculum gastrale with basal plate, ventral view. Scale bar = 0.5 mm.

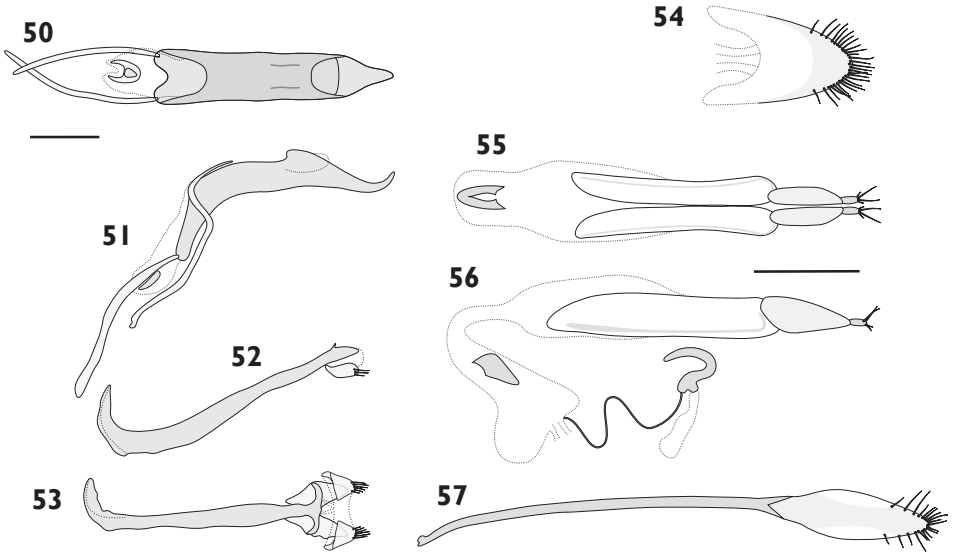

Figures 50–57. Genitalia of *Austromonticola furcatus*. **50** penis, dorsal view **51** aedeagus, lateral view **52** male hemisternites 8 and spiculum gastrale, lateral view (membrane between hemisternites 8 and basal plate indicated) **53** male hemisternites 8 and spiculum gastrale with basal plate, ventral view **54** female tergite 8, dorsal view **55** ovipositor, dorsal view **56** ovipositor and spermatheca, lateral view **57** female sternite 8, ventral view. Scale bars = 0.5 mm; **50–53** at same scale; **54–57** at same scale.

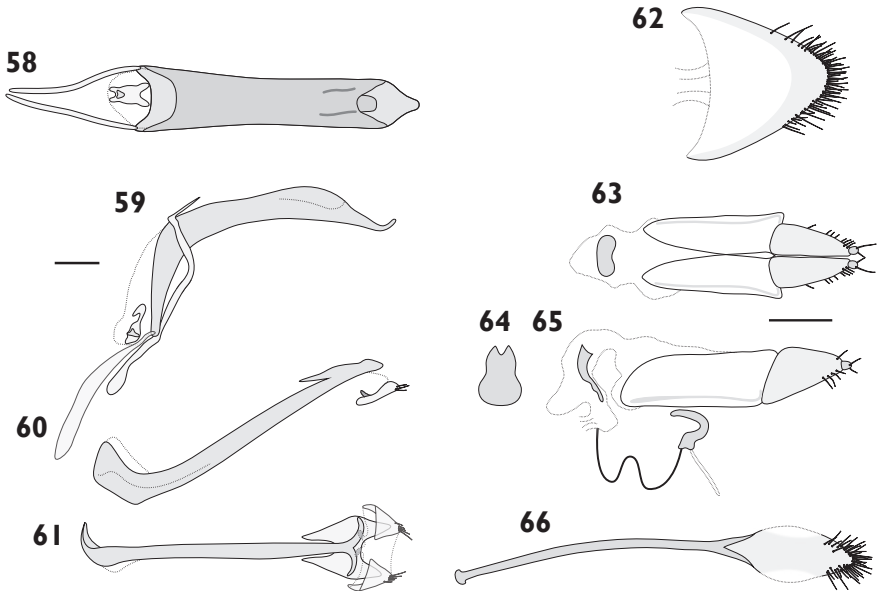

Figures 58–66. Genitalia of *Austromonticola inflatus*. **58** penis, dorsal view **59** aedeagus, lateral view **60** male hemisternites 8 and spiculum gastrale, lateral view (muscles between hemisternites 8 and basal plate indicated) **61** male hemisternites 8 and spiculum gastrale with basal plate, ventral view **62** female tergite 8, dorsal view **63** ovipositor, dorsal view **64** bursal sclerite, anterior view **65** ovipositor and spermatheca, lateral view **66** sternite 8, ventral view. Scale bars = 0.5 mm; **58–61** at same scale; **62–66** at same scale.

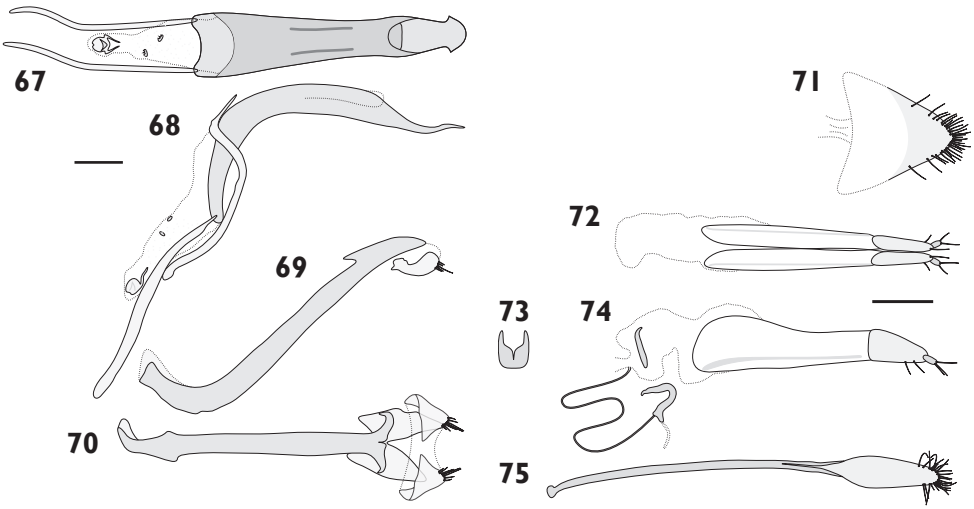

Figures 67–75. Genitalia of *Austromonticola planulatus*. **67** penis, dorsal view **68** aedeagus, lateral view **69** male hemisternites 8 and spiculum gastrale, lateral view (muscles between hemisternites 8 and basal plate indicated) **70** male hemisternites 8 and spiculum gastrale with basal plate, ventral view **71** tergite 8, dorsal view **72** ovipositor, dorsal view **73** bursal sclerite, anterior view **74** ovipositor and spermatheca, lateral view **75** female sternite 8, ventral view. Scale bars = 0.5 mm; 67–70 at same scale; 71–75 at same scale.

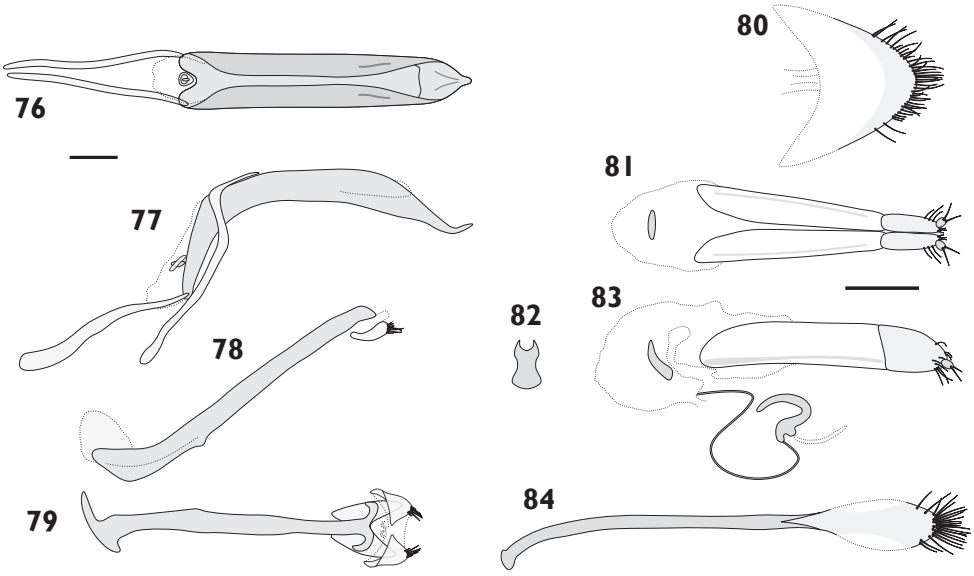

Figures 76–84. Genitalia of *Austromonticola postinventus*. **76** penis, dorsal view **77** aedeagus, lateral view **78** male hemisternites 8 and spiculum gastrale, lateral view (muscles between hemisternites 8 and basal plate indicated) **79** male hemisternites 8 and spiculum gastrale with basal plate, ventral view **80** female tergite 8, dorsal view **81** ovipositor, dorsal view **82** bursal sclerite, anterior view **83** ovipositor and spermatheca, lateral view **84** female sternite 8, ventral view. Scale bars = 0.5 mm; **75–79** at same scale; **80–84** at same scale.

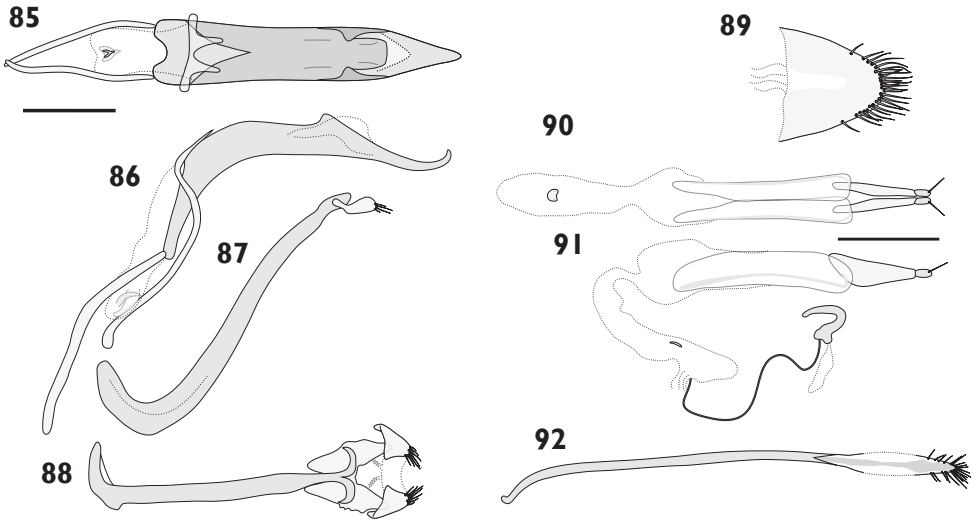

Figures 85–92. Genitalia of *Austromonticola mataura*. **85** aedeagus, dorsal view **86** aedeagus, lateral view **87** male hemisternites 8 and spiculum gastrale, lateral view (muscles between hemisternites 8 and basal plate indicated) **88** male hemisternites 8 and spiculum gastrale with basal plate, ventral view **89** female tergite 8, dorsal view **90** ovipositor, dorsal view **91** ovipositor and spermatheca, lateral view **92** female sternite 8, ventral view. Scale bars = 0.5 mm; **85–88** at same scale; **89–92** at same scale.

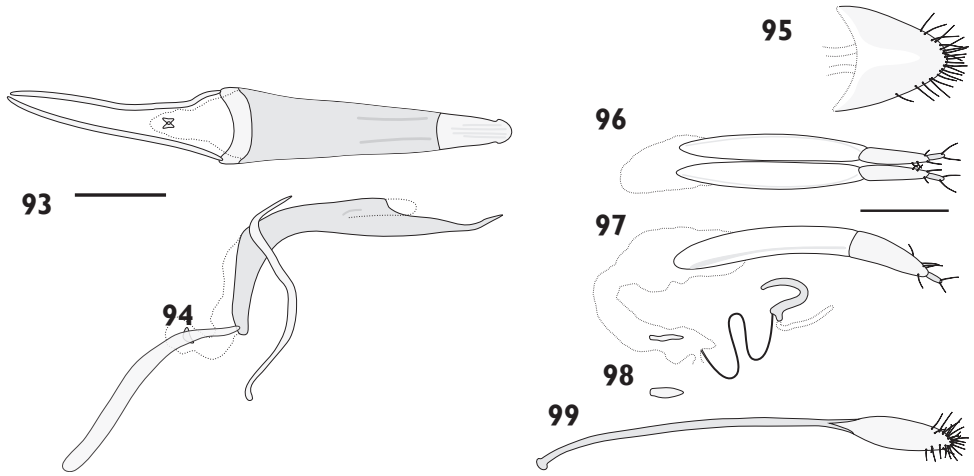

Figures 93–99. Genitalia of *Austromonticola rotundus*. **93** penis, dorsal view **94** aedeagus, lateral view **95** female tergite 8, dorsal view **96** ovipositor, dorsal view **97** ovipositor and spermatheca, lateral view **98** bursal sclerite, ventral view **99** female sternite 8, ventral view. Scale bars = 0.5 mm; **93–94** at same scale; **95–99** at same scale.

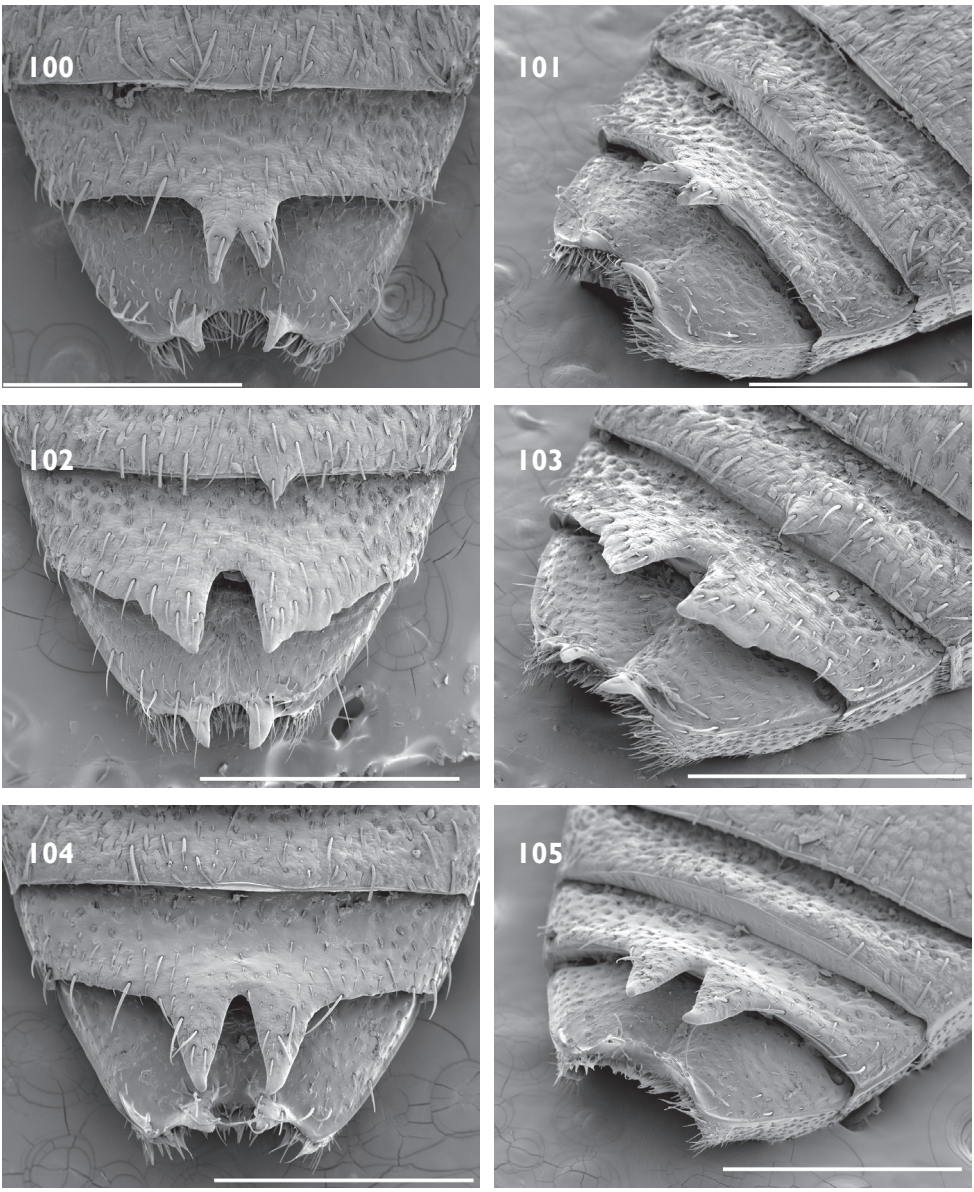

Figures 100–105. SEM photographs of abdominal ventrites 4 and 5 of *Austromonticola* females. **100, 101** *A. atriarius* **102, 103** *A. furcatus* **104, 105** *A. mataura*. Left: ventral view. Right: ventroposterolateral view. Scale bars = 0.5 mm.

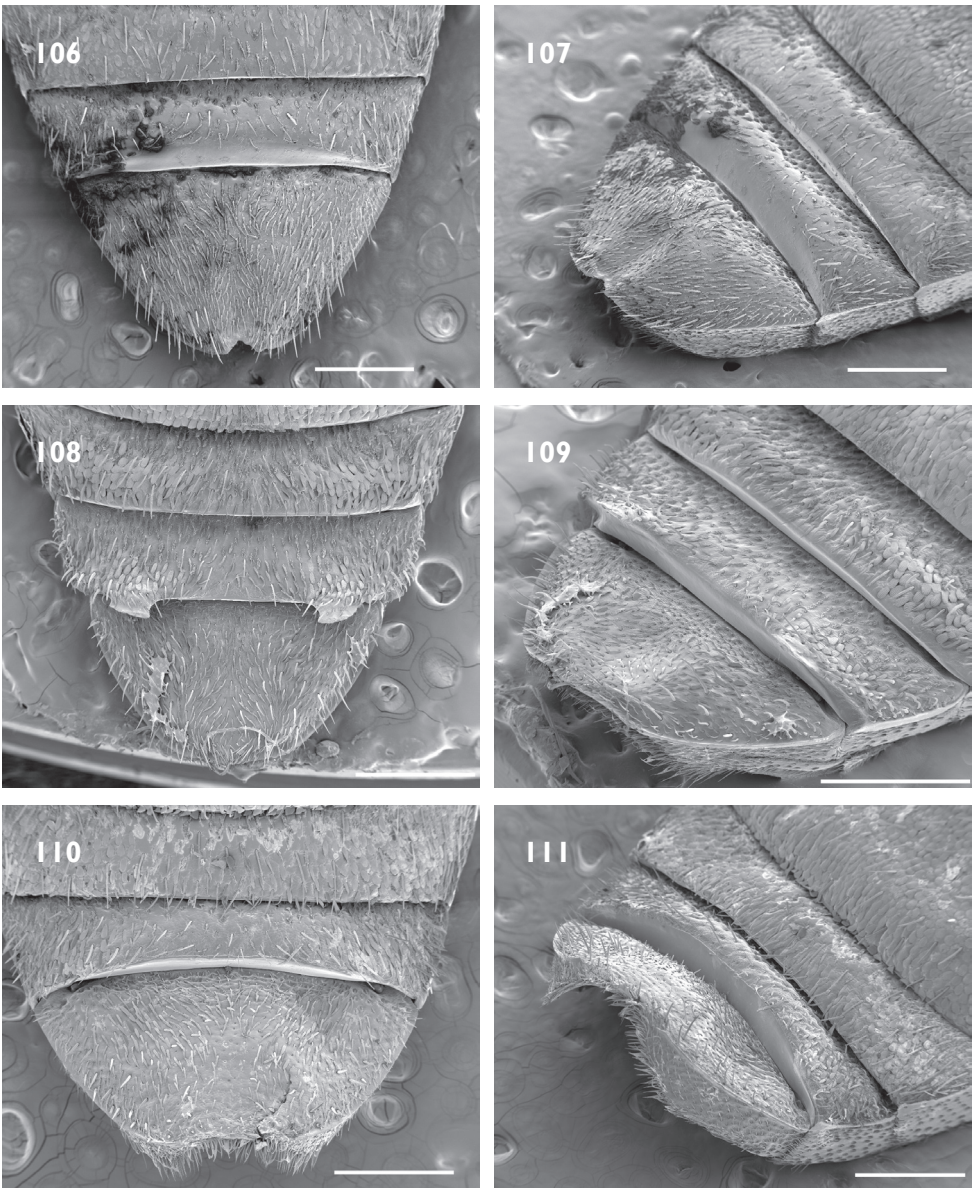

Figures 106–111. SEM photographs of abdominal ventrites 4 and 5 of *Austromonticola* females. **106, 107** *A. inflatus*, holotype **108, 109** *A. planulatus*, holotype **110, 111** *A. postinventus*, holotype. Left: ventral view. Right: ventroposterolateral view. Scale bars = 0.5 mm.

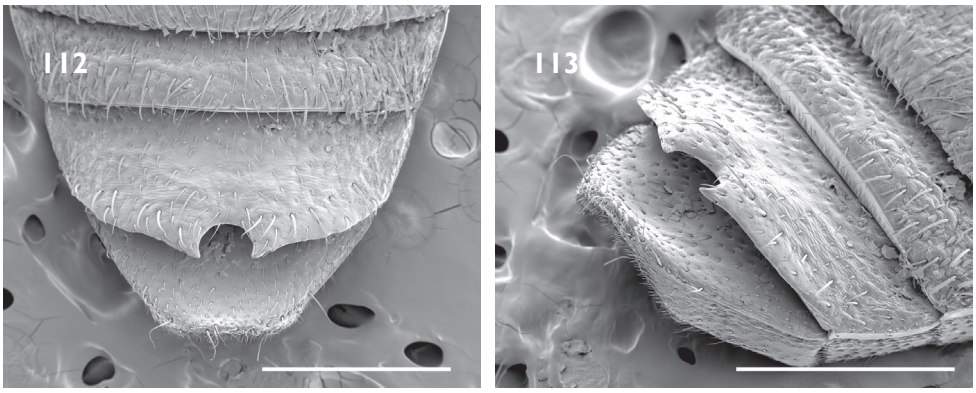

Figures 112–113. SEM photographs of abdominal ventrites 4 and 5 of female *Austromonticola rotundus.* **112** ventral view **113** ventroposterolateral view. Scale bars = 0.5 mm.

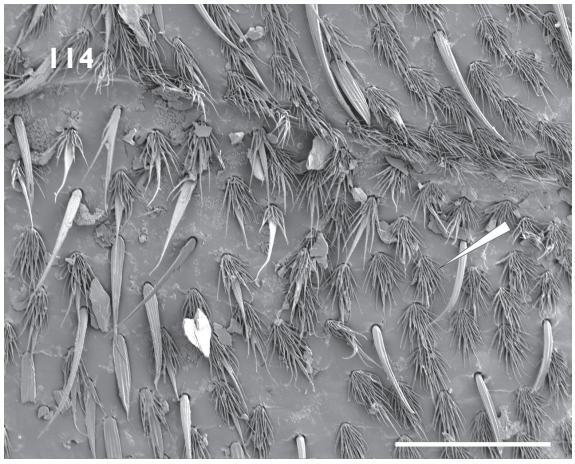

Figure 114. SEM photograph of *Austromonticola furcatus* abdominal ventrite 2 showing pappolepidia (arrowed). Scale bar = 0.1 mm.

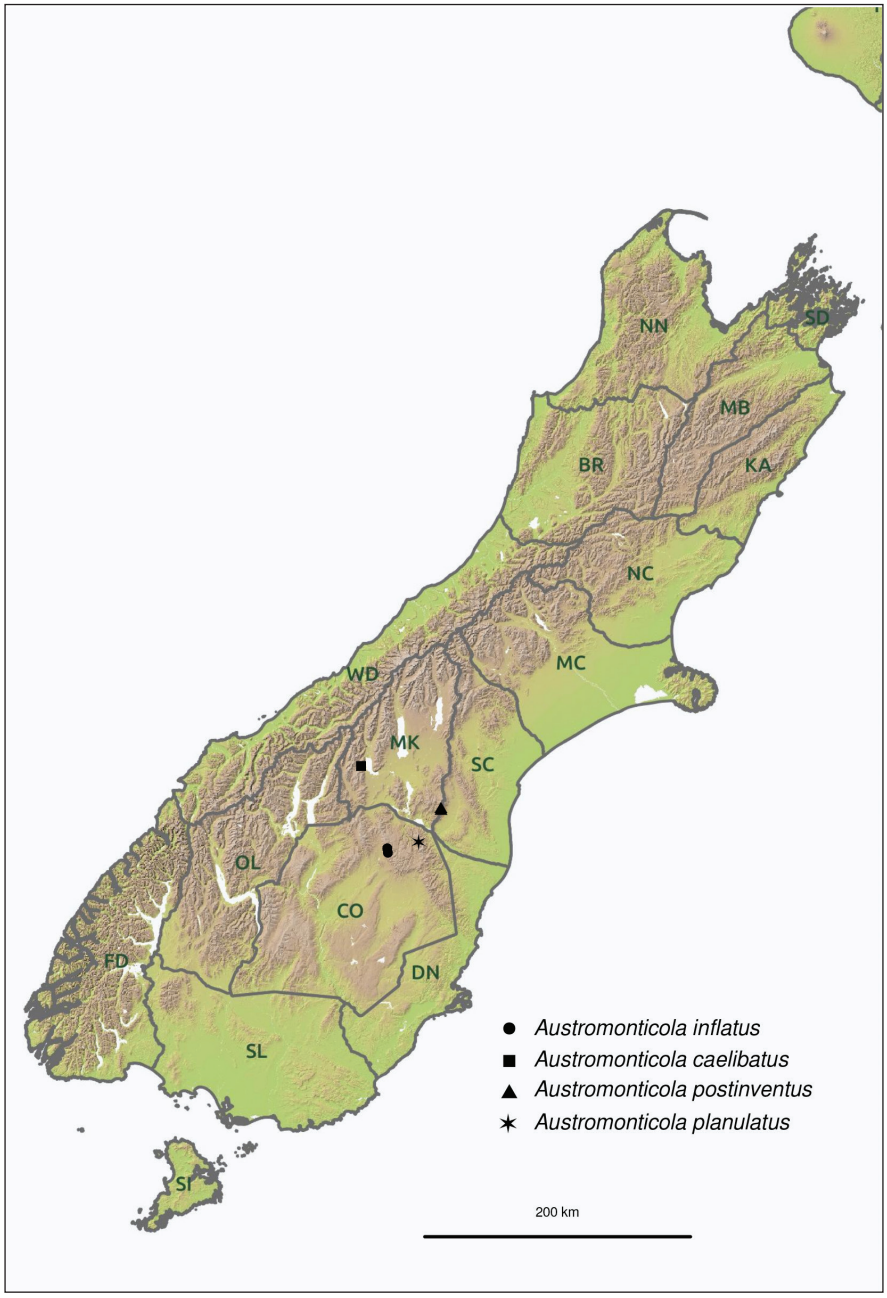

Figure 115. Distributions of *Austromonticola inflatus* (circles), *A. caelibatus* (squares), *A. postinventus* (triangles) and *A. planulatus* (stars).

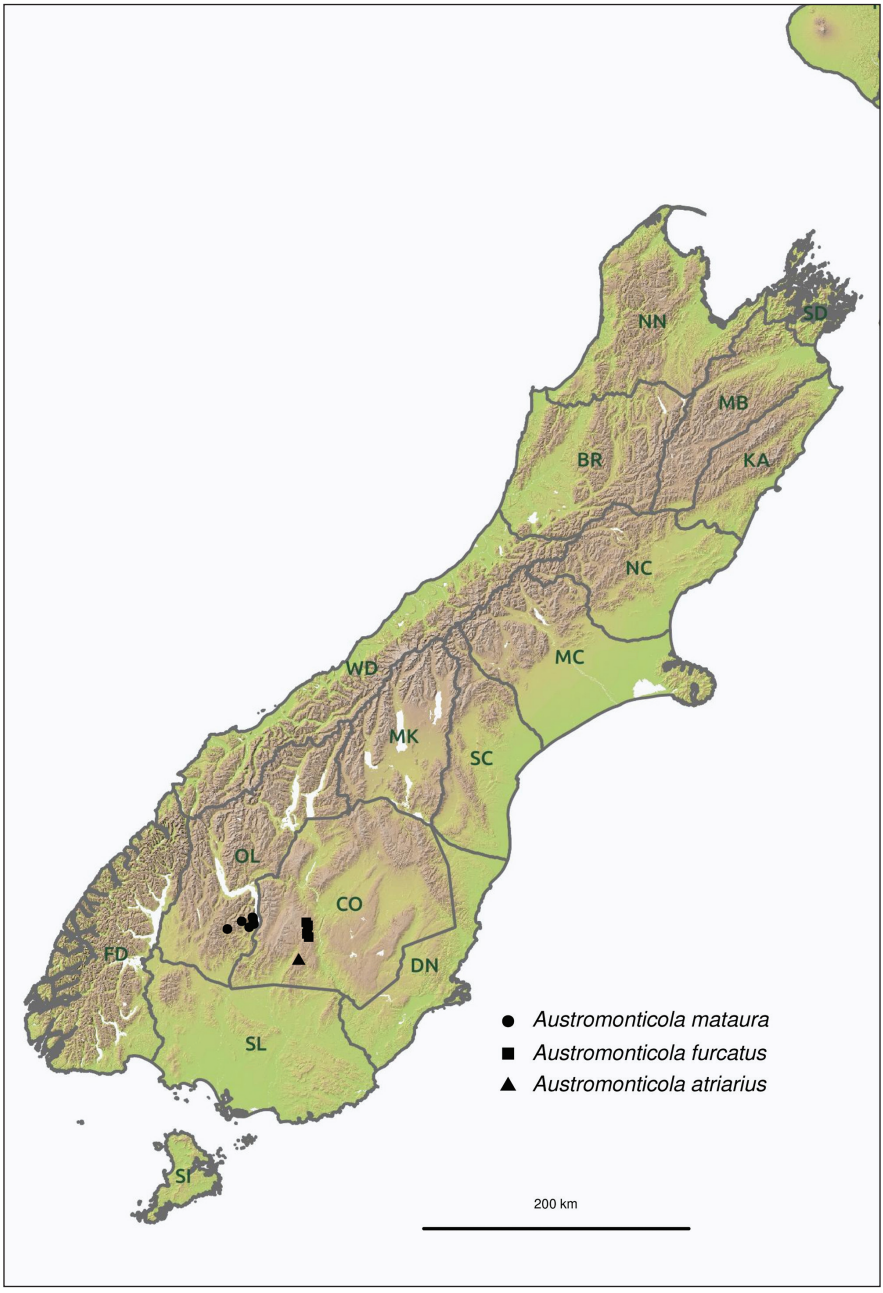

Figure 116. Distributions of *Austromonticola mataura* (circles), *A. furcatus* (squares) and *A. atriarius* (triangles).

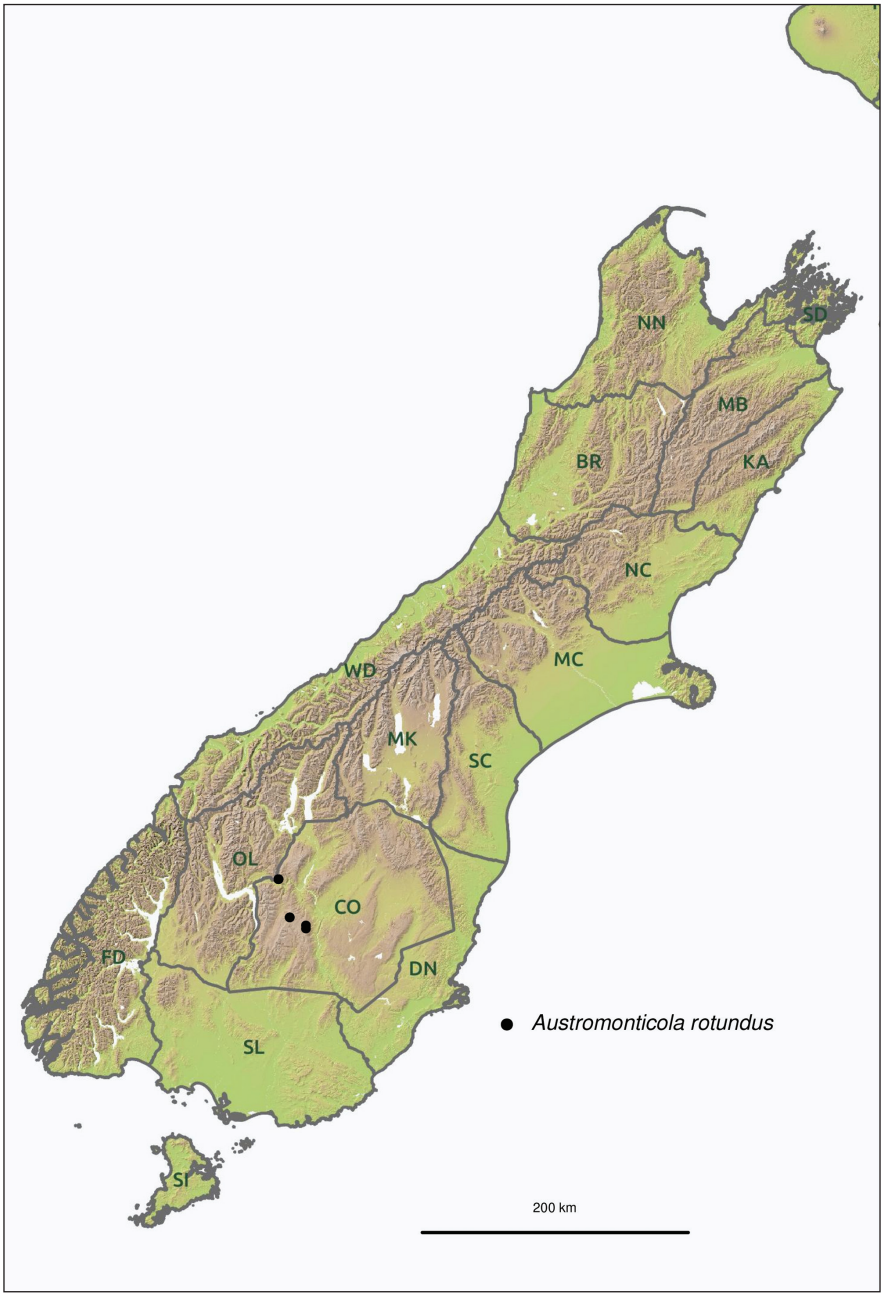

Figure 117. Distribution of *Austromonticola rotundus*.

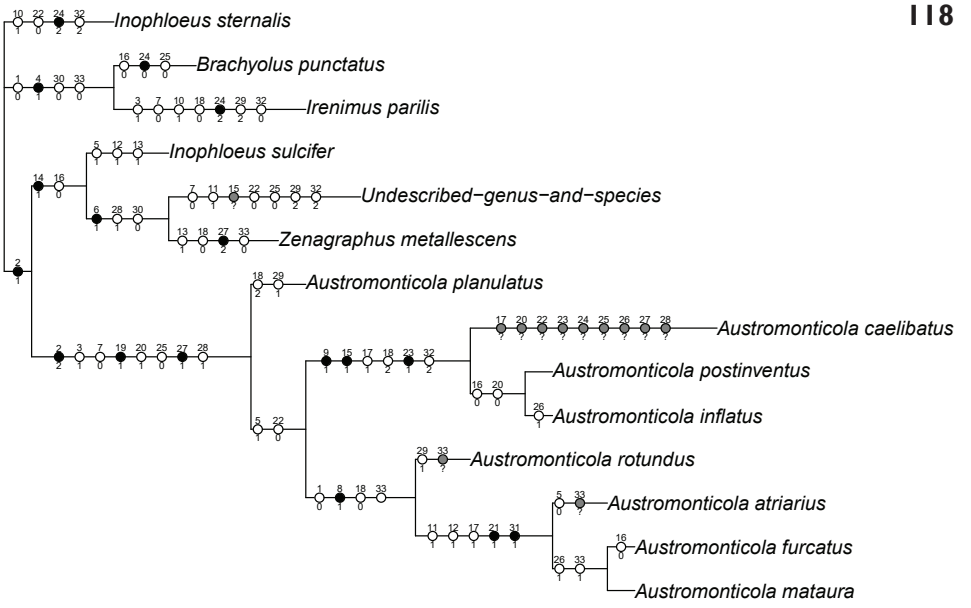

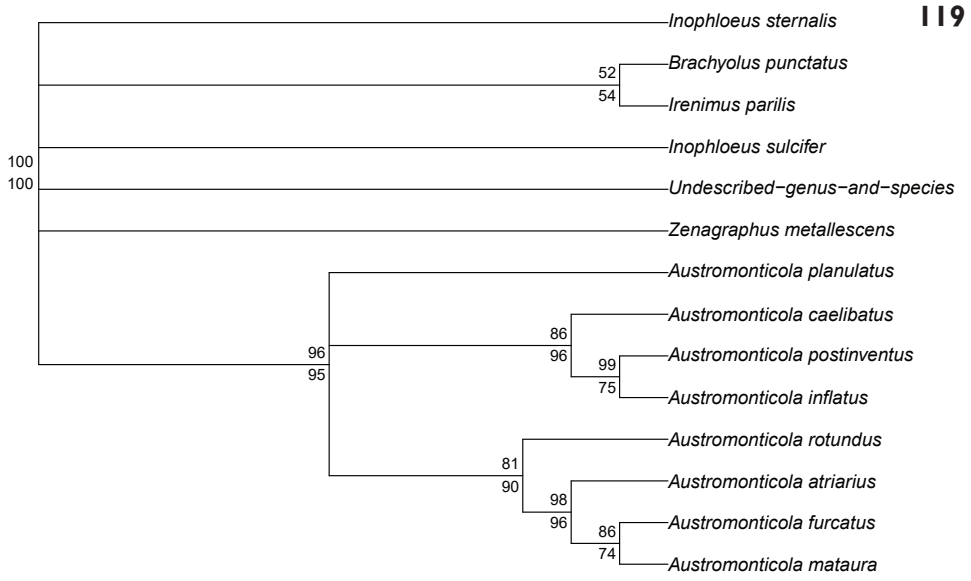

Figures 118–119. Cladograms showing phylogenetic relationships between *Austromonticola* species as inferred from morphological data. **118** single most parsimonious tree inferred from 33 characters scored for 14 species **119** phylogenetic tree of *Austromonticola* with bootstrap values above nodes and jackknife values below. Nodes with lower than 50% support were collapsed.

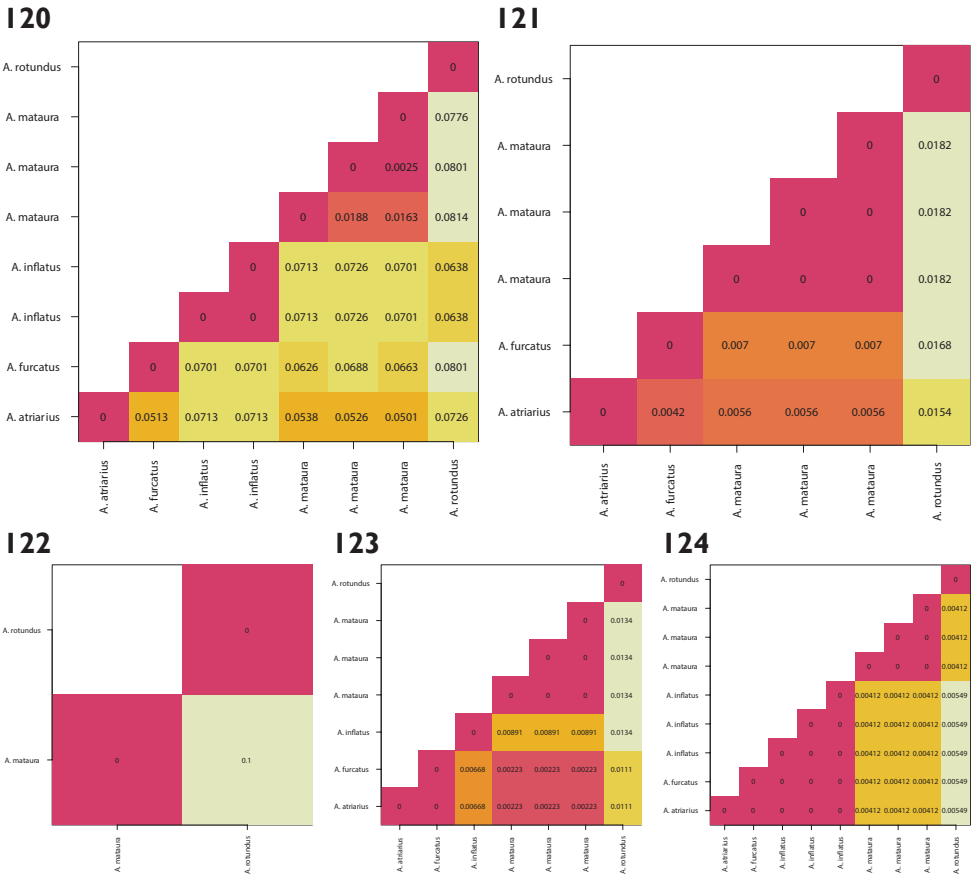

Figures 120–124. Heatmaps of the uncorrected pairwise genetic distances between *Austromonticola* specimens sampled. Lighter colours indicate greater distances. **120** the 3' region of the COI mitochondrial protein-coding gene **121** CAD nuclear protein-coding gene **122** the 5' ("barcoding") region of COI **123** ArgK nuclear protein-coding gene **124** 28S nuclear ribosomal RNA gene.

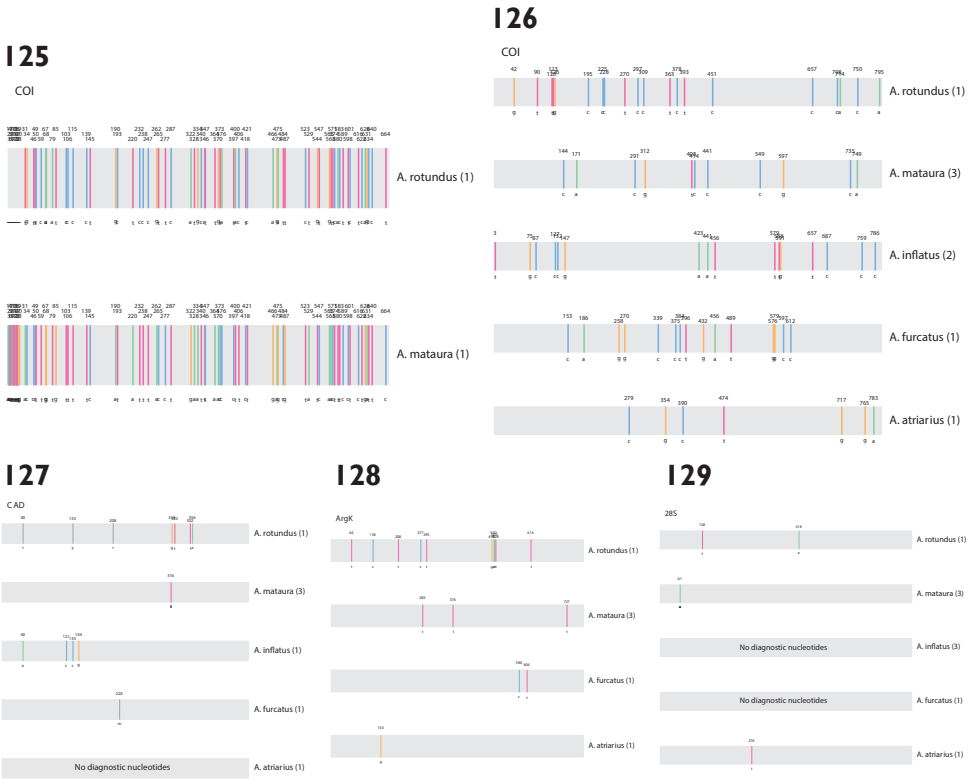

Figures 125–129. Diagnostic nucleotides within the *Austromonticola* specimens sampled. Numbers above the bars indicate the position of the diagnostic base within the alignment. Numbers in parentheses beside species names indicate the numbers of specimens included in the alignment. Letters below the bars and the colour of the vertical bar indicate the value of the diagnostic nucleotide. **125** the 5' ("barcoding") region of the COI mitochondrial protein-coding gene **126** the 3' region of COI **127** CAD nuclear protein-coding gene **128** ArgK nuclear protein-coding gene **129** 28S nuclear ribosomal RNA gene.

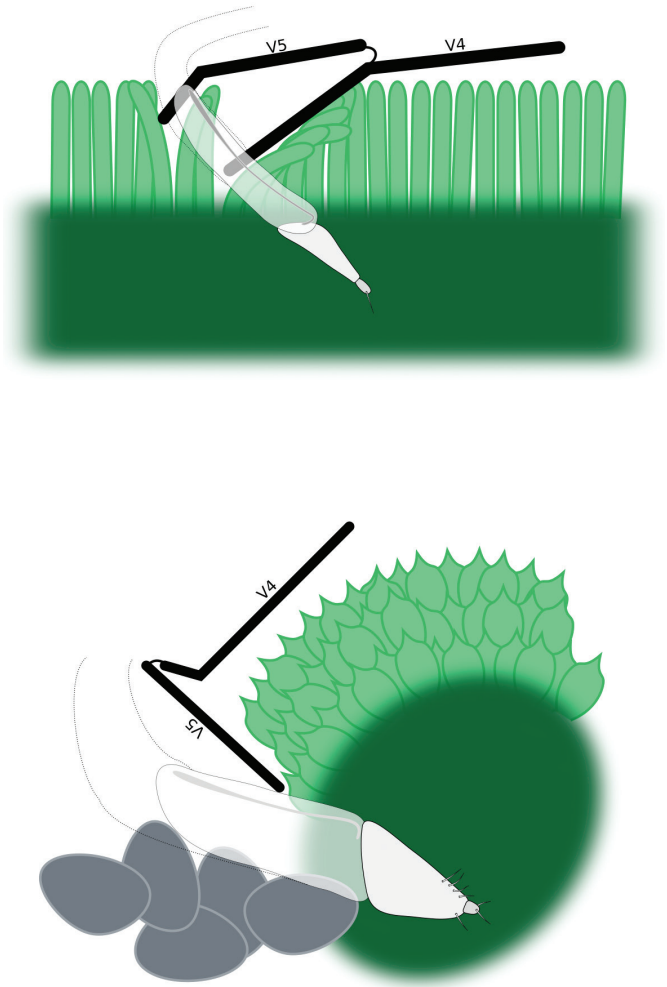

Figures 130–131. Schematic diagrams of hypothesised oviposition posture. **130** hypothesised function of lamina on ventrite 4 and horns surrounding genital orifice on ventrite 5, which force apart dense foliage of cushion plants to allow oviposition in peaty layer underneath **131** hypothesised function of recurved margin of ventrite 4 which allows maximum flexion of ventrite 5, enabling oviposition under the side of cushions between the plant and the surrounding substrate. Abbreviations: V4–ventrite 4; V5–ventrite 5. Figures not drawn to scale.

Acknowledgements

This research was funded by Lincoln University, the Miss E. L. Hellaby Indigenous Grasslands Research Trust and AgResearch (MSI contract LINX0304, Ecosystems Bioprotection), as part of the author's doctoral programme. The basemap of distribution maps was provided courtesy of Geographx. Miguel Alonso-Zarazaga (Museo Nacional de Ciencias Naturales), Robert Anderson (Canadian Museum of Nature), Karen Armstrong (Bio-Protection Research Centre), John Marris (Bio-Protection Research Centre) and Rolf Oberprieler (CSIRO Ecosystem Services) critically commented on the manuscript. Robert Hoare (Landcare Research) provided guidance on name formation. Mike Flaws (University of Canterbury) assisted with scanning electron microscopy, while Cor Vink (Canterbury Museum) provided access to photomicroscopy facilities. Gregory Holwell (University of Auckland), Ren Li (Institute of Zoology, Chinese Academy of Sciences) and Greg Setliff (Kutztown University) provided useful comments and discussion about morphological features.

The following curators and institutions that provided specimens are most gratefully acknowledged: Barbara Barratt (Invermay Agricultural Centre Collection, Mosgiel), Rich Leschen (New Zealand Arthropod Collection, Auckland), John Marris (Lincoln University Entomology Research Museum, Christchurch), and Cor Vink (Canterbury Museum, Christchurch).

References

Álvarez Padilla F, Hormiga G (2008) A protocol for digesting internal soft tissues and mounting spiders for scanning electon microscopy. The Journal of Arachnology 35: 538–542. https://doi.org/10.1636/Sh06-55.1

Arnqvist G, Rowe L (1995) Sexual conflict and arms races between the sexes: a morphological adaptation for control of mating in a female insect. Proceedings of the Royal Society of London B: Biological Sciences 261(1360): 123–127. https://doi.org/10.1098/rspb.1995.0126

Aslam NA (1969) Revision of Indo-Pakistan *Parisomias* Faust (Coleoptera, Curculionidae) with some notes on *Leptomias* Faust. Journal of Natural History 3: 543–560. https://doi.org/10.1080/00222936900770461

Astrin JJ, Stüben PE (2008) Phylogeny in cryptic weevils: molecules, morphology and new genera of western Palaearctic Cryptorhynchinae (Coleoptera: Curculionidae). Invertebrate Systematics 22: 503–522. https://doi.org/10.1071/IS07057

Barlow ND, Barratt BIP, Ferguson CM (2004) Using models to estimate parasitoid impacts on nontarget host abundance. Environmental Entomology 33(4): 941–948. https://doi.org/10.1603/0046-225X-33.4.941

Barratt BIP, Ferguson CM, Bixley AS, Crook KE, Barton DM, Johnstone PD (2007) Field parasitism of nontarget weevil species (Coleoptera: Curculionidae) by the introduced biological control agent *Microctonus aethiopoides* Loan (Hymenoptera: Braconidae) over an altitude gradient. Environmental Entomology 36(4): 826–839. https://doi.org/10.1603/0046-225X(2007)36

Barratt BIP, Kuschel G (1996) Broad-nosed weevils (Curculionidae: Brachycerinae: Entimini) of the Lammermoor and Rock and Pillar Ranges in Otago, with descriptions of four new species of *Irenimus*. New Zealand Journal of Zoology 23: 359–374. https://doi.org/10.1080/03014223.1996.9518096

Bell TP, Patterson GB (2008) A rare alpine skink *Oligosoma pikitanga* n. sp. (Reptilia: Scincidae) from Llawrenny Peaks, Fiordland, New Zealand. Zootaxa 1882: 57–68.

Broun T (1880) Manual of the New Zealand Coleoptera, Volume 1. Government Printer, Wellington, 651 pp. https://doi.org/10.5962/bhl.title.9559

Broun T (1881) Manual of the New Zealand Coleoptera, Volume 2. Government Printer, Wellington, 101 pp. https://doi.org/10.5962/bhl.title.9559

Broun T (1886) Manual of the New Zealand Coleoptera, Volume 3 & 4. Government Printer, Wellington, 245 pp. https://doi.org/10.5962/bhl.title.9559

Broun T (1903) Descriptions of new genera and species of New Zealand Coleoptera. Annals and Magazine of Natural History (7) 12(67): 69–86. https://doi.org/10.1080/00222930308678830

Broun T (1909a) Descriptions of Coleoptera from the Subantarctic Islands of New Zealand with remarks on the affinities of the genera, etc. In: Chilton C (Ed.) The Subantarctic Islands of New Zealand, Volume 1. Philosophical Society of Canterbury, Wellington, 78–123.

Broun T (1909b) Descriptions of new genera and species of New Zealand Coleoptera. Annals and Magazine of Natural History (8) 4(20): 130–161. https://doi.org/10.1080/00222930908692651

Broun T (1911) Additions to the Coleopterous fauna of the Chatham Islands. Transactions and Proceedings of the New Zealand Institute 43(12): 92–115.

Broun T (1913) Descriptions of new genera and species of Coleoptera. Transactions and Proceedings of the New Zealand Institute 45(16): 97–163.

Broun T (1915) Descriptions of new genera and species of Coleoptera. Bulletin of the New Zealand Institute 1(4): 267–346. https://doi.org/10.5962/bhl.title.12470

Broun T (1921) Descriptions of new genera and species of Coleoptera. Bulletin of the New Zealand Institute 1(6): 475–590. https://doi.org/10.5962/bhl.title.12470

Brown RW (1956) Composition of Scientific Words. Revised Edition. Smithsonian Institution Press, Washington DC, 882 pp.

Brown SDJ (2017) A revision of the New Zealand weevil genus *Irenimus* Pascoe, 1876 (Coleoptera: Curculionidae: Entiminae). Zootaxa 4263(1): 1–42. https://doi.org/10.11646/zootaxa.4263.1.1

Brown SDJ, Collins RA, Boyer S, Lefort MC, Malumbres-Olarte J, Vink CJ, Cruickshank RH (2012) Spider: An R package for the analysis of species identity and evolution, with particular reference to DNA barcoding. Molecular Ecology Resources 12(3): 562–565. https://doi.org/10.1111/j.1755-0998.2011.03108.x

Buckley TR, Simon C (2007) Evolutionary radiation of the cicada genus *Maoricicada* Dugdale (Hemiptera: Cicadoidea) and the origins of the New Zealand alpine biota. Biological Journal of the Linnean Society 91: 419–435. https://doi.org/10.1111/j.1095-8312.2007.00807.x

Chen J, Schöb C, Zhou Z, Gong Q, Li X, Yang Y, Li Z, Sun H (2015) Cushion plants can have a positive effect on diversity at high elevations in the Himalayan Hengduan Mountains. Journal of Vegetation Science 26: 768–777. https://doi.org/10.1111/jvs.12275

Chinn WG, Gemmell NJ (2004) Adaptive radiation within New Zealand endemic species of the cockroach genus *Celatoblatta* Johns (Blattidae): a response to Plio-Pleistocene mountain building and climate change. Molecular Ecology 13(6): 1507–1518. https://doi.org/10.1111/j.1365-294X.2004.02160.x

Cockayne L (1921) The vegetation of New Zealand. Im Engelmann, Leipzig, 364 pp.

Craw D, Upton P, Walcott R, Burridge CP, Waters JM (2012) Tectonic controls on the evolution of the Clutha River catchment, New Zealand. New Zealand Journal of Geology and Geophysics 55(4): 345–359. https://doi.org/10.1080/00288306.2012.709184

Crosby TK, Dugdale JS, Watt JC (1998) Area codes for recording specimen localities in the New Zealand subregion. New Zealand Journal of Zoology 25: 175–183. https://doi.org/10.1080/03014223.1998.9518148

Dolezal J, Dvorsky M, Kopecky M, Liancourt P, Hiiesalu I, Macek M, Altman J, Chlumska Z, Rehakova K, Capkova K, Borovec J, Mudrak O, Wild J, Schweingruber F (2016) Vegetation dynamics at the upper elevational limit of vascular plants in Himalaya. Scientific Reports 6:24881. https://doi.org/10.1038/srep24881

Dugdale JS, Fleming CA (1978) New Zealand cicadas of the genus *Maoricicada* (Homoptera: Tibicinidae). New Zealand Journal of Zoology 5(2): 295–340. https://doi.org/10.1080/03014223.1978.10428319.

Dunning LT, Dennis AB, Sinclair BJ, Newcomb RD, Buckley TR (2014) Divergent transcriptional responses to low temperature among populations of alpine and lowland species of New Zealand stick insects (*Micrarchus*). Molecular Ecology, 23(11): 2712–2726. https://doi.org/10.1111/mec.12767

Felsenstein J (2004) Inferring phylogenies. Sinauer, Sunderland, 580 pp.

Forsyth PJ (2001) Geology of the Waitaki area. Institute of Geological and Nuclear Sciences Ltd, Lower Hutt, New Zealand, 73 pp.

Franz NM, Cardona-Duque J (2013) Description of two new species and phylogenetic reassessment of *Perelleschus* O'Brien & Wibmer, 1986 (Coleoptera: Curculionidae), with a complete taxonomic concept history of *Perelleschus* sec. Franz & Cardona-Duque, 2013. Systematics and Biodiversity 11(2): 209–236. https://doi.org/10.1080/14772000.2013.806371

Gaskin DE (1975) Revision of the New Zealand Crambini (Lepidoptera: Pyralidae: Crambinae). New Zealand Journal of Zoology 2(3): 265–363. https://doi.org/10.1080/03014223.1975.9517878

Gibson N, Kirkpatrick JB (1985) A comparison of the cushion plant communities of New Zealand and Tasmania. New Zealand Journal of Botany 23(4): 549–566. https://doi.org/10.1080/0028825X.1985.10434227

Gillespie JJ, Cannone J, Gutell R, Cognato AI (2004) A secondary structural model of the 28S rRNA expansion segments D2 and D3 from rootworms and related leaf beetles (Coleoptera: Chrysomelidae; Galerucinae). Insect Molecular Biology 13(5): 495–518. https://doi.org/10.1111/j.0962-1075.2004.00509.x

Gómez-Zurita J, Jolivet P, Vogler AP (2005) Molecular systematics of Eumolpinae and the relationships with Spilopyrinae (Coleoptera, Chrysomelidae). Molecular Phylogenetics and Evolution 34: 584–600. https://doi.org/10.1016/j.ympev.2004.11.022

Grebennikov VV (2015) Neglected *Trichalophus* (Coleoptera: Curculionidae): DNA barcode and phylogeography of high-altitude flightless weevils rediscovered in Southwest China. Bonn Zoological Bulletin 64(2): 59–76.

Guoy M, Guindon S, Gascuel O (2010) SeaView version 4: a multiplatform graphical user interface for sequence alignment and phylogenetic tree building. Molecular Biology and Evolution 27(2): 221–224. https://doi.org/10.1093/molbev/msp259

Halloy SRP, Mark AF (2003) Climate-change effects on alpine plant biodiversity: A New Zealand perspective on quantifying the threat. Arctic, Antarctic, and Alpine Research 35(2): 248–254. https://doi.org/10.1657/1523-0430(2003)035[0248:CEOAPB]2.0.CO;2

Hebert PDN, Cywinska A, Ball SL, de Waard JR (2003) Biological identification through DNA barcodes. Proceedings of the Royal Society of London B 270: 313–321. https://doi.org/10.1098/rspb.2002.2218

Heenan PB, McGlone MS (2013) Evolution of New Zealand alpine and open-habitat plant species during the late Cenozoic. New Zealand Journal of Ecology 37(1): 105–113.

Hoare RJB (2012) A new species of *Hierodoris* Meyrick (Lepidoptera: Oecophoridae) with a telescopic ovipositor, from granite sand plains in Fiordland. New Zealand Entomologist 35(1): 51–57. https://doi.org/10.1080/00779962.2012.651776

Inkscape Team (2004–2017) Inkscape: A vector drawing tool http://www.inkscape.org

Jaffer A (2011) Color-Name Dictionaries: NBS/ISCC centroids http://people.csail.mit.edu/jaffer/Color/Dictionaries#nbs-iscc

Jordal BH, Sequeira AS, Cognato AI (2011) The age and phylogeny of wood boring weevils and the origin of subsociality. Molecular Phylogenetics and Evolution 59: 708–724. https://doi.org/10.1016/j.ympev.2011.03.016

Kelly KL, Judd DB (1976) Color: universal language and dictionary of names. U.S. Department of Commerce, National Bureau of Standards, Washington DC, 196 pp. https://doi.org/10.6028/NBS.SP.440

Kuschel G (1964) Insects of Campbell Island. Coleoptera: Curculionidae of the subantarctic islands of New Zealand. Pacific Islands Monograph 7: 415–493.

Kuschel G (1969) The genus *Catoptes* Schönherr and two species oblitae of Fabricius from New Zealand (Coleoptera Curculionidae). New Zealand Journal of Science 12: 789–810.

Kuschel G (1972) The foreign Curculionoidea established in New Zealand (Insecta: Coleoptera). New Zealand Journal of Science 15: 273–289. https://doi.org/10.1080/03036758.1982.10415349

Kuschel G (1982) Apionidae and Curculionidae (Coleoptera) from the Poor Knights Islands, New Zealand. Journal of the Royal Society of New Zealand 12(3): 273–282.

Land Information New Zealand (2016) New Zealand Gazetteer of place names http://www.linz.govt.nz/regulatory/place-names/find-place-name/new-zealand-gazetteer-place-names

Landcare Research (2010a) NZDEM North Island 25 metre https://lris.scinfo.org.nz/layer/131-nzdem-north-island-25-metre/

Landcare Research (2010b) NZDEM South Island 25 metre https://lris.scinfo.org.nz/layer/127-nzdem-south-island-25-metre/

Lawrence JF, Beutel RG, Leschen RAB, Ślipiński A (2010) 2. Glossary of Morphological Terms. In: Leschen RAB, Beutel RG, Lawrence JF (Eds) Handbuch der Zoologie/Handbook of

Zoology. Band/Volume IV Arthropoda: Insecta Teilband/Part 38. Coleoptera, Beetles. Vol. 2. Morphology and Systematics (Polyphaga partim), W. DeGruyter, Berlin, 9–20. https://doi.org/10.1515/9783110911213.9

Leschen RAB, Buckley TR (2015) Revision and phylogeny of *Syrphetodes* (Coleoptera: Ulodidae): implications for biogeography, alpinization and conservation. Systematic Entomology 40: 143–168. https://doi.org/10.1111/syen.12094

Liberti G (2005) Improved solutions of two water-soluble media for mounting beetle genitalia. The Coleopterist 14(1): 29–35.

Lin CP, Danforth BN (2004) How do insect nuclear and mitochondrial gene substitution patterns differ? Insights from Bayesian analyses of combined datasets. Molecular Phylogenetics and Evolution 30: 686–702. https://doi.org/10.1016/S1055-7903(03)00241-0

Lyal CHC, Favreau EA (2015) The rectal valve in Curculionoidea (Insecta: Coleoptera). Zootaxa 3926 (4): 451–479. https://doi.org/10.11646/zootaxa.3926.4.1

Maddison WP, Maddison DR (2016) Mesquite: A modular system for molecular analysis http://mesquiteproject.wikispaces.com

Magnhagen C (1991) Predation risk as a cost of reproduction. Trends in Ecology and Evolution 6(6): 183–186. https://doi.org/10.1016/0169-5347(91)90210-O

Mark AF (2012) Above the treeline. A nature guide to alpine New Zealand. Craig Potton Publishing, Nelson, 472 pp.

Marshall GAK (1926) Some new Curculionidae from New Zealand (Col.). The Annals and Magazine of Natural History (9) 18(103): 1–16. https://doi.org/10.1080/00222932608633472

Marshall GAK (1931) New injurious Curculionidae (Col.). Bulletin of Entomological Research 22(3): 417–421. https://doi.org/10.1017/S000748530002993X

Marshall GAK (1937) New Curculionidae (Col.) from New Zealand. Transactions of the Royal Society of New Zealand 67(3): 316–340.

Marshall GAK (1956) The Otiorrhynchine Curculionidae of the tribe Celeuthetini (Col.). The British Museum (Natural History), London, 133 pp.

McGlone MS (2009) Postglacial history of New Zealand wetlands and implications for their conservation. New Zealand Journal of Ecology 33(1): 1–23.

McGlone MS, Duncan RP, Heenan PB (2001) Endemism, species selection and the origin and distribution of the vascular plant flora of New Zealand. Journal of Biogeography 28: 199–216. https://doi.org/10.1046/j.1365-2699.2001.00525.x

McKenna DD, Sequeira AS, Marvaldi AE, Farrell BD (2009) Temporal lags and overlap in the diversification of weevils and flowering plants. Proceedings of the National Academy of Science 106(17): 7083–7088. https://doi.org/10.1073/pnas.0810618106

Michelsen-Heath S, Gaze P (2007) Changes in abundance and distribution of the rock wren (*Xenicus gilviventris*) in the South Island, New Zealand. Notornis 54: 71–78.

Mildenhall DC (1989) Summary of the age and paleoecology of the miocene Manuherikia Group, Central Otago, New Zealand. Journal of the Royal Society of New Zealand 19(1): 19–29. https://doi.org/10.1080/03036758.1989.10426452

Molina-Montenegro MA, Badano EI, Cavieres LA (2006) Cushion plants as microclimatic shelters for two ladybird beetles in alpine zone of central Chile. Arctic, Antarctic, and Alpine Research 38(2): 224–227. https://doi.org/10.1657/1523-0430(2006)38[224:CPAMSF]2.0.CO;2

Nixon KC (1999) The parsimony ratchet, a new method for rapid parsimony analysis. Cladistics 15: 407–414. https://doi.org/10.1111/j.1096-0031.1999.tb00277.x

O'Donnell CFJ, Weston KA, Monks JM (2017) Impacts of introduced mammalian predators on New Zealand's alpine fauna. New Zealand Journal of Ecology 41(1): 1–22. https://doi.org/10.20417/nzjecol.41.18

Oberprieler RG, Anderson RS, Marvaldi AE (2014) 3 Curculionoidea Latreille, 1802: Introduction, Phylogeny. In: Leschen RAB, Beutel RG (Eds) Handbook of Zoology, Arthropoda: Insecta. Coleoptera, Beetles Volume 3: Morphology and Systematics (Phytophaga), Walter De Gruyter, Berlin, 285–300. https://doi.org/10.1515/9783110274462.285

Paradis E, Claude J, Strimmer K (2004) APE: analyses of phylogenetics and evolution in R language. Bioinformatics 20: 289–290. https://doi.org/10.1093/bioinformatics/btg412

Pascoe FP (1875) Descriptions of new genera and species of New Zealand Coleoptera. Part I. Annals and Magazine of Natural History (4) 16: 210–223. https://doi.org/10.1080/00222937508681155.

Pascoe FP (1876a) Descriptions of new genera and species of New Zealand Coleoptera. Part II. Annals and Magazine of Natural History (4) 17: 48–60. https://doi.org/10.1080/00222937608681895.

Pascoe FP (1876b) Descriptions of new genera and species of New Zealand Coleoptera. Part III. Annals and Magazine of Natural History (4) 18: 57–67. https://doi.org/10.1080/00222937608682007

Pascoe FP (1877) Descriptions of new genera and species of New Zealand Coleoptera. Part IV. Annals and Magazine of Natural History (4) 19: 140–147. https://doi.org/10.1080/00222937708682109

Sarkar I, Planet P, DeSalle R (2008) CAOS software for use in character-based DNA barcoding. Molecular Ecology Resources 8: 1256–1259. https://doi.org/10.1111/j.1755-0998.2008.02235.x

Schliep K (2011) phangorn: phylogenetic analysis in R. Bioinformatics 27(4): 592–593. https://doi.org/10.1093/bioinformatics/btq706

Schweiger AH, Beierkuhnlein C (2016) Size dependency in colour patterns of Western Palearctic carabids. Ecography 39: 846–857. https://doi.org/10.1111/ecog.01570

Seago AE, Leschen RAB, Newton AF (2015) Two new high altitude genera of Camiarini (Coleoptera: Leiodidae: Camiarinae) from Australia and New Zealand. Zootaxa 3957(3): 300–312. https://doi.org/10.11646/zootaxa.3957.3.3

Sequeira AS, Normark BB, Farrell BD (2000) Evolutionary assembly of the conifer fauna: distinguishing ancient from decent associations in bark beetles. Proceeding of the Royal Society of London B 267: 2359–2366. https://doi.org/10.1098/rspb.2000.1292

Sharp D (1886) On New Zealand Coleoptera, with descriptions of new genera and species. Scientific transactions of the Royal Dublin Society 2(3): 351–454.

Simon C, Frati F, Beckenbach AT, Crespi B, Liu H, Flook P (1994) Evolution, weighting, and phylogenetic utility of mitochondrial gene sequences and a compilation of conserved polymerase chain reaction primers. Annals of the Entomological Society of America 87(6): 651–701. https://doi.org/10.1093/aesa/87.6.651

Stone GN (1995) Female foraging responses to sexual harassment in the solitary bee *Anthophora plumipes*. Animal Behaviour 50: 405–412. https://doi.org/10.1006/anbe.1995.0255

Sutherland R (1996) Transpressional development of the Australia-Pacific boundary through southern South Island, New Zealand: Constraints from Miocene-Pliocene sediments, Waiho-1 borehole, South Westland. New Zealand Journal of Geology and Geophysics 39(2): 251–264. https://doi.org/10.1080/00288306.1996.9514709

Tanner VM (1969) A study of the weevil tribe Celeuthetini of the Solomon Islands (Coleoptera: Curculionidae). Brigham Young University Science Bulletin Biological Series 10(3).

Thompson RT (1992) Observations on the morphology and classification of weevils (Coleoptera, Curculionidae) with a key to major groups. Journal of Natural History 26: 835–891. https://doi.org/10.1080/00222939200770511

Torre-Bueno JR (1979) A Glossary of Entomology. New York Entomological Society, New York, 394 pp.

Townsend AJ, de Lange PJ, Duffy CAJ, Miskelly CM, Molloy J, Norton DA (2008) New Zealand Threat Classification System manual. Department of Conservation, Wellington, 36 pp.

Trewick SA (2008) DNA barcoding is not enough: mismatch of taxonomy and genealogy in New Zealand grasshoppers (Orthoptera: Acrididae). Cladistics 24: 240–254. https://doi.org/10.1111/j.1096-0031.2007.00174.x

Trewick SA, Wallis GP, Morgan-Richards M (2000) Phylogeographical pattern correlates with Pliocene mountain building in the alpine scree weta (Orthoptera, Anostostomatidae). Molecular Ecology 9: 657–666. https://doi.org/10.1046/j.1365-294x.2000.00905.x

Volkov IV, Volkova II (2015) More than just a plant: cushion plants as biodiversity protectors in high mountains of Siberia. International Journal of Environmental Studies 72: 474–489. https://doi.org/10.1080/00207233.2015.1027594

Wanat M (2007) Alignment and homology of male terminalia in Curculionoidea and other Coleoptera. Invertebrate Systematics 21: 147–171. https://doi.org/10.1071/IS05055

Watson PJ, Arnqvist G, Stallman RR (1998) Sexual conflict and the energetic costs of mating and mate choice in water striders. The American Naturalist 151(1): 46–58. https://doi.org/10.1086/286101

Wharton DA (2011) Cold tolerance of New Zealand alpine insects. Journal of Insect Physiology 57: 1090–1095. https://doi.org/10.1016/j.jinsphys.2011.03.004

Whitaker AH (1984) *Hoplodactylus kahutarae* n. sp. (Reptilia: Gekkonidae) from the Seaward Kaikoura Range, Marlborough, New Zealand. New Zealand Journal of Zoology 11 (3): 259–270. https://doi.org/10.1080/03014223.1984.10428239

Wilkins JS (2009) Species. A History of the Idea. University of California Press, Berkeley, 320 pp.

Wilkins JS (2010) What is a species? Essences and generation. Theory in Biosciences 129: 141–148. https://doi.org/10.1007/s12064-010-0090-z

Williams JR (2000) A revision of the Mascarene weevil genus *Syzygops* Schöenherr (Coleoptera: Curculionidae: Entiminae). Invertebrate Taxonomy 14: 411–432. https://doi.org/10.1071/IT99004

Winkworth RC, Wagstaff SJ, Glenny D, Lockhart PJ (2005) Evolution of the New Zealand mountain flora: origins, diversification and dispersal. Organisms, Diversity and Evolution 5: 237–247. https://doi.org/10.1016/j.ode.2004.12.001

Youngson JH, Craw D, Landis CA, Schmitt KR (1998) Redefinition and interpretation of late Miocene-Pleistocene terrestrial stratigraphy, Central Otago, New Zealand. New Zealand Journal of Geology and Geophysics 41(1): 51–68. https://doi.org/10.1080/00288306.1998.9514790

ZooKeys 707: 131–156 (2017)
doi: 10.3897/zookeys.707.14029
http://zookeys.pensoft.net

RESEARCH ARTICLE

A peer-reviewed open-access journal
ZooKeys
Launched to accelerate biodiversity research

Herpetofaunal assemblages of a lowland broadleaf forest, an overgrown orchard forest and a lime orchard in Stann Creek, Belize

Russell Gray[1], Colin T. Strine[2]

1 *Toucan Ridge Ecology & Education Society, 27.5 Hummingbird Highway, Stann Creek District, Belize* **2** *Sakaerat Environmental Research Station 1 Moo 9 Udom Sab Subdistrict, Wang Nam Khieo District, Nakhon Ratchasima 30370, Thailand*

Corresponding author: *Colin T. Strine* (strine.conservation@gmail.com)

Academic editor: *J. Penner* | Received 6 June 2016 | Accepted 22 August 2017 | Published 11 October 2017

http://zoobank.org/BCAEB074-0FE8-45A3-BBC5-F34F92F61746

Citation: Gray R, Strine CT (2017) Herpetofaunal assemblages of a lowland broadleaf forest, an overgrown orchard forest and a lime orchard in Stann Creek, Belize. ZooKeys 707: 131–165. https://doi.org/10.3897/zookeys.707.14029

Abstract

Understanding and monitoring ecological impacts of the expanding agricultural industry in Belize is an important step in conservation action. To compare possible alterations in herpetofaunal communities due to these anthropogenic changes, trapping arrays were set in a manicured orchard, a reclaimed orchard and a lowland broadleaf forest in Stann Creek district at Toucan Ridge Ecology and Education Society (TREES). Trapping efforts were carried out during the rainy season, from June to September, 2016, during which time the study site was hit by a category one hurricane between sampling sessions. Trapping yielded 197 individual herpetofauna and 40 different species overall; 108 reptile captures (30 species) and 88 amphibian captures (ten species). Reptiles and amphibians were more abundant in the lowland broadleaf forest and the manicured orchard area. Amphibian species diversity was relatively similar in each habitat type. Reptile captures were most diverse in the Overgrown Orchard Forest (OGF) and Overgrown Orchard Riparian Forest (OGR) and least diverse in the Lowland Broadleaf Forest (LBF). The findings of this study suggest that reptile and amphibian sensitivity to anthropogenically altered areas is minimal when enveloped by natural habitat buffers, and additionally, that extreme weather events have little impact on herpetofauna communities in the area.

Keywords

Amphibians, funnel-traps, human-altered habitats, passive-trapping, reptiles, lowland broadleaf forest

Introduction

Negative effects of agricultural development are well known for a number of taxa across the neotropics (Harvey et al. 2006; Offerman et al. 1995; Saab and Petit 1992). However, there is still contention regarding the impacts on herpetofauna and their assemblages (Lips et al. 2003; Suazo-Ortuno et al. 2008). Along with 391 reptiles and 307 amphibians endemic to the region, the Mesoamerica hotspot has remarkable herpetofauna species diversity in proportion to its surface area (Conservation International 2011; Mittermeier et al. 2011; Myers et al. 2000). According to the Mesoamerica Hotspot: Northern Mesoamerica Briefing Book (CEPF 2004), the Mesomerican hotspot is ranked first in reptile and second in amphibian species diversity when compared to other biodiversity hotspots around the world. Belize encompasses a great deal of undisturbed natural forest areas (Redo et al. 2012). However, due to lack of preventative legal framework and rising poverty rate, the country has been experiencing high rates of deforestation and large-scale sprawl of land for agricultural use (Young 2008). As a consequence of high deforestation rates, and its immense diversity of flora and fauna, Belize is an import part of the Mesoamerican biodiversity hotspot (Cherrington et al. 2012; DeClerck et al. 2010; Young 2008).

The Stann Creek district of Belize (Fig. 1) is dominated by Mountain Pine Savannah and humid Lowland Broadleaf Forests, covered by granitic intrusions and limestone karst topography (Bridgewater 2012). Mountain Pine Savannah habitats are dominated by *Pinus oocarpa, Clusia* sp. and various grasses. Lowland Broadleaf Forest areas in Stann Creek, east of the Maya Mountains, are categorized as Class 3 Semi Evergreen Forests which are dominated by *Attalea cohune*, *Manilkara chicle, Pouteria reticulate, Terminalia amazonia*, *Bursera simaruba*, Eyma and *Brosimum alicastrum* (Penn et al. 2004). Montane habitats have a significant influence on biodiversity; the Maya Mountains extend southwest from the Stann Creek district of Belize into Guatemala and envelope 785,379 ha of the fourth key biodiversity area in the Selva Maya corridor (CEPF 2004). Limestone karsts, have been shown to have significant changes in diversity and species endemism, although are often overlooked for study (Brewer et al. 2003; Hughes 2017; Latinne et al. 2013). Flowing water bodies found throughout the district are fed by the Sibun River Watershed (SRW); the SRW drains the central portion of the country's water and empties into the Caribbean Sea (Boles 1999). Sprawling agricultural lands have reduced the forest cover of the Caribbean and Mesoamerican lowlands rapidly, attributed to a half-century of expansion from the Central American dry Pacific lowlands (Harvey et al. 2005; Pasos et al. 1994; Utting 1993). Forested areas of Belize are fragmented by approximately 19,424 ha of citrus orchard plantations, the majority of which are in the Stann Creek district (Smith 2016; Bridgewater 2012). Evidence suggests that agricultural and developmental land clearing can diminish forest-dwelling wildlife populations (Brownet al. 2014; Yue et al. 2015). Tropical forests are important in preserving wildlife assemblages and are very slow to regenerate to their original functions when cleared, if they return at all (Frost 1981; Gibson et al. 2011).

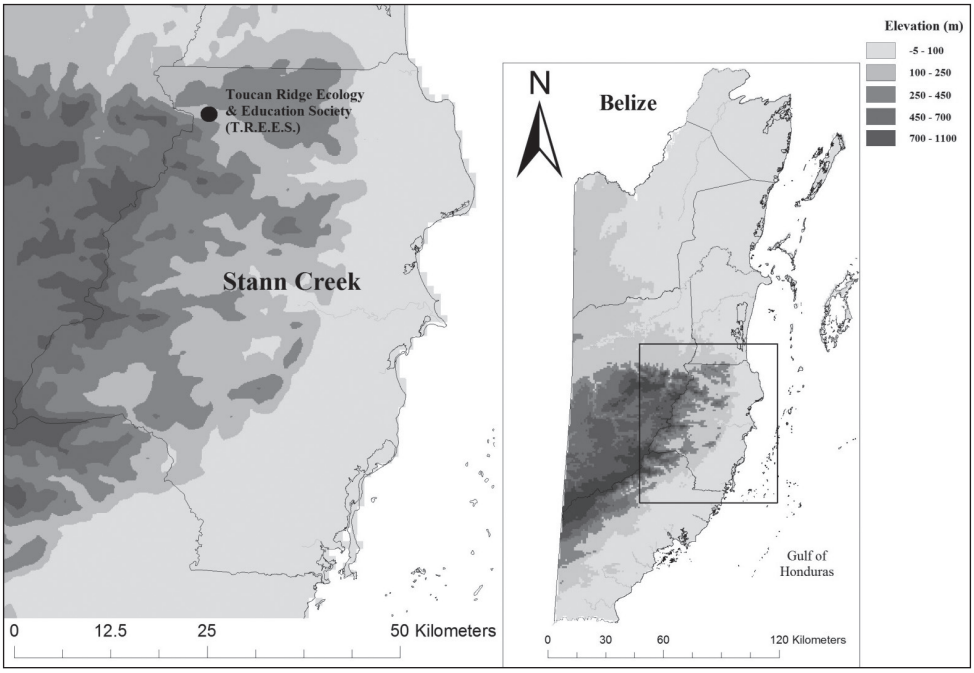

Figure 1. Stann Creek District, Belize, with the location of Toucan Ridge Ecology and Education Society (TREES).

Biodiversity conservation is necessary in Central America and the whole of the neotropics in order to maintain ecosystem functions (Islebe et al. 2015; Spangler 2015). Furthermore, habitat loss driven by deforestation is a major driving factor for loss of ecosystem function (Hinsley et al. 2015). According to the study of seven Central American countries by Redo (2012), Belize was the highest ranking in woody vegetation cover (63%). However, deforestation in Belize between 2001 and 2014 was estimated to be 141,711 ha; a forest-cover decrease of 96.9% to 85.72% (Chicas et al. 2016; GFW 2017). With this increased deforestation, it is of paramount importance to monitor and evaluate effects on the fauna of Belize in order to develop counteractive conservation methods.

Five major ecological assemblages characterize Central American herpetofauna: 1) humid tropical, 2) arid tropical, 3) humid montane, 4) arid montane and 5) high montane; the humid tropical assemblages of lowland habitat areas contain highest species richness and endemism (Duellman 1966). After the global assessment, the status of Mesoamerican amphibians has been extensively evaluated (Stuart et al. 2004). Habitat loss has been correlated with 89% of threatened amphibian species; 52% of the 685 amphibian species in Mesoamerica (Young et al. 2004). Another major factor of amphibian decline is the chytrid fungal pathogen *Batrachochytrium dendrobatidis* which has been found to be prevalent in the Maya Mountains of Belize (Kaiser and Pollinger 2012). In comparison, the status of reptiles in Mesoamerica is less well-known (John-

son et al. 2015; Wilson et al. 2013). According to the Environmental Vulnerability Score (EVS) of Mesoamerican herpetofauna described by Johnson et al. (2015), amphibians have an average EVS of 14.7 and reptiles have an average EVS of 13.3; these scores indicate that amphibians are generally more vulnerable to habitat decline than reptiles, and overall, at a mid-range of vulnerability.

Therefore, the objective of this study was to monitor herpetofauna assemblages in forested areas and various anthropogenic altered areas in order to compare any possible differences in community structure. Comparisons of this nature test the hypothesis of whether or not agricultural land clearings reduce herpetofauna diversity and richness, and if so, whether or not reclamation of these habitats restores diversity and richness. An imperative facet of wildlife conservation is the understanding of how anthropogenic change affects fauna. It is with this understanding that proper conservation methods and mitigation techniques can be implemented.

Materials and methods

Study site.—The study site was chosen at Toucan Ridge Ecology and Education Society (TREES) located between DMS; 17°03'07.98–17°02'46.16N, 88°34'14.43–88°33'44.66 W; WGS84 (Fig. 2). The TREES property encompasses approximately 200 acres (0.809 km^2) of private land located at the foothills of the Maya Mountains. The dominant habitat on the property is lowland broadleaf forest, characteristic of the moist rainforest habitats commonly found throughout Belize (Stafford et al. 2010). The land also has an open and regularly manicured lime orchard which converges with the lowland broadleaf forest through a large area of overgrown citrus orchard, ecotone, and moist broadleaf riparian forest. A large stream, approx. 4–5 m in width, runs north to south (with some curvature) through the property, which is fed by several headwater streams from the Maya Mountains and floods regularly during heavy rains. Average rainfall for the study period was 7.04 mm during the day and 8.84 during mm during the night with the highest overnight rainfall during hurricane Earl (>150 mm).

Site selection and herpetofaunal sampling.—Herpetofaunal assemblages were assessed and monitored within four habitats using drift fence and funnel trapping systems. These study sites included: 1) a heavily manicured lime orchard (HMO), 2) an old orange orchard overgrowth forest (OGF), 3) an old orange orchard overgrowth forest with an adjacent riparian forest area (OGR) and 4) a virgin lowland broadleaf forest area disturbed only by walking trails (LBF). Both reclaimed orchard study sites have been undisturbed for approximately 15 years. Each habitat chosen for sampling in the study was identified and verified by knowledge of the current owners of the property, caretakers who have managed it since early 2000, and additionally by updated habitat analysis conducted over the span of three years (V. Kilburn and M. Charette, pers. comm. May 2015). We used previously conducted habitat analysis of the TREES property from former interns who used several plots with transect lines

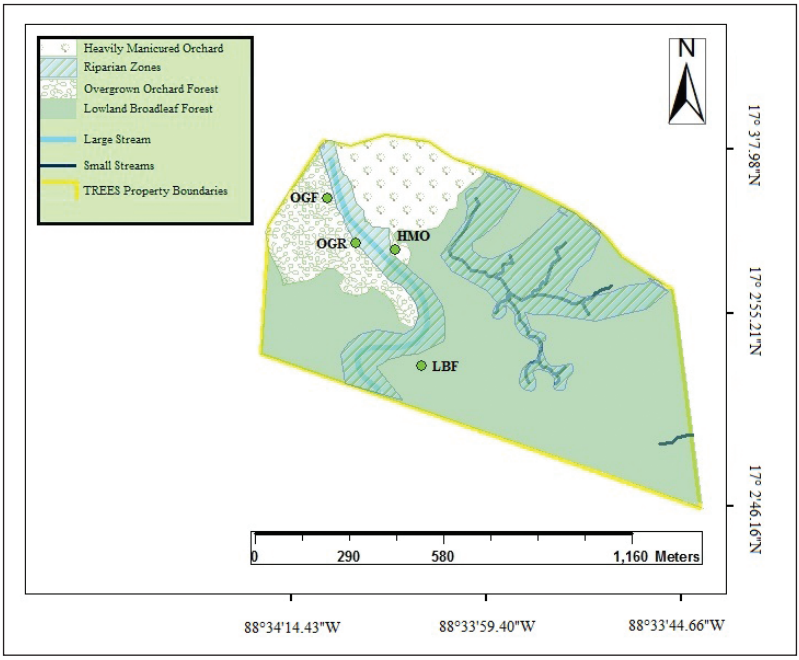

Figure 2. Toucan Ridge Ecology and Education Society (TREES) habitat map showing the Heavily Manicured Orchard (HMO), Overgrown Orchard Forest (OGF), Lowland Broadleaf Forest (LBF), and Overgrown Orchard Riparian Forest (OGR) areas, including locations where trapping arrays were set. Additionally, the map indicates the large stream which runs through the property and smaller streams that can be found throughout the forested areas.

running through them in order to determine habitat diversity through Gap Analysis, using vegetation as key biodiversity elements.

Trapping arrays (one per study site) were constructed in convenient sample sites within the chosen study areas that conformed to three major requirements: 1) Besides the HMO, each end of drift fence arrays should be ≥10 m from any walking trails; 2) trapping arrays should be 30–40 m from the large stream running through the property and 3) the trapping arrays should be placed on relatively flat ground to prevent fence wings from being placed in a levy, valley or dip, in order to avoid flood risk which could result in mortality of trapped fauna.

The trapping array in the HMO was set in a secluded part of the orchard area (DDM; 17°03.144N, 088°34.148W; WGS84) at an elevation of approximately 177.394 m. This area was regularly manicured, though did not experience the same amount of human interference as other parts of the orchard as a transit and fruit harvesting area. This was an important factor to avoid human interference with traps. The OGF trapping system (DDM; 17°03.030N, 088°34.046W; WGS84) was set at an elevation of approximately 190.5 m, 10m away from a trail system that leads to the adjacent broadleaf forest area. The second trapping system in the overgrown orchard habitat (OGR) was set in a riparian zone approximately 119.9 m from the OGF trap-

ping system (DDM; 17°03.050N, 88°34.138W; WGS84) at an elevation of 186.8 m. The Lowland Broadleaf Forest trapping array was set deep into the heavily forested area (DDM; 17°03.028N, 88°34.044W; WGS84) at an elevation of 192.0 m.

In order to cover sufficient surface area for trapping herpetofauna, each of the fences were set up in a 'Y' shaped formation, with the one wing of the 'Y' facing west, one facing south east and the other wing extending to the north west, the length of the formation running perpendicular to the nearby stream. Each wing of the array was 10 m in length and approximately 1 m high, relative to the terrain it crosses; the bottom of the fence were buried approximately 10–15 cm to reduce chances of fossorial and subfossorial herpetofauna from evading capture. Fencing material was 1.2 m black nylon mesh material which was supported by bamboo stakes set at every meter from the vertex of the array; bamboo stakes were cut at approximately 1.4 m in length to allow for the 1 m height to be maintained when set in the ground and buried; nylon fencing material was attached and secured to the bamboo via zip-ties and staples. Each of the four drift fence arrays were set with 12 funnel traps. Outer trap openings, on the ends of the drift fence, faced inward toward the vertex of the array and the inner trap openings faced away from the vertex. Traps were double-funnel and assembled using aluminium mesh screen material, with a 60 cm long entry chamber and a 70 cm long holding chamber; chamber height and width was approximately 30×30cm. Wire and staples were used to hold shape and secure the canters and ends of the traps. Funnel openings were approximately 6-8 cm in diameter and were fitted with a flap to reduce capture escape probability. Trap ends were secured with removable wire for convenient fauna release. All traps had the front lip buried in the soil to reduce trap avoidances; traps within HMO area or open canopy areas of the OGF and OGR were covered with a white sheet to prevent direct sunlight and overheating of trapped fauna and reduce risk of stress and fatality. Traps and fence damage issues were repaired and addressed on a same-day basis when needed. Trapping sample sessions ran for 14 days each month of the rainy season between June and late September, 2016 for a total of eight weeks of sampling. These dates were chosen in order to capture and assess herpetofauna during their most active period of the year. According to the historical temperature and rainfall averages recorded between 1991 and 2015 on The Climate Change Knowledge Portal by the World Bank Group (no date), the overall climate of the study period was a standard representative of previous years, and can therefore accurately represent data extrapolations.

Environmental variables.—In order to better understand the chosen study sites and the area surrounding the trapping systems, habitat variables were taken into account. We conducted a micro/macro-habitat analysis at each study site. Macro-habitat data was collected by measuring and forming a 10×10 m quadrat at the end of each wing of the drift fence array with colored flagging tape. Once the quadrats were established, several participating assistants walked, at a full arm's length apart from each other through the quadrat and collected plants to be identified in order to find the dominant vegetative species in the habitat area. Plant identification was verified with the assistance of Belizean botanist David Tzul using the Checklist of the Vascular Plants of Belize, with Common Names and Uses (Balick 2000) and Trees of Belize (Harris 2009).

Microhabitat data was collected at each of the four study sites to evaluate understory vegetation, ground cover/composition and canopy cover. A 1×1m quadrat divided into four equal sub-sections was used to evaluate understory vertical vegetation density, leaf/grass cover and composition, and canopy cover. The quadrat was placed beside the 12 traps of each array. To evaluate standing vegetation, a 2m measuring pole was placed in the centres of the four subsections in the quadrat and touch points were tallied within every 20 cm (Valentine et al. 2012: Table 1). We used a visual estimate of the four subsections for leaf litter percentage. Leaf litter and grass cover was calculated by pushing a 30 cm ruler in each subsection until solid ground was felt, and the four recorded values (± 0.5 cm) were averaged. A spherical handheld crown densitometer was used at each side of the quadrat to derive an average canopy cover percentage. Microhabitat analysis was conducted before and after Hurricane Earl to assess any possible significant changes to the immediate study area.

As another measure of environmental variable analysis, we took general microclimate data (temperature and Relative Humidity [RH]) at each plotted site every day during trap checks (between 0800h and 1000h) using a HTC-1 temperature and humidity meter (Temperature Accuracy: Â ± 1°C; Humidity Range :10-99%; RH accuracy: 60% Â ± 5% RH). Along with this, we recorded rain data each day at 0800h and 2000h from a plastic rain gauge set in an open area.

Data analysis.—We performed all statistical analyses in RStudio V. 0.99.903 using packages "vegan" and "BiodiversityR" (Kindt and Coe 2005; Oksansen et al. 2016; R Core Development Team 2016); we created maps using ArcMapper V10.4; basemaps and other map datum for Belize were obtained from the Biodiversity & Environmental Resource Data System (BERDS) website (Meerman and Clabaugh 2016). We used the field guides "A Field Guide to the Amphibians and Reptiles of the Mayan World: The Lowlands of Mexico, Northern Guatemala, and Belize" by Julian C. Lee and "Amphibians and Reptiles of Northern Guatemala, the Yucatan, and Belize" by Jonathan A. Campbell to identify herpetofauna, when necessary; Identifications were further verified by the publication on their holotype and most recently updated taxonomic papers (AmphibiaWeb 2016; IUCN 2016; Uetz n.d.). We added analysis of Hurricane Earl; however, the capture data was not significantly different between reptiles and amphibians caught before and after the hurricane, so the focus remains on the habitat variations with the hurricane included as an important variable, as there are no comparative data from previous years of herpetofauna trapping in this area. We compared canopy changes before and after the hurricane using a Wilcoxon signed-rank test, and performed other habitat comparisons by averages. Herpetofauna species capture data were analysed to compare any trends or patterns in species capture rates, species richness and species diversity between the different study sites. Amphibian and reptile community assemblages and capture data were analysed separately, as their reactions and sensitivity to habitats affected by anthropogenic change can be disparate and the capture rates between them in the study were significantly different in all habitat types. Reptile and amphibian capture rates were compared between all habitat types using a Kruskal-Wallace ranked sum test, and a post-hoc Wilcoxon signed-rank test

Table 1. Comparison of microhabitat variables averaged from 12 points at each sampling site pre/post Hurricane Earl (note: HMO grass is regularly manicured and not constant, therefore it is ranked "-" on the chart for litter (%) and depth analysis; vertical vegetation density was factored in with exceptions (≤ 20 cm)); Before (B) and After (A) vertical vegetation values are shown side-by-side in the table.

Microhabitat variable	*HMO*		*OGF*		*OGR*		*LBF*	
	Mean	**SD (±)**	**Mean**	**SD (±)**	**Mean**	**SD (±)**	**Mean**	**SD (±)**
Canopy cover (%) pre	23	30	91	4	77	24	98	1
Canopy cover (%) post	12	12	44	27	13	28	95	3
Leaf Litter (%) pre	-	-	59	22	51	30	56	25
Leaf Litter (%) post	-	-	87	12	87	12	75	28
Litter depth (cm) pre	-	-	7.02	60	4.90	2.24	2.98	1.61
Litter depth (cm) post	-	-	2.69	95	1.71	1.42	2.05	1.36
Vertical Vegetation Density (Number of touch points)								
0–20 cm(B:A)	-	-	1.75:0.17	4.94:0.58	0.75:0.08	1.76:0.29	3.91:0.58	3.5:0.67
20–40 cm(B:A)	0.58:0.08	1.16:0.29	1.33:1.25	3.70:2.93	0.08:0.5	0.29:0.67	0.5:0.5	1:0.90
40–60 cm(B:A)	0.08:0	0.29:0	0.43:0.08	0.67:0.29	0.33:0.58	0.78:1.16	0:0.08	0:0.28
60–80 cm(B:A)	0.08:0.08	0.29:0.28	0.25:0.08	0.62:0.29	0.08:0.17	0.29:0.39	0:0.25	0:0.62
80–100 cm(B:A)	1.67:0.33	0.58:0.78	0.17:0.08	0.58:0.29	0.41:0	0.67:0	0:0.08	0:0.29
100–150 cm(B:A)	0.67:0.42	1.62:1.0	0.5:0.5	0.80:1	0.75:0.58	0.97:0.79	0.5:0.58	1.24:0.90
150–200 cm (B:A)	0.45:0.08	1.44:0.29	1.5:0.5	2.39:0.67	1.08:0.5	1.31:1.24	1.08:0.25	1.44:0.62

to compare habitats that appeared significantly different after forming boxplots. An ANOVA was used to test for overall variations in species diversity. For all statistical analysis tests, $\alpha = 0.05$. Numbers of individuals and species were evaluated at each site with a calculated Shannon-Weiner diversity index (Krebs 1989). Further analysis was conducted to quantify extrapolated richness values for unseen reptile species.

Results

Habitat variation.—Habitat variations were recorded using the micro/macro-habitat analysis for each of the four habitat areas studied:

Heavily Manicured Orchard.—The HMO had an average temperature of 31.15°C and an average RH of 76.2% throughout the duration of the study. The soil was relatively dry in comparison to the other plotted areas and was covered in grass rather than leaf litter as groundcover, the open area was thinly spotted with *Citrus aurantifolia* lime trees covered in water bearing *Aechmea* sp. bromeliads. There were no canopies over the trapping systems; however there were dense canopy edges (> 2 m) on the west and north-west wings. After the hurricane, large trees fell over top of the north-west wing providing a heavily shaded canopy area over two of the traps.

Overgrown Orchard Forest.—The OGF habitat area had an average temperature of 27.45°C and average RH of 84.1% throughout the duration of the study. The ground of this site was covered in leaf litter and moist soil which turns to soft mud after rains. Vegetation consisted of small scattered bryophytes and lycophytes with dominant tree species being *Cupania* sp. The site was covered by relatively heavy canopy with an extensive liana complex extending from tree to tree. Following the hurricane, the canopy cover decreased and tangled liana complexes hung large concentrations of vegetation over the centre and west wing of the trapping system.

Overgrown Orchard/Riparian Forest.—The vegetation, soil composition and canopy cover in the OGR were relatively similar to the OGF habitat with the exception of a small wetland area, composed of a thick patch *Costus* sp. and shallow muddy water approximately 15-25 cm in depth, approximately >5m from the end of the west wing and extending further past the 10×10 quadrat area documented. The site had an average temperature of 26.71 and average humidity of 84.3% throughout the study. After the hurricane, the canopy cover was significantly altered with nearly all vegetation falling away from the trapping array and none overhanging, as has occurred in the other sites.

Lowland Broadleaf Forest.—The canopy cover of the LBF was very heavy; soil was moist; ground cover consisted of leaf litter, scattered bryophytes, lycophytes and many sapling trees. Scattered *Bactris major* and large *Attalea cohune* were surrounding the trapping system; the dominant tree species were *Xylopia* sp., *Hirtella Americana,* and *Vochisia hondurensis*. The site had an average temperature was 26.89 °C and RH was 83.2% throughout the study. After the study, there was very little alteration to the vegetation in the study site, assumedly the thick vegetation levels inhibited and broke down the heavy winds.

Microhabitat variables pre/post hurricane.—In order to show the difference in canopy changes from Hurricane Earl which occurred after two of the four sample sessions, we took canopy cover data before and after hurricane Earl (Fig. 3). The data shows that there were significant alterations in canopy percentages in the OGF (Wilcoxon signed-rank; V = 78, P = 0.002) and OGR (Wilcoxon signed-rank; V = 78, P = 0.002) and slight canopy reductions in the HMO (Wilcoxon signed-rank; V = 42, P = 0.423); there were no significant canopy alterations in the LBF (Wilcoxon signed-rank; V = 75, P = 0.005).

Pre/post hurricane species richness and diversity.—The analysis of each habitat studied shows that although habitat areas were significantly altered after the hurricane there were no significant comparable differences in capture rates, species richness or diversity (Fig. 4). Reptiles caught before the hurricane yielded 23 species (53 individuals) and after yielded 23 species (55 individuals). Amphibian captures before the hurricane yielded 7 species (43 individuals, and after yielded 8 species (46 individuals).

Before the hurricane, the trapping system in the LBF yielded six species (12 individuals); HMO yielded 12 species (20 individuals); OGF yielded ten species (eleven individuals) and OGR yielded 8 species (10 individuals). Amphibian captures before the hurricane in the LBF yielded 4 species (18 individuals); HMO yielded 4 species (17 individuals); OGF yielded 2 species (2 individuals) and OGR yielded 2 species

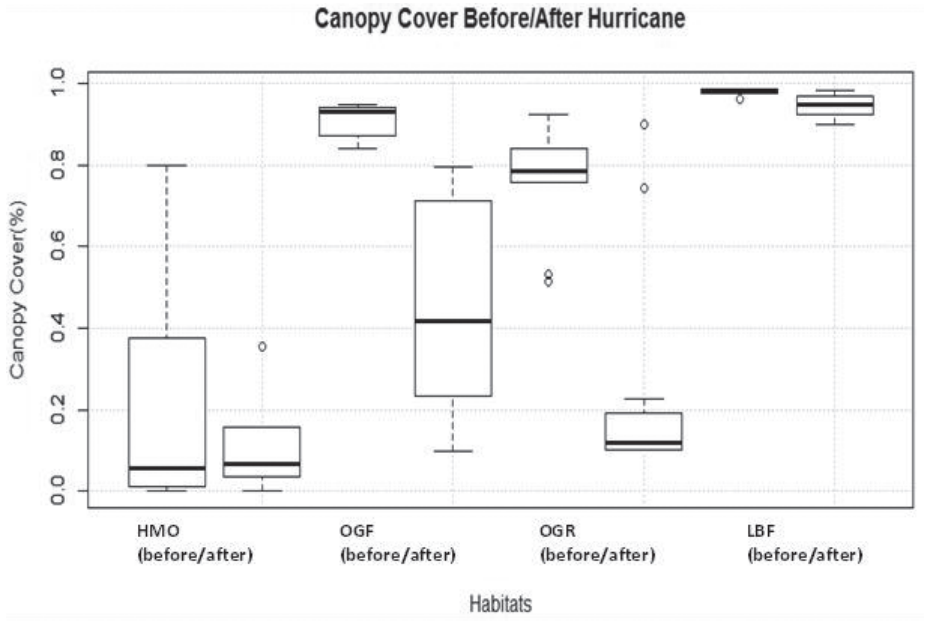

Figure 3. Boxplots representing the values (%) of canopy cover in each habitat taken before and after Hurricane Earl.

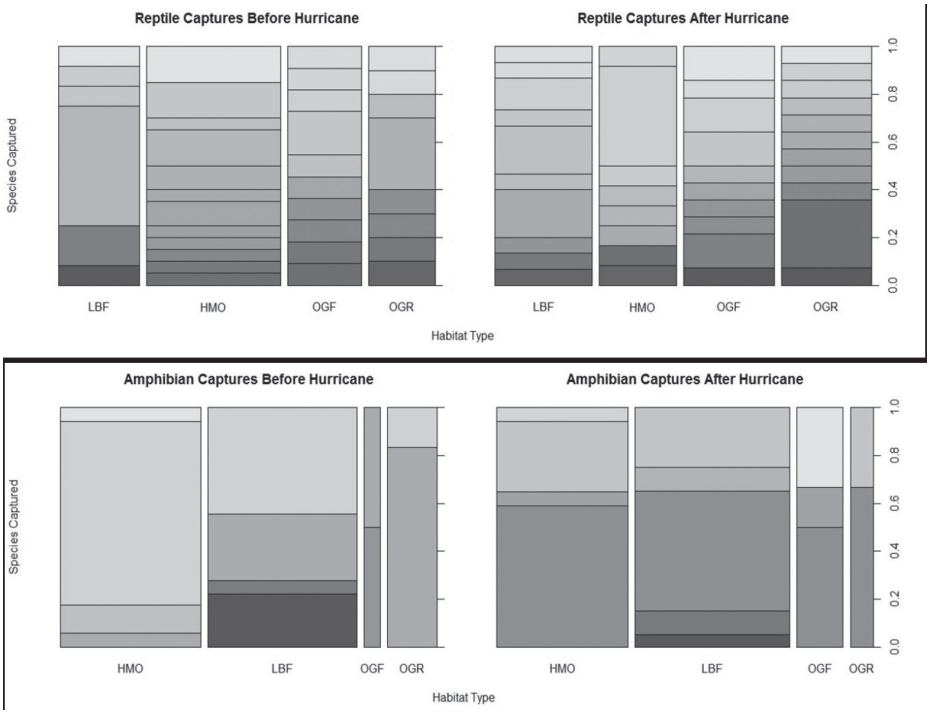

Figure 4. Bar graphs exhibiting species capture diversity and richness in reptiles and amphibians before and after Hurricane Earl.

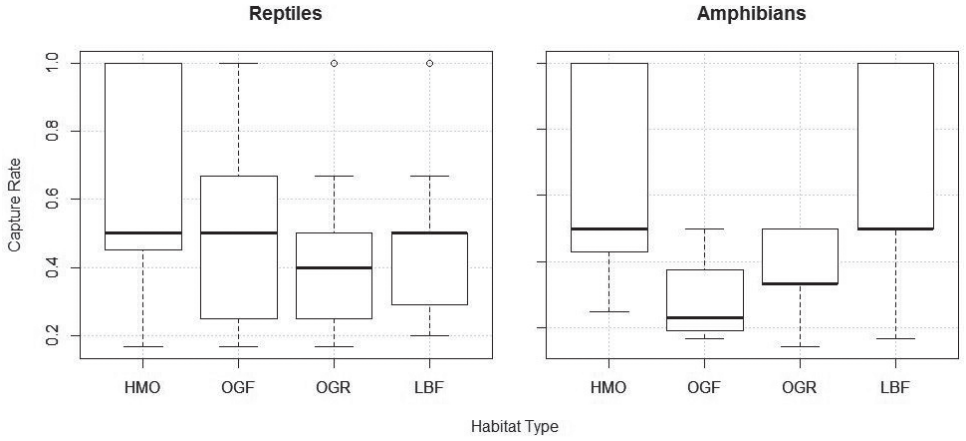

Figure 5. Boxplots of reptile and amphibian capture rates by trap night in the Heavily Manicured Orchard (HMO), Overgrown Orchard Forest (OGF), Overgrown Orchard/Riparian Forest, (OGR) and Lowland Broadleaf Forest (LBF).

(6 individuals). Post-hurricane reptiles in the LBF yielded 10 species (15 individuals); HMO yielded 8 species (12 individuals); OGF yielded ten species (14 individuals) and OGR yielded 11 species (14 individuals). Post-hurricane amphibian captures in the LBF yielded 4 species (20 individuals); HMO yielded 4 species (17 individuals); OGF yielded 3 species (6 individuals) and OGR yielded 2 species (3 individuals).

Capture rates.—During this study, trapping efforts yielded 197 individual herpetofauna and 40 different species overall; 108 reptile captures (30 species) and 89 amphibian captures (ten species) (Table 2). Furthermore, traps captured 22 species unique to their particular habitat, 17 reptiles, and five amphibians.

Reptile and amphibian capture rates were analysed per plot-night for differences between habitat areas (Fig. 5). Amphibian capture rates per trap night were not significantly different between habitat types collectively (Kruskal-Wallis; $\chi^2 = 6.0478$, df = 3, $P = 0.109$); however, the capture rates in the OGF were significantly lower than both the HMO (Wilcoxon signed-rank; W = 8, P = 0.016) and LBF (Wilcoxon signed-rank; W = 14, P = 0.027). Although reptiles were captured in higher numbers than amphibians, there were no significant differences in capture rates collectively (Kruskal-Wallis; $\chi^2 = 4.2267$, df = 3, $P = 0.238$) or between habitats individually.

Rank abundances.—Amphibian rank abundance curves between the four sites show no cogent species richness in amphibians (Fig. 6). Two species, *Incilius valliceps* and *Lithobates vaillanti*, had the highest ranking abundance in all habitats except OGF; the curves show that amphibian diversity and abundance is most prominent in LBF and least prominent in OGR; with OGF and HMO having relatively similar curves. Reptile rank abundance curves had relatively different slopes among the habitat types (Fig. 7). Although most habitats produced a low quantity of individuals captured, all of the plots have a relatively high number of species diversity; the lowest diversity habi-

Table 2. Amphibian and reptile pecies captured in each habitat type throughout the study.

Family	Species	Habitat type				
		HMO	OGF	OGR	LBF	Total
Ranidae	*Lithobates brownorum*	3	1			**4**
	Lithobates juliani				2	**2**
	Lithobates vaillanti	18		2	12	**32**
Craugastoridae	*Craugastor chac*				7	**7**
	Craugastor sabrinus		1			**1**
Bufonidae	*Incilius valliceps*	3	12	7	15	**37**
	Rhinella horribilis	1				**1**
Eleutherodactylidae	*Eleutherodactylus leprus*	1				**1**
Hylidae	*Smilisca baudinii*		2			**2**
Plethodontidae	*Bolitoglossa dofleini*				1	**1**
Kinosternidae	*Kinosternon leucostomum*			2		**2**
Corytophanidae	*Basiliscus vittatus*		1	2		**3**
Xantusiidae	*Lepidophyma flavimaculatum*		1		1	**2**
Dactyloidae	*Norops lemurinus*				4	**4**
Gekkonidae	*Coleonyx elegans*	2	1	5		**8**
Scincidae	*Scincella cherriei*	8	2	1	3	**14**
	Marisora brachypoda	1				**1**
Teiidae	*Holcosus undulatus*				1	**1**
Colubridae	*Coniophanes fissidens*				1	**1**
	Coniophanes imperialis				2	**2**
	Drymarchon melanurus		2	1		**3**
	Drymobius margaritiferus		1	1		**2**
	Imantodes cenchoa	1				**1**
	Lampropeltis abnorma		1			**1**
	Leptodeira polysticta	1				**1**
	Leptophis ahaetulla			1		**1**
	Leptophis mexicanus	2	1	1		**4**
	Mastigodryas melanolomus	1	1	1		**3**
	Ninia diademata	2	2			**4**
	Ninia sebae	4	2	1	2	**9**
	Phrynonax poecilonotus		3		1	**4**
	Pliocercus elapoides				1	**1**
	Rhadinaea decorata				1	**1**
	Scaphiodontophis annulatus		1			**1**
	Sibon nebulatus	1	1	2		**4**
	Spilotes pullatus	1				**1**
	Tantilla hendersoni		1		1	**2**
	Tropidodipsas sartorii			1		**1**
	Xenodon rabdocephalus		2	1		**3**
Viperidae	*Bothrops asper*	2	1		1	**4**
Elapidae	*Micrurus diastema*	2	1	3		**6**
	Micrurus hippocrepis	4		1	9	**14**
Grand Totals		**58**	**41**	**33**	**65**	**197**

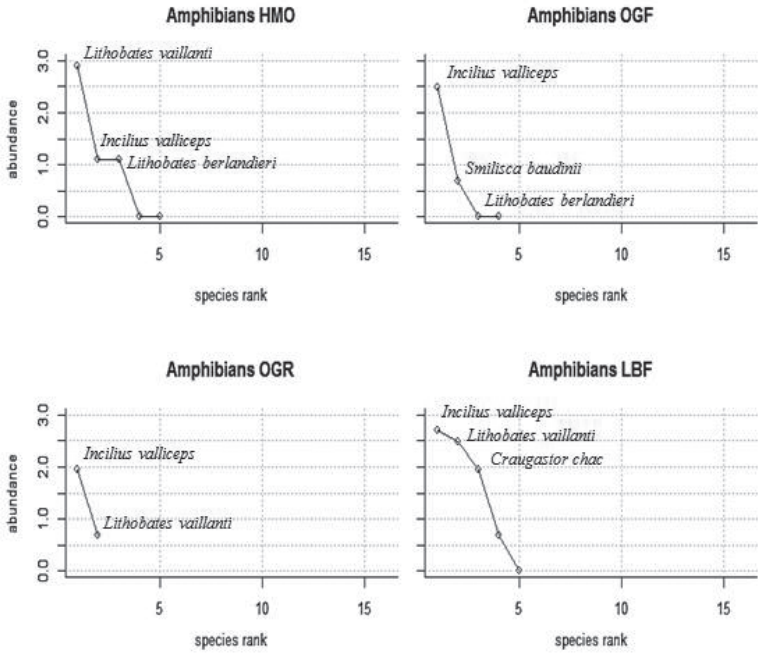

Figure 6. Amphibian rank abundance curves (using the logarithm of abundances) for the Heavily Manicured Orchard (HMO), Overgrown Orchard Forest (OGF), Overgrown Orchard Riparian Forest (OGR) and Lowland Broadleaf Forest (LBF); the three most abundant species captured in each site is labeled in each of the four plots.

tat being HMO and the highest diversity habitat being OGF. When comparing these plots, it is evident that some species (i.e., *Scincella cherriei*) appear to be abundant in HMO, OGF, and LBF habitats, though the species is not present in the OGR habitat.

Species richness and diversity.—Both species richness and diversity contrasted significantly between reptiles and amphibians in each habitat site (Fig. 8). Low levels of species richness and diversity was uniform for amphibians captured; curves show relatively similar slopes for HMO, OGF and LBF and indicate that species richness decreases from LBF, HMO, OGF to OGR in that respective order.

Reptiles had comparatively higher species richness and diversity in each habitat with HMO and LBF showing similarities in their richness, although HMO is slightly higher in diversity. Diversity is highest in OGF and lowest in LBF; richness is highest in HMO and lowest in OGR. The curves appear to indicate there is significant probability of discovering unseen species in their extrapolated richness values.

There were no significant differences in reptile diversity between each of the habitats studied, (ANOVA; F = 0.661, P = 0.869); similarly, amphibians too showed no significant difference in diversity of captured species in each habitat (ANOVA; F = 0.258, P = 0.854).

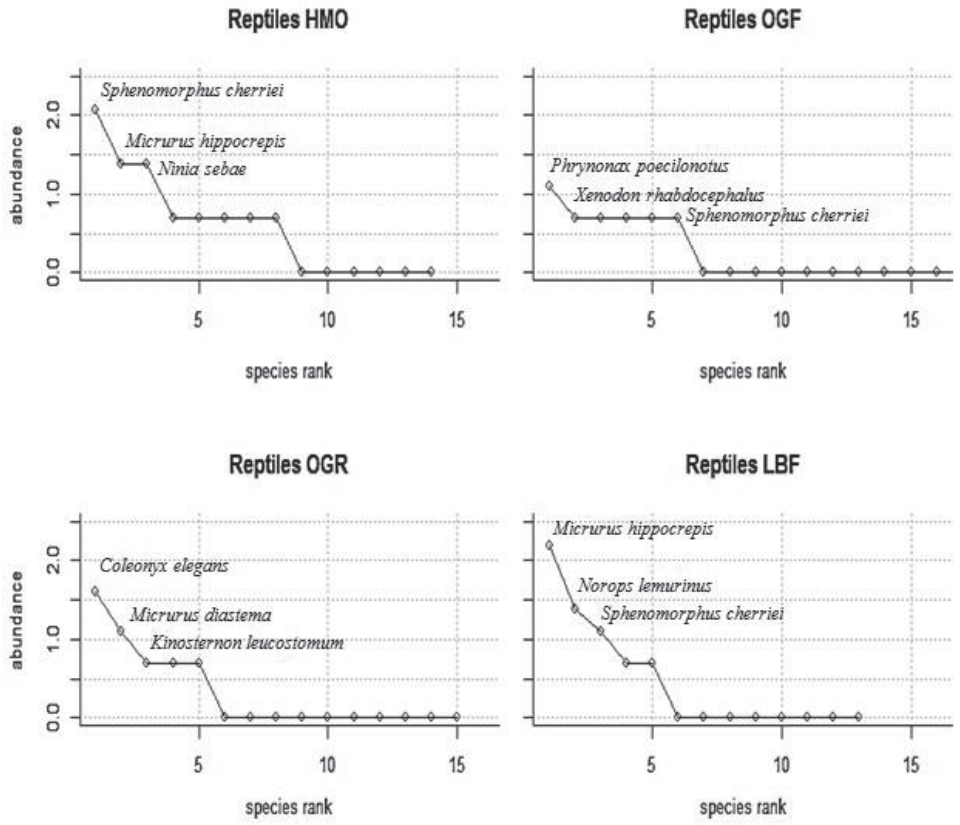

Figure 7. Reptile rank abundance curves (using the logarithm of abundances) for the Heavily Manicured Orchard (HMO), Overgrown Orchard Forest (OGF), Overgrown Orchard Riparian Forest (OGR) and Lowland Broadleaf Forest (LBF) study sites; the three most abundant species captured in each site is labeled in each of the four plots.

Table 3. Shannon-Wiener diversity indexes, means and standard deviations of reptiles and amphibians between each sample site are compared.

Forest Type	Amphibians			Reptiles		
	Average observed species	Average Shannon Diversity	SD (±)	Average observed species	Average Shannon Diversity	SD (±)
Heavily Manicured Orchard	2.6	1.00	5.54	0.5	3.26	0.63
Overgrown Orchard Forest Overgrown	1.6	0.82	3.71	0.46	2.97	0.69
Orchard Riparian Forest	0.9	0.52	2.23	0.43	2.83	0.68
Lowland Broadleaf Forest	3.70	1.30	5.64	0.48	3.07	0.66

Table 4. Extrapolated richness estimates evaluated through Chao1 index and Abundance-based Coverage Estimator (A.C.E.)

Forest Type	Reptiles				
	observed species	Chao1 Index	SE (±)	A.C.E.	SE (±)
Heavily Manicured Orchard	14	16.50	2.89	21.39	2.64
Overgrown Orchard Forest Overgrown	18	29.0	8.46	34.61	2.39
Orchard Riparian Forest	15	26.25	9.52	34.13	2.95
Lowland Broadleaf Forest	13	22.33	8.82	32.3	3.82

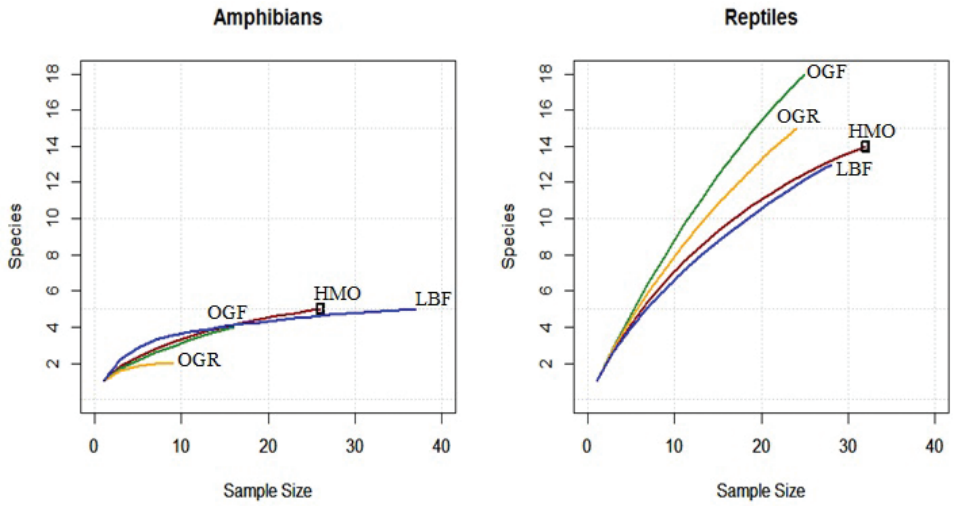

Figure 8. Rarefaction curves displaying sample based species richness and diversity for amphibian and reptiles captured in each habitat type.

Possibility of unseen species.—We calculated values using the Chao 2 richness estimator and Abundance-based Coverage Estimation (A.C.E.) in order to estimate extrapolated richness values in each habitat for reptile species (Chao 1984; Chao et al. 2000; Colwell and Coddington 1994) (Table 4); Amphibian curves appeared to flatten out, indicating low probability of unseen species and were therefore omitted from the analysis.

Discussion

A total of 56 trap nights, spanning four months of the rainy season, yielded 40 species of herpetofauna (197 individuals); 108 reptile captures (30 species) and 88 amphibian captures (ten species). Trapping systems captured 49 frogs (seven species), 38 toads (two species), and only one species of salamander. Gulf coast toads *Incilius valliceps*

and ranid frogs from the *Lithobates* genus were the most abundant amphibians captured (*Lithobates vaillanti* being the most abundant species); *Rhinella horribilis* (HMO), *Craugastor sabrinus* (OGF), *Eleutherodactylus leprus* (HMO) and *Bolitoglossa dofleini* (LBF) were the rarest, with only one individual of each species being caught in traps. In regards to reptiles, traps captured 74 snakes (25 species), 10 lizards (4 species), 8 geckos (1 species), 15 skinks (2 species) and two turtles (1 species).

Since the study sites were restricted to the TREES property, the trapping systems were all within close proximity to one another (μ = 267.6 m). In addition to this, there are several variations in habitat types; some are drastic (i.e., heavily manicured orchard areas bordering unaltered broadleaf forest areas), whereas some can be as miniscule as vegetation variations (i.e., lowland santamaria variant and lowland negrito-nargusta variant) within the broadleaf forest area (Penn et al. 2004). Habitat heterogeneity could result in increased species richness and diversity throughout the study areas (MacArthur and MacArthur 1961). However, this hypothesis must be factored in with the probability of decreased herpetofaunal species diversity due to open, human altered areas which lack significant shelter, such as woody debris (Whiles and Grubaugh 1996). It has been previously documented that herpetofauna species richness in agricultural areas with nearby strips of natural habitats can be greater than those without (Biaggini and Corti 2015). Natural broadleaf forest habitat strips were surrounding the trapping array in the HMO, possibly contributing to the species richness. This may indicate that small pockets of manicured land for agriculture may have reduced effects on herpetofauna communities so long as they have surrounding natural forest areas.

Herpetofaunal species diversity exhibited some extent of variation between the habitats studied; species richness was higher in reptiles than amphibians. Individual captures were highest in the LBF (n = 65) and HMO (n = 58) and lowest in the OGR (n = 33); diversity of species was highest in OGF (n=22) and relatively similar in HMO (n = 19), LBF (n = 18) and OGR (n = 17). Since this study only utilized standard Y-shaped funnel trapping system per habitat, incorporating pitfall traps and using different or modified funnel traps/drift fence configurations could increase trapping potential, particularly for anurans (Crosswhite 1999; Greenberg et al. 1994; Ribeiro Júnior et al. 2008). Moreover, including one or two more systems per habitat could increase capture rates and representativeness, providing better insight to herpetofaunal assemblages and species diversity; unfortunately, herpetological research in Belize is underfunded, so the study was performed under strict financial restraints. Conjointly, the study spanned through the rainy season, due to higher probability of capturing herpetofauna in what is generally their most active period. Nevertheless, if the study duration was extended throughout the year it may be a more acute representation of herpetofaunal assemblages in respects to seasonal variations, as some species may be more active at other times of the year (Todd et al. 2007). In addition to the sampling time constraint, the second trapping system set in the Overgrown Orchard Forest was set after the first sample session, providing a reduced capture capability; nevertheless, the trapped fauna accurately represented an abundant species diversity potential of the habitat areas so the data simply may not represent the richness potential individuals captured.

As this project was run for a single season, there are a number of cautions necessary for interpreting our dataset. The richness and abundance estimates may have been inflated or deflated by temporary boom and bust cycles of prey items during this particular season. It is also possible that we simply had an anomalous season and therefore recommend more extensive monitoring through a longer sampling period. Multi-year studies allow for monitoring survivorship of marked individuals, and trends in both activity and movement throughout the seasons, making them more robust. However, our study is intended as a snapshot view of the herpetofaunal communities within the different forest types of the study area in hopes to generate more interest for community level research within Belize, and to provide a baseline dataset from which to work.

The findings of this study can be used in conjunction with future herpetology and ecology work within the Belize in regards to community structure in anthropogenically-altered habitat areas. Monitoring efforts of herpetofauna in various habitats may assist in the creation of feasible conservation methods. Overall, there is now evidence of the effectiveness of drift fence and funnel trapping system use to monitor herpetofauna in Belize. Furthermore, the limitations of this study regarding lack of previous replicate studies, spatial autocorrelations, and changing environmental variables are understood.

The suitability of funnel traps in conjunction with drift fences is known to be an effective passive capture method for monitoring terrestrial herpetofauna (Dorcas and Williams 2009; Todd et al. 2007). Although these trapping systems may result in fewer captures, they promote more standardization of effort, which allows for more robust comparisons among different sites. Many methods in Belize have been utilized to study herpetofauna, although no published studies have included drift fences and funnel traps for passive trapping efforts. That being said, there have been efforts to use drift fences and pitfall traps to monitor other fauna, such as small mammals and amphibians (Engilis et al. 2012). Replicate studies using similar trapping methods should be implemented in the future for further verification of our findings.

Hurricane Earl significantly effected study site vegetation (i.e. canopy cover and standing vegetation), though didn't significantly alter capture diversity. One possible result of post-hurricane habitat alterations were the captures of two individuals of *Tantilla hendersoni*, a data deficient species of centipede eating snake known from only one prior individual record (Hofmann et al. 2017; Wilson and Mata-Silva 2015). Both snakes were captured after the hurricane struck the study sites. *Tantilla* are known to be fossorial and cryptozoic snakes and their activity during the post-hurricane sample sessions may have been to relocate due to damaged habitat areas or deracination of prey items. Other interesting occurrence, were the captures of arboreal snake species *Imantodes cenchoa,* and *Leptodeira polysticta*, both in the HMO just a few days before the hurricane. This was the only instance of capture for both species, which brings to question whether the captures were coincidental or influenced by the snakes seeking shelter in the manicured area, away from falling trees.

Predated fauna may also account for species capture data to be reduced. R. Gray and A. Pelletier observed a *Micrurus hippocrepis* captured underneath a trap in the

OGF, seemingly attempting to access the *Ninia sebae* captured within. This leads to the assumption that some herpetofauna trap-mates could potentially have been taken by other predatory herpetofauna, as many of the snake species caught are known to have diets consisting of lizards, skinks, frogs, toads and other snakes (Lee 2000; Campbell 1999). Due to the possibilities of trap mates being predated, data may lack some unique or rare species occurrences; however, the general trend of dominant species in each habitat would likely remain the same.

A study by McCoy (1970) in Middlesex (a village area near TREES) yielded similar information on snake species and their abundances in citrus plantations, *Ninia sebae* and *Micrurus hippocrepis* being found in higher abundances than other snakes. Our study suggests a similar trend, as the two most abundant species in the HMO were *N. sebae* and *M. hippocrepis*.

Conclusions

Intensive trapping studies should be implemented throughout the year to collect additional data on seasonal variations of herpetofauna in Belize. Herpetofauna that are of

Table 5. Herpetofauna species that occur in Belize considered as a concern for conservation (Critically Endangered = CE; Endangered = EN; Vulnerable = V; Near Threatened = NT; Lower Risk/Conservation Dependant = LR/CD).

REPTILES			
Species Name	**Common Name**	**Conservation Status**	**Status Authority**
Dermatemys mawii	Central American River Turtle	CE	Vogt et al. 2006
Chelydra rossignonii	Yucatan Snapping Turtle	V	Van Dijk et al. 2007a
Rhinoclemmys areolata	Furrowed Wood Turtle	NT	Van Dijk et al. 2007b
Crocodylus moreletii	Morlete's Crocodile	LR/CD	Cedeño-Vázquez et al. 2012
Crocodylus acutus	American Crocodile	V	Ponce-Campos et al. 2012
Celestus rozellae	Rozella's Lesser Galliwasp	NT	Sunyer et al. 2013a
Phyllodactylus insularis	Belize Leaf-tailed Gecko	V	Townsend and Walker 2014
Agkistrodon bilineatus	Cantil	NT	Lee and Hammerson 2007
AMPHIBIANS			
Species Name	**Common Name**	**Conservation Status**	**Status Authority**
Lithobates juliani	Maya Mountain Frog	NT	Lee and Walker 2004
Smilisca cyanosticta	Blue Spotted Mexican Treefrog	NT	Santos-Barrera et al. 2004a
Incilius campbelli	Campbell's Forest Toad	NT	Lee et al. 2004a
Craugastor laticeps	Broadheaded Rainfrog	NT	Santos-Barrera et al. 2004b
Craugastor chac	Chac's Rainfrog	NT	Walker et al. 2004
Craugastor sandersoni	Sanderson's Streamfrog	EN	Lee et al. 2004b
Craugastor sabrinus	Long-legged Streamfrog	NT	IUCN SSC 2016
Craugastor psephosypharus	Limestone Rainfrog	V	Lee et al. 2004c
Bolitoglossa dofleini	Mushroom-tongue Salamander	NT	Cruz et al. 2010
Eleutherodactylus leprus	Leprus Chirping Frog	V	Santos-Barrera et al. 2004c
Agalychnis moreletii	Morelet's Treefrog	CE	Santos-Barrera et al. 2004d

conservation concern in Belize (Table 5) still require continued monitoring and observations in order to target possible reasons for population decline and limiting factors for their distributions. Future research within Belize is important to provide data-based insight on herpetofauna species occurrences and the effects of anthropogenic change on their assemblages. Although there were some variations in reptile and amphibian species richness and diversity between habitats, our data shows the variations to be insignificant indicators of sensitivity towards anthropogenic changes in the study site. In fact, the Heavily Manicured Orchard was proportionate in herpetofauna species diversity and richness to the natural Lowland Broadleaf Forest, thus concluding that even constant anthropogenic activity had little effect on herpetofaunal assemblages in the area. The suspected reason for this lack of sensitivity is that each anthropogenically-altered habitat area had a surrounding natural forest edge, which could provide fauna with abundances of shelter and prey when necessary. Additionally, considering the significant alterations to standing vegetation and canopy percentages within each sampled habitat, the after effects of Hurricane Earl were minimal on herpetofaunal community composition within the study site. This data can be used to implement effective conservation methods by providing evidence that agricultural areas, when surrounded by natural habitat buffers, have little effect on herpetofaunal community assemblages.

Acknowledgements

We would like to express gratitude to the Forest Department of Belize for providing permissions for this research project (Scientific Collection/Research Permit Act No. 14/2000; Ref. No. WL/1/1/16(48) and to Mathieu Charette and Vanessa Kilburn, the directors of TREES for making this study possible by providing lodgings and facilitating research efforts on their property. We would also like to acknowledge Zach Dunseith, Ryan Dickson, Antoine Pelletier, Mathilde Poirier and Mireille Levesque for their tireless assistance with data records and field work. Finally, we would like to thank César Barrio-Amorós/Doc Frog Photography (César Luis Barrio Amorós www.docfrogphotography.com, email: cesarlba@yahoo.com) for the photos provided of *S. cherriei* and *L. vaillanti*.

References

Acevedo M, Ariano-Sánchez D, Johnson J (2013) *Micrurus hippocrepis*. The IUCN Red List of Threatened Species 2013: e.T203626A2769214. http://dx.doi.org/10.2305/IUCN.UK.2013-2.RLTS.T203626A2769214.en [Downloaded on 10 January 2017]

AmphibiaWeb. Information on amphibian biology and conservation.[web application] (2016) Berkeley, California, AmphibiaWeb. http://www.amphibiaweb.org/

Balick MJ, Nee MH, Atha DE (2000) Checklist of the vascular plants of Belize, with common names and uses. New York Botanical Garden Press, New York, 246 pp.

Biaggini M, Corti C (2015) Reptile assemblages across agricultural landscapes: Where does biodiversity hide? Animal Biodiversity and Conservation 38(2): 163–174. http://www.raco.cat/index.php/ABC/article/view/301565/391155

Boles E (1999) The Sibun River Watershed Atlas. The Government Printer, Belmopan, Belize. http://www.worldcat.org/title/sibun-river-watershed-atlas/oclc/61198224

Brewer SW, Rejmánek M, Webb MA, Fine PV (2003) Relationships of phytogeography and diversity of tropical tree species with limestone topography in southern Belize. Journal of Biogeography 30(11): 1669–1688. https://doi.org/10.1046/j.1365-2699.2003.00971.x

Bridgewater S (2012) A natural history of Belize: inside the Maya Forest. University of Texas Press, Austin, 11–13.

Brown ML, Donovan TM, Schwenk WS, Theobald DM (2014) Predicting impacts of future human population growth and development on occupancy rates of forest-dependent birds. Biological conservation, 170: 311–320. https://doi.org/10.1016/j.biocon.2013.07.039

Campbell JA (1999) Amphibians and reptiles of northern Guatemala, the Yucatán, and Belize (Vol. 4) University of Oklahoma Press, Norman.

Cedeño-Vázquez JR, Platt SG, Thorbjarnarson J (IUCN Crocodile Specialist Group) (2012) *Crocodylus moreletii.* The IUCN Red List of Threatened Species 2012: e.T5663A3045579. http://dx.doi.org/10.2305/IUCN.UK.2012.RLTS.T5663A3045579.en. [Downloaded on 08 January 2017]

CEPF (2004) Mesoamerica hotspot: Northern Mesoamerica briefing book, 7-10. http://www.cepf.net/Documents/final.mesoamerica.northernmesoamerica.briefingbook2005.pdf

Chao A (1984) Nonparametric estimation of the number of classes in a population. Scandinavian Journal of Statistics 11(4): 265–270. http://www.jstor.org/stable/4615964

Chao A, Hwang WH, Chen YC, Kuo CY (2000) Estimating the number of shared species in two communities. Statistica Sinica 10(2000): 227–246. http://www.jstor.org/stable/24306714

Chaves G, Köhler G, Lamar W, Nicholson K (2013b) *Sphenomorphus cherriei*. The IUCN Red List of Threatened Species 2013: e.T198510A2527609. http://dx.doi.org/10.2305/IUCN.UK.2013-2.RLTS.T198510A2527609.en [Downloaded on 10 January 2017]

Chaves G, Köhler G, Nicholson K, Porras LW (2013a) *Ninia sebae*. The IUCN Red List of Threatened Species 2013: e.T198388A2523671. http://dx.doi.org/10.2305/IUCN.UK.2013-2.RLTS.T198388A2523671.en [Downloaded on 10 January 2017]

Cherrington EA, Cho P, Waight I, Santos TY, Escalante AE, Nabet J, Usher L (2012) Executive Summary: Forest Cover and Deforestation in Belize, 2010–2012. SERVIR (El Sistema Regional de Visualización y Monitoreo), Belmopan, Belize: CATHALAC (El Centro del Agua del Trópico Húmedo para América Latina y el Caribe). http://eprints.uberibz.org/id/eprint/1381

Chicas SD, Omine K, Arevalo B, Ford JB, Sugimura K (2016) Deforestation Along the Maya Mountain Massif Belize-Guatemala Border. ISPRS-International Archives of the Photogrammetry, Remote Sensing and Spatial Information Sciences, 597–602. http://www.int-arch-photogramm-remote-sens-spatial-inf-sci.net/XLI-B8/597/2016/isprs-archives-XLI-B8-597-2016.pdf

Colwell RK, Coddington JA (1994) Estimating terrestrial biodiversity through extrapolation. Philosophical Transactions: Biological Sciences 345: 101–118. http://dx.doi.org/10.1098/rstb.1994.0091

Conservation International (2011) Biodiversity Hotspots Revisited. https://databasin.org/maps/new#datasets=23fb5da1586141109fa6f8d45de0a260

Crosswhite DL (1999) Comparison of methods for monitoring reptiles and amphibians in upland forests of the Ouachita Mountains. Proceedings of the Oklahoma Academy of Science 79: 45-50. http://s3.amazonaws.com/academia.edu.documents/45022359/p45_50.pdf?AWSAccessKeyId=AKIAIWOWYYGZ2Y53UL3A&Expires=1496577698&Signature=291Y996VITtfwWZkggE4M5U2UpM%3D&response-content-disposition=inline%3B%20filename%3DComparison_of_Methods_for_Monitoring_Rep.pdf

Cruz G, Wilson LD, McCranie R, Acevedo M, Wake D, Lee J, Papenfuss T, Castañeda F, Rovito S, KolbyJ (2010) *Bolitoglossa dofleini*. (errata version published in 2016) The IUCN Red List of Threatened Species 2010: e.T59156A87541574. [Downloaded on 08 January 2017]

DeClerck FA, Chazdon R, Holl KD, Milder JC, Finegan B, Martinez-Salinas A, Imbach P, Canet L, Ramos Z (2010) Biodiversity conservation in human-modified landscapes of Mesoamerica: Past, present and future. Biological conservation 143(10): 2301–2313. https://doi.org/10.1016/j.biocon.2010.03.026

Dorcas ME, Willson JD (2009) Innovative methods for studies of snake ecology and conservation. Snakes: ecology and conservation, 5–37. http://comp.uark.edu/~jwillson/publications/2009%20-%20Dorcas%20&%20Willson%20-%20SNAKES%20ECOLOGY%20AND%20CONSERVATION%20-%20Chapter1.PDF

Duellman WE (1966) The Central American herpetofauna: an ecological perspective. Copeia 1966(4): 700–719. https://doi.org/10.2307/1441403

Engilis A, Cole RE, Caro TM (2012) Small mammal survey of Chiquibul forest reserve, Maya mountains, Belize, 2001. Museum of Texas Tech University, Lubbock 308, 1–23. https://pdfs.semanticscholar.org/b732/bbaf9718e43e89518c49b3c4e0c9c9d0f8aa.pdf

Frost MD (1981) Patterns of human influence on landscape and wildlife: Selected case studies in Belize. Revista Geográfica 94: 89-100. http://www.jstor.org/stable/40992403

GFW (Global Forest Watch) (2017) World Resources Institute, Washington, DC. http://www.globalforestwatch.org. [Accessed on 08 January 2017]

Gibson L, Lee TM, Koh LP, Brook BW, Gardner TA, Barlow J, Sodhi NS (2011) Primary forests are irreplaceable for sustaining tropical biodiversity. Nature 478(7369): 378–381. https://doi.org/10.1038/nature10425

Greenberg CH, Neary DG, Harris LD (1994) A comparison of herpetofaunal sampling effectiveness of pitfall, single-ended, and double-ended funnel traps used with drift fences. Journal of Herpetology 28(3): 319-y65t324. https://doi.org/10.2307/1564530

Greene HW (1975) Ecological observations on the red coffee snake, Ninia sebae, in southern Veracruz, Mexico. American Midland Naturalist 93(2): 478–484. https://doi.org/10.2307/2424185

Harris KL (2009) Trees of Belize. BRC Printing, Benque Viejo Del Carmen.

Harvey CA, Medina A, Sánchez DM, Vílchez S, Hernández B, Saenz JC, Sinclair FL (2006) Patterns of animal diversity in different forms of tree cover in agricultural landscapes. Ecological applications 16(5): 1986–1999. https://doi.org/10.1890/1051-0761(2006)016[1986:POADID]2.0.CO;2

Harvey C, Alpízar F, Chacón M, Madrigal R (2005) Assessing linkages between agriculture and biodiversity in Central America: Historical overview and future perspectives. Mesoamerican, Caribbean Region Conservation Science Program, 1–140.

Hinsley A, Entwistle A, Pio DV (2015) 'Does the long-term success of REDD+ also depend on biodiversity?' Oryx 49(2): 216–221. https://doi.org/10.1017/S0030605314000507

Hofmann EP, Gray RJ, Wilson LD, Townsend JH (2017) Discovery of the first male specimen of *Tantilla hendersoni* Stafford, 2004 (Squamata: Colubridae), from a new locality in central Belize. Herpetology Notes 10: 53–57.

Hughes AC (2017) Understanding the drivers of Southeast Asian biodiversity loss. Ecosphere 8(1): e01624. https://doi.org/10.1002/ecs2

Islebe GA, León-Cortés JL, Schmook B, Calmé S (2015) Biodiversity and Conservation of the Yucatán Peninsula. Springer International Publishing, Cham, 1–401. https://doi.org/10.1007/978-3-319-06529-8

IUCN (2016) The IUCN Red List of Threatened Species. Version 2016-3. http://www.iucnredlist.org [Downloaded on 07 December 2016]

IUCN SSC Amphibian Specialist Group (2014) *Bromeliohyla bromeliacia*. The IUCN Red List of Threatened Species 2014: e.T55422A53953100. http://dx.doi.org/10.2305/IUCN.UK.2014-3.RLTS.T55422A53953100.en [Downloaded on 08 January 2017]

IUCN SSC Amphibian Specialist Group (2016) *Craugastor sabrinus*. The IUCN Red List of Threatened Species 2016: e.T56940A54370744. http://dx.doi.org/10.2305/IUCN.UK.2016-3.RLTS.T56940A54370744.en [Downloaded on 08 January 2017]

Johnson JD, Mata-Silva V, Wilson LD (2015) A conservation reassessment of the Central American herpetofauna based on the EVS measure. Amphibian, Reptile Conservation 9(2): 1–94. http://amphibian-reptile-conservation.org/pdfs/Volume/Vol_9_no_2/ARC_9_2_[General_Section]_1-94_e100_low_res.pdf

Kaiser K, Pollinger J (2012) *Batrachochytrium dendrobatidis* shows high genetic diversity and ecological niche specificity among haplotypes in the Maya Mountains of Belize. PloS ONE 7(2): e32113. https://doi.org/10.1371/journal.pone.0032113

Kindt R, Coe R (2005) Tree diversity analysis. A manual and software for common statistical methods for ecological and biodiversity studies. World Agroforestry Centre (ICRAF), Nairobi.

Krebs CJ (1989) Ecological methodology. Harper, Row, New York.

Latinne A, Waengsothorn S, Rojanadilok P, Eiamampai K, Sribuarod K, Michaux JR (2013) Diversity and endemism of Murinae rodents in Thai limestone karsts. Systematics and Biodiversity 11(3): 323–344. http://dx.doi.org/10.1080/14772000.2013.818587

Lee J, Acevedo M, Wilson LD, Walker P (2004a) *Incilius campbelli*. The IUCN Red List of Threatened Species 2004: e.T54601A11170251. http://dx.doi.org/10.2305/IUCN.UK.2004.RLTS.T54601A11170251.en [Downloaded on 08 January 2017]

Lee J, Walker P, Acevedo M (2004b) *Craugastor sandersoni*. The IUCN Red List of Threatened Species 2004: e.T56946A11558459. http://dx.doi.org/10.2305/IUCN.UK.2004.RLTS.T56946A11558459.en [Downloaded on 08 January 2017]

Lee J, Walker P, Acevedo M (2004c). *Craugastor psephosypharus*. The IUCN Red List of Threatened Species 2004: e.T56882A11536599. http://dx.doi.org/10.2305/IUCN.UK.2004.RLTS.T56882A11536599.en [Downloaded on 08 January 2017]

Lee J, Hammerson GA (2007) *Agkistrodon bilineatus*. The IUCN Red List of Threatened Species 2007:e.T64296A12755881. http://dx.doi.org/10.2305/IUCN.UK.2007.RLTS.T64296A12755881.en [Downloaded on 08 January 2017]

Lee J, Walker P (2004) *Lithobates juliani*. The IUCN Red List of Threatened Species 2004:e.T58630A11816243.

Lee JC (2000) A field guide to the amphibians and reptiles of the Maya world: the lowlands of Mexico, northern Guatemala, and Belize. Comstock Pub Assoc.

Lips KR, Reeve JD, Witters LR (2003) Ecological traits predicting amphibian population declines in Central America. Conservation Biology 17(4): 1078–1088. https://doi.org/10.1046/j.1523-1739.2003.01623.x

MacArthur RH, MacArthur JW (1961) On bird species diversity. Ecology 42(3): 594–598. https://doi.org/10.1046/j.1523-1739.2003.01623.x

McCoy CJ (1970) The Snake Fauna of Middlesex, British Honduras. Journal of Herpetology 4(3): 135–140. https://doi.org/10.2307/1562888

Meerman J, Clabaugh J 2016. Biodiversity and Environmental Resource Data System of Belize. Online. http://www.biodiversity.bz

Mittermeier RA, Turner WR, Larsen FW, Brooks TM, Gascon C (2011) Global biodiversity conservation: the critical role of hotspots. Biodiversity hotspots. Springer Berlin, Heidelberg. https://doi.org/10.1007/978-3-642-20992-5_1

Myers N, Mittermeier RA, Mittermeier CG, Da Fonseca GA, Kent J (2000) Biodiversity hotspots for conservation priorities. Nature 403(6772): 853–858. https://doi.org/10.1038/35002501

Offerman HL, Dale VH, Pearson SM, O'Neill RV, Bierregaard Jr RO (1995) Effects of forest fragmentation on neotropical fauna: current research and data availability. Environmental Reviews 3(2): 191–211. https://doi.org/10.1139/a95-009

Oksanen JFG, Blanchet R, Kindt P, Legendre PR, Minchin RB, O'Hara G, Simpson G, Solymos P, Stevens H, Wagner H (2015) Vegan: Community Ecology Package. R package version 2.3–0. http://CRAN.R-project.org/package=vegan

Pasos R, Girot P, Laforge M, Torrealba P, Kaimowitz D (1994) El último despale: la frontera agrícola en Centroamérica. FUNDESCA. Garnier Relaciones Públicas, San José, Costa Rica.

Penn MG, Sutton DA, Monro A (2004) Vegetation of the greater Maya mountains, Belize. Systematics and biodiversity 2(1): 21–44. http://dx.doi.org/10.1017/S1477200004001318

Ponce-Campos P, Thorbjarnarson J, Velasco A (IUCN SSC Crocodile Specialist Group) (2012) *Crocodylus acutus*. The IUCN Red List of Threatened Species 2012: e.T5659A3043244. http://dx.doi.org/10.2305/IUCN.UK.2012.RLTS.T5659A3043244.en [Downloaded on 08 January 2017]

R Core Team (2014) R:A language and environment for statistical computing. R Foundation for Statistical Computing. Vienna, Austria. http://www.R-project.org/

Radachowsky J (2002) Endemism in the Maya Forest. A report prepared by Wildlife Conservation Society for FIPA and USAID. http://www.areasprotegidas.info/upload/document/endemisminthemayaforest.pdf

Redo DJ, Grau HR, Aide TM, Clark ML (2012) Asymmetric forest transition driven by the interaction of socioeconomic development and environmental heterogeneity in Central

America. Proceedings of the National Academy of Sciences of the United States of America 109(23): 8839–8844. http://doi.org/10.1073/pnas.1201664109

Ribeiro Júnior MA, Gardner TA, Ávila Pires TC (2008) Evaluating the effectiveness of herpetofaunal sampling techniques across a gradient of habitat change in a tropical forest landscape. Journal of Herpetology 42(4): 733–749. http://dx.doi.org/10.1670/07-097R3.1

Saab VA, Petit DR (1992) Impact of pasture development on winter bird communities in Belize, Central America. Condor 94(1): 66–71. https://doi.org/10.2307/1368796

Santos-Barrera G, Acevedo M, Walker P, Lee J, Cruz G, Wilson LD (2004b). *Craugastor laticeps*. The IUCN Red List of Threatened Species 2004: e.T56703A11517589. http://dx.doi.org/10.2305/IUCN.UK.2004.RLTS.T56703A11517589.en [Downloaded on 08 January 2017]

Santos-Barrera G, Canseco-Márquez L, Lee J, Acevedo M (2004c).*Eleutherodactylus leprus*. The IUCN Red List of Threatened Species 2004: e.T56714A11521644. http://dx.doi.org/10.2305/IUCN.UK.2004.RLTS.T56714A11521644.en [Downloaded on 08 January 2017]

Santos-Barrera G, Lee J, Acevedo M, Wilson LD (2004d) *Agalychnis moreletii*. The IUCN Red List of Threatened Species 2004: e.T55293A11275690. http://dx.doi.org/10.2305/IUCN.UK.2004.RLTS.T55293A11275690.en [Downloaded on 08 January 2017]

Santos-Barrera G, Lee J, Acevedo M, Walker P (2004a). *Smilisca cyanosticta*. The IUCN Red List of Threatened Species 2004: e.T56007A11405713. http://dx.doi.org/10.2305/IUCN.UK.2004.RLTS.T56007A11405713.en [Downloaded on 08 January 2017]

Santos-Barrera G, Solís F, Ibáñez R, Chaves G, Bolaños F, Wilson LD, Castro F, Coloma LA, Ron SR, Acosta-Galvis A, Morales M (2008) *Lithobates vaillanti*. The IUCN Red List of Threatened Species 2008: e.T58744A11835860. http://dx.doi.org/10.2305/IUCN.UK.2008.RLTS.T58744A11835860.en [Downloaded on 11 January 2017]

Santos-Barrera G, Wilson LD, Savage J, Bolaños F, Acevedo M (2010) *Incilius valliceps*. The IUCN Red List of Threatened Species 2010: e.T54789A11191593. http://dx.doi.org/10.2305/IUCN.UK.2010-2.RLTS.T54789A11191593.en [Downloaded on 10 January 2017]

Smith F (2016) The citrus industry. http://belizeinfocenter.org/industries/citrus-industry/

Spangler M (2015) Conservation of a Neotropical Herpetofauna: An Introduction to the Crisis of Amphibians and Reptiles in Central America and Beyond. Central American Biodiversity. Springer, New York, 323–349. https://doi.org/10.1007/978-1-4939-2208-6_14

Stafford PJ, Walker P, Edgar P, Penn MG (2010) Distribution and conservation of the herpetofauna of Belize. In: Wilson LD, Townsend JH, Johnson JD (Eds) Conservation of Mesoamerican Amphibians and Reptiles. Eagle Mountain Publishing, LC, Eagle Mountain, Utah, USA, 370–405.

Stuart SN, Chanson JS, Cox NA, Young BE, Rodrigues AS, Fischman DL, Waller RW (2004) Status and trends of amphibian declines and extinctions worldwide. Science 306(5702): 1783-1786. https://doi.org/10.1126/science.1103538

Suazo-Ortuño I, Alvarado-Díaz J, Martínez-Ramos M (2008) Effects of conversion of dry tropical forest to agricultural mosaic on herpetofaunal assemblages. Conservation Biology 22(2): 362-374. https://doi.org/10.1111/j.1523-1739.2008.00883.x

Sunyer J, Ariano-Sánchez D, Lee J (2013b) *Coleonyx elegans*. The IUCN Red List of Threatened Species 2013: e.T197470A2487594. http://dx.doi.org/10.2305/IUCN.UK.2013-2.RLTS.T197470A2487594.en [Downloaded on 10 January 2017]

Sunyer J, Ariano-Sánchez D, Lee J, Mandujano RC (2013a) *Celestus rozellae*. The IUCN Red List of Threatened Species 2013: e.T63698A3128241. http://dx.doi.org/10.2305/IUCN.UK.2013-2.RLTS.T63698A3128241.en [Downloaded on 08 January 2017]

Todd BD, Winne CT, Willson JD, Gibbons JW (2007) Getting the drift: examining the effects of timing, trap type and taxon on herpetofaunal drift fence surveys. The American Midland Naturalist 158(2): 292–305. http://dx.doi.org/10.1674/0003-0031(2007)158[292:GTDETE]2.0.CO;2

Townsend JH, Walker P (2014) *Phyllodactylus insularis*. The IUCN Red List of Threatened Species 2014: e.T203074A2759895. http://dx.doi.org/10.2305/IUCN.UK.2014-1.RLTS.T203074A2759895.en [Downloaded on 08 January 2017]

Uetz P (2016) [Ed.] The Reptile Database. http://www.reptile-database.org [accessed on 10 October 2016]

Utting P (1993) Trees, people and power: social dimensions of deforestation and forest protection in Central America. Earthscan Publications Ltd.

Valentine LE, Reaveley A, Johnson B, Fisher R, Wilson BA (2012) Burning in banksia woodlands: how does the firefree period influence reptile communities? PloS ONE 7 (4): e34448. https://doi.org/10.1371/journal.pone.0034448

Van Dijk PP, Lee J, Calderón Mandujano R, Flores-Villela O, Lopez-Luna MA, Vogt RC (2007a) *Chelydra rossignonii*. (errata version published in 2016) The IUCN Red List of Threatened Species 2007: e.T63660A97408221 [Downloaded on 08 January 2017]

Van Dijk PP, Lee J, Calderón Mandujano R, Flores-Villela O, Lopez-Luna, MA (2007b).*Rhinoclemmys areolata*. (errata version published in 2016) The IUCN Red List of Threatened Species 2007: e.T63664A97375601 [Downloaded on 08 January 2017]

Vogt RC, Gonzalez-Porter GP, Van Dijk PP (2006) *Dermatemys mawii*. (errata version published in 2016) The IUCN Red List of Threatened Species 2006: e.T6493A97409830 [Downloaded on 08 January 2017]

Walker P, Acevedo M, Cruz G, Wilson LD, McCranie R, Köhler G (2004) *Craugastor chac*. The IUCN Red List of Threatened Species 2004: e.T56504A11484970. http://dx.doi.org/10.2305/IUCN.UK.2004.RLTS.T56504A11484970.en [Downloaded on 08 January 2017]

Whiles MR, Grubaugh JW (1996) Importance of coarse woody debris to southern forest herpetofauna. Biodiversity of coarse woody debris in Southern Forests: effects on biodiversity. Proc. Work. Coarse Woody Debris in Southern Forests. US For. Serv., Gen. Tech. Rep. SE94 146: 94–100.

Wilson LD, Mata-Silva V (2015) A checklist and key to the snakes of the Tantilla clade (Squamata: Colubridae), with comments on taxonomy, distribution, and conservation. Mesoamerican Herpetology 2: 418–498. http://mesoamericanherpetology.com/uploads/3/5/0/0/3500871/wilson_mata-silva_dec_2015.pdf

Wilson LD, Mata-Silva V, Johnson JD (2013) A conservation reassessment of the reptiles of Mexico based on the EVS measure. Amphibian, Reptile Conservation 7(1): 1–47. http://ww.w.redlist-arc.org/Article-PDFs/Special_Mexico_Issue_ARC_7(1)_1-47_low_res.pdf

World Bank Group (no date) Climate Change Knowledge Portal For Developmental Practitioners and Policy Makers. http://sdwebx.worldbank.org/climateportal/index.cfm?page=country_historical_climate&ThisCCode=BLZ

Young BE, Stuart SN, Chanson JS, Cox NA, Boucher TM (2004) Disappearing jewels: the status of new world amphibians. NatureServe Virginia Arlington. https://portals.iucn.org/library/sites/library/files/documents/2004-107.pdf

Young CA (2008) Belize's ecosystems: Threats and challenges to conservation in Belize. Tropical Conservation Science 1(1): 18–33. http://journals.sagepub.com/doi/pdf/10.1177/194008290800100102

Yue S, Brodie JF, Zipkin EF, Bernard H (2015) Oil palm plantations fail to support mammal diversity. Ecological Applications 25(8): 2285–2292. https://doi.org/10.1890/14-1928.1

Supplementary material 1

Common captures during study

Authors: Russell Gray, Colin T. Strine

Data type: Occurrence Data

Explanation note: Photos of reptiles and amphibians most commonly captured during the study. Information is provided regarding the habitats each species was caught in during the study, their IUCN Redlist conservation status, and EVS scores according to Johnson et al. (2015).

Link: https://doi.org/10.3897/zookeys.707.14029.suppl1